Emiliano Molinaro

*PhD Thesis:*

# CP Violation in the Lepton Sector,

# Thermal Leptogenesis and

# Lepton Flavour Violating Processes

Supervisor: Prof. Serguey T. Petcov

*September 2010*

*International School for Advanced Studies*
*(SISSA/ISAS)*

# Acknowledgments

It is a pleasure for me to acknowledge here all the people who gave an important contribution to my life and scientific activity during the years of Ph.D. in SISSA.

First, I would like to thank my supervisor Serguey Petcov for his continuous encouragement and the deep physical insight he could transmit to me.

I cannot forget all the guys who started the Ph.D. with me and shared several nice moments of my life in Trieste: Luca Lepori, wonderful officemate, Marco Nardecchia (the Buffone), Raffaele Savelli (Fuffi), Andrea Prudenziati (Bond), Robert Ziegler, Jorge Noreña, Guido D'amico, Gaurav Narain and Tom Varley. Among the other SISSA Ph.D. students and the people who shared their time with me in Trieste: Pratika Dayal, Fabio Ferrari Ruffino, Laura Bonavera, Vincenzo Vitagliano, Omar Zanusso, Daniel Arean Fraga, Zaynep Varley, Marilena Griguoli, Anna Griguoli, Margherita Cavallo, Nicola Majorano, Francesca Nani, Carlo Mercuri, Stefano Benvegnú, Davide Masoero, Emanuele Costa, Giulia Migliori, Alena Streltsova, Liuba Papeo, Claudia Civai.

I had the pleasure to collaborate with several physicists during my research activity: Tetsuo Shindou, Yasutaka Takanishi, Claudia Hagedorn, Florian Plentinger, Michael Schmidt, Silvia Pascoli, Anupam Mazumdar, Roberto Petronzio, Nazario Tantalo, Giulia de Divitiis. From everybody I learned a lot about physics and science in general.

I have to remember also the people I met at the IPPP, in Durham, for their special company and the very nice environment they managed to create. In particular, I would like to thank Carina Popovici for her warm help and support when I was completing this Ph.D. thesis.

Finally, I am grateful to my parents and my brothers for the high regard they have for me.

A very special thanks to Tamara, for being always present in the most important moments of my life.

*to the memory of Alessandro Conti*

# Contents

# Introduction

It is a well established experimental fact that the Universe is strongly asymmetric in its matter and antimatter content. Indeed, there is no direct/indirect evidence up to now about the formation of primordial stars or galaxies made entirely of antiparticles. The only clear observation of antimatter in the Universe, besides the one created in particle accelerators, resides on the measurement of the cosmic ray flux through the Earth. The antiproton number density in the cosmic rays is about $10^{-4}$ smaller than the density of protons [1] and it is consistent with antiproton secondary production through accelerator-like processes, $p + p \to 3p + \overline{p}$. This suggests that there is no remnant of a primordial antimatter abundance in our galaxy. Experimental evidences of a baryonic asymmetric Universe are also observed at larger scales [2, 3].

An indirect measurement of the relative abundance of baryonic (protons and neutrons) matter and antimatter can be deduced empirically in two different ways : $i$) from Big Bang Nucleosynthesis (BBN) [4] and $ii$) from the cosmic microwave background (CMB) anisotropies [5]. The theory of BBN predicts that the light elements of the Universe, namely D, $^{3}$He, $^{4}$He and $^{7}$Li were produced in the first three minutes after the Big Bang. The relative density of these elements depend crucially on the following quantity:

$$\eta \; \equiv \; \frac{n_b - n_{\bar{b}}}{n_\gamma} \, , \tag{1}$$

where $n_b$, $n_{\bar{b}}$ and $n_\gamma$ are number densities of baryons, antibaryons and photons, respectively. The quantity $\eta$ is by definition the *baryon asymmetry* of the Universe. It can be shown that the same value of $\eta$ explain, within the BBN scenario, all the primordial abundances of the light elements listed above, which can be inferred, independently, from different observations [4]. This is considered a great success of the Standard Cosmological Model. The range of $\eta$ (at 95% CL), compatible with BBN constraints [4], is

$$4.7 \times 10^{-10} \le \eta^{\text{BBN}} \le 6.5 \times 10^{-10} \, . \tag{2}$$

The second way in which $\eta$ can be measured is from the CMB anisotropies. The CMB radiation has a thermal blackbody spectrum with a nearly constant temperature $T \cong 2.73$ K. Temperature fluctuations $\Delta T/T \sim 10^{-5}$ in different directions in the sky, were measured quite in detail by the satellite WMAP [5]. Such anisotropies are connected to acoustic oscillations of the baryon-photon fluid at the time of recombination, about 400 thousand years after the Big Bang, when protons and electrons formed neutral hydrogen atoms and photons decoupled from the thermal plasma. The seeds of these tiny temperature variations can be traced back to quantum fluctuations during the inflationary era. The baryon energy density strongly affects the shape of the CMB power spectrum. From the analysis of the spectrum it is possible to obtain a measurement of $\eta$ which is independent

from the one given by BBN. The WMAP 5 year data [5] report the value

$$\eta^{\mathrm{CMB}} = (6.17 \pm 0.17) \times 10^{-10} \,, \tag{3}$$

in perfect agreement with the determination obtained from the primordial nucleosynthesis.

An alternative way to express the matter-antimatter asymmetry is to use the ratio between the baryon number density and the entropy density $s$ of the Universe:

$$Y_B \;=\; \frac{n_b - n_{\bar{b}}}{s}\,. \tag{4}$$

The two formulations in terms of $Y_B$ and $\eta$, at the present time, [1] are easily related:

$$Y_B \;=\; \frac{n_\gamma^0}{s^0}\eta \;=\; 0.142\,\eta \;=\; (8.77 \pm 0.24) \times 10^{-11}\,, \tag{5}$$

where $n_\gamma^0$ and $s^0$ denote the current photon and the entropy densities.

A simple computation shows that the Standard Cosmological Model, which gives the correct description of the evolution of the Universe after the BBN era, fails in explaining the small number reported in (5). To be more concrete, starting with an initial equal number density of matter and antimatter, $\eta = 0$, as predicted within the Standard Big Bang Model, at temperatures $T \lesssim m_p \simeq 1$ GeV, the baryon and antibaryon number densities are Boltzmann suppressed and result: $n_b \approx n_{\bar{b}} \approx (m_p/T)^{3/2} \exp(-m_p/T)\, n_\gamma$. Owing to the expansion (cooling) of the Universe, $n_b$ and $n_{\bar{b}}$ decrease as long as the annihilation rate $\Gamma \approx n_b \langle \sigma_{\mathrm{ann}} v \rangle$ is larger than the expansion rate of the Universe $H$. Taking a thermally averaged annihilation cross-section $\langle \sigma_{\mathrm{ann}} v \rangle \approx m_\pi^{-2}$, with $m_\pi \simeq 135$ MeV, the annihilation rate of nucleons and antinucleons equals the expansion rate of the Universe at the freeze-out temperature $T_{\mathrm{f}} \approx 20$ MeV. Consequently, nucleons and antinucleons become so rare that they cannot interact anymore and their comoving number densities remain constant until present time: $n_b/n_\gamma \approx n_{\bar{b}}/n_\gamma \approx (m_p/T_{\mathrm{f}})^{3/2} \exp(-m_p/T_{\mathrm{f}}) \approx 10^{-18}$. In order to avoid this *annihilation catastrophe*, a primordial asymmetry between baryons and antibaryons, at the level of 1 part in $10^{10}$, should be dynamically generated so that, after the annihilation process, the Universe remains with an excess of baryons over antibaryons, in the amount given by (5). The generation of the baryon asymmetry of the Universe is called *baryogenesis*.

The necessary and sufficient conditions under which baryogenesis occurs in the early Universe, were pointed out for the first time by Sakharov in 1967 [6]. These conditions, which should be simultaneously satisfied at some epoch of the evolution of the Universe, consist in: *i*) baryon number violation, *ii*) C (charge conjugation symmetry) and CP violation and *iii*) departure from thermal equilibrium. All the mentioned criteria are already verified inside the Standard Model (SM) of elementary particles: due to the chiral anomaly of the electroweak (EW) interactions, the baryon number $B$ and lepton number $L$ are not conserved at the quantum level. Only the combination $B - L$, which is anomaly free, is preserved. At zero temperature, $B + L$ violating interactions are determined by instanton configurations of the gauge fields which allow tunneling between two inequivalent vacua of the theory. Non-perturbative transitions of this type create 9 quarks and

---

[1]Throughout the thesis the computation of the baryon asymmetry is compared to the measurement reported in (5), which is obtained from the CMB analysis in [5].

3 leptons, one for each family. The associated $B + L$ violating rate at zero temperature is exponentially suppressed and does not produce observable effects. However, when temperature effects are included, thermal fluctuations can excite static gauge field configurations, called sphalerons [7], which correspond to an energy equal to the energy barrier between two adjacent vacua. The sphaleron interaction rates were shown [8] to approach thermal equilibrium at temperatures larger than the EW symmetry breaking scale and at such temperatures can mediate fast $B + L$ violating processes in the thermal bath. The second Sakharov condition is satisfied in the SM: C is maximally violated by the weak interaction, while CP is broken due to the Cabibbo-Kobayashi-Maskawa mixing [9, 10], *i.e.* quarks mass eigenstates and electroweak flavour states are mixed via a complex unitary matrix, the so-called CKM matrix, which contains one CP violating phase that is different from zero. Finally, the departure from thermal equilibrium can be determined by a strongly first order electroweak phase transition in the early Universe. This mechanism for the generation of the baryon asymmetry, which resides only on the SM field content, is called *electroweak baryogenesis* [11]. Unfortunately, it cannot provide sufficient primordial baryon production, since the source of CP violation in the quark sector of the theory is too small, due to the smallness of some of the quark masses and of the quark mixing angles [12]. Moreover, the first order EW phase transition does not result strong enough to allow successful baryogenesis, because of the lower bound on the Higgs mass [13]. In conclusion, in order to obtain the observed value of $Y_B$, it is necessary to go beyond the SM, providing new sources of CP violation and a new mechanism for realizing departure from thermal equilibrium.

Several scenarios of baryogenesis have been proposed in the literature, each one with proper variations. Some examples are provided by GUT baryogenesis, MSSM electroweak baryogenesis, Affleck-Dine mechanism and leptogenesis.

In this thesis phenomenological aspects related to the thermal leptogenesis mechanism [2] of baryon asymmetry generation are analyzed in detail. The leptogenesis mechanism was introduced for the first time by Fukugita and Yanagida in 1986 [15]. What makes it appealing is the fact that it is intimately related to neutrino physics. Neutrino oscillation experiments [16] have provided compelling evidences for existence of transitions in flight between the different flavour neutrinos, caused by non-zero neutrino masses and neutrino mixing. Massive neutrinos cannot be implemented in the SM, therefore some type of new physics is necessary to explain their small mass.

One of the most viable theoretical frameworks used to yield neutrino masses is the see-saw mechanism [17]. The basic features of this scenario are the following: the SM Lagrangian is extended with the addition of at least two heavy right-handed (RH) Majorana neutrinos which are SM singlets and have masses much larger than the EW symmetry breaking scale, close to the GUT scale. These particles are coupled to the left-handed charged lepton and Higgs doublets and have a Majorana mass term which violate total lepton number by two units. At low energy the heavy fields are integrated out leaving an effective SM invariant dimension-5 operator, suppressed by the RH neutrino mass scale, which generate a Majorana mass term for the light left-handed flavour neutrinos after EW symmetry breaking.

Thermal leptogenesis, in its standard formulation, is based on the see-saw extension of the SM. It provides a dynamical mechanism which produces a primordial lepton charge asymmetry $L$. The latter is partially converted into a baryon number asymmetry when the $B + L$ violating sphaleron

---

[2]For a recent review on the subject of thermal leptogenesis see [14].

3

interactions of the SM enter in thermal equilibrium. All the Sakharov criteria are naturally satisfied in this scenario: $i$) lepton number is violated by RH neutrinos, because of their Majorana nature; $ii$) C is violated by the chiral nature of the see-saw interactions and a source of CP violation is given by the (complex) neutrino Yukawa couplings; $iii$) the heavy Majorana fields are produced in the thermal bath at a temperature close to their mass scale, via the neutrino Yukawa interactions: the most efficient processes are inverse decays and two-by-two scatterings involving the top quark or EW gauge bosons. When the temperature drops below their mass, they start to decay and departure from thermal equilibrium is reached, provided their decay rate in the thermal bath is not too big when compared with the expansion rate of the Universe. The out-of-equilibrium decays of the RH neutrinos generate an asymmetry in the lepton flavour charge which can survive at lower temperature. The evolution of the RH neutrino number density and the lepton asymmetry can be computed solving the corresponding system of Boltzmann equations, which take into account the production and wash-out of the lepton charge asymmetry via all the lepton number violating processes present at the time of leptogenesis.

The main topic of this thesis is the role played by CP violation in the thermal leptogenesis scenario. CP violation in the lepton sector can be revealed, in principle, in future neutrino experiments. Observable CP violating effects in such experiments can put constraints on the Dirac and the Majorana phases which enter in the neutrino mixing matrix. These "low energy" CP violating phases may play an important role in the generation of the baryon asymmetry of the Universe via the leptogenesis mechanism. Their contribution to the CP asymmetry generated in the decays of the Majorana neutrinos is studied in a model independent way, emphasizing the region of the parameter space in which they can give a dominant/unsuppressed input.

The thesis is organized as follows. In Chapter 1 the type I see-saw mechanism of neutrino mass generation is introduced and the connection of this with leptogenesis is explained thoroughly. The CP asymmetry in the RH neutrino decays is derived and the different sources of CP violation are pointed out. The computation of the baryon asymmetry in a generic see-saw framework is hence performed in Chapters 2 and 3. It is shown, in particular, on the basis of a complete numerical analysis, that in large regions of the parameter space, the production of the baryon asymmetry depends crucially on low energy observables, namely the lightest neutrino mass and the CP violating phases in the neutrino mixing matrix. The last two chapter of the thesis consider supersymmetric see-saw scenarios which are based on the discrete $A_4$ flavour symmetry. The interesting feature of this kind of models is that they predict a mixing pattern of neutrinos which is naturally compatible with the tri-bimaximal scheme. Moreover the CP violating phases which enter in the expression of the CP asymmetry and drive successful leptogenesis are given exclusively by the Majorana phases of the neutrino mixing matrix. The leptogenesis scale in such supersymmetric models is correlated to lepton flavour violating processes which can be probed in flavour physics experiments. Charged lepton flavour violating rates are computed in the minimal supergravity scenario. A summary of the main results obtained in this work is reported in the concluding chapter.

This Ph.D. thesis is based on the following papers:

**1.** E. Molinaro, S. T. Petcov, T. Shindou and Y. Takanishi, *Effects of lightest neutrino mass in leptogenesis*, Nucl. Phys. B **797** (2008) 93.

**2.** E. Molinaro and S. T. Petcov, *The interplay between the 'low' and 'high' energy CP violation in leptogenesis*, Eur. Phys. J. C **61** (2009) 93.

**3.** E. Molinaro and S. T. Petcov, *A case of subdominant/suppressed 'high energy' contribution to the baryon asymmetry of the Universe in flavoured leptogenesis*, Phys. Lett. B **671** (2009) 60.

**4.** C. Hagedorn, E. Molinaro and S. T. Petcov, *Majorana phases and leptogenesis in see-saw models with $A_4$ symmetry*, JHEP **0909** (2009) 115.

**5.** C. Hagedorn, E. Molinaro and S. T. Petcov, *Charged lepton flavour violating radiative decays $\ell_i \to \ell_j + \gamma$ in see-saw models with $A_4$ symmetry*, JHEP **1002** (2010) 047.

# Chapter 1

# See-Saw Mechanism and Thermal Leptogenesis

## 1.1 Type I See-Saw Extension of the Standard Model

In the simplest thermal leptogenesis scenario, the SM is extended by the addition of two or three RH Majorana neutrinos, which are SM singlets and have a mass much larger than the electroweak EW symmetry breaking scale. This is the well known type I see-saw scenario [17]. These heavy fields are integrated out at low energies and generate an effective Majorana mass term for light active neutrinos:

$$\mathcal{L}_{m_\nu}(x) \;=\; \frac{1}{2}\overline{\nu}^c_{\alpha R}(x)\,(m_\nu)_{\alpha\beta}\,\nu_{\beta L}(x) \;+\; \text{h.c.}\,, \tag{1.1}$$

where $\nu_{\alpha L}$ and $\nu^c_{\alpha R} \equiv C\overline{\nu}^T_{\alpha L}$, for $\alpha = e,\mu,\tau$, are the left-handed light neutrino field and the corresponding (right-handed) charge conjugated field [1], respectively.

In the case of three RH neutrino fields $N_i(x)$ [2], $i = 1,2,3$, with masses $M_3 > M_2 > M_1$, the interaction and $L$ violating Lagrangian in the lepton sector, $\mathcal{L}^{\text{lep}}$, is given by:

$$\mathcal{L}^{\text{lep}}(x) \;=\; \mathcal{L}_{CC}(x) \;+\; \mathcal{L}_Y(x) \;+\; \mathcal{L}^N_M(x)\,, \tag{1.2}$$

where $\mathcal{L}_{CC}$ and $\mathcal{L}_Y$ denote the charged current and the Yukawa Lagrangians, respectively, while $\mathcal{L}^N_M$ involve the lepton number violating Majorana mass term of the RH neutrino fields. In the basis in which the RH neutrino mass matrix and the charged lepton Yukawa matrix are diagonal with real eigenvalues, (see-saw flavour basis), the terms in the interaction Lagrangian $\mathcal{L}^{\text{lep}}$ are:

$$\mathcal{L}_{CC}(x) \;=\; -\frac{g}{\sqrt{2}}\,\overline{e}_{\alpha L}(x)\gamma_\mu\nu_{\alpha L}(x)W^{\mu\dagger}(x) \;+\; \text{h.c.}\,, \tag{1.3}$$

$$\mathcal{L}_Y(x) \;=\; \lambda_{k\alpha}\overline{N}_k(x)H^T(x)\,i\sigma_2\,\ell_\alpha(x) \;-\; h_\alpha\overline{e}_{\alpha R}(x)H^{cT}(x)\,i\sigma_2\,\ell_\alpha(x) \;+\; \text{h.c.}\,, \tag{1.4}$$

$$\mathcal{L}^N_M(x) \;=\; -\frac{1}{2}M_k\overline{N}_k(x)N_k(x)\,. \tag{1.5}$$

---

[1]$C$ is the usual charge conjugation matrix of Dirac spinors: $C\gamma^T_\alpha C^{-1} = -\gamma_\alpha$, $C^\dagger C = 1$ and $C^T = -C$.

[2]Throughout this chapter the greek subscript in the definition of the fields and matrix elements is always intended as a flavour index (e.g. $\alpha = e,\mu$ and $\tau$). The latin indices, instead, are used to label the RH neutrino fields, unless differently specified.

The left-handed $SU(2)$ lepton doublets and the right-handed charged lepton singlets are indicated as $\ell_\alpha^T \equiv (\nu_{\alpha L}, e_{\alpha L})$ and $e_{\alpha R}$, while $W^\mu$ and $H \equiv (h^+, h^0)$ represent the charged $SU(2)$ gauge boson and Higgs doublets, respectively. The field $H^c(x) \equiv i\sigma_2 H(x)^*$ ($\sigma_2$ is the second Pauli matrix) denotes the charge conjugated Higgs doublet with hypercharge $Y = -1$. The RH neutrino fields $N_k(x)$ satisfy the Majorana condition:

$$C(\overline{N}_k)^T(x) = N_k(x). \tag{1.6}$$

Note that the see-saw Lagrangian $\mathcal{L}_Y + \mathcal{L}_M^N$ contains 18 independent parameters: three RH neutrino masses $M_k$ and 15 real parameters in the neutrino Yukawa matrix $\lambda$. [3] In contrast, as discussed below, the low energy effective theory described by $\mathcal{L}_{m_\nu} + \mathcal{L}_{CC}$ contains only 9 independent (measurable) elements: three light neutrino masses, three mixing angles and three CP violating phases.

The effective Majorana mass term $m_\nu$ in (1.1) is a combination of the (high energy) see-saw parameters $\lambda_{k\alpha}$ and $M_k$. Below the EW symmetry breaking scale, the see-saw Lagrangian can be written in the matrix form:

$$\mathcal{L}_{\text{mass}}(x) = -\frac{1}{2} \left( \overline{\nu}_R^c(x)\, N_R(x) \right) \begin{pmatrix} O & m_D \\ m_D^T & M_N \end{pmatrix} \begin{pmatrix} \nu_L(x) \\ N_L^c(x) \end{pmatrix} + \text{h.c.}. \tag{1.7}$$

The $3 \times 3$ matrix $O$ has all null entries and

$$m_D \equiv \lambda\, v, \quad M_N \equiv \text{diag}\, (M_1, M_2, M_3) \tag{1.8}$$

are the $3 \times 3$ Dirac and Majorana mass matrices, where $v \equiv \langle h^0 \rangle \cong 174$ GeV is the SM Higgs vacuum expectation value (VEV). The fields $N_R$ and $N_L^c \equiv C N_R^T$ are the two chiral components of the Majorana neutrino (vector) $N$. In the see-saw mechanism, the Majorana mass term is much larger than the Dirac mass, i.e. $M_N \gg m_D$. This implies that the mixing between left-handed, $\nu_{\alpha L}$, and right-handed, $N_{kR}$, fields is of the order $\theta \sim m_D/m_N \ll 1$, i.e. the heavy neutrino mass eigenstates are decoupled and have a mass matrix equal to $M_N$ at leading order in $\theta$. The effective Majorana mass matrix $m_\nu$, given in Eq. (1.1), is obtained from the diagonalization of the $6 \times 6$ mass matrix in (1.7). At leading order in $\theta$, one has in the flavour basis:

$$(m_\nu)_{\alpha\beta} \cong v^2 \lambda_{\alpha k}^T M_k^{-1} \lambda_{k\beta} = U_{\alpha j}^* m_j U_{j\beta}^\dagger, \tag{1.9}$$

where $m_j > 0$, for $j = 1, 2, 3$ are the light neutrino mass eigenvalues. Assuming a light neutrino mass scale $m_\nu \approx 0.1$ eV, from Eq. (1.9) one obtains that RH Majorana neutrinos $N_k$ should have a mass $M_N \approx 10^{14}$ GeV.

The neutrino mass matrix $m_\nu$ is diagonalized by a unitary transformation $U$, with neutrino mass eigenstates $\nu_j$ given by:

$$\nu_j = \sum_\alpha U_{j\alpha}^\dagger \nu_{\alpha L} \tag{1.10}$$

Light neutrino mass eigenstates resulting from the see-saw are Majorana fermions. They satisfy the Majorana condition [4]: $\nu_j^c \equiv C(\overline{\nu_j})^T = \nu_j$. In the basis in which the charged lepton mass matrix

---

[3]One can always remove three phases of the complex Yukawa matrix $\lambda$ with a redefinition of the lepton doublet fields $\ell_e$, $\ell_\mu$ and $\ell_\tau$.

[4]Majorana fermions can be defined more generally through the condition: $C\overline{\psi}^T = \xi\psi$, with $|\xi| = 1$. However the phase $\xi$ has no physical meaning and therefore it can be neglected (see e.g. [20]).

is diagonal, $U$ coincides with the Pontecorvo-Maki-Nakagawa-Sakata (PMNS) neutrino mixing matrix [21]. The unitary matrix $U$ parametrizes the flavor mixing in the lepton sector, in analogy to the CKM matrix [9, 10], which correctly describe the analogous mixing in the quark sector [22]. However, as discussed in the next section, the lepton mixing is characterized by two large and one small (approximately zero) angles, which give rise to a mixing pattern completely different from the one determined by the CKM matrix.

## 1.2 Neutrino Mixing Parameters and CP violating Phases

Throughout the thesis the PMNS neutrino mixing matrix $U$ is always expressed in the standard parametrization:

$$
U = \begin{pmatrix}
c_{12}c_{13} & s_{12}c_{13} & s_{13}e^{-i\delta} \\
-s_{12}c_{23} - c_{12}s_{23}s_{13}e^{i\delta} & c_{12}c_{23} - s_{12}s_{23}s_{13}e^{i\delta} & s_{23}c_{13} \\
s_{12}s_{23} - c_{12}c_{23}s_{13}e^{i\delta} & -c_{12}s_{23} - s_{12}c_{23}s_{13}e^{i\delta} & c_{23}c_{13}
\end{pmatrix} \operatorname{diag}(1, e^{i\frac{\alpha_{21}}{2}}, e^{i\frac{\alpha_{31}}{2}}), \quad (1.11)
$$

where $c_{ij} \equiv \cos\theta_{ij}$, $s_{ij} \equiv \sin\theta_{ij}$, $\theta_{ij} \in [0, \pi/2]$, $\delta \in [0, 2\pi]$ is the Dirac CP violating phase and $\alpha_{21}$ and $\alpha_{31}$ are the two Majorana CP violating phases [23, 24, 25], $\alpha_{21,31} \in [0, 2\pi]$. As discussed below, the source of low energy CP violation in the lepton sector is directly related to the existence of three observable rephasing invariants, $J_{\text{CP}}$, $S_1$ and $S_2$.

The best fit values of the neutrino mixing angles with the corresponding errors are reported in Tab. 1.1. These are obtained from a global fit [26] of all neutrino oscillation data including solar, atmospheric, reactor (KamLAND and CHOOZ) and accelerator (K2K and MINOS) experiments [16].

The main features of the neutrino mixing pattern, mixing angles and CP violating phases, as well as the experimental probes of the neutrino mass spectrum are briefly discussed below.

### 1.2.1 Neutrino mass spectrum

The solar and atmospheric neutrino oscillations are driven by two different mass scales, $\Delta m_\odot^2$ and $\Delta m_{\text{A}}^2$, respectively. The solar neutrino mass difference is standardly defined as:

$$
\Delta m_\odot^2 = \Delta m_{21}^2 \equiv m_2^2 - m_1^2 > 0. \quad (1.12)
$$

In this case

$$
|\Delta m_{\text{A}}^2| = |\Delta m_{31}^2| \equiv |m_3^2 - m_1^2| \quad (1.13)
$$

and $\Delta m_{\text{A}}^2 > 0$ ($\Delta m_{\text{A}}^2 < 0$) for a light neutrino mass spectrum with normal (inverted) ordering: $m_1 < m_2 < m_3$ ($m_3 < m_2 < m_1$).

Oscillation experiments are not able to provide information on the absolute neutrino mass scale, but only on two mass squared differences. Direct measurements of the absolute mass scale are performed in different types of experiments. Some of them put limits on the upper end of the spectral

| Parameter | Best Fit | $2\sigma$ | $3\sigma$ |
|:---:|:---:|:---:|:---:|
| $\Delta m_{21}^2 \, (10^{-5} \, \mathrm{eV}^2)$ | $7.59^{+0.23}_{-0.18}$ | $[7.22, 8.03]$ | $[7.03, 8.27]$ |
| $\lvert\Delta m_{31}^2\rvert \, (10^{-3} \, \mathrm{eV}^2)$ | $2.40^{+0.12}_{-0.11}$ | $[2.18, 2.64]$ | $[2.07, 2.75]$ |
| $\sin^2\theta_{12}$ | $0.318^{+0.019}_{-0.016}$ | $[0.29, 0.36]$ | $[0.27, 0.38]$ |
| $\sin^2\theta_{23}$ | $0.50^{+0.07}_{-0.06}$ | $[0.39, 0.63]$ | $[0.36, 0.67]$ |
| $\sin^2\theta_{13}$ | $0.013^{+0.013}_{-0.009}$ | $\le 0.039$ | $\le 0.053$ |

**Table 1.1:** Best fit values with $1\sigma$ errors and $2\sigma$ and $3\sigma$ intervals for the three flavour neutrino oscillation parameters. The global fit is performed on data including solar, atmospheric, reactor (KamLAND and CHOOZ) and accelerator (K2K and MINOS) experiments (see [26] and references therein).

distribution of electrons in tritium $\beta-$decay, ${}^3\mathrm{H}\rightarrow{}^3\mathrm{He}+\overline{\nu}_e + e^-$. They provide a determination of the electron neutrino mass

$$m_{\nu_e} = \sqrt{\sum_{j=1}^{3} |U_{ej}|^2 \, m_j^2}. \tag{1.14}$$

The Mainz experiment obtained the bound $m_{\nu_e} < 2.2$ eV [27] and the Troitsk experiment $m_{\nu_e} < 2.5$ eV [28], both at 95% CL. The KATRIN experiment [29], which is under construction at the moment, aims to search for the mass of the electron neutrino with a sensitivity of 0.2 eV.

Indirect determination of the absolute neutrino mass can be derived from CMB data as well as data from large scale structures, which are sensitive to the sum of the neutrino masses. They allow to set the conservative upper limit [30, 31]: $\sum_j m_j < 0.5$ eV at 95% CL.

### 1.2.2 Tri-bimaximal mixing pattern

The data reported in Tab. 1.1 suggest a pattern of the PMNS matrix which is remarkably similar to the so called "tri-bimaximal" (TB) mixing [32]. In the case of TB mixing, the solar and atmospheric neutrino mixing angles $\theta_{12}$ and $\theta_{23}$ are very close to, or coincide with, the best fit values determined in global analyses of neutrino oscillation data:

$$\sin^2\theta_{12} = 1/3, \quad \sin^2\theta_{23} = 1/2. \tag{1.15}$$

The reactor mixing angle $\theta_{13}$ is predicted to be exactly zero. Correspondingly, the PMNS matrix (1.11) takes the form:

$$U = U_{TB} \, \mathrm{diag}\left(1, e^{i\alpha_{21}/2}, e^{i\alpha_{31}/2}\right), \tag{1.16}$$

where

$$U_{TB} = \begin{pmatrix} \sqrt{2/3} & 1/\sqrt{3} & 0 \\ -1/\sqrt{6} & 1/\sqrt{3} & 1/\sqrt{2} \\ -1/\sqrt{6} & 1/\sqrt{3} & -1/\sqrt{2} \end{pmatrix} . \tag{1.17}$$

The TB scheme suggests the interesting possibility that the neutrino mixing originates from some flavour symmetry in the lepton sector. An example of such symmetry is provided by the tetrahedral group $A_4$. Supersymmetric (SUSY) models based on the discrete flavour group $A_4$ will be introduced in Chapters 4 and 5, where several results concerning leptogenesis and lepton flavour violating processes within these models will be derived.

### 1.2.3  CP violation in neutrino oscillations

CP violation in the lepton sector, due to the Dirac phase $\delta$, can be probed in neutrino oscillations experiments and is directly related to the rephasing invariant [33]:

$$J_{\mathrm{CP}} = \mathrm{Im}\left\{ U_{e1} U_{\mu2} U_{e2}^* U_{\mu1}^* \right\} = \frac{1}{4} \sin 2\theta_{12} \sin 2\theta_{23} \cos^2 \theta_{13} \sin \theta_{13} \sin \delta , \tag{1.18}$$

which is analogous to the rephasing invariant associated with the Dirac CP violating phase in the CKM quark mixing matrix [34, 35].

If $J_{\mathrm{CP}} \neq 0$, *i.e.* if $\sin\theta_{13}\sin\delta \neq 0$, there is no CP violation coming from the Dirac phase $\delta$ in the PMNS matrix. An experimental signature of CP violation associated to the Dirac phase $\delta$ can in principle be obtained searching for CP asymmetries in neutrino flavour oscillations: [33, 36, 37]:

$$A_{\mathrm{CP}}^{\alpha\beta} = P(\nu_{\alpha L} \to \nu_{\beta L}) - P(\overline{\nu}_{\alpha L} \to \overline{\nu}_{\beta L}) , \tag{1.19}$$

where $P(\nu_{\alpha L} \to \nu_{\beta L})$ is vacuum oscillation probability [20] for three massive neutrinos:

$$P(\nu_{\alpha L} \to \nu_{\beta L}) = \delta_{\alpha\beta} - 4 \sum_{j>k} \mathrm{Re}\left( U_{\alpha j}^* U_{\beta j} U_{\alpha k} U_{\beta k}^* \right) \sin^2 \left( \frac{\Delta m_{jk}^2}{4E} L \right)$$
$$+ 2 \sum_{j>k} \mathrm{Im}\left( U_{\alpha j}^* U_{\beta j} U_{\alpha k} U_{\beta k}^* \right) \sin \left( \frac{\Delta m_{jk}^2}{4E} L \right) . \tag{1.20}$$

In the previous equation $E$ is the mean energy of neutrinos in the beam and $L$ denotes the distance between the detector and the source. Using (1.18) and (1.20), one can get the following expressions for the CP asymmetries [33]:

$$A_{\mathrm{CP}}^{e,\mu} = A_{\mathrm{CP}}^{\mu,\tau} = -A_{\mathrm{CP}}^{e,\tau} = J_{\mathrm{CP}} \, F_{\mathrm{vacuum}} , \tag{1.21}$$

$$F_{\mathrm{vacuum}} = \sin\left( \frac{\Delta m_{21}^2}{2E} L \right) + \sin\left( \frac{\Delta m_{31}^2}{2E} L \right) + \sin\left( \frac{\Delta m_{32}^2}{2E} L \right) . \tag{1.22}$$

Because of CPT invariance, effects of CP violation can also be inferred from T asymmetries [33], $A_{\mathrm{T}}^{\alpha,\beta}$, in neutrino oscillation, with

$$A_{\mathrm{T}}^{\alpha\beta} = P(\nu_{\alpha L} \to \nu_{\beta L}) - P(\nu_{\beta L} \to \nu_{\alpha L}) , \tag{1.23}$$

$$A_{\mathrm{T}}^{\alpha\beta} = A_{\mathrm{CP}}^{\alpha\beta} . \tag{1.24}$$

Future experiments [38, 39] on neutrino oscillations aim to constraints the reactor angle $\theta_{13}$ and measure CP violating effects associated to the Dirac phase $\delta$. Hints of a non-zero value of $\theta_{13}$ at $1.6\sigma$ where found in a recent analysis on global neutrino oscillation data [40].

### 1.2.4 Majorana phases and neutrinoless double beta decay

The Majorana phases $\alpha_{21}$ and $\alpha_{31}$, entering in the PMNS matrix (1.11), can have physical effects only if the neutrino mass eigenstates $\nu_j$ in (1.10) are Majorana particles. As explained in Section 1.1, the see-saw mechanism provides naturally an effective Majorana mass term for the three flavour neutrinos, Eq. (1.9) and thus, in this framework, massive active neutrinos behave as Majorana particles. In analogy to the Dirac phase, $\alpha_{21}$ and $\alpha_{31}$ can be related to a particular combination of the neutrino mixing matrix elements, invariant under a basis transformation of the lepton fields. Such rephasing invariants are not unique [41, 42]. A possible choice is

$$
\begin{aligned}
S_1 &= \mathrm{Im}\left\{U_{\tau 1}^* U_{\tau 2}\right\}, & (1.25) \\
S_2 &= \mathrm{Im}\left\{U_{\tau 2}^* U_{\tau 3}\right\}. & (1.26)
\end{aligned}
$$

The two Majorana phases $\alpha_{21}$ and $\alpha_{31}$ can be expressed in terms $S_1$ and $S_2$ in the following way:

$$
\cos\alpha_{31} = 1 - 2\frac{S_1^2}{|U_{e1}|^2 |U_{e3}|^2}, \tag{1.27}
$$

$$
\cos(\alpha_{31} - \alpha_{21}) = 1 - 2\frac{S_2^2}{|U_{e2}|^2 |U_{e3}|^2}. \tag{1.28}
$$

As will be discussed in more detail in Section 1.3.2, all the CP violating effects associated with the Majorana nature of the massive neutrinos are generated by $\alpha_{21} \neq k\pi$ and/or $\alpha_{31} \neq k'\pi$ ($k, k' = 0, \pm 1, \pm 2, \ldots$).

The Majorana nature of massive neutrinos [5] can be inferred from the existence of processes which violate the lepton number by two units, $\Delta L = 2$. The only viable experiments that currently may prove if neutrinos are Majorana particles and possibly put constraints on the Majorana phases of the PMNS matrix are the ones searching for neutrinoless double beta $((\beta\beta)_{0\nu}$-) decay [44] of even-even nuclei:

$$
(A, Z) \rightarrow (A, Z + 2) + e^- + e^-. \tag{1.29}
$$

The corresponding decay rate is proportional to the effective Majorana mass $m_{ee}$, which contains all the dependence on the neutrino mixing parameters:

$$
m_{ee} = \sum_{j=1}^{3} U_{ej}^2 m_j. \tag{1.30}
$$

One can distinguish two possible scenarios, compatible with neutrino mixing data (see Tab. 1.1): $i$) normal ordered mass spectrum, $m_1 < m_2 < m_3$; $ii$) inverted ordered mass spectrum, $m_3 < m_1 <$

---

[5]As is well known, oscillations of neutrinos are insensitive [23, 43] to the phases $\alpha_{21}$ and $\alpha_{31}$ in the PMNS matrix.

$m_2$. The corresponding expression of the Majorana mass term $m_{ee}$ is the following:

**Normal Ordering:**

$$m_{ee} \;\cong\; \left| m_1 \cos^2 \theta_{12} + \sqrt{m_1^2 + \Delta m_\odot^2} \sin^2 \theta_{12} e^{i\alpha_{21}} + \sqrt{m_1^2 + \Delta m_A^2} \sin^2 \theta_{13} e^{i(\alpha_{31}-2\delta)} \right| \quad (1.31)$$

**Inverted Ordering:**

$$m_{ee} \;\cong\; \sqrt{m_3^2 + |\Delta m_A^2|} \left| \cos^2 \theta_{12} + e^{i\alpha_{21}} \sin^2 \theta_{12} \right|. \quad (1.32)$$

The latest results of the CUORICINO experiment [45] set an upper limit on the effective Majorana mass: $m_{ee} < 0.20 - 0.68$ eV, at 90% CL. Next generation experiments [46, 47, 48] searching for $(\beta\beta)_{0\nu}$-decay, currently under preparation, will probe the quasi-degenerate and inverted hierarchical ranges of $m_{ee}$. They aim to reach the sensitivity of $m_{ee} \approx 50$ meV.

The measurement of the $(\beta\beta)_{0\nu}$-decay rate in oncoming experiments might allow to obtain constraints on the Majorana phase $\alpha_{21}$ in the PMNS matrix (see *e.g.* [49, 50] and also [51]).

## 1.3   Casas-Ibarra Parametrization and CP Invariance Constraints

### 1.3.1   Bottom-up parametrization of the see-saw

The amount of CP violation necessary to generate the baryon asymmetry of the Universe, can be related to both "low" and "high" energy contributions, the first being correlated to a particular combination of the Dirac and Majorana CP violating phases in the neutrino mixing matrix, studied in the previous section. In order to distinguish and analyze quantitatively the different sources of CP violation in the lepton sector, it is useful to work in the Casas-Ibarra [52] parametrization of the neutrino Yukawa coupling matrix $\lambda$, which appears in $\mathcal{L}_Y$ (see Eq. (1.4)):

$$\lambda \;=\; \frac{1}{v} \sqrt{M_N} \, R \, \sqrt{m} \, U^\dagger \,, \quad (1.33)$$

where $M_N = \text{diag}(M_1, M_2, M_3)$ and $m = \text{diag}(m_1, m_2, m_3)$. The unitary matrix $U$ is the PMNS neutrino mixing matrix introduced in Section 1.2. From the expression (1.4) and the type I see-saw mass relation given in (1.9), it comes out that $R$ is a $3 \times 3$ (complex) orthogonal matrix: $RR^T = R^T R = \mathbf{1}$. It contains three mixing angles and three phases, which together with $M_N$, $U$ and $m$ provide the 18 independent parameters of the see-saw Lagrangian, $\mathcal{L}_Y + \mathcal{L}_M^N$.

The parametrization (1.33) is derived in the *see-saw flavour basis*, which corresponds to diagonal mass matrices for the charged leptons and RH neutrinos, both with real eigenvalues. In a *generic see-saw basis*, given by the neutrino Yukawa matrix $\widehat{\lambda}$, the charged lepton Yukawa matrix $\widehat{\lambda}_\ell$ and the RH neutrino mass matrix $\widehat{M}_N$, Eq. (1.33) can be written in the form [52, 53]:

$$v \left(\sqrt{M_N}\right)^{-1} V_R^\dagger \widehat{\lambda} \;=\; R \, \sqrt{m} \, V_\nu^\dagger. \quad (1.34)$$

The unitary matrices $V_R$, $V_{e_L}$ and $V_\nu$ define the basis transformation:

$$V_R^T \, \widehat{M}_N \, V_R \;=\; \mathrm{diag}\,(M_1, M_2, M_3)\,, \tag{1.35}$$

$$V_{e_L}^\dagger \, \widehat{\lambda}_\ell^\dagger \, \widehat{\lambda}_\ell \, V_{e_L} \;=\; \mathrm{diag}\,\big(h_e^2, h_\mu^2, h_\tau^2\big)\,, \tag{1.36}$$

$$V_\nu \;=\; V_{e_L} U\,, \tag{1.37}$$

where $V_\nu$ diagonalizes the neutrino mass matrix $m_\nu \cong v^2 \widehat{\lambda}^T \widehat{M}_N^{-1} \widehat{\lambda}$ in $\mathcal{L}_{m_\nu}$, Eq. (1.1):

$$V_\nu^T m_\nu V_\nu \;=\; \mathrm{diag}\,(m_1, m_2, m_3)\,. \tag{1.38}$$

Equation (1.34) can be derived directly from (1.33), using the basis transformation defined above. Thus, given any see-saw model $\{\widehat{\lambda}, \widehat{\lambda}_\ell, \widehat{M}_N\}$, in some particular basis, the orthogonal matrix $R$ can be computed directly form Eq. (1.34) and is an invariant see-saw quantity [53], *i.e.* it doesn't change under basis transformations. [6] Actually, $R$ parametrizes basis invariant classes of see-saw models, $\mathcal{C}(R)$, in the sense that, each see-saw model defined by the set $\{\widehat{\lambda}, \widehat{\lambda}_\ell, \widehat{M}_N\} \in \mathcal{C}(R)$, which is consistent with a set of low energy parameters $\{m_e, m_\mu, m_\tau, m_i, U\}$, is related to another model of the same class by applying lepton basis changes. Models belonging to distinct classes are associated to different $R$ matrices and cannot be related to one another.

## 1.3.2 CP transformation properties

If CP is a symmetry of the lepton Lagrangian (1.2), then the neutrino Yukawa couplings $\lambda_{k\alpha}$ should satisfy specific constraints [20]. Using the parametrization given in (1.33), such constraints translate into conditions on matrix $R$ elements. Indeed, if CP is preserved, the Majorana fields $N_k$ and $\nu_j$ have definite CP parities [20] $\eta_k^{\mathrm{NCP}}$ and $\eta_j^{\nu\mathrm{CP}}$, respectively, and transform as:

$$U_{\mathrm{CP}} N_k(x) U_{\mathrm{CP}}^\dagger \;=\; \eta_k^{\mathrm{NCP}} \gamma^0 N_k(x')\,, \quad \text{with} \quad \eta_k^{\mathrm{NCP}} = \pm i\,, \tag{1.39}$$

$$U_{\mathrm{CP}} \nu_j(x) U_{\mathrm{CP}}^\dagger \;=\; \eta_j^{\nu\mathrm{CP}} \gamma^0 \nu_j(x')\,, \quad \text{with} \quad \eta_j^{\nu\mathrm{CP}} = \pm i\,. \tag{1.40}$$

The RH neutrino mass term defined in $\mathcal{L}_M^N$ is invariant under the above transformation. The Yukawa part of the lepton Lagrangian $\mathcal{L}_Y$ is also CP invariant if and only if the following transformation of the neutrino Yukawa matrix elements occurs:

$$\lambda_{j\alpha}^* \;=\; \lambda_{j\alpha} (\eta_j^{\mathrm{NCP}})^* \eta^\alpha \eta^{H*}\,, \tag{1.41}$$

where $\eta^\alpha$ and $\eta^H$ are the (unphysical) phase factors which enter in the CP transformation of the left-hand lepton and Higgs doublets, respectively. One can fix, without loss of generality: $\eta^\alpha = i$ and $\eta^H = 1$. [7] Using the above assumptions, the CP invariance constraints satisfied by the neutrino Yukawa matrix, $\lambda$, become [54]:

$$\lambda_{j\alpha}^* \;=\; \lambda_{j\alpha} \, \rho_j^N\,, \quad \rho_j^N = \pm 1\,. \tag{1.42}$$

---

[6]More generally, $R$ is invariant under a non-unitary RH neutrino trasformation, namely $N_k \to S_{kj} N_j$, where $S$ is a non-singular matrix [53].

[7]Such values of the parameters $\eta^\alpha$ and $\eta^H$ can always be obtained due to a convenient redefinition of the phases of the lepton and Higgs doublets in the lepton Lagrangian (1.2).

Thus, under CP the neutrino Yukawa matrix elements would be real or purely imaginary, depending on the CP parities of the RH neutrino fields. Note that CP invariance in the high energy see-saw model would imply that CP is conserved in the lepton sector even after EW symmetry breaking. In such a case, the phases which enter in the neutrino mixing matrix take the values (see Section 1.2):

$$\delta = \pi q \,, \qquad q = 0, \pm 1, \pm 2, \dots \,, \tag{1.43}$$

$$\alpha_{21} = \pi q' \,, \qquad q' = 0, \pm 1, \pm 2, \dots \,, \tag{1.44}$$

$$\alpha_{31} = \pi q'' \,, \qquad q'' = 0, \pm 1, \pm 2, \dots \,, \tag{1.45}$$

or equivalently [20]

$$U_{\alpha j}^* = U_{\alpha j} \, \rho_j^\nu \,, \qquad \rho_j^\nu = \pm 1 \,. \tag{1.46}$$

Taking into account Eqs (1.42) and (1.46), one can derive the CP transformation properties of the orthogonal matrix $R$ [54]:

$$R_{jk}^* = R_{jk} \, \rho_j^\nu \, \rho_k^N \,. \tag{1.47}$$

All the constraints derived above can be conveniently expressed in terms of the following quantity [54, 55]:

$$P_{jkm\alpha} \equiv R_{jk} R_{jm} U_{\alpha k}^* U_{\alpha m} \,. \tag{1.48}$$

Indeed, from Eqs (1.42), (1.46) and (1.47) one has:

$$P_{jkm\alpha}^* = (\rho_j^N)^2 (\rho_k^\nu)^2 (\rho_m^\nu)^2 P_{jkm\alpha} = P_{jkm\alpha} \,. \tag{1.49}$$

The previous equation implies that CP is violated in the lepton sector, provided $P_{jkm\alpha}$ is complex:

$$\text{CP violation} \quad \Longleftrightarrow \quad \text{Im}(P_{jkm\alpha}) \neq 0 \,. \tag{1.50}$$

Notice that $P_{jkm\alpha}$ is a see-saw invariant quantity, because it is defined in terms of the matrix $R$ and the neutrino mixing matrix $U$, which are basis independent.

In the next section CP violation in the lepton sector, enclosed in the CP violating phases of the matrices $R$ and $U$, will be discussed in connection with thermal leptogenesis. In particular, it will be shown that the condition (1.50) "triggers" CP violation in the thermal leptogenesis scenario, when the dynamics of the flavour states plays a role in the generation of the baryon asymmetry of the Universe.

## 1.4  CP Violation in Thermal Leptogenesis

The different sources of CP violation that enter in the lepton sector play a crucial role in the generation of the baryon asymmetry of the Universe via the leptogenesis mechanism. In the following the expression of the CP asymmetry in the decays of the heavy Majorana neutrinos is derived and the connection to the CP violating phases in the PMNS is discussed in detail.

### 1.4.1 Implications of CPT and unitarity

A non zero CP asymmetry can be generated in the out-of-equilibrium decays of the heavy RH Majorana neutrinos, only if the neutrino Yukawa couplings $\lambda_{k\alpha}$ are complex and are not constrained by relation (1.41) or, equivalently, if the condition (1.50) is verified. The lepton CP asymmetry in the decays of the RH field $N_k$, $\epsilon_{k\alpha}$, which determines the evolution of the lepton charge $L_\alpha$ ($\alpha = e, \mu, \tau$), is defined as:

$$\epsilon_{k\alpha} = \frac{\Gamma(N_k \to \ell_\alpha H) - \Gamma(N_k \to \overline{\ell}_\alpha \overline{H})}{\Gamma_{Dk}}, \tag{1.51}$$

where $\Gamma_{Dk}$ is the total decay rate of $N_k$:

$$\begin{aligned} \Gamma_{Dk} &= \sum_\alpha \left[ \Gamma(N_k \to \ell_\alpha H) + \Gamma(N_k \to \overline{\ell}_\alpha \overline{H}) \right] \\ &= \frac{[\lambda\lambda^\dagger]_{kk} M_k}{8\pi}. \end{aligned} \tag{1.52}$$

The evaluation of the CP asymmetry in RH neutrino decays, given in (1.51), can be handled taking into account the constraints on the transition matrix elements derived from CPT invariance and unitarity of the $\mathbf{S}$ matrix [56]. Indeed, considering $\mathbf{S} = \mathbf{1} + i\mathbf{T}$, the unitarity condition, $\mathbf{S}\mathbf{S}^\dagger = \mathbf{S}^\dagger\mathbf{S} = \mathbf{1}$, implies:

$$i\mathbf{T}_{ab} - i\mathbf{T}^*_{ba} = [\mathbf{T}\mathbf{T}^\dagger]_{ab} = [\mathbf{T}^\dagger\mathbf{T}]_{ab}. \tag{1.53}$$

The matrix element $\mathbf{T}_{ba}$ is related to the decay amplitude $\mathcal{M}(a \to b)$, from an initial state of particles $a \equiv \{a_1(p_1), \ldots, a_n(p_n)\}$ to the final set $b \equiv \{b_1(k_1), \ldots, b_m(k_m)\}$:

$$\mathbf{T}_{ba} = \mathcal{M}(a \to b)\,(2\pi)^4\,\delta^{(4)}\left(\sum_{i=1}^n p_i - \sum_{j=1}^m k_j\right), \tag{1.54}$$

where $p_i$ $(i = 1, \ldots, n)$ and $k_j$ $(j = 1, \ldots, m)$ are the momenta of the incoming and outgoing particles, respectively. Notice that if CP is preserved, $\mathbf{T}$ is a hermitian matrix and $\mathcal{M}(a \to b) = \mathcal{M}(b \to a)^*$. The absolute value of (1.53) provides a relation between the transition rates of the processes $a \leftrightarrow b$:

$$|\mathbf{T}_{ab}|^2 - |\mathbf{T}_{ba}|^2 = -2\mathrm{Im}\left\{[\mathbf{T}\mathbf{T}^\dagger]^*_{ab}\mathbf{T}^*_{ba}\right\} + \left|[\mathbf{T}\mathbf{T}^\dagger]_{ab}\right|^2. \tag{1.55}$$

Assuming that the transition rate for the process $a \to b$ can be perturbatively expanded in powers of a small coupling constant $\alpha$, i.e. $|\mathcal{M}^{(k)}(a \to b)|^2 = \mathcal{O}(\alpha^k)$, it follows from (1.55) that the CP asymmetry $|\mathcal{M}^{(k)}(a \to b)|^2 - |\mathcal{M}^{(k)}(b \to a)|^2$ must be at least of order $\alpha^{k+1}$. Therefore, CP violating effects may arise only from loop corrections to the amplitude of the process $a \to b$. These corrections should arise from CP violating vertices and the particles running in the loops should correspond to physical eigenstates. Notice that, even if the particles running in the loops have CP violating coupling constants, they can produce a CP asymmetry of the form (1.55) only if their masses are small enough to let them propagate on their mass-shells.
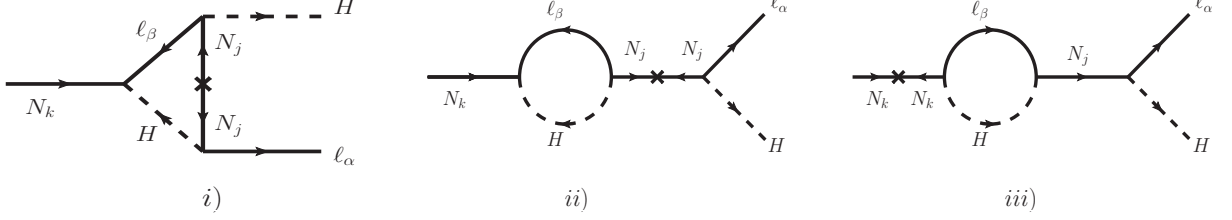
**Figure 1.1:** Diagrams contributing to the CP asymmetry $\epsilon_{k\alpha}$. The lepton field $\ell_\beta$ and the Higgs field $H$ in the loop are taken on-shell (see the text for details). The sum over the lepton doublets $\ell_\beta$ ($\beta = e, \mu, \tau$) and RH Majorana fields $N_j$ ($j \neq k$) is implicit. Diagrams $i$) and $ii$) are lepton flavour and lepton number violating, while the amplitude given in $iii$) is flavour changing but conserves total lepton number, *i.e.* it does not contribute to the total CP asymmetry $\epsilon_k$.

The previous considerations can be applied directly to the neutrino Yukawa interactions in the see-saw Lagrangian. From CPT invariance, the rate of inverse decays, $\ell_\alpha + H \to N_k$, is:

$$|\mathcal{M}\left(\ell_\alpha\, H \to N_k\right)|^2 \;=\; \left|\mathcal{M}\left(N_k \to \overline{\ell}_\alpha\, \overline{H}\right)\right|^2 . \tag{1.56}$$

At tree-level, CP and T are conserved. Therefore, the RH neutrino decay amplitude satisfies:

$$\mathcal{M}^{(0)}\left(N_k \to \ell_\alpha\, H\right) \;=\; \mathcal{M}^{(0)}\left(\ell_\alpha\, H \to N_k\right)^* , \tag{1.57}$$

where the superscript "(0)" indicates that the amplitude is evaluated at tree-level. From expressions (1.54)$-$(1.56), the CP asymmetry in the decays, $\epsilon_{k\alpha}$, defined in (1.51), can be computed as the convolution of tree-level amplitudes [8] $\mathcal{M}^{(0)}(N_k \to \ell_\alpha\, H)$, $\mathcal{M}^{(0)}(N_k \to \ell_\beta\, H\,(\overline{\ell}_\beta\, \overline{H}))$ and $\mathcal{M}^{(0)}(\ell_\beta\, H\,(\overline{\ell}_\beta\, \overline{H}) \to \ell_\alpha\, H)$, for $\beta = e, \mu, \tau$ (see Fig. 1.1). An explicit calculation gives:

$$\epsilon_{k\alpha} \;=\; \frac{\mathrm{Im}\left\{\int d\tilde{\Pi}_{\ell_\alpha, H}\, \mathcal{M}^{(0)}(N_k \to \ell_\alpha\, H)^* \sum\limits_{\{n\}} \int d\tilde{\Pi}_{\{n\}}\, \mathcal{M}^{(0)}(N_k \to \{n\})\, \mathcal{M}^{(0)}(\{n\} \to \ell_\alpha\, H)\right\}}{\int d\tilde{\Pi}_{\ell_\alpha, H}\, \left|\mathcal{M}^{(0)}(N_k \to \ell_\alpha\, H)\right|^2} , \tag{1.58}$$

where $\sum_{\{n\}}$ indicates the sum over all possible on-shell states in the loops of Fig. 1.1, while the phase space factor in the integral is, in general

$$d\tilde{\Pi}_{n_1, \ldots, n_k} \;\equiv\; \frac{d^3 p_{n_1}}{(2\pi)^3 2E_{n_1}} \cdot \ldots \cdot \frac{d^3 p_{n_k}}{(2\pi)^3 2E_{n_k}} \,(2\pi)^4\, \delta^{(4)}\left(p_{N_k} - \sum_{j=1}^{k} p_{n_j}\right) , \qquad k \geq 2\,, \tag{1.59}$$

$p_{N_k}$ and $p_{n_j}$ ($j = 1, \ldots, k$) being the 4-momentum of the decaying RH neutrino $N_k$ and the final state $n_j$, respectively.

---

[8] At leading order in the small coupling constant the last term on the r.h.s. of (1.55) gives a negligible contribution.

For a non degenerate RH neutrino mass spectrum, $|M_i - M_j| \gg \Gamma_{Di}$, expression (1.58) becomes:

$$
\begin{aligned}
\epsilon_{k\alpha} &= -\frac{1}{(8\pi)} \frac{1}{[\lambda\lambda^\dagger]_{kk}} \sum_j \mathrm{Im}\left\{ \lambda_{k\alpha} [\lambda\lambda^\dagger]_{kj} \lambda_{j\alpha}^* \right\} f(x_j) \\
&\quad -\frac{1}{(8\pi)} \frac{1}{[\lambda\lambda^\dagger]_{kk}} \sum_j \mathrm{Im}\left\{ \lambda_{k\alpha} [\lambda\lambda^\dagger]_{jk} \lambda_{j\alpha}^* \right\} \frac{1}{1-x_j} \,,
\end{aligned}
\tag{1.60}
$$

where $x_j \equiv M_j^2/M_1^2$ and the loop function $f(x_j)$ is [57]:

$$
f(x) = \sqrt{x}\left[ \frac{1}{1-x} + 1 - (1+x)\log\left(1+\frac{1}{x}\right) \right] \longrightarrow -\frac{3}{2\sqrt{x}} + \dots, \text{ for } x_j \gg 1 \,.
\tag{1.61}
$$

Thus, the total CP asymmetry $\epsilon_k$ associated to the decays of the RH neutrino $N_k$ is:

$$
\begin{aligned}
\epsilon_k &\equiv \sum_\alpha \epsilon_{k\alpha} \\
&= \frac{1}{(8\pi)} \frac{1}{[\lambda\lambda^\dagger]_{kk}} \sum_{j\neq k} \mathrm{Im}\left\{ \left[ [\lambda\lambda^\dagger]_{jk} \right]^2 \right\} f(x_j) \,.
\end{aligned}
\tag{1.62}
$$

A similar computation can be done in supersymmetric [9] (SUSY) see-saw models. In this case, the RH neutrino $N_k$ and its supersymmetric partner $\widetilde{N}_k$ decay into the channels: $N_k, \widetilde{N}_k \to \ell_\alpha H \, (\widetilde{\ell}_\alpha \widetilde{H})$. The sum of the asymmetries into leptons and sleptons is given by the expression (1.60), with the loop function [57]: [10]

$$
f(x) = -\sqrt{x}\left[ \frac{2}{x-1} + \log\left(1+\frac{1}{x}\right) \right] \longrightarrow -\frac{3}{\sqrt{x}} + \dots, \text{ for } x_j \gg 1 \,.
\tag{1.63}
$$

### 1.4.2 Sources of CP violation

The necessary amount of CP violation which allows to produce the observed value of the baryon asymmetry of the Universe via the thermal leptogenesis mechanism, stems from both the "high" energy CP violating phases in the matrix $R$ ($R$−phases) and by the "low" energy Dirac phase $\delta$ and Majorana phases $\alpha_{21}$ and $\alpha_{31}$, which enter in the PMNS matrix (1.11). The latter can, in principle, be measured in neutrino physics experiments, as discussed in Section 1.2. Conversely, the purely "high" energy CP violating $R$−phases produce physical effects only in processes that arise at some high energy scale, such as in the production and decays of the heavy RH fields. Related to this, there are three possibilities that should be considered [54]:

---

[9]SUSY soft breaking terms do not contribute to the CP asymmetries for a RH neutrino mass much larger than the EW symmetry breaking scale, as in the standard see-saw scenario considered here.

[10]Notice that, in what concerns the CP asymmetry of RH neutrino decays, in the supersymmetric scenario one has to consider the contribution of three additional diagrams, which are equivalent to the diagrams shown in Fig. 1.1, provided one replaces the particles in the loops with the corresponding (on-shell) sparticles. Similar diagrams arise when the final states in the RH neutrino decays are the SUSY partners of the left-handed lepton and Higgs doublets.

*i*) CP is a symmetry of the lepton sector at "high" energies, *i.e.* neutrino Yukawa couplings $\lambda_{k\alpha}$ satisfy the constraints reported in Eq. (1.42). Then, CP is also preserved in the "low" energy limit and the neutrino mixing matrix $U$ is constrained by Eq. (1.46). Moreover, as a consequence of the CP symmetry, the $R$ matrix elements are real or purely imaginary, Eq. (1.47).

*ii*) CP symmetry is violated at "low" energies by the charged current interactions in (1.3), *i.e.* at least one of Eqs (1.43) − (1.45) does not hold. Therefore, CP is also violated at "high" energy scales through the neutrino Yukawa couplings and it is not possible to use the matrix $R$ to cancel all the phases present in $\lambda$. In this case, CP violating effects in "high" energy phenomena are determined, in general, by the *interplay* between the phases $\delta$, $\alpha_{21}$ and $\alpha_{31}$ and the $R$−phases.

*iii*) Charge current interactions are CP conserving and $U$ satisfies constraints in Eq. (1.46), but CP is violated at some "high" energy scale, *i.e.* not all the neutrino Yukawa couplings verify the transformation properties given in Eq. (1.42). CP violation in this case is due to the matrix $R$.

A phenomenological interesting situation within point *ii*) corresponds to the particular case of a CP conserving [11] matrix $R$, Eq. (1.47). In such scenario the effective CP violating phases which enter in "high" energy phenomena, can be directly linked to the Dirac and/or Majorana phases of the PMNS matrix, accessible in neutrino experiments (see Section 1.2). In particular, the source of CP violation necessary for the generation of the observed baryon asymmetry of the Universe in thermal leptogenesis can be identified, exclusively, with the phases $\delta$, $\alpha_{21}$ and $\alpha_{31}$. A thorough analysis on this issue was performed in [54, 59, 60, 61] in the context of *flavoured leptogenesis*, where flavour effects [62, 63, 64, 65, 66, 67, 68] may play an important role in the determination of the observed baryon asymmetry. The topic of flavour effects in thermal leptogenesis will be briefly discussed in Section 1.5.

Before analyzing the role of flavour effects in leptogenesis, it is convenient to express the CP asymmetry $\epsilon_{k\alpha}$, derived Eq. (1.60), in terms of the Casas-Ibarra parametrization of the neutrino mixing matrix $\lambda$, Eq. (1.33). Henceforth, it is assumed a see-saw scenario in which the RH neutrino mass spectrum is strongly hierarchical: $M_{2,3} \gg M_1$. In this case, the lepton number and flavour asymmetries, which are partially converted into a baryon number symmetry by fast sphaleron processes, are generated only in the out-of-equilibrium decays of the lightest one, $N_1$. A possible lepton charge asymmetry produced in the decays of the heavier states, is expected to be washed out by the Yukawa interactions of $N_1$. Thus, the CP asymmetry $\epsilon_{1\alpha}$, relevant for leptogenesis, can

---

[11]It should be noted, however, that constructing a viable see-saw model which leads to real or purely imaginary $R_{ij}$ might encounter serious difficulties (see *e.g.* [58]).

be written as [54]:

$$
\begin{aligned}
\epsilon_{1\alpha} &= -\frac{3M_1}{16\pi v^2} \frac{\text{Im}\left(\sum_{jk} m_j^{1/2} m_k^{3/2} U_{\alpha j}^* U_{\alpha k} R_{1j} R_{1k}\right)}{\sum_i m_i |R_{1i}|^2} \\
&= -\frac{3M_1}{16\pi v^2} \frac{\text{Im}\sum_{jk} m_j^{1/2} m_k^{3/2} P_{1jk\alpha}}{\sum_i m_i |R_{1i}|^2} \, .
\end{aligned}
\tag{1.64}
$$

where $P_{1jk\alpha}$ was defined in (1.48). Notice that, the CP asymmetry (1.64) depends only on basis invariant quantities and, therefore, is unique in all the see-saw models belonging to a particular invariant class $\mathcal{C}(R)$ (see Section 1.3). From the previous formulation of $\epsilon_{k\alpha}$ one can see that the source of CP violation required in order to have successful leptogenesis is provided, in general, by the *interplay* between the three "high" energy phases that enter in the elements of the orthogonal matrix $R$ and the "low" energy CP violating phases $\delta$, $\alpha_{21}$ and $\alpha_{31}$ in the neutrino mixing matrix $U$. The total CP asymmetry $\epsilon_1$, defined in (1.62), is easily derived:

$$
\epsilon_1 = -\frac{3M_1}{16\pi v^2} \frac{\text{Im}\left(\sum_k m_k^2 R_{1k}^2\right)}{\sum_i m_i |R_{1i}|^2} \, .
\tag{1.65}
$$

Thus, $\epsilon_1$ is sensitive only to the $R-$phases and there is no correlation with any of the low energy sources of CP violation in the lepton sector. It can be shown [66] that scenarios in which $\epsilon_1 = 0$ while $\epsilon_{1\alpha} \neq 0$, entail the possibility that the phases in the light neutrino mixing matrix $U$ provide enough CP violation for successful leptogenesis. In [54, 55], in particular, it was shown that if flavour effects are relevant and the heavy Majorana neutrinos $N_k$ have a hierarchical mass spectrum, then the observed baryon asymmetry can be produced even if the only source of CP violation is the Majorana and/or Dirac phase(s) in the PMNS matrix. The same result was shown to hold also for quasi-degenerate in mass heavy RH Majorana neutrinos [54, 55].

## 1.5 Flavour Effects in Thermal Leptogenesis

The notion of flavour enters in the total lepton Lagrangian, $\mathcal{L}^{\text{lep}}$, via the charged lepton Yukawa interactions, mediated by the couplings $h_e$, $h_\mu$ and $h_\tau$ (see Eq. (1.4)). They give rise to the masses of charged leptons in the SM, after the spontaneous breaking of the EW symmetry. In the early Universe these interactions can be fast enough to put in thermal equilibrium processes like: $e_{\alpha L} + \overline{e}_{\alpha R} \to h^0$, $\nu_{\alpha L} + \overline{e}_{\alpha R} \to h^+$ or $e_{\alpha L} + \overline{e}_{\alpha R} \to h^{0,\pm} + A^{0,\mp}$, $\nu_{\alpha L} + \overline{e}_{\alpha R} \to h^{0,+} + A^{+,0}$, with $A^0 = W^3, B$ and $A^\pm = W^\pm$ being the $SU(2) \times U(1)$ gauge bosons. These interactions are in equilibrium if the corresponding rate $\Gamma_\alpha$ is larger than the expansion rate of the Universe. The rate $\Gamma_\alpha$ can be estimated as [69]:

$$
\Gamma_\alpha \approx 5 \times 10^{-3} \, h_\alpha^2 T \, .
\tag{1.66}
$$

## 1.5 Flavour Effects in Thermal Leptogenesis

The expansion rate of the Universe is $H \cong 1.66 g_*^{1/2} T^2 / M_{\rm Pl}$, where $M_{\rm Pl} \cong 10^{19}$ GeV is Planck mass, while $g_*$ indicates the number of relativistic degrees of freedom present in the thermal bath. When the temperature drops due to the expansion of the Universe, the tau Yukawa interactions enter in thermal equilibrium, *i.e.* $\Gamma_\tau > H$. This condition is realized as soon as $T \lesssim 10^{12}$ GeV. For the muon the same will happen at $T \lesssim 10^9$ GeV. [12] Hence, for $T \gg 10^{12}$ GeV the charged lepton Yukawa interactions are negligible and the notion of flavour in the thermal plasma has no meaning. The physical lepton states arise from the combination of the (flavour) fields $\ell_\alpha$ coupled to the RH Majorana neutrino $N_k$, *i.e.* [13]

$$|\ell_k\rangle \equiv \frac{1}{[\lambda\lambda^\dagger]_{kk}} \sum_\alpha \lambda_{k\alpha}^* |\ell_\alpha\rangle, \tag{1.67}$$

$$|\overline{\ell}_k\rangle \equiv \frac{1}{[\lambda\lambda^\dagger]_{kk}} \sum_\alpha \lambda_{k\alpha} |\overline{\ell}_\alpha\rangle. \tag{1.68}$$

When the charged lepton Yukawa interactions are in thermal equilibrium ($\Gamma_\alpha > H$) and they are faster than the inverse decay processes $\overline{\ell}_k + \overline{H}, \ell_k + H \to N_k$, the coherence of the state $|\ell_k\rangle$ is spoiled and the physical basis is given by $|\ell_\alpha\rangle$ and the component of $|\ell_k\rangle$ which is orthogonal to $|\ell_\alpha\rangle$. In this case, the Higgs bosons will interact with the incoherent lepton flavour combinations given in the physical basis instead of the coherent superpositions $|\ell_k\rangle$ and $|\overline{\ell}_k\rangle$, produced in the $N_k$ decays.

Following the previous discussion, there are *three possible regimes* of generation of the baryon asymmetry in the thermal leptogenesis scenario [65, 66, 67]. Considering a hierarchical neutrino mass spectrum, $M_{2,3} \gg M_1$, as already done at the end of Section 1.4.2, the leptogenesis time scale is set at a temperature $T \sim M_1$. For $T \sim M_1 > 10^{12}$ GeV the lepton flavours are indistinguishable and the *one-flavour* approximation is valid: the physical states interacting in the plasma at the leptogenesis scale are $|\ell_1\rangle$ and $|\overline{\ell}_1\rangle$. The relevant CP asymmetry in this case is $\epsilon_1 \equiv \epsilon_{1e} + \epsilon_{1\mu} + \epsilon_{1\tau}$ and it depends only on the $R-$phases. Hence for real or purely imaginary CP conserving $R_{1j}$, it is impossible to produce any baryon asymmetry (see Eq. (1.65)). If $10^9$ GeV $\lesssim T \sim M_1 \lesssim 10^{12}$ GeV, the tau Yukawa interactions enter in thermal equilibrium and the Boltzmann evolution of the lepton charge $L_\tau$, proportional to the CP asymmetry $\epsilon_{1\tau}$ is distinct from the evolution of the $(e+\mu)-$flavour number density (lepton charge $L_o \equiv L_e + L_\mu$), which is related to the CP asymmetry $\epsilon_{1o} \equiv \epsilon_{1e} + \epsilon_{1\mu}$. This corresponds to the so-called *two-flavour regime*. [14] At smaller temperatures, $T \sim M_1 \lesssim 10^9$ GeV, also charged muon Yukawa interactions reach thermal equilibrium and the evolution of the $\mu-$flavour number density (lepton charge $L_\mu$) becomes distinguishable in the thermal plasma. In this *three-flavour regime* the physical basis coincides with the standard flavour basis: $\ell_e$, $\ell_\mu$ and $\ell_\tau$.

In the one-flavour scenario, $T \sim M_1 > 10^{12}$ GeV, the baryon asymmetry of the Universe $Y_B$, in

---

[12] In SUSY we have $h_\tau = m_\tau / (v \sin\beta)$, so that the tau Yukawa is in equilibrium at temperatures $T < (1 + \tan^2\beta) \times 10^{12}$ GeV, where $\tan\beta$ is the ratio of the VEV of the two Higgs doublets present in the minimal SUSY extension of the Standard Model.

[13] Note that, if neutrino Yukawa coupling are complex, the state $\overline{\ell}_k$ defined in (1.68) *does not* correspond to the charge conjugated state of $\ell_k$ in (1.67).

[14] As was suggested in [54] and confirmed in the more detailed study [70, 71], in the two-flavour regime of leptogenesis the flavour effects are fully developed at $M_1 \lesssim 5 \times 10^{11}$ GeV.

the formulation given in Eq. (4), can be computed as:

$$Y_B \cong -\frac{12}{37g_*} \epsilon_1 \, \eta \, (\widetilde{m}_1) \, . \tag{1.69}$$

In the previous equation, $g_* = 217/2$ is the number of (SM) relativistic degrees of freedom in the thermal bath and $\widetilde{m}_1$ is the wash-out mass term:

$$\widetilde{m}_1 \equiv \frac{[\lambda\lambda^\dagger]_{11}}{M_1} v^2 = \sum_k |R_{1k}|^2 m_k \, , \tag{1.70}$$

where the Casas-Ibarra parametrization was used in the last equality. The dimensional parameter $\widetilde{m}_1$ measures the strength of neutrino Yukawa interactions at the leptogenesis time. Indeed, one has:

$$\frac{\Gamma_{D1}}{H} \equiv \frac{\widetilde{m}_1}{m_*} \, , \tag{1.71}$$

where $\Gamma_{D1}$ is the total decay rate of $N_1$ (see Eq. (1.52)) and

$$m_* = 8\pi \frac{v^2}{M_1^2} \, H|_{T=M_1} \cong 1.1 \times 10^{-3} \, \text{eV} \, . \tag{1.72}$$

From the orthogonality condition of the matrix $R$, one has: $\widetilde{m}_1 > \left| \sum_k R_{1k}^2 m_k \right| > \min(m_k)$. The range of parameters for which $\widetilde{m}_1 \gtrsim m_*$ is referred to as *strong wash-out*. Conversely, if $\widetilde{m}_1 < m_*$, the leptogenesis scenario is said to happen in a *weak wash-out* regime.

The efficiency function $0 < \eta < 1$, that takes into account the wash-out effects of the total lepton charge asymmetry produced by the out-of-equilibrium decays $N_1$, can be parametrized as [72]:

$$\eta \, (X) \cong \left( \frac{3.3 \times 10^{-3} \, \text{eV}}{X} + \left( \frac{X}{0.55 \times 10^{-3} \, \text{eV}} \right)^{1.16} \right)^{-1} \, . \tag{1.73}$$

The previous expression is obtained by performing a fit of the numerical solution of the set of Boltzmann equations relevant for leptogenesis. The main processes that enter in the computation are: $i$) decays and inverse decays, $N_1 \leftrightarrow \ell_1 H$ and $N_1 \leftrightarrow \overline{\ell}_1 \overline{H}$; $ii$) $\Delta L = 1$ Higgs-mediated scattering processes, $N_1 \ell_1 \leftrightarrow \overline{q}_{3L} t_R$ (s-channel) and $N_1 \overline{q}_{3L} \leftrightarrow \ell_1 \overline{t}_R$, $N_1 t_R \leftrightarrow \ell_1 q_{3L}$ (t- and u-channels), where $q_{3L}$ and $t_R$ are the third family $SU(2)$ quark doublet and singlet, respectively; $iii$) $\Delta L = 1$ gauge scatterings, $N_1 \ell_1 \to \overline{H} \, A$, with $A = W^{\pm,0}$ and $B$; $iv$) $\Delta L = 2$ scattering processes, $\ell_1 H \to \overline{\ell}_1 \overline{H}$ (s-channel), $\ell_1 \ell_1 \to H H$ (t- and u-channels), where in the s-channel process only the off-shell contribution of the RH neutrino fields is considered (the on-shell part is already taken into account in the decay and inverse decays). One can prove [72] that the $\Delta L = 2$ scattering processes are out-of-equilibrium if leptogenesis happens at $T \sim M_1 < 10^{14}$ GeV and can be safely neglected. In this case, the efficiency factor $\eta$ will depend only on the effective wash-out mass parameter $\widetilde{m}_1$, according to Eq. (1.73). For $M_1 \gtrsim 10^{14}$ GeV, Eq. (1.73) is not anymore a good approximation.

In the two-flavour regime, $10^9$ GeV $\lesssim T \sim M_1 \lesssim 10^{12}$ GeV, the baryon asymmetry predicted in the case of interest is:

$$Y_B \cong -\frac{12}{37g_*} \left( \epsilon_{1o} \, \eta \left( \frac{417}{589} \widetilde{m}_{1o} \right) + \epsilon_{1\tau} \, \eta \left( \frac{390}{589} \widetilde{m}_{1\tau} \right) \right) \, , \tag{1.74}$$

## 1.5 Flavour Effects in Thermal Leptogenesis

with $\epsilon_{1o} = \epsilon_{1e} + \epsilon_{1\mu}$, $\widetilde{m}_{1o} = \widetilde{m}_{1e} + \widetilde{m}_{1\mu}$, $\widetilde{m}_{1\alpha}$ defined as [65, 66, 67],

$$\widetilde{m}_{1\alpha} = \left| \sum_k R_{1k}\, m_k^{1/2}\, U_{\alpha k}^* \right|^2 . \tag{1.75}$$

The terms $\eta(390\widetilde{m}_{1\tau}/589) \cong \eta(0.66\widetilde{m}_{1\tau})$ and $\eta(417\widetilde{m}_{1o}/589) \cong \eta(0.71\widetilde{m}_{1o})$ are the efficiency factors for generation of the asymmetries $\epsilon_{1\tau}$ and $\epsilon_{1o}$. In the flavoured scenario, such efficiency factors are well approximated by the expression [67]:

$$\eta\left(X\right) \cong \left( \frac{8.25 \times 10^{-3}\,\mathrm{eV}}{X} + \left( \frac{X}{2 \times 10^{-4}\,\mathrm{eV}} \right)^{1.16} \right)^{-1} . \tag{1.76}$$

At $T \sim M_1 \lesssim 10^9$ GeV, the three-flavour regime is realized and [67]:

$$Y_B \cong -\frac{12}{37g_*} \left( \epsilon_{1e}\, \eta\left( \frac{151}{179}\widetilde{m}_{1e} \right) + \epsilon_{1\mu}\, \eta\left( \frac{344}{537}\widetilde{m}_{1\mu} \right) + \epsilon_{1\tau}\, \eta\left( \frac{344}{537}\widetilde{m}_{1\tau} \right) \right) . \tag{1.77}$$

The expression of the CP asymmetries $\epsilon_{1\alpha}$ which enter in the computation of the total baryon asymmetry $Y_B$ (see Eqs (1.74) and (1.77)) in the thermal flavoured leptogenesis scenario, depend on the Dirac and Majorana CP violating phases in the PMNS neutrino mixing matrix. As pointed out in the previous section, one can distinguish different scenarios according to the dominant source of CP violation which determines the CP asymmetry.

A phenomenological interesting case is obtained when the only source of CP violation which enters in the CP asymmetries is provided exclusively by the phases of the PMNS matrix, that is, when the elements of the matrix $R$ are all real or purely imaginary (see Eq. (1.47)). Actually, it can be shown [54] that such scenario is encountered if the less restrictive condition $\mathrm{Re}(R_{1j}R_{1k}) = 0$ or $\mathrm{Im}(R_{1j}R_{1k}) = 0$, for $j \neq k$, is fulfilled. In this case, it proves convenient to cast the flavour CP asymmetries $\epsilon_{1\alpha}$ in the form [73]:

$$\mathrm{Im}\left(R_{1k}R_{1j}\right) = 0 :$$

$$\epsilon_{1\alpha} = -\frac{3M_1}{16\pi v^2} \frac{\sum_k \sum_{j>k} \sqrt{m_k m_j}\,(m_j - m_k)\,\rho_{kj}|R_{1k}R_{1j}|\,\mathrm{Im}\left(U_{\alpha k}^* U_{\alpha j}\right)}{\sum_i m_i\,|R_{1i}|^2} , \tag{1.78}$$

$$\mathrm{Re}\left(R_{1k}R_{1j}\right) = 0 :$$

$$\epsilon_{1\alpha} = -\frac{3M_1}{16\pi v^2} \frac{\sum_k \sum_{j>k} \sqrt{m_k m_j}\,(m_j + m_k)\,\rho_{kj}|R_{1k}R_{1j}|\,\mathrm{Re}\left(U_{\alpha k}^* U_{\alpha j}\right)}{\sum_i m_i\,|R_{1i}|^2} . \tag{1.79}$$

where it is assumed that $R_{1j}R_{1k} = \rho_{jk}\,|R_{1j}R_{1k}|$ (1.78) or $R_{1j}R_{1k} = i\rho_{jk}\,|R_{1j}R_{1k}|$ (1.79), with $\rho_{jk} = \pm 1$, for $j \neq k$. One can easily prove that for real or purely imaginary $R_{1j}R_{1k}$, for $j \neq k$, in the two flavour regime and for a hierarchical RH neutrino mass spectrum, the two relevant CP

asymmetries in the computation of the baryon asymmetry $Y_B$ (1.74), are related in the following way:

$$\epsilon_{1\tau} = -\epsilon_{1o}\,, \tag{1.80}$$

where $\epsilon_{1o} \equiv \epsilon_{1\mu} + \epsilon_{1e}$.

Few comments are here in order:

i) Real (purely imaginary) $R_{1k}R_{1j}$ and purely imaginary (real) $U^*_{\alpha k}U_{\alpha j}$, $j \neq k$, implies violation of CP symmetry by the matrix $R$.

ii) In order to break CP at low energies [41, 42], both $\text{Re}(U^*_{\alpha k}U_{\alpha j}) \neq 0$ and $\text{Im}(U^*_{\alpha k}U_{\alpha j}) \neq 0$ should be satisfied (see [54] for further details).

iii) If $R_{1j}$, for $j = 1, 2, 3$, is real or purely imaginary, as the condition of CP invariance requires, Eq. (1.47), of the three quantities $R_{11}R_{12}$, $R_{11}R_{13}$ and $R_{12}R_{13}$, relevant for the computation of the CP asymmetries $\epsilon_{1\alpha}$, not more than two can be purely imaginary, i.e. if, for instance, $R_{11}R_{12} = i\rho_{12}\,|R_{11}R_{12}|$ and $R_{12}R_{13} = i\rho_{23}\,|R_{12}R_{13}|$, then one has $R_{11}R_{13} = \rho_{13}\,|R_{11}R_{13}|$.

In Chapter 2 a detailed analysis of thermal flavoured leptogenesis is reported in the case when the source of CP violation, necessary for successful leptogenesis, is provided only by the the Dirac and/or Majorana CP violating phases in the PMNS matrix. Particular emphasis is given to the effects played by the lightest neutrino mass, $\min(m_1, m_2, m_3)$, in the determination of the baryon asymmetry $Y_B$.

In the general case of complex matrix elements $R_{1j}$, the $R-$phases provide a further source of CP violation in the lepton sector, which can be relevant at the time scale of leptogenesis, $T \sim M_1$. In order to study the *interplay* of the different sources of CP violation, it proves convenient to write the general expression of the CP asymmetry $\epsilon_{1\alpha}$, $\alpha = e, \mu, \tau$, given in (1.64), in the following form [74, 75]:

$$\epsilon_{1\alpha} = -\frac{3\,M_1}{16\,\pi\,v^2}\,\frac{1}{\sum_k\,m_k|R_{1k}|^2}\left\{\sum_\beta m_\beta^2\,|R_{1\beta}|^2\,|U_{\alpha\beta}|^2\,\sin 2\tilde\varphi_{1\beta} + \sum_\beta\sum_{\rho>\beta}\sqrt{m_\beta\,m_\rho}\,|R_{1\beta}R_{1\rho}| \right. \tag{1.81}$$

$$\left. \times\left[(m_\rho - m_\beta)\cos(\varphi_{\beta\rho})\,\text{Im}\left(U^*_{\alpha\beta}\,U_{\alpha\rho}\right) + (m_\rho + m_\beta)\sin(\varphi_{\beta\rho})\,\text{Re}\left(U^*_{\alpha\beta}\,U_{\alpha\rho}\right)\right]\right\}\,,$$

where $\tilde\varphi_{1j}$ are the CP violating $R-$phases:

$$R_{1j} \equiv |R_{1j}|\,e^{i\,\tilde\varphi_{1j}} \quad \text{and} \quad \varphi_{ij} \equiv \tilde\varphi_{1i} + \tilde\varphi_{1j}\,. \tag{1.82}$$

The first term in the curly brackets in Eq. (1.81) represents the contribution to $\epsilon_{1\alpha}$ from the "high energy" CP violation, originating entirely from the matrix $R$, while the terms in the square brackets are "mixed", i.e. they are due both to the "low" and "high" energy CP violation, generated by the neutrino mixing matrix $U$ and by the matrix $R$. Obviously, if $\tilde\varphi_{1j} = k_j\pi/2$ ($k_j = 0, 1, 2, ...$, and $j = 1, 2, 3$) the "high energy" part is zero, while the "mixed" term reduces to a "low energy" contribution, in the sense that, with exception of very special cases discussed before, the only

source of CP violation in leptogenesis will be the PMNS matrix $U$ and the expression of the CP asymmetry $\epsilon_{1\alpha}$ reduces to the formulas (1.78) or (1.79). It is easy to show, taking into account the unitarity of the matrix $U$, that in the two flavour regime the expression for the CP asymmetry $\epsilon_{1o}$ can be simply obtained from $\epsilon_{1\tau}$:

$$\epsilon_{1o} \equiv \epsilon_{1e} + \epsilon_{1\mu} = \epsilon_{1\tau}(|U_{\tau k}|^2 \to 1 - |U_{\tau k}|^2 , \, U_{\tau 2}^* U_{\tau 3} \to -U_{\tau 2}^* U_{\tau 3}), \quad \text{for} \quad k = 2, 3 \,. \qquad (1.83)$$

The interplay between the "high energy" source of CP violation, provided by the $R-$phases and the "low energy" phases $\delta$ and $\alpha_{21,31}$ of the PMNS neutrino mixing matrix, will be analyzed in detail in Chapter 3.

# Chapter 2

# Effects of Lightest Neutrino Mass

In this chapter a model independent analysis of the thermal leptogenesis scenario is presented. The amount of CP violation necessary for the generation of the observed baryon asymmetry of the Universe is provided only by the Dirac and/or Majorana CP violating phases in the PMNS matrix $U$.

The RH neutrino mass spectrum is strongly hierarchical ($M_1 \ll M_{2,3}$) and the results derived in Chapter 1 are used. Leptogenesis takes place in the two-flavour regime ($10^9$ GeV $\lesssim M_1 \lesssim 10^{12}$ GeV). Analytical estimates and a numerical study of the effects of the lightest neutrino masses in the generation of the baryon asymmetry are reported. Such results are based on the work [73].

The analysis is performed for two possible types of light neutrino mass spectrum allowed by the data: $i$) with normal ordering ($\Delta m_A^2 > 0$), $m_1 < m_2 < m_3$, and $ii$) with inverted ordering ($\Delta m_A^2 < 0$), $m_3 < m_1 < m_2$. The case of inverted hierarchical (IH) spectrum, $m_3 \ll m_{1,2}$, and real (and CP conserving) matrix $R$ is investigated in detail. Results for the normal hierarchical (NH) case, $m_1 \ll m_{2,3}$, are also derived.

The computation is performed neglecting renormalisation group (RG) running [76] of $m_j$ and of the parameters in the PMNS matrix $U$, from $M_Z$ to $M_1$. This is a good approximation for $\min(m_j) \lesssim 0.10$ eV, $i.e.$ for the NH and IH neutrino mass spectra, as well as for a spectrum with partial hierarchy (see, $e.g.$ [77]). Under the indicated condition $m_j$, and correspondingly $\Delta m_A^2$ and $\Delta m_\odot^2$, and $U$ can be taken at the scale of the order $M_Z$, at which the neutrino mixing parameters are measured.

## 2.1   Inverted hierarchical light neutrino mass spectrum

The case of IH neutrino mass spectrum, $m_3 \ll m_1 < m_2$, $m_{1,2} \cong \sqrt{|\Delta m_A^2|}$, is of particular interest since, within the leptogenesis scenario discussed here, for real $R_{1j}$ ($j = 1, 2, 3$), IH spectrum and $negligible$ lightest neutrino mass $m_3 \cong 0$, it is impossible to generate the observed baryon asymmetry $Y_B$ in the flavoured regime, [1] if the only source of CP violation are the Majorana and/or Dirac phases in the PMNS matrix. Indeed, for $m_3 \ll m_1 < m_2$ and real $R_{1j}$, the terms proportional to $\sqrt{m_3}$ in the expressions of the CP asymmetries $\epsilon_{1\alpha}$, Eq. (1.78), and wash-out mass parameters

---

[1]A detailed treatment of this region of the parameter space is reported in [54].

$\widetilde{m}_{1\alpha}$, Eq. (1.75), are negligible if $m_3 \approx 0$, or if $R_{13} \approx 0$ and $R_{11}, R_{12} \neq 0$, with $R_{11}^2 + R_{12}^2 \approx 1$ from the orthogonality condition. This implies that the CP asymmetries $\epsilon_{1\alpha}$ are suppressed by the factor $\Delta m_\odot^2 / (2\Delta m_A^2) \cong 1.6 \times 10^{-2}$, while $|R_{11}|, |R_{12}| \leq 1$ and the resulting baryon asymmetry is too small [54]. The same suppression is also present in the one-flavour regime, $M_1 > 10^{12}$ GeV, when $R_{13} \approx 0$ and the product $R_{11}R_{12}$ has non-trivial real and imaginary parts [78].

On the other hand, if the lightest active neutrino mass $m_3$ is not negligible, with still $m_3 \ll m_{1,2}$, the terms $\propto \sqrt{m_3}$ in $\epsilon_{1\alpha}$ are the dominant contributions, provided that:

$$2 \left( \frac{m_3}{\sqrt{\Delta m_\odot^2}} \right)^{\frac{1}{2}} \left( \frac{\Delta m_A^2}{\Delta m_\odot^2} \right)^{\frac{3}{4}} \frac{|R_{13}|}{|R_{11(12)}|} \gg 1 \,. \tag{2.1}$$

This inequality can be fulfilled in the limits $R_{11} \approx 0$, or $R_{12} \approx 0$, and if $m_3$ is sufficiently large. The latter condition can be satisfied for $m_3 \lesssim 5 \times 10^{-3}$ eV $\ll \sqrt{|\Delta m_A^2|}$.

In the following, the parameter space relevant for successful leptogenesis is discussed more quantitatively. A complete numerical analysis as well as useful analytical approximations of the baryon asymmetry $Y_B$ (see Eq. (1.74)) are perfomed.

### 2.1.1 Analytical estimates: the case $R_{11} = 0$

For $R_{11} = 0$ the CP asymmetry $\epsilon_{1\tau} = -\epsilon_{1o} \equiv (\epsilon_{1e} + \epsilon_{1\mu})$ reported in (1.78) can be expressed as:

$$\epsilon_{1\tau} \cong -\frac{3M_1}{16\pi v^2} \sqrt{m_3 \, m_2} \left( 1 - \frac{m_3}{m_2} \right) \rho_{23} \, r \, \mathrm{Im} \left( U_{\tau 2}^* U_{\tau 3} \right) \,, \tag{2.2}$$

where

$$m_2 = \sqrt{m_3^2 + |\Delta m_A^2|} \,, \tag{2.3}$$

$$r = \frac{|R_{13}R_{12}|}{|R_{12}|^2 + \frac{m_3}{m_2}|R_{13}|^2} \,, \tag{2.4}$$

$$\mathrm{Im} \left( U_{\tau 2}^* U_{\tau 3} \right) = -c_{23}c_{13} \, \mathrm{Im} \left( e^{i(\alpha_{31} - \alpha_{21})/2} (c_{12}s_{23} + s_{12}c_{23}s_{13}e^{-i\delta}) \right) \,. \tag{2.5}$$

The two relevant wash-out mass parameters are in this case:

$$\widetilde{m}_{1\tau} = m_2 R_{12}^2 |U_{\tau 2}|^2 + m_3 R_{13}^2 |U_{\tau 3}|^2 + 2\sqrt{m_2 m_3} \, \rho_{23} |R_{12}R_{13}| \, \mathrm{Re} \left( U_{\tau 2}^* U_{\tau 3} \right), \tag{2.6}$$

$$\widetilde{m}_{1o} \equiv \widetilde{m}_{1e} + \widetilde{m}_{1\mu} = m_2 R_{12}^2 + m_3 R_{13}^2 - \widetilde{m}_{1\tau} \,, \tag{2.7}$$

where $\rho_{23} = \mathrm{sign}(R_{12}R_{13})$.

The orthogonality of the matrix $R$ implies that $R_{11}^2 + R_{12}^2 + R_{13}^2 = 1$, which in the case under consideration reduces to $R_{12}^2 + R_{13}^2 = 1$. It is not difficult to show that for real $R_{12}$ and $R_{13}$ satisfying this constraint, the maximum of the function $r$, and therefore of the CP asymmetry $|\epsilon_{1\tau}|$, is realized for $R_{12}$ and $R_{13}$ given by:

$$R_{12}^2 = \frac{m_3}{m_3 + m_2} \,, \quad R_{13}^2 = \frac{m_2}{m_3 + m_2} \,, \quad \text{with} \quad R_{12} < R_{13} \,. \tag{2.8}$$

## 2.1 Inverted hierarchical light neutrino mass spectrum

At the maximum, $|r|$ is equal to:

$$\max(|r|) = \frac{1}{2}\left(\frac{m_2}{m_3}\right)^{\frac{1}{2}} \cong \frac{1}{2}\left(\frac{\sqrt{|\Delta m_{\rm A}^2|}}{m_3}\right)^{\frac{1}{2}} , \tag{2.9}$$

and the CP asymmetry $|\epsilon_{1\tau}|$ takes the form:

$$|\epsilon_{1\tau}| \cong \frac{3M_1}{32\pi v^2}\,(m_2 - m_3)\,|{\rm Im}\,(U_{\tau2}^* U_{\tau3})| \cong \frac{3M_1}{32\pi v^2}\sqrt{|\Delta m_{\rm A}^2|}\,|{\rm Im}\,(U_{\tau2}^* U_{\tau3})| . \tag{2.10}$$

The second approximate equalities in Eqs (2.9) and (2.10) correspond to IH spectrum, *i.e.* to $m_3 \ll m_2 \cong \sqrt{|\Delta m_{\rm A}^2|}$. Thus, the maximum of the asymmetry $|\epsilon_{1\tau}|$ *i*) is not suppressed by the factor $\Delta m_\odot^2/(\Delta m_{\rm A}^2)$ and *ii*) practically does not depend on $m_3$ in the case of IH spectrum. One can estimate

$$|\epsilon_{1\tau}| \cong 5.0 \times 10^{-8}\,\frac{m_2 - m_3}{\sqrt{|\Delta m_{\rm A}^2|}}\left(\frac{\sqrt{|\Delta m_{\rm A}^2|}}{0.05~{\rm eV}}\right)\left(\frac{M_1}{10^9~{\rm GeV}}\right)|{\rm Im}\,(U_{\tau2}^* U_{\tau3})| , \tag{2.11}$$

Because of $\max(|{\rm Im}(U_{\tau2}^* U_{\tau3})|) \cong 0.46$, for, *e.g.* $\sin^2 2\theta_{23} = 1$, $\sin^2\theta_{12} = 0.30$ and $\sin^2\theta_{13} < 0.04$ and $\max(|\eta(0.66\widetilde{m}_{1\tau}) - \eta(0.71\widetilde{m}_{1o})|) \cong 7\times 10^{-2}$, an absolute upper bound on the baryon asymmetry $Y_B$ in the two flavour regime for IH light neutrino mass spectrum and real matrix $R$ (*i.e.* real $R_{1j}R_{1k}$) is derived:

$$|Y_B| \lesssim 4.8 \times 10^{-12}\left(\frac{\sqrt{|\Delta m_{\rm A}^2|}}{0.05~{\rm eV}}\right)\left(\frac{M_1}{10^9~{\rm GeV}}\right) . \tag{2.12}$$

This upper bound allows to determine the minimal value of $M_1$ for which it is possible to reproduce the observed value of $|Y_B|$ [2] for IH spectrum, real matrix $R$ and $R_{11} = 0$:

$$M_1 \gtrsim 1.7 \times 10^{10}~{\rm GeV} . \tag{2.13}$$

The values of $R_{12}$, for which $|\epsilon_{1\tau}|$ is maximal, can differ, in general, from those that maximize $|Y_B|$ due to the dependence of the wash-out mass parameters and of the corresponding efficiency factors on $R_{12}$. However, this difference, when it is present, does not exceed 30%.

For $R_{12}$ and $R_{13}$, which maximize the ratio $|r|$ and the asymmetry $|\epsilon_{1\tau}|$, the relevant wash-out mass parameters are given by:

$$\widetilde{m}_{1\tau} = \frac{m_2\,m_3}{m_3 + m_2}\left[\,|U_{\tau2}|^2 + |U_{\tau3}|^2 + 2\,\rho_{23}\,{\rm Re}\,(U_{\tau2}^* U_{\tau3})\right] , \tag{2.14}$$

$$\widetilde{m}_{1o} = 2\,\frac{m_2\,m_3}{m_3 + m_2} - \widetilde{m}_{1\tau} . \tag{2.15}$$

---

[2] In all the numerical analysis performed in this chapter, the baryon asymmetry $|Y_B|$ takes values in the interval $8.0 \times 10^{-11} \lesssim |Y_B| \lesssim 9.2 \times 10^{-11}$, which is compatible with the observed value reported in (5).

Equations (2.11), (2.14) and (2.15) suggest that in the case of IH light neutrino mass spectrum with non-negligible $m_3$, $m_3 \ll \sqrt{|\Delta m_{\rm A}^2|}$, the generated baryon asymmetry $|Y_B|$ can be strongly enhanced in comparison with the asymmetry $|Y_B|$ produced if $m_3$ were approximately zero. The *enhancement* can be by *a factor of* $\sim 100$. Indeed, the maximum of the CP asymmetry $|\epsilon_{1\tau}|$ (with respect to $|R_{12}|$), Eq. (2.10), does not contain the suppression factor $\Delta m_{\odot}^2/(2\Delta m_{\rm A}^2) \cong 1.6 \times 10^{-2}$ and its magnitude is not controlled by $m_3$, but rather by $\sqrt{|\Delta m_{\rm A}^2|}$. At the same time, the wash-out mass parameters $\widetilde{m}_{1\tau}$ and $\widetilde{m}_{1o}$, Eqs (2.14) and (2.15), are determined by $m_2 m_3/(m_2 + m_3) \cong m_3$. The latter in the case under discussion can take values as large as $m_3 \sim 5 \times 10^{-3}$ eV. The efficiency factors $\eta(0.66\widetilde{m}_{1\tau})$ and $\eta(0.71\widetilde{m}_{1o})$, which enter into the expression for the baryon asymmetry, Eq. (1.74), have a maximal value $\eta(X) \cong (6 \div 7) \times 10^{-2}$ when $X \cong (0.7 \div 1.5) \times 10^{-3}$ eV (weak wash-out regime). Since the range of values of $m_3$ for IH spectrum extends to about $5 \times 10^{-3}$ eV, one can always find a value of $m_3$ in this range such that $\widetilde{m}_{1\tau}$ or $\widetilde{m}_{1o}$ takes a value maximizing $\eta(0.66\widetilde{m}_{1\tau})$ or $\eta(0.71\widetilde{m}_{1o})$, and $|\eta(0.66\widetilde{m}_{1\tau}) - \eta(0.71\widetilde{m}_{1o})|$. This qualitative discussion suggests that there always exists an interval of values of $m_3$ for which the baryon asymmetry is produced in the weak wash-out regime. On the basis of the above considerations, one can expect that *successful leptogenesis is possible for non-negligible $m_3$* in the case of IH spectrum even if the requisite CP violation is provided by the Majorana or Dirac phase(s) in the PMNS matrix.

### 2.1.2 Leptogenesis due to Majorana CP violation

For $\delta = 0$ $(\pi)$, one has $|{\rm Im}(U_{\tau 2}^* U_{\tau 3})| = c_{23}c_{13}(s_{23}c_{12} \overset{+}{\underset{(-)}{}} c_{23}s_{12}s_{13})|\sin\alpha_{32}/2|$ and correspondingly $0.36|\sin\alpha_{32}/2| \lesssim |{\rm Im}(U_{\tau 2}^* U_{\tau 3})| \lesssim 0.46|\sin\alpha_{32}/2|$, where $\alpha_{32} = \alpha_{31} - \alpha_{21}$. [3] The terms proportional to $s_{13}$ have a subdominant effect on the magnitude of the calculated $|\epsilon_{1\tau}|$ and $|Y_B|$.

It is easy to check that the CP asymmetry $|\epsilon_{1\tau}|$ and the wash-out mass parameters $\widetilde{m}_{1\tau,1o}$ remain invariant with respect to the changes $\rho_{23} \to -\rho_{23}$ and $\alpha_{32} \to 2\pi - \alpha_{32}$. Thus, the baryon asymmetry $|Y_B|$ satisfies the following relation:

$$|Y_B(\rho_{23}, \alpha_{32})| = |Y_B(-\rho_{23}, 2\pi - \alpha_{32})|. \tag{2.16}$$

Therefore, one can work with a fixed value of the parameter $\rho_{23}$ without loss of generality. In the following, $\rho_{23} = +1$ is assumed.

In the case of $\alpha_{32} = \pi$, $\delta = 0$; $\pi$, and real $R_{1j}R_{1k}$, the CP asymmetry $\epsilon_{1\tau}$ is still different from zero and the source of CP violation is provided only by the matrix $R$ (see discussion after Eq. (1.79)). For such value of the effective Majorana phase $\alpha_{32}$ $|\epsilon_{1\tau}|$ is maximized. The maximum of the baryon asymmetry $Y_B$, instead, is reached for $\alpha_{32} \in [\pi/2, 2\pi/3]$ if $\rho_{23} = +1$ or $\alpha_{32} \in [4\pi/3, 3\pi/2]$ if $\rho_{23} = -1$. The maximal value of $|Y_B|$ at $\alpha_{32} = \pi$ is smaller at least by a factor of two than the value of $|Y_B|$ at its absolute maximum (see further Fig. 2.3). Indeed, for $\alpha_{32} \sim \pi$ there is a rather strong mutual compensation between the asymmetries in the lepton charges $L_\tau$ and $(L_e + L_\mu)$ owing to the fact that, due to ${\rm Re}(U_{\tau 2}^* U_{\tau 3}) = 0$, $\widetilde{m}_{1\tau}$ and $\widetilde{m}_{1o}$ have relatively close values and $|\eta(0.66\widetilde{m}_{1\tau}) - \eta(0.71\widetilde{m}_{1o})| \lesssim 10^{-2}$. Actually, in certain cases one can even have $|\eta(0.66\widetilde{m}_{1\tau}) - \eta(0.71\widetilde{m}_{1o})| \approx 0$, and thus $|Y_B| \approx 0$, for $\alpha_{32}$ lying in the interval $\alpha_{32} \in [\pi, 4\pi/3]$

---

[3] In the following estimates, it is always assumed $\sin^2 2\theta_{23} = 1$, $\sin^2 \theta_{12} = 0.3$ and the limit $\sin^2 \theta_{13} < 0.04$, which are compatible with the $3\sigma$ bounds on neutrino mixing angles (see Tab. 1.1).

## 2.1 Inverted hierarchical light neutrino mass spectrum
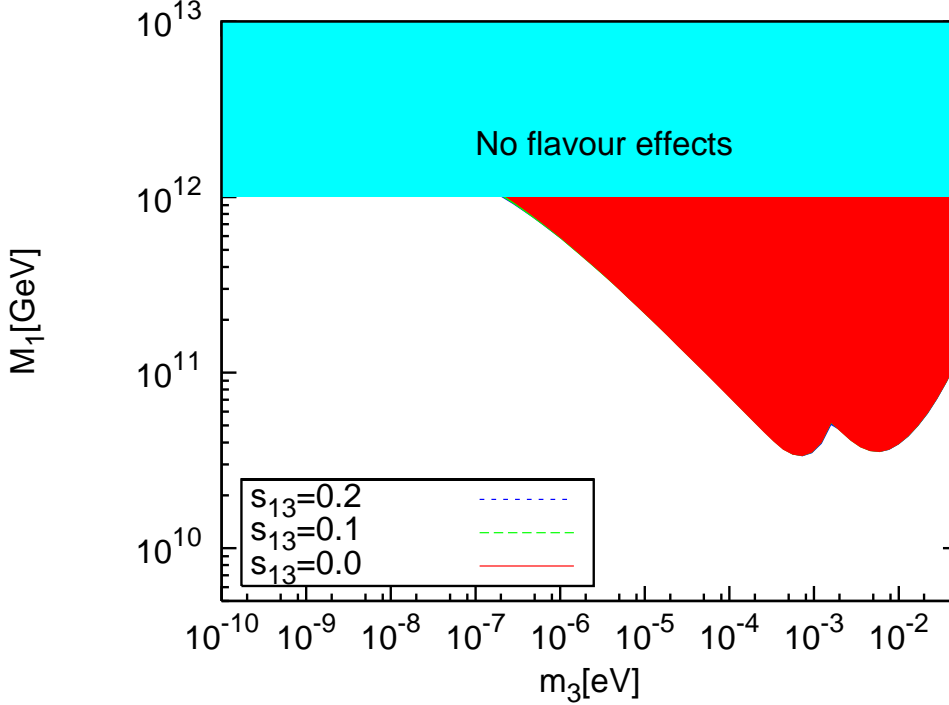


**Figure 2.1:** Values of $m_3$ and $M_1$ for which the flavoured leptogenesis is successful, generating baryon asymmetry $|Y_B| = 8.6 \times 10^{-11}$ (red/dark shaded area). The figure corresponds to hierarchical heavy Majorana neutrinos, light neutrino mass spectrum with inverted ordering (hierarchy), $m_3 < m_1 < m_2$, and real elements $R_{1j}$ of the matrix $R$. The minimal value of $M_1$ at given $m_3$, for which the measured value of $|Y_B|$ is reproduced, corresponds to CP violation due to the Majorana phases in the PMNS matrix. The results shown are obtained using the best fit values of neutrino oscillation parameters: $\Delta m^2_\odot = 8.0 \times 10^{-5}$ eV$^2$, $\Delta m^2_{\rm A} = 2.5 \times 10^{-3}$ eV$^2$, $\sin^2 \theta_{12} = 0.30$ and $\sin^2 2\theta_{23} = 1$.

(see Fig. 2.3). Similar cancellation can occur for $s_{13} = 0.2$ at $\alpha_{32} \sim \pi/6$. Obviously, $|Y_B| = 0$ for $\alpha_{32} = 0$ and $2\pi$.

As $m_3$ increases from the value of $10^{-10}$ eV up to $10^{-4}$ eV, in the case of $R_{11} = 0$, the maximum possible $|Y_B|$ for a given $M_1$ increases monotonically, starting from a value which for $M_1 \leq 10^{12}$ GeV is much smaller than the observed one, $\max(|Y_B|) \ll 8.77 \times 10^{-11}$ (see Fig. 2.2 further in the text). At approximately $m_3 = 2 \times 10^{-6}$ eV, $\max(|Y_B|) \approx 8.77 \times 10^{-11}$ for $M_1 \approx 5 \times 10^{11}$ GeV. As $m_3$ increases beyond $2 \times 10^{-6}$ eV, $\max(|Y_B|)$ for a given $M_1$ continues to increase until it reaches a maximum. This maximum occurs for $m_3$ such that $0.71\widetilde{m}_{1o} \cong 9.0 \times 10^{-4}$ eV and $\eta(0.71\widetilde{m}_{1o})$ is maximal, *i.e.* $\eta(0.71\widetilde{m}_{1o}) \cong 6.8 \times 10^{-2}$, while $\eta(0.66\widetilde{m}_{1\tau})$ is considerably smaller. As can be shown, for $\rho_{23} = +1$, the maximum value of $|Y_B|$ always takes place at $\alpha_{32} \cong \pi/2$. For $\alpha_{32} = \pi/2$, $s_{13} = 0$ and $\rho_{23} = +1$, $\max(|Y_B|)$ is located at $m_3 \cong 7 \times 10^{-4}$ eV. It corresponds to the CP asymmetry being predominantly in the $(e + \mu)$−flavour. As $m_3$ increases further, $|\eta(0.66\widetilde{m}_{1\tau}) - \eta(0.71\widetilde{m}_{1o})|$ and correspondingly $|Y_B|$, rapidly decrease. At certain value of $m_3$, typically lying in the interval $m_3 \sim (1.5 \div 2.5) \times 10^{-3}$ eV, one has $|\eta(0.66\widetilde{m}_{1\tau}) - \eta(0.71\widetilde{m}_{1o})| \approx 0$ and $|Y_B|$ goes through a deep

minimum (see Fig. 2.2).This minimum of $|Y_B|$ corresponds to a partial or complete cancellation between the CP asymmetries in the $\tau-$flavour and in the $(e+\mu)-$flavour. In the previous example of $\alpha_{32} = \pi/2$, $s_{13} = 0$ and $\rho_{23} = +1$, the indicated minimum of $|Y_B|$ occurs at $m_3 \cong 2.3 \times 10^{-3}$ eV. As $m_3$ increases further, $|\eta(0.66\widetilde{m}_{1\tau}) - \eta(0.71\widetilde{m}_{1o})|$ and $|Y_B|$ rapidly increase and $|Y_B|$ reaches a second maximum, which in magnitude is of the order of the first one. This maximum corresponds to the CP asymmetry being predominantly in the $\tau-$flavour rather than in the $(e + \mu)-$flavour. Indeed, $\eta(0.66\widetilde{m}_\tau) \cong 6.8 \times 10^{-2}$ and $\eta(0.71\widetilde{m}_2)$ is substantially smaller. For $\rho_{23} = +1$, $s_{13} = 0$ or $s_{13} = 0.2$ and $\delta = 0$, it takes place at a value of $\alpha_{32}$ close to $\pi/2$, while for $s_{13} = 0.2$ and $\delta = \pi$, it occurs at $\alpha_{32} \cong 2\pi/3$. In the case of $\rho_{23} = +1$, $s_{13} = 0$ and $\alpha_{32} = \pi/2$, the second maximum of $|Y_B|$ is located at $m_3 \cong 7 \times 10^{-3}$ eV. As $m_3$ increases further, $|Y_B|$ decreases monotonically rather slowly.

These features of the dependence of $|Y_B|$ on $m_3$ discussed above for $R_{11} = 0$ are confirmed by a more general analysis in which, in particular, the value of $R_{11}$ is not set to zero a priori. The results of this analysis are presented in Fig. 2.1, while Fig. 2.2 illustrates the dependence of $|Y_B|$ on $m_3$ in the case of $R_{11} = 0$.

The correlation between the values of $M_1$ and $m_3$ for which one can have successful leptogenesis is shown in Fig. 2.1. The figure is obtained by performing, for given $m_3$ from the interval $10^{-10} \le m_3 \le 0.05$ eV, a thorough scan of the relevant parameter space searching for possible enhancement or suppression of the baryon asymmetry with respect to that found for $m_3 = 0$. The real elements $R_{1j}$ are allowed to vary in their full ranges determined by the condition of orthogonality of the matrix $R$: $R_{11}^2 + R_{12}^2 + R_{13}^2 = 1$. The Majorana phases $\alpha_{21,31}$ are varied in the interval $[0, 2\pi]$. The calculations are performed for three values of the CHOOZ angle $\theta_{13}$, corresponding to $\sin\theta_{13} = 0$; 0.1; 0.2. In the cases of $\sin\theta_{13} \ne 0$, the Dirac phase $\delta$ is allowed to take values in the interval $[0, 2\pi]$. The heavy Majorana neutrino mass $M_1$ takes values in the two-flavour regime of thermal leptogenesis, $10^9$ GeV $\le M_1 \le 10^{12}$ GeV. For given $m_3$, the minimal value of the mass $M_1$, for which the leptogenesis is successful, generating $|Y_B| \approx 8.77 \times 10^{-11}$, is obtained for the values of the other parameters which maximize $|Y_B|$. The $\min(M_1)$ obtained in this way does not exhibit any significant dependence on $s_{13}$. If $m_3 \lesssim 2.5 \times 10^{-7}$ eV, leptogenesis cannot be successful for $M_1 \le 10^{12}$ GeV: the baryon asymmetry produced in this regime is too small. As $m_3$ increases starting from the indicated value, the maximal $|Y_B|$ for a given $M_1 \le 10^{12}$ GeV, increases monotonically. Correspondingly, the $\min(M_1)$ for which one can have successful leptogenesis decreases monotonically and for $m_3 \gtrsim 5 \times 10^{-6}$ eV one has $\min(M_1) \lesssim 5 \times 10^{11}$ GeV. The first maximum of $|Y_B|$ (minimum of $M_1$), as $m_3$ increases, is reached at $m_3 \cong 5.5 \times 10^{-4}$ eV, $\alpha_{32} \cong \pi/2$ ($\alpha_{21} \cong 0.041$, $\alpha_{31} \cong 1.65$), $R_{11} \cong -0.061$, $R_{12} \cong 0.099$, and $R_{13} \cong 0.99$. At the maximum one has $|Y_B| = 8.77 \times 10^{-11}$ for $M_1 \approx 3.4 \times 10^{10}$ GeV. The second maximum of $|Y_B|$ (or minimum of $M_1$) seen in Fig. 2.1 corresponds to $m_3 \approx 5.9 \times 10^{-3}$ eV, $\alpha_{32} \cong \pi/2$ ($\alpha_{21} \cong -0.022$, $\alpha_{31} \cong 1.45$), $R_{11} \cong -0.18$, $R_{12} \cong 0.29$ and $R_{13} \cong -0.94$. The observed value of $|Y_B|$ is reproduced, in this case, for $M_1 \approx 3.5 \times 10^{10}$ GeV.

Similar features are seen in Fig. 2.2, which shows the dependence of $|Y_B|$ on $m_3$ for $R_{11} = 0$, fixed $M_1 = 10^{11}$ GeV, $\alpha_{32} = \pi/2$ , $s_{13} = 0$ and $\rho_{23} = \pm 1$. In the case of $\alpha_{32} = \pi/2$, $s_{13} = 0.2$, $\delta = 0$ and $\rho_{23} = +1$, the absolute maximum of $|Y_B|$ is obtained for $m_3 \cong 6.7 \times 10^{-3}$ eV and $|R_{12}| = 0.34$
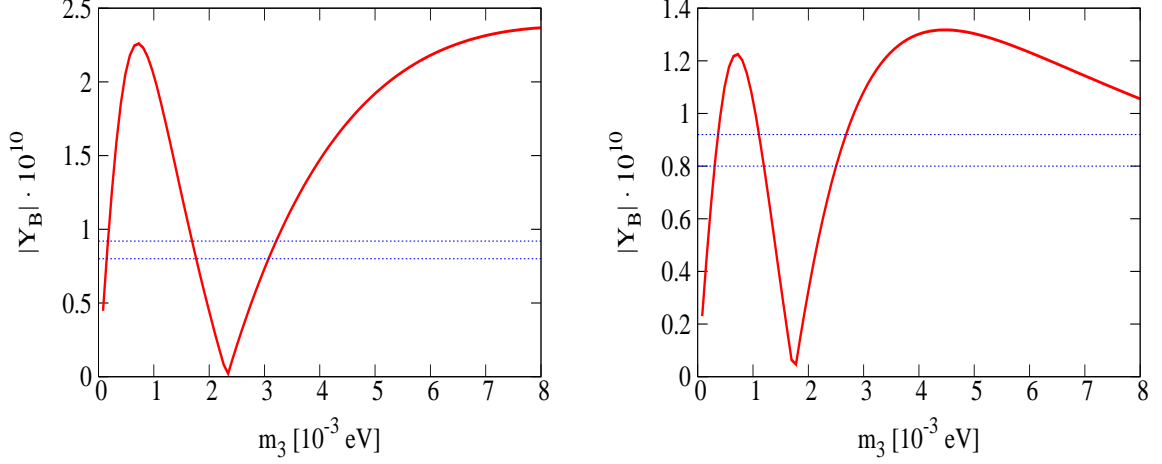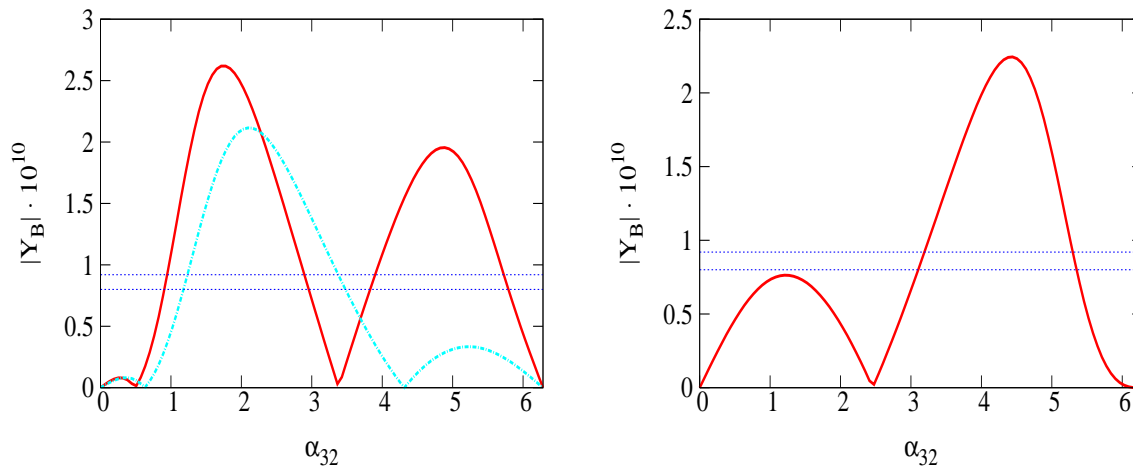
**Figure 2.2:** The dependence of $|Y_B|$ on $m_3$ in the case of IH spectrum, real $R_{1j}R_{1k}$, Majorana CP violation, $R_{11} = 0$, $\alpha_{32} = \pi/2$, $s_{13} = 0$, $M_1 = 10^{11}$ GeV, and for $i)$ $\text{sign}(R_{12}R_{13}) = +1$ (left panel), and $ii)$ $\text{sign}(R_{12}R_{13}) = -1$ (right panel). The baryon asymmetry $|Y_B|$ was calculated for a given $m_3$, using the value of $|R_{12}|$, for which the asymmetry $|\epsilon_{1\tau}|$ has the maximum value. The horizontal dotted lines indicate the range of $|Y_B|$ compatible with observations: $|Y_B| \in [8.0, 9.2] \times 10^{-11}$.

(see Fig. 2.3, left panel). At this maximum $\eta(0.66\widetilde{m}_{1\tau}) \cong 0.067$, $\eta(0.71\widetilde{m}_{1o}) \cong 0.013$ and

$$|Y_B| \cong 2.6 \times 10^{-12} \left( \frac{\sqrt{|\Delta m_A^2|}}{0.05 \text{ eV}} \right) \left( \frac{M_1}{10^9 \text{ GeV}} \right) . \tag{2.17}$$

Correspondingly, the observed baryon asymmetry $|Y_B|$ can be reproduced if $M_1 \gtrsim 3.0 \times 10^{10}$ GeV. If $s_{13} = 0$, the same result holds for $M_1 \gtrsim 3.5 \times 10^{10}$ GeV. The minimal values of $M_1$ thus found are somewhat smaller than $\min(M_1) \cong 5.3 \times 10^{10}$ GeV obtained in the case of negligible $m_3 \cong 0$ ($R_{13} = 0$) and purely imaginary $R_{11}R_{12}$ [54]. The dependence of the baryon asymmetry on $\alpha_{32}$ in the case of $s_{13} = 0$; 0.2 discussed above is illustrated in Fig. 2.3.

Summarizing, the results corresponding to the case of $R_{1j} \neq 0$, $j = 1, 2, 3$, which are shown in Fig. 2.1, are very different from the results obtained for, $e.g.$ $R_{11} = 0$ and $R_{12}, R_{13} \neq 0$. According to the values of $M_1$ in Fig. 2.1, for which successful leptogenesis is possible, one finds either $\widetilde{m}_{1o} \sim 10^{-3}$ eV and $\widetilde{m}_{1\tau} \sim 2 \times 10^{-4}$ eV, or $\widetilde{m}_{1\tau} \sim 2 \times 10^{-3}$ eV and $\widetilde{m}_{1o} \gg 10^{-3}$ eV, practically for any $m_3$ from the interval $10^{-10}$ eV $\leq m_3 \leq 5.0 \times 10^{-2}$ eV. This explains why successful leptogenesis is reached for $\min(M_1) \lesssim 5 \times 10^{11}$ GeV even when $m_3 \cong 5 \times 10^{-6}$ eV. If $R_{11} = 0$, for $m_3 \ll m_2$ and $R_{12}$ and $R_{13}$ which maximize the asymmetry $|\epsilon_{1\tau}|$, as it follows from Eqs (2.14) and (2.15), the relevant wash-out mass parameters are $\widetilde{m}_{1\tau} \approx \widetilde{m}_{1o} \approx m_3$. Consequently, for $m_3 \ll 10^{-3}$ eV, one also has $\widetilde{m}_{1\tau}, \widetilde{m}_{1o} \ll 10^{-3}$ eV and for $M_1 < 10^{12}$ GeV the baryon asymmetry generated under these conditions is strongly suppressed, $|Y_B| \ll 8.6 \times 10^{-11}$.

**Figure 2.3:** The dependence of $|Y_B|$ on $\alpha_{32}$ (Majorana CP violation), in the case of IH spectrum, real $R_{1j}R_{1k}$, $R_{11} = 0$, $M_1 = 10^{11}$ GeV, and for $i$) $s_{13} = 0.2$, $\delta = 0$ $(\pi)$, $|R_{12}| = 0.34$ $(0.38)$, $m_3 = 6.7$ $(4.3) \times 10^{-3}$eV, sign$(R_{12}R_{13}) = +1$ (left panel, red (blue) line), and $ii$) $s_{13} = 0$, sign$(R_{12}R_{13}) = -1$, $|R_{12}| = 0.41$, $m_3 = 4.2 \times 10^{-3}$eV (right panel). The values of $m_3$ and $|R_{12}|$ used maximise $|Y_B|$ at $i$) $\alpha_{32} = \pi/2$ $(2\pi/3)$ and $ii$) $\alpha_{32} = 3\pi/2$. The horizontal dotted lines indicate the range of $|Y_B|$ compatible with observations: $|Y_B| \in [8.0, 9.2] \times 10^{-11}$.

### 2.1.3 Analytical estimates: the case $R_{12} = 0$

One obtains similar conclusions in the case of $R_{12} = 0$ and $R_{11}, R_{13} \neq 0$. The corresponding formulae can be obtained from those derived previously for $R_{11} = 0$ by replacing $R_{12}$ with $R_{11}$, $U^*_{\tau 2}$ with $U^*_{\tau 1}$ and $m_2$ with $m_1 = \sqrt{m_3^2 + |\Delta m_A^2| - \Delta m_\odot^2} \cong \sqrt{m_3^2 + |\Delta m_A^2|} = m_2$. In this case $|\epsilon_{1\tau}| \propto |\text{Im}(U^*_{\tau 1}U_{\tau 3})| = |c_{23}c_{13}(s_{12}s_{23} \mp c_{12}c_{23}s_{13}) \sin \alpha_{31}/2|$, where the minus (plus) sign corresponds to $\delta = 0$ $(\pi)$. Evidently, the relevant Majorana phase [4] is $\alpha_{31}/2$. Moreover, one has $0.19|\sin \alpha_{31}/2| \lesssim |\text{Im}(U^*_{\tau 1}U_{\tau 3})| \lesssim 0.35|\sin \alpha_{31}/2|$, while for $s_{13} = 0$, $|\text{Im}(U^*_{\tau 1}U_{\tau 3})| \cong 0.27|\sin \alpha_{31}/2|$. Therefore, the maximal value of $|\epsilon_{1\tau}|$ for $R_{12} = 0$ is smaller approximately by a factor of 1.3 than the maximal value of $|\epsilon_{1\tau}|$ when $R_{11} = 0$. As a consequence, the minimal $M_1$ for which successful leptogenesis is realized can be expected to be bigger by a factor of approximately 1.3 than the one obtained previously in the case of $R_{11} = 0$. This is confirmed by the numerical computation. For example, for $s_{13} = 0.2$, $\delta = \pi$, sign$(R_{12}R_{13}) = -1$ and the values of $|R_{11}| = 0.38$ and $m_3 = 4.5 \times 10^{-3}$eV (which maximize $|Y_B|$ at $\alpha_{31} = 2\pi/3$), one obtain:

$$\max(|Y_B|) \cong 2.2 \times 10^{-12} \left( \frac{\sqrt{|\Delta m_A^2|}}{0.05 \text{ eV}} \right) \left( \frac{M_1}{10^9 \text{ GeV}} \right). \tag{2.18}$$

---

[4]Note that the Majorana phase $\alpha_{32}$ $(R_{11} = 0)$ or $\alpha_{31}$ $(R_{12} = 0)$, relevant for leptogenesis in the case of IH spectrum and real matrix $R$, does not coincide with the Majorana phase $\alpha_{21}$, which together with $\sqrt{|\Delta m_A^2|}$ and $\sin^2 \theta_{12}$ determines the values of the effective Majorana mass in neutrinoless double beta decay (see Section 1.2.4).

Consequently, the observed value of $|Y_B|$ can be reproduced for $M_1 \gtrsim 3.7 \times 10^{10}$ GeV.

### 2.1.4 Leptogenesis due to Dirac CP violation

Now the Majorana phases are assumed to be CP conserving, $\alpha_{21} = 2\pi k$ and $\alpha_{31} = 2\pi k'$ $(k, k' = 0, 1, 2, ...)$ and the *only* source of CP violation is provided by the Dirac phase $\delta$.

Note that the case in which $\text{Im}(R_{1j}R_{1k}) \neq 0$, $R_{11} = 0$ $(R_{12} = 0)$ and the Majorana phase $\alpha_{32}$ $(\alpha_{31})$ entering into the expression for $\epsilon_{1\tau}$ takes the CP conserving value $\alpha_{32(31)} = \pi$, corresponds to *CP violation* given not only by the *Dirac phase* $\delta \neq k\pi$ $(k = 0, 1, 2, ...)$, but also by the *orthogonal matrix $R$* (see discussion in the end of Section 1.5). Therefore this case is not taken into account in the present analysis.

For $R_{11} = 0$ and $\alpha_{32} = 0$, $|\epsilon_{1\tau}| \propto |\text{Im}(U_{\tau 2}^* U_{\tau 3})| = c_{23}^2 c_{13} s_{12} s_{13} |\sin\delta| \lesssim 0.054 |\sin\delta|$. Thus, for given $M_1$ the maximum baryon asymmetry $|Y_B|$ is smaller by a factor of about 10 than the possible $\max(|Y_B|)$ in the case of CP violation due to the Majorana phase(s) in $U$. The wash-out mass parameter $\widetilde{m}_{1\tau}$, corresponding to $R_{12}$ maximizing $|\epsilon_{1\tau}|$ (see Eq. (2.8)), is given by:

$$\widetilde{m}_{1\tau} \cong \frac{m_2 \, m_3}{m_3 + m_2} \left[ (c_{12} s_{23} - \rho_{23} c_{13} c_{23})^2 + s_{12}^2 s_{13}^2 c_{23}^2 + 2 s_{12} s_{13} c_{23} (c_{12} s_{23} - \rho_{23} c_{13} c_{23}) \cos\delta \right] , \quad (2.19)$$

while $\widetilde{m}_{1o}$ is determined by Eq. (2.15). Depending on the value of $\rho_{23}$, there are two quite different cases to be considered.

If $\rho_{23} = -1$, the terms $s_{12}^2 s_{13}^2 c_{23}^2$ and proportional to $2 s_{12} s_{13} c_{23} \cos\delta$ in the expression for $\widetilde{m}_{1\tau}$, Eq. (2.19), are subdominant and can be neglected. [5] Thus, $\widetilde{m}_{1\tau}$ and $\widetilde{m}_{1o}$ practically do not depend on $\delta$ and for $c_{23} = s_{23} = 1/\sqrt{2}$ one has: $\widetilde{m}_{1\tau} \cong 0.5 (c_{12} + c_{13})^2 m_2 m_3 / (m_2 + m_3) \cong 1.66 m_2 m_3 / (m_2 + m_3)$, $\widetilde{m}_{1o} \cong 0.34 m_2 m_3 / (m_3 + m_2)$. Both the CP asymmetry $|\epsilon_{1\tau}|$ and the baryon asymmetry $|Y_B|$ have a maximum value for $\delta = \pi/2 + k\pi$ $(k = 0, 1, ...)$. The dependence of $|Y_B|$ on $m_3$ is analogous to that in the case of CP violation due to the Majorana phase(s) in $U$: there are two similar maxima corresponding to the CP asymmetry being predominantly in the $\tau-$flavour and in the $(e + \mu)-$flavour, respectively. The two maxima are separated by a deep minimum of $|Y_B|$ (see Fig. 2.4). The maxima occur at $m_3 \cong 7.5 \times 10^{-4}$ eV $(|R_{12}| \cong 0.12)$ and at $m_3 \cong 4.9 \times 10^{-3}$ eV $(|R_{12}| \cong 0.30)$, *i.e.* at values of $m_3$ which differ by a factor of about seven. At the first (second) maximum, $\eta(0.66\widetilde{m}_{1\tau}) - \eta(0.71\widetilde{m}_{1o}) \cong 0.044 (-0.046)$ and the absolute value of the baryon asymmetry is given by:

$$|Y_B| \cong 3.5 \ (3.7) \times 10^{-13} |\sin\delta| \left( \frac{\sin\theta_{13}}{0.2} \right) \left( \frac{\sqrt{|\Delta m_A^2|}}{0.05 \ \text{eV}} \right) \left( \frac{M_1}{10^9 \ \text{GeV}} \right) . \quad (2.20)$$

Therefore, the measured value of $|Y_B|$ can be reproduced for $M_1 \gtrsim 2.3 \ (2.2) \times 10^{11}$ GeV. This upper bound allows to derive a lower limit on $|\sin\theta_{13} \sin\delta|$ and thus on $\sin\theta_{13}$:
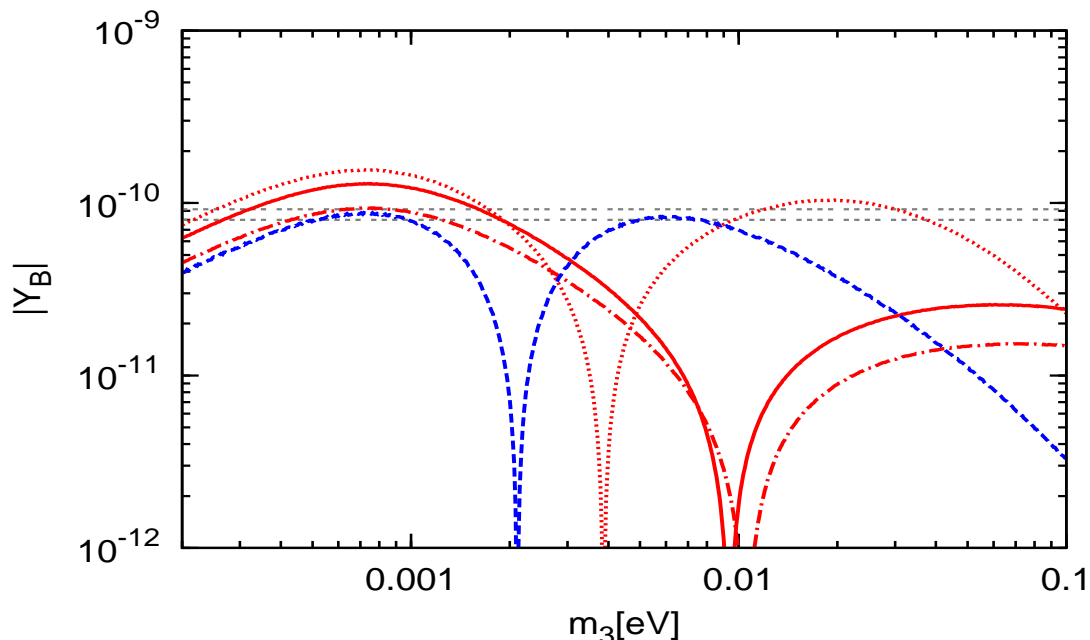
$$|\sin\theta_{13} \sin\delta| \gtrsim 0.087 \,, \quad \sin\theta_{13} \gtrsim 0.087 \,. \quad (2.21)$$

The preceding lower bound corresponds to

$$|J_{\text{CP}}| \gtrsim 0.02 \,, \quad (2.22)$$

---

[5] The term $\propto 2 s_{12} s_{13} c_{23} \cos\delta$, for instance, gives a relative contribution to $\widetilde{m}_{1\tau}$ not exceeding 10%.

**Figure 2.4:** The dependence of $|Y_B|$ on $m_3$ in the case of spectrum with inverted ordering (hierarchy), real $R_{1j}R_{1k}$ and Dirac CP violation, for $R_{11} = 0$, $\delta = \pi/2$, $s_{13} = 0.2$, $s_{12}^2 = 0.3$, $\alpha_{32} = 0$, $M_1 = 2.5 \times 10^{11}$ GeV and $\text{sign}(R_{12}R_{13}) = +1\ (-1)$ (red lines (blue dashed line)). The baryon asymmetry $|Y_B|$ was calculated for a given $m_3$, using the value of $|R_{12}|$ for which the CP asymmetry $|\epsilon_{1\tau}|$ has a maximum. The results shown for $\text{sign}(R_{12}R_{13}) = +1$ are obtained for $\sin^2\theta_{23} = 0.50\ (0.36)\ [0.64]$, red solid (dotted) [dash-dotted] line, while those for $\text{sign}(R_{12}R_{13}) = -1$ correspond to $\sin^2\theta_{23} = 0.5$. The horizontal dotted lines indicate the range of $|Y_B|$ compatible with observations: $|Y_B| \in [8.0, 9.2] \times 10^{-11}$.

where $J_{\text{CP}}$ is the rephasing invariant associated with the Dirac phase $\delta$ (see Eq. (1.18)), which controls the magnitude of CP violating effects in neutrino oscillations. Values of $s_{13}$ larger than the bound given in Eq. (2.21) can be probed in the forthcoming Double CHOOZ [38] and future reactor neutrino experiments [39]. CP violating effects with magnitude determined by $|J_{\text{CP}}|$ satisfying (2.22) are within the sensitivity of the next generation of neutrino oscillation experiments, designed to search for CP or T symmetry violations in the oscillations [39]. Since in the case under discussion the wash-out factor $|\eta_B| \equiv |\eta(0.66\widetilde{m}_{1\tau}) - \eta(0.71\widetilde{m}_{1o})|$ in the expression for $|Y_B|$ practically does not depend on $s_{13}$ and $\delta$, while both $|Y_B| \propto |s_{13}\sin\delta|$ and $|J_{\text{CP}}| \propto |s_{13}\sin\delta|$, there is a direct relation between $|Y_B|$ and $|J_{\text{CP}}|$ for given $m_3$ (or $m_2$) and $M_1$:

$$|Y_B| \cong 1.8 \times 10^{-10}\, |J_{\text{CP}}|\, |\eta_B|\, \frac{m_2 - m_3}{\sqrt{|\Delta m_A^2|}} \left(\frac{\sqrt{|\Delta m_A^2|}}{0.05\ \text{eV}}\right) \left(\frac{M_1}{10^9\ \text{GeV}}\right), \qquad (2.23)$$

where $\eta_B = \eta_B(m_2 m_3/(m_2 + m_3), \theta_{12}, \theta_{23})$ and, again, the best fit values of $\sin^2\theta_{12}$ and $\sin^2\theta_{23}$ are assumed in the computation. In the case of IH spectrum one has $(m_2 - m_3)/\sqrt{|\Delta m_A^2|} \cong 1$ and

## 2.1 Inverted hierarchical light neutrino mass spectrum

$m_2 m_3/(m_2 + m_3) \cong m_3$. A similar relation between $|Y_B|$ and $|J_{CP}|$ holds in an analogous case of normal hierarchical light neutrino mass spectrum [54].

Relatively different results are obtained if $\rho_{23} = +1$. Now there is a strong compensation between the terms in the round brackets in the expression (2.19) for $\widetilde{m}_{1\tau}$, such that: $\widetilde{m}_{1\tau} \ll m_2 m_3/(m_2+m_3)$. Correspondingly, one has $\widetilde{m}_{1o} \cong 2m_2 m_3/(m_2+m_3) \gg \widetilde{m}_{1\tau}$. Thus, $\widetilde{m}_{1o}$ practically does not depend on $\delta$ and on the neutrino mixing angles. The two wash-out mass parameters $\widetilde{m}_{1o}$ and $\widetilde{m}_{1\tau}$ can differ by a factor $\sim 100$. Indeed, for $s_{23}^2 = c_{23}^2 = 0.5$ and $s_{13} = 0.2$ and $s_{12}^2 = 0.30$ one finds $\widetilde{m}_{1\tau}/\widetilde{m}_{1o} \cong 0.5(0.0162 - 0.0156\cos\delta)$. For fixed $\sin^2\theta_{12} = 0.30$, the magnitude of the ratio $\widetilde{m}_{1\tau}/\widetilde{m}_{1o}$ (which is practically independent of $m_2 m_3/(m_2 + m_3)$) is very sensitive to the value of $\theta_{23}$: for $s_{23}^2 = 0.64$ one has $\widetilde{m}_{1\tau}/\widetilde{m}_{1o} \cong 0.5(0.0066 + 0.0043 s_{13}^2/0.04 - 0.0107(s_{13}/0.2)\cos\delta)$, while if $s_{23}^2 = 0.36$ one obtains $\widetilde{m}_{1\tau}/\widetilde{m}_{1o} \cong 0.5(0.0794 + 0.0077 s_{13}^2/0.04 - 0.0494(s_{13}/0.2)\cos\delta)$. The maxima of the asymmetry $|Y_B|$ take place at $\delta = \pi/2 + k\pi$ ($k = 0, 1, 2, ...$). For $\delta = \pi/2$, $s_{13} = 0.2$ and $s_{23}^2 = 0.64\,(0.5)\,[0.36]$ one has $\widetilde{m}_{1\tau}/\widetilde{m}_{1o} \cong 0.52 \times 10^{-2}\,(0.81 \times 10^{-2})\,[4.36 \times 10^{-2}]$. Therefore the two maxima of $|Y_B|$ as a function of $m_3$, corresponding to the CP asymmetry being predominantly in the $(e + \mu)-$flavour and in the $\tau-$flavour, can be expected to occur at values of $m_3$ which for $s_{23}^2 = 0.36\,(0.5)\,[0.64]$ and $s_{12}^2 = 0.30$ would differ by a factor of $\widetilde{m}_{1o}/\widetilde{m}_{1\tau} \sim 20\,(120)\,[190]$. The position of the deep minimum of $|Y_B|$ between the two maxima would also be very different for $s_{23}^2 = 0.36$ and $s_{23}^2 = 0.5\,(0.64)$. Obviously, the relative position on the $m_3$ axis of two maxima and the minimum of $|Y_B|$ under discussion will depend not only on the precise value of $\sin^2\theta_{23}$, but also on the precise value of $\sin^2\theta_{12}$.

To be more concrete, the maximum of $|Y_B|$ (as a function of $m_3$), associated with the CP asymmetry being predominantly in the $(e + \mu)-$flavour, takes place at $m_3 \cong 7.5 \times 10^{-4}$ eV, *i.e.* in the region of IH spectrum. At this value of $m_3$, $\eta(0.71\widetilde{m}_{1o})$ is maximum, $\eta(0.71\widetilde{m}_{1o}) \cong 0.068$, while $\eta(0.66\widetilde{m}_{1\tau}) \lesssim 0.005 \ll \eta(0.71\widetilde{m}_{1o})$, resulting in

$$|Y_B| \cong 5.1 \times 10^{-13}\,|\sin\delta|\,\frac{\sin\theta_{13}}{0.2}\,\left(\frac{\sqrt{|\Delta m_A^2|}}{0.05\text{ eV}}\right)\left(\frac{M_1}{10^9\text{ GeV}}\right)\,. \qquad (2.24)$$

The position of this maximum does not depend on $\theta_{12}$, $\theta_{23}$, $\theta_{13}$ and $\delta$ (see Fig. 2.4). Thus, the measured value of $|Y_B|$ can be reproduced for a somewhat smaller value of $M_1 \gtrsim 1.6 \times 10^{11}$ GeV than the corresponding value of $M_1$ found for $\rho_{23} = -1$ (compare Eqs (2.20) and (2.24)). In the vicinity of the maximum there exists a correlation between the values of $|Y_B|$ and $|J_{CP}|$ similar to the one given in Eq. (2.23). Now the requirement of successful leptogenesis leads for $M_1 \lesssim 5 \times 10^{11}$ GeV to a somewhat less stringent lower limit on $|\sin\theta_{13}\sin\delta|$, and thus on $\sin\theta_{13}$ and $|J_{CP}|$:

$$|\sin\theta_{13}\sin\delta|,\ \sin\theta_{13} \gtrsim 0.063,\quad |J_{CP}| \gtrsim 0.015\,. \qquad (2.25)$$

The second maximum of $|Y_B|$, related to the possibility of the CP asymmetry being predominantly in the $\tau-$flavour, takes place, instead, at $m_2 m_3/(m_2 + m_3) \gtrsim 10^{-2}$ eV, *i.e.* for values of $m_3 \gtrsim 1.2 \times 10^{-2}$ eV in the region of neutrino mass spectrum with partial inverted hierarchy. In this case the factor in $|Y_B|$, which determines the position of the maximum as a function of $m_3$, is $\left((m_2 - m_3)/\sqrt{|\Delta m_A^2|}\right)\eta(0.66\widetilde{m}_{1\tau})$, rather than just $\eta(0.66\widetilde{m}_{1\tau})$. Taking this observation into account, it is not difficult to show that for $\delta = \pi/2$ and $s_{13} = 0.2$ maximizing $|Y_B|$, $s_{12}^2 = 0.30$ and,

*e.g.* $s_{23}^2 = 0.36$ (0.50), the maximum occurs at $m_3 \cong 1.8$ (5.0) $\times 10^{-2}$ eV. If $M_1 = 10^{11}$ GeV and $\sqrt{|\Delta m_A^2|} = 5.0 \times 10^{-2}$ eV, the value of $|Y_B|$ at this maximum reads: $|Y_B| \cong 4.4$ (1.1) $\times 10^{-11}$. For $s_{23}^2 = 0.64$ one has for the same values of the other parameters $\max(|Y_B|) \cong 0.6 \times 10^{-11}$. Obviously, if $m_3 \gtrsim 10^{-2}$ eV, the observed value of $|Y_B|$ can be reproduced for $M_1 \lesssim 5 \times 10^{11}$ GeV only if $s_{23}^2 < 0.50$. The position of the deep minimum of $|Y_B|$ at $m_3 \gtrsim 10^{-3}$ eV is also very sensitive to the value of $s_{23}^2$: for $\delta = \pi/2$, $s_{13} = 0.2$ and $s_{12}^2 = 0.30$, it takes place at $m_3 \cong 2 \times 10^{-3}$ eV if $s_{23}^2 = 0.36$, and at $m_3 \cong 10^{-2}$ eV in the case of $s_{23}^2 = 0.50$. These features of the dependence of $|Y_B|$ on $m_3$ are illustrated in Fig. 2.4.

One can perform a similar analysis in the case of real $R_{1j}R_{1k}$, $R_{12} = 0$ and $R_{11}, R_{13} \neq 0$. In this case, $|\epsilon_{1\tau}| \propto |\mathrm{Im}(U_{\tau 1}^* U_{\tau 3})| = c_{23}^2 c_{13} c_{12} s_{13} |\sin \delta| \lesssim 0.082 |\sin \delta|$ and

$$\widetilde{m}_{1\tau} \cong \frac{m_1 \, m_3}{m_3 + m_1} \left[ (s_{12}s_{23} + \rho_{13}c_{13}c_{23})^2 + c_{12}^2 c_{23}^2 s_{13}^2 - 2s_{13}c_{12}c_{23}(s_{12}s_{23} + \rho_{13}c_{23}c_{13})\cos\delta \right] , \quad (2.26)$$

$\widetilde{m}_{1o} = 2m_1 m_3/(m_3 + m_1) - \widetilde{m}_{1\tau}$, where $\rho_{13} \equiv \mathrm{sign}(R_{11}R_{13}) = \pm 1$ and $m_1 \cong m_2 = \sqrt{m_3^2 + |\Delta m_A^2|}$. For $\rho_{13} = +1$, the two maxima of $|Y_B|$ (as a function of $m_3$) have the same magnitude. They occur at $\delta \cong 3\pi/4$, $s_{13} = 0.2$ and $m_3 \cong 7.5 \times 10^{-4}$ (3.5 $\times 10^{-3}$) eV. The maximum baryon asymmetry exhibits rather strong dependence on $s_{23}^2$: for $s_{23}^2 = 0.36$ (0.50), $M_1 = 5 \times 10^{11}$ GeV and $\sqrt{|\Delta m_A^2|} = 5.0 \times 10^{-2}$ eV, $\max(|Y_B|)$ is approximately 1.7 (0.9) $\times 10^{-10}$. If $s_{23}^2 > 0.50$, however, it is impossible to reproduce the observed value of $|Y_B|$ for $M_1 \lesssim 5 \times 10^{11}$ GeV. The same negative result holds for any $s_{23}^2$ in the interval [0.36,0.64] if $s_{13} \lesssim 0.10$.

In the case of $\rho_{13} = -1$, $|Y_B| \propto c_{23}^2$ in the region of the maximum of $|Y_B|$ at $m_3 \cong 7.5 \times 10^{-4}$ eV, associated with the CP asymmetry being predominantly in the $(e + \mu)-$ flavour. The baryon asymmetry $|Y_B|$ has a maximum for $\delta = \pi/2$, which maximizes the CP asymmetry $|\epsilon_{1\tau}|$ as well. For $s_{13} = 0.2$, $c_{23}^2 = 0.5$, $M_1 = 5 \times 10^{11}$ GeV and $\sqrt{|\Delta m_A^2|} = 5.0 \times 10^{-2}$ eV, the absolute value of the baryon asymmetry is therefore:

$$|Y_B| \cong 9.0 \times 10^{-13} \, |\sin\delta| \, \frac{\sin\theta_{13}}{0.2} \left( \frac{\sqrt{|\Delta m_A^2|}}{0.05 \text{ eV}} \right) \left( \frac{M_1}{10^9 \text{ GeV}} \right) . \quad (2.27)$$

Thus, the observed value of the baryon asymmetry can be reproduced for relatively small values of $|\sin\theta_{13} \sin\delta|$ and correspondingly of $|J_{\mathrm{CP}}|$:

$$|\sin\theta_{13} \sin\delta|, \ \sin\theta_{13} \gtrsim 0.036 , \quad |J_{\mathrm{CP}}| \gtrsim 0.0086 . \quad (2.28)$$

In contrast, the position (with respect to $m_3$) of the maximum of $|Y_B|$, associated with the CP asymmetry being predominantly in the $\tau-$flavour, and its magnitude, exhibit rather strong dependence on $s_{23}^2$. For $s_{23}^2 = 0.36$ (0.50) [0.64], the maximum of $|Y_B|$ is located at $m_3 \cong 0.7$ (1.5) [3.0] $\times 10^{-2}$ eV. For $M_1 \lesssim 5 \times 10^{11}$ GeV, the measured value of $|Y_B|$, $8.0 \times 10^{-11} \lesssim |Y_B| \lesssim 9.2 \times 10^{-11}$, can be reproduced provided $|\sin\theta_{13} \sin\delta| \gtrsim 0.046$ (0.053) [0.16] if $s_{23}^2 = 0.36$ (0.50) [0.64].

## 2.2 Normal hierarchical neutrino mass spectrum

Results for light neutrino mass spectrum with normal ordering are presented in the following. The case of negligible $m_1$ and real (CP conserving) elements $R_{1j}$ of $R$ was analysed in detail in [54]. It was found that, if the only source of CP violation is the Dirac phase $\delta$ in the PMNS matrix, the observed value of the baryon asymmetry can be reproduced if $|\sin\theta_{13}\sin\delta| \gtrsim 0.09$. Given the upper limit $|\sin\theta_{13}\sin\delta| < 0.2$, this requires $M_1 \gtrsim 2 \times 10^{11}$ GeV. The quoted lower limit on $|\sin\theta_{13}\sin\delta|$ implies that $\sin\theta_{13} \gtrsim 0.09$ and that $|J_{\mathrm{CP}}| \gtrsim 2 \times 10^{-2}$. If, however, the Dirac phase $\delta$ has a CP conserving value $\delta \cong k\pi$ ($k = 0, 1, 2, ...$) and the requisite CP violation is due exclusively to the Majorana phases $\alpha_{21,31}$ in $U$, the observed $Y_B$ can be obtained for $M_1 \gtrsim 4 \times 10^{10}$ GeV [54]. For $M_1 = 5 \times 10^{11}$ GeV, for which the flavour effects are fully developed, the measured value of $Y_B$ can be reproduced for a rather small value of $|\sin\alpha_{32}/2| \cong 0.15$, where, as usual, $\alpha_{32} \equiv \alpha_{31} - \alpha_{21}$.

In searching for possible significant effects of non negligible $m_1$ in leptogenesis, values of $m_1$ as large as 0.05 eV are taking into account. For $3 \times 10^{-3}$ eV $\lesssim m_1 \lesssim 0.10$ eV, the neutrino mass spectrum is not hierarchical, but the spectrum exhibits a partial hierarchy, *i.e.* $m_1 < m_2 < m_3$.

Two simple possibilities are analyzed in the following: $|R_{11}| \ll 1$ and $|R_{12}| \ll 1$. Results of a more general analysis performed without making a priori assumptions about the real parameters $R_{11}$ and $R_{12}$ are discussed further in the text.

### 2.2.1 Analytical estimates: the case $R_{11} = 0$

The CP asymmetry $\epsilon_{1\tau}$ in this case is given by:

$$\epsilon_{1\tau} \cong -\frac{3M_1\sqrt{\Delta m_{\mathrm{A}}^2}}{16\pi v^2}\left(\frac{m_3}{m_2}\right)^{\frac{1}{2}}\frac{\sqrt{\Delta m_{\mathrm{A}}^2}}{m_2 + m_3}\,\rho_{23}\,r\,\mathrm{Im}\left(U_{\tau 2}^* U_{\tau 3}\right),\qquad(2.29)$$

where now

$$r = \frac{|R_{12}R_{13}|}{|R_{12}|^2 + \frac{m_3}{m_2}|R_{13}|^2}\qquad(2.30)$$

and $\mathrm{Im}(U_{\tau 2}^* U_{\tau 3})$ is given in Eq. (2.5). The ratio in (2.30) is similar to the ratio in Eq. (2.4). Note, however, that the masses $m_{2,3}$ present in Eqs (2.2) and (2.4) are very different from the masses $m_{2,3}$ in Eqs (2.29) and (2.30). Using again the fact that $R_{12}^2 + R_{13}^2 = 1$, it is easy to find that $r$ has a maximum for

$$R_{12}^2 = \frac{m_3}{m_2 + m_3},\quad R_{13}^2 = \frac{m_2}{m_2 + m_3},\quad R_{13} < R_{12},\qquad(2.31)$$

where $m_2 = \sqrt{m_1^2 + \Delta m_{\odot}^2}$ and $m_3 = \sqrt{m_1^2 + \Delta m_{\mathrm{A}}^2}$, with $\Delta m_{\mathrm{A}}^2 > 0$. At the maximum:

$$\max(r) = \frac{1}{2}\left(\frac{m_2}{m_3}\right)^{\frac{1}{2}}.\qquad(2.32)$$

For the value of $R_{12}$ ($R_{13}$), which maximizes the ratio $|r|$ and, correspondingly, the asymmetry $|\epsilon_{1\tau}|$ in (2.29), the relevant wash-out mass parameters $\widetilde{m}_{1\tau}$ and $\widetilde{m}_{1o}$ are given by Eqs (2.14) and

(2.15) with $m_2$ and $m_3$ given above. Since now $m_2 \gtrsim \sqrt{\Delta m_\odot^2} \cong 0.9 \times 10^{-2}$ eV and $m_3 \gtrsim \sqrt{\Delta m_A^2} \cong 5.0 \times 10^{-2}$ eV, one has $m_2 m_3/(m_2 + m_3) \gtrsim 0.7 \times 10^{-2}$ eV. The lightest neutrino mass $m_1$ can have any effect on the generation of the baryon asymmetry $Y_B$ only if $m_1^2 \gg \Delta m_\odot^2$ and if $m_1$ is non negligible with respect to $\sqrt{\Delta m_A^2}$. Indeed, for the values of $m_1$ of interest, one has $m_2 m_3/(m_2 + m_3) \gtrsim 10^{-2}$ eV and the baryon asymmetry will be generated in the "strong wash-out" regime, unless there is a strong cancellation between the first two and the third terms in the expression for $\widetilde{m}_{1\tau}$ (see Eq. (2.14)). Obviously, the possibility of such a cancellation depends critically on $\rho_{23} \equiv \text{sign}(R_{12} R_{13})$. Moreover, it results from the dependence of $\max(|\epsilon_{1\tau}|)$, $\widetilde{m}_{1\tau}$ and $\widetilde{m}_{1o}$ on $m_{2,3}$, that with the increasing of $m_1$ beyond $10^{-2}$ eV the predicted baryon asymmetry decreases.

### 2.2.2  Leptogenesis due to Majorana CP violation

Suppose first that the Dirac phase $\delta$ in the PMNS matrix has a CP conserving value, $\delta = \pi k$ ($k = 0, 1, 2, ...$) and that the only source of CP violation are the Majorana phases $\alpha_{21,31}$ in the PMNS matrix $U$. In the specific case of $R_{11} = 0$, the relevant CP violating parameter is the effective Majorana phase $\alpha_{32}$. In this case $|\epsilon_{1\tau}| \propto \text{Im}(U_{\tau 2}^* U_{\tau 3}) \cong c_{23}^2 c_{12} |\sin \alpha_{32}/2| \cong 0.42 |\sin \alpha_{32}/2|$. The effect of $\theta_{13}$ is always subleading in the present computation and in what follows it is always assumed $\sin \theta_{13} = 0.2$, unless differently specified. The wash-out mass parameter $\widetilde{m}_{1\tau}$ is:

$$\widetilde{m}_{1\tau} \cong m_2 \frac{m_3}{m_2 + m_3} \left[ c_{12}^2 s_{23}^2 + c_{23}^2 - 2\,\rho_{23}\, c_{23}\, s_{23}\, c_{12}\, \cos \frac{\alpha_{32}}{2} \right]. \tag{2.33}$$

Therefore, if $\cos \alpha_{32}/2 \cong 0$, the baryon asymmetry $Y_B$ is produced in the strong wash-out regime and for $M_1 < 10^{12}$ GeV the calculated baryon asymmetry is too small to reproduce observed value, $Y_B \cong 8.77 \times 10^{-11}$. On the other hand, the maximum of $|Y_B|$ in the case under discussion occurs for $\alpha_{32} \cong \pi/2 + \pi k$ ($k = 0, 1, 2, ...$). There are two distinctive possibilities to be considered, corresponding to the two possible signs of $\rho_{23}\,\text{sign}(\cos \alpha_{32}/2)$. If $\rho_{23}\,\text{sign}(\cos \alpha_{32}/2) = +1$, then $\widetilde{m}_{1\tau} \cong 0.25 m_2 m_3/(m_2 + m_3)$, the asymmetry in the $\tau-$flavour (($e + \mu)-$flavour) is produced in the weak (strong) wash-out regime and for, $e.g.$ $m_1 = 2 \times 10^{-2}$ ($5 \times 10^{-2}$) eV, one obtains the following value of the baryon asymmetry $|Y_B|$:

$$|Y_B| \cong 1.20\,(0.36) \times 10^{-12} \left( \frac{\sqrt{\Delta m_A^2}}{0.05\ \text{eV}} \right) \left( \frac{M_1}{10^9\ \text{GeV}} \right), \quad \text{for} \quad \alpha_{32} \cong \pi/2 + \pi k. \tag{2.34}$$

Thus, for $m_1 = 2 \times 10^{-2}\,(5 \times 10^{-2})$ eV the measured value of $Y_B$ can be obtained if $M_1 \gtrsim 7.2 \times 10^{10}\,(2.4 \times 10^{11})$ GeV.

These results are illustrated in Fig. 2.5, showing the correlated values of $M_1$ and $m_1$ for which one can have successful leptogenesis. The figure is obtained using the same general method of analysis employed before in order to realize Fig. 2.1: for fixed $m_1$, in the interval $10^{-10} \leq m_1 \leq 0.05$ eV, a thorough scan of the relevant parameter space is performed in the calculation of $|Y_B|$, searching for a possible enhancement or suppression of the baryon asymmetry with respect to the case $m_1 = 0$. The real matrix elements $R_{1j}$, are allowed to vary in their full ranges determined by the condition
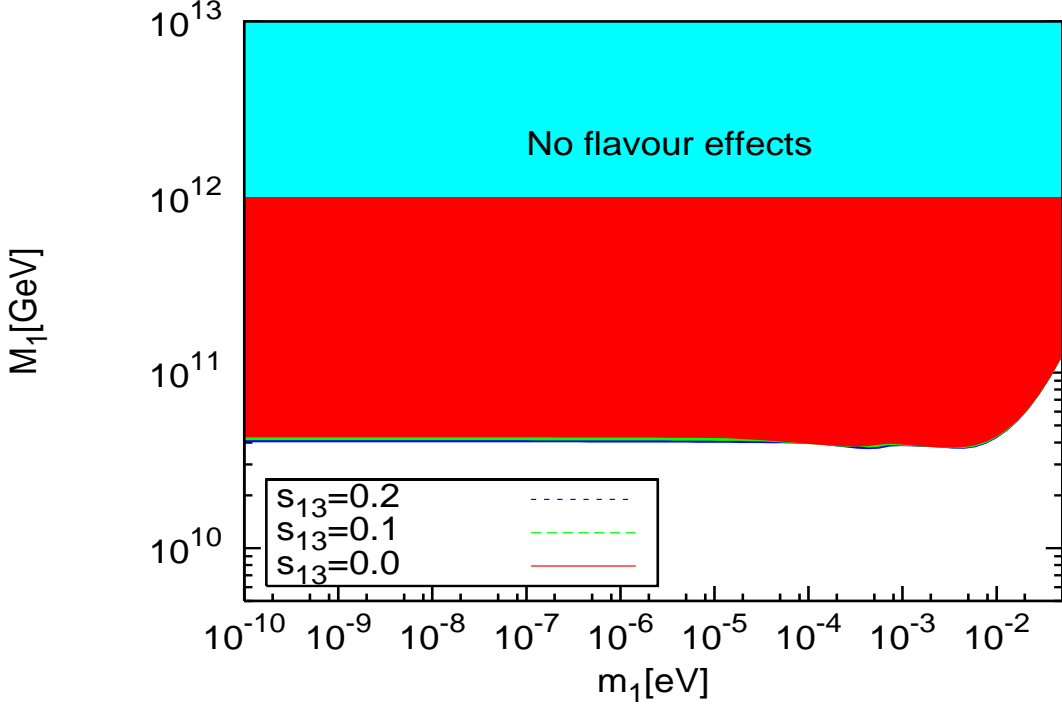
**Figure 2.5:** Values of $m_1$ and $M_1$ for which flavoured leptogenesis is successful and baryon asymmetry $Y_B = 8.6 \times 10^{-11}$ can be generated (red shaded area). The figure corresponds to light neutrino mass spectrum with normal ordering. The CP violation necessary for leptogenesis is due to the Majorana and Dirac phases in the PMNS matrix. The results shown are obtained using the best fit values of neutrino oscillation parameters: $\Delta m_\odot^2 = 8.0 \times 10^{-5}$ eV$^2$, $\Delta m_A^2 = 2.5 \times 10^{-3}$ eV$^2$, $\sin^2 \theta_{12} = 0.30$ and $\sin^2 2\theta_{23} = 1$.

of orthogonality of $R$: $R_{11}^2 + R_{12}^2 + R_{13}^2 = 1$. The Majorana and Dirac phases $\alpha_{21,31}$ and $\delta$ are varied in the interval $[0, 2\pi]$. The calculations are performed again for three values of the CHOOZ angle, $\sin \theta_{13} = 0; 0.1; 0.2$. The relevant heavy Majorana neutrino mass $M_1$ is varied in the interval $10^9$ GeV $\lesssim M_1 \lesssim 10^{12}$ GeV. For given $m_1$, the minimal value of the mass $M_1$, for which the leptogenesis is successful, generating $Y_B \cong 8.77 \times 10^{-11}$, is obtained for the values of the other parameters which maximize $|Y_B|$. The $\min(M_1)$ thus calculated does not show any significant dependence on $s_{13}$. For $m_1 \lesssim 7.5 \times 10^{-3}$ eV there are not relevant effects of $m_1$ in leptogenesis: the behavior practically coincide with that corresponding to $m_1 = 0$ and derived in [54]. The value of $\min(M_1) \cong 4 \times 10^{10}$ GeV, shown in Fig. 2.5, corresponds to $R_{12}^2 \cong 0.85$, $R_{13}^2 \cong 0.15$ and $\alpha_{32} \cong \pi/2$ ($\rho_{23}\mathrm{sign}(\cos \alpha_{32}/2) = +1$). For $7.5 \times 10^{-3}$ eV $\lesssim m_1 \leq 5 \times 10^{-2}$ eV, the predicted baryon asymmetry $Y_B$, for given $M_1$, is generically smaller with respect to the asymmetry $Y_B$ one finds for $m_1 = 0$. Thus, successful leptogenesis is possible for larger values of $\min(M_1)$. The corresponding suppression factor increases with $m_1$ and for $m_1 \cong 5 \times 10^{-2}$ eV values of $M_1 \gtrsim 10^{11}$ GeV are required.

For the second choice, $\rho_{23} \mathrm{sign}(\cos \alpha_{32}/2) = -1$, both the asymmetries in the $\tau-$flavour and in

the $(e+\mu)-$flavour are generated under the conditions of strong wash-out effects. Correspondingly, it is impossible to have a successful leptogenesis for $M_1 < 10^{12}$ GeV, if $m_1 \cong 5 \times 10^{-2}$ eV. If $m_1$ has a somewhat lower value, say $m_1 = 2 \times 10^{-2}$ eV, the wash-out of the $(e+\mu)-$flavour asymmetry is less severe ($\widetilde{m}_{1o} \cong 8.6 \times 10^{-3}$ eV) and the observed $Y_B$ can be reproduced for $\alpha_{32} = \pi/2 + \pi k$ and $M_1 \gtrsim 2.5 \times 10^{11}$ GeV.

### 2.2.3  Leptogenesis due to Dirac CP violation

If the Majorana phases $\alpha_{21,31}$ have CP conserving values and the only source of CP violation is the Dirac phase $\delta$ in $U$, one has $|\epsilon_{1\tau}| \propto |c_{23}^2 c_{13} s_{12} s_{13} \sin \delta| \lesssim 0.054 |\sin \delta|$. The factor $c_{23}^2 c_{13} s_{12} s_{13}$ in $|\epsilon_{1\tau}|$ is smaller by approximately one order of magnitude than the analogous factor $c_{23}^2 c_{12}$ which enters in the case, considered before, of a CP asymmetry due only to Majorana-type CP violation in the PMNS matrix. Such relative suppression, encountered in the Dirac-type CP violating scenario, makes it impossible to generate the observed value of the baryon asymmetry for $M_1 \lesssim 5 \times 10^{11}$ GeV.

### 2.2.4  Analytical estimates: the cases $R_{13} = 0$ and $R_{12} = 0$

For a light neutrino mass spectrum with normal ordering (hierarchy) and real matrix $R$, with $R_{13}$ approximately zero, the term $\propto R_{11} R_{12}$ in the expression for $\epsilon_{1\tau}$ is the dominant one. The numerical analysis shows, indeed, that for $R_{13} = 0$ it is impossible to have successful leptogenesis for $m_1 \lesssim 0.05$ eV and $M_1 < 10^{12}$ GeV, if the requisite CP violation is due to the Majorana and/or Dirac phases in $U$.

On the other hand, very different results are obtained if $R_{12} = 0$, while $R_{11} R_{13} \neq 0$. In this case the expression for the CP asymmetry $\epsilon_{1\tau}$ can be derived formally from Eq. (2.29) by replacing $m_2$ with $m_1$, $\rho_{23}$ with $\rho_{13}$, $U_{\tau 2}^*$ with $U_{\tau 1}^*$ and the ratio $r$ with

$$r = \frac{|R_{11} R_{13}|}{|R_{11}|^2 + \frac{m_3}{m_1} |R_{13}|^2} \ , \quad R_{11}^2 + R_{13}^2 = 1 \ . \tag{2.35}$$

As in the similar cases discussed earlier, the ratio $r$ and $|\epsilon_{1\tau}|$ take the maximum value for

$$R_{11}^2 = \frac{m_3}{m_1 + m_3} \ , \quad R_{13}^2 = \frac{m_1}{m_1 + m_3} \ , \tag{2.36}$$

with $\max(r) = 0.5(m_1/m_3)^{\frac{1}{2}}$, while the expression of the CP asymmetry $|\epsilon_{1\tau}|$ at the maximum reads:

$$|\epsilon_{1\tau}| \cong \frac{3M_1 \sqrt{\Delta m_{\mathrm{A}}^2}}{32 \pi v^2} \frac{\sqrt{\Delta m_{\mathrm{A}}^2}}{m_1 + m_3} |\mathrm{Im}\,(U_{\tau 1}^* U_{\tau 3})| \ . \tag{2.37}$$

The wash-out mass parameters $\widetilde{m}_{1\tau}$ and $\widetilde{m}_{1o}$, corresponding to the maximum of $|\epsilon_{1\tau}|$, are then

$$\widetilde{m}_{1\tau} = \frac{m_1 m_3}{m_1 + m_3} \left[ |U_{\tau 1}|^2 + |U_{\tau 3}|^2 + 2\rho_{13} \,\mathrm{Re}\,(U_{\tau 1}^* U_{\tau 3}) \right] \tag{2.38}$$

$$= \frac{m_1 m_3}{m_1 + m_3} \left( s_{12}^2 s_{23}^2 + c_{23}^2 + 2\rho_{13} c_{23} s_{23} s_{12} \cos \frac{\alpha_{31}}{2} \right) \ , \tag{2.39}$$
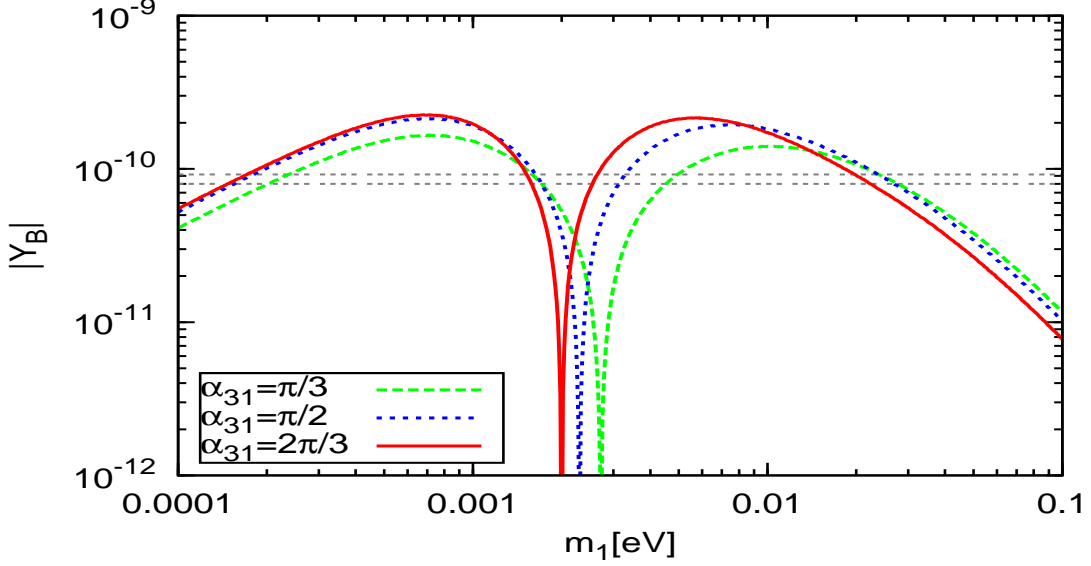
**Figure 2.6:** The dependence of $|Y_B|$ on $m_1$ in the case of neutrino mass spectrum with normal ordering and real $R_{1j}R_{1k}$, for $R_{12} = 0$, $s_{13} = 0$, $M_1 = 1.5 \times 10^{11}$ GeV and sign$(R_{11}R_{13}) = -1$. The red solid, the blue dotted, and the green dashed lines correspond to $\alpha_{31} = 2\pi/3$, $\pi/2$, and $\pi/3$ respectively. The figure is obtained for $\theta_{23} = \pi/4$.

where $s_{13} = 0$ in the second expression and $\widetilde{m}_{1o} = 2m_1m_3/(m_1 + m_3) - \widetilde{m}_{1\tau}$, as usual. Note that if $m_1 \ll m_3 \cong 5 \times 10^{-2}$ eV, the CP asymmetry $|\epsilon_{1\tau}|$ practically does not depend on $m_1$, while $\widetilde{m}_{1\tau,1o} \sim \mathcal{O}(m_1)$. This implies that the dependence of max($|Y_B|$) on $m_1$ as the latter increases, will exhibit the same features as in the case of IH spectrum discussed in previous sections: $|Y_B|$ has two maxima, corresponding to the CP asymmetry being predominantly in the $\tau-$flavour and in the $(e + \mu)-$flavour, respectively, separated with a deep minimum. The previous analysis of the similar case of IH light neutrino mass spectrum suggests that, for $s_{13} = 0$, the largest baryon asymmetry $|Y_B|$ is obtained for $\alpha_{31} \neq \pi(2k + 1)$ and $\rho_{13}\,\text{sign}(\cos\alpha_{31}/2) = -1$. These features are confirmed by the numerical calculations performed here and are illustrated in Fig. 2.6. The results shown in Fig. 2.6 are obtained for $\rho_{13} = -1$, $\sin\theta_{13} = 0$, $M_1 = 3 \times 10^{11}$ GeV, and three CP violating values of the Majorana phase $\alpha_{31}$, relevant for the calculation of $|Y_B|$: $2\pi/3$; $\pi/2$; $\pi/3$. There are two maxima and a deep minimum of $|Y_B|$ in the figure. The maximum values of $|Y_B|$ are reached for $\alpha_{31} \cong 2\pi/3$. As regards the dependence of $|Y_B|$ on $\alpha_{31}$ and $\rho_{13}$ in the case of $s_{13} = 0$, the following relation holds: $|Y_B(\rho_{13}, \alpha_{31})| = |Y_B(-\rho_{13}, 2\pi - \alpha_{31})|$. More precisely, these two maxima occur at $m_1 \cong 7.7 \times 10^{-4}$ eV and at $m_1 \cong 5.5 \times 10^{-3}$ eV, for which $\eta(0.66\widetilde{m}_{1\tau}) - \eta(0.71\widetilde{m}_{1o}) \cong -0.044$ and $0.047$, respectively. The complete compensation between $\eta(0.66\widetilde{m}_{1\tau})$ and $\eta(0.71\widetilde{m}_{1o})$, leading to $|Y_B| \cong 0$, takes place at $m_1 \sim 1.5 \times 10^{-3}$ eV. For $\alpha_{31} = 2\pi/3$, the baryon asymmetry at the two maxima reads:

$$|Y_B| \cong 1.5\,(1.4) \times 10^{-12} \left(\frac{\sqrt{|\Delta m_A^2|}}{0.05\text{ eV}}\right) \left(\frac{M_1}{10^9\text{ GeV}}\right). \tag{2.40}$$

Thus, one can have successful leptogenesis for $M_1 \gtrsim 5.3 \times 10^{10}$ GeV.

## 2.3 Summary

In the present chapter, the dependence of the baryon asymmetry of the Universe $Y_B$ on the lightest neutrino mass, $\min(m_j)$, was numerically studied, in the context of flavoured thermal leptogenesis, when the source of CP violation necessary for the generation of the observed baryon asymmetry is due exclusively to the Majorana and/or Dirac CP violating phases in the PMNS neutrino mixing matrix $U$.

The two possible types of light neutrino mass spectrum allowed by the data were considered: $i$) with normal ordering ($\Delta m_A^2 > 0$), $m_1 < m_2 < m_3$, and $ii$) with inverted ordering ($\Delta m_A^2 < 0$), $m_3 < m_1 < m_2$. The study was performed within the simplest type I see-saw scenario with three heavy Majorana neutrinos $N_j$, $j = 1, 2, 3$, having a hierarchical mass spectrum with masses $M_1 \ll M_{2,3}$.

As regards the case of IH spectrum with non negligible $m_3$, $m_3 \ll \sqrt{|\Delta m_A^2|}$, the generated baryon asymmetry $|Y_B|$ can be strongly enhanced in comparison with the asymmetry $|Y_B|$ produced if $m_3 \cong 0$. The enhancement can be roughly by a factor of 100. As a consequence, one can have successful leptogenesis for IH spectrum with $m_3 \gtrsim 5 \times 10^{-6}$ eV even if the elements $R_{1j}$ of the orthogonal matrix are real and the requisite CP violation is provided by the Majorana and/or Dirac phase(s) in the PMNS matrix (see Figs 2.1-2.4).

The results obtained for light neutrino mass spectrum with normal ordering (hierarchy) depend on whether $R_{11} \cong 0$ or $R_{12} \cong 0$. If $R_{11} \cong 0$, there is not any significant enhancement of the baryon asymmetry $|Y_B|$, generated within the flavoured leptogenesis scenario with real matrix $R$ and CP violation provided only by the PMNS matrix. When the lightest neutrino mass is varied in the interval $10^{-10}$ eV $\le m_1 \lesssim 7.5 \times 10^{-3}$ eV, the produced asymmetry $|Y_B|$ practically coincides with that corresponding to $m_1 = 0$ (see Fig. 2.5). For $m_1 \gtrsim 10^{-2}$ eV, the lightest neutrino mass $m_1$ has a suppressing effect on the baryon asymmetry $|Y_B|$. If, however, $R_{12} \cong 0$ (see Fig. 2.6), the dependence of $|Y_B|$ on $m_1$ exhibits qualitatively the same features as the dependence of $|Y_B|$ on $m_3$ in the case of neutrino mass spectrum with inverted ordering (hierarchy): $|Y_B|$ possesses two maxima separated by a deep minimum. Quantitatively, $\max(|Y_B|)$ is somewhat smaller than in the corresponding IH spectrum case. As a consequence, it is possible to reproduced the observed value of $Y_B$ if the CP violation is due to the Majorana phase(s) in $U$, provided $M_1 \gtrsim 5.3 \times 10^{10}$ GeV.

The results obtained show clearly that the value of the lightest neutrino mass in the cases of neutrino mass spectrum with inverted and normal ordering (hierarchy) can have strong effects on the magnitude of the baryon asymmetry of the Universe, generated within the flavoured leptogenesis scenario with hierarchical heavy Majorana neutrinos.

# Chapter 3

# Interplay Between High and Low Energy CP Violation

In the present chapter the possible connection between flavoured leptogenesis and the low energy CP violation in the lepton (neutrino) sector is further investigated. In particular, on the basis of the discussion reported in Chapter 1, great attention is devoted to the interplay between the "low energy" CP violation, originating from the PMNS neutrino mixing matrix, and the "high energy" CP violation in the neutrino Yukawa couplings that can manifest itself only at some "high" energy scale, like $e.g.$ in leptogenesis. The leptogenesis mechanism is studied in the framework introduced in Chapter 1, which includes the Lagrangian of the Standard Model with the addition of three heavy RH Majorana neutrinos $N_j$ with masses $M_1 \ll M_{2,3}$ and Yukawa couplings $\lambda_{j\alpha}$ (see Eq. (1.2)). Therefore, the CP asymmetries, relevant for leptogenesis, are generated in out-of-equilibrium decays of the lightest one, $N_1$. As in the analysis performed in Chapter 2, the baryon asymmetry is produced in the two-flavour regime ($10^9$ GeV $\lesssim T \sim M_1 \lesssim 10^{12}$ GeV). The general form of each of the flavoured CP asymmetries $\epsilon_{1\alpha}$ is provided, for the case under discussion, by expression (1.81). The total baryon asymmetry $Y_B$ is thus computed according to Eq. (1.74). The effect of both the *high energy* and *the mixed terms* in $Y_B$ is discussed in detail. Both type of light neutrino mass spectrum, with normal and inverted hierarchy are taken into account.

The results derived are based on the papers [74] and [75].

## 3.1 Neutrino Mass Spectrum with Normal Hierarchy

In this section the leptogenesis mechanism is implemented in a framework corresponding to NH light neutrino mass spectrum: $m_1 \ll m_2 < m_3$. The analysis is performed in this case for negligible lightest neutrino mass $m_1$. [1] In particular, in what follows $m_1$ is set equal to zero. In this case the

---

[1]As already pointed out in the introduction to Chapter 2, RG effects are negligible for both NH and IH light neutrino mass spectra (see $e.g.$ [76]).

asymmetry $\epsilon_{1\tau}$, given in Eq. (1.81), takes the form [74]:

$$
\epsilon_{1\tau} \cong -\frac{3\,M_1}{16\,\pi\,v^2} \frac{\sqrt{\Delta m_{\rm A}^2}}{\left(\dfrac{\Delta m_\odot^2}{\Delta m_{\rm A}^2}\right)^{1/2} |R_{12}|^2 + |R_{13}|^2}
$$

$$
\times \left\{ \left(\frac{\Delta m_\odot^2}{\Delta m_{\rm A}^2}\right) |R_{12}|^2\,|U_{\tau 2}|^2\,\sin 2\tilde{\varphi}_{12} + |R_{13}|^2\,|U_{\tau 3}|^2\,\sin 2\tilde{\varphi}_{13} \right.
$$

$$
+ \left(\frac{\Delta m_\odot^2}{\Delta m_{\rm A}^2}\right)^{1/4} |R_{12}|\,|R_{13}| \left[\left(1 - \frac{\sqrt{\Delta m_\odot^2}}{\sqrt{\Delta m_{\rm A}^2}}\right) \cos(\tilde{\varphi}_{12} + \tilde{\varphi}_{13})\,{\rm Im}\,(U_{\tau 2}^*\,U_{\tau 3})\right.
$$

$$
\left.\left. + \left(1 + \frac{\sqrt{\Delta m_\odot^2}}{\sqrt{\Delta m_{\rm A}^2}}\right) \sin(\tilde{\varphi}_{12} + \tilde{\varphi}_{13})\,{\rm Re}\,(U_{\tau 2}^*\,U_{\tau 3})\right]\right\}, \tag{3.1}
$$

where, as usual, $\tilde{\varphi}_{12}$ and $\tilde{\varphi}_{13}$ are the CP violating phases ($R-$phases) of the matrix elements $R_{12}$ and $R_{13}$, respectively. The expression of the CP asymmetry in the second flavour, $\epsilon_{1o}$, can be derived from $\epsilon_{1\tau}$ using Eq. (1.83).

The first term in the brackets in Eq. (3.1) is suppressed by the factor $\Delta m_\odot^2/\Delta m_{\rm A}^2 \cong 0.03$. A more detailed study shows that it always plays a subdominant role in the generation of baryon asymmetry compatible with observations and can be safely neglected. From the expression of $\epsilon_{1\tau}$ in Eq. (3.1), as well as the analogous for $\epsilon_{1o}$, it follows that the CP violation due to the PMNS matrix $U$ can play a significant role in leptogenesis only if the *mixed term* proportional to $|R_{12}R_{13}|$ in Eq. (3.1) is comparable in magnitude, or exceeds, the *high energy term* proportional to $|R_{13}|^2|U_{\tau 3}|^2 \sin 2\tilde{\varphi}_{13}$. The latter will not give a contribution to the asymmetries $\epsilon_{1\tau}$ and $\epsilon_{1o}$ if $\sin 2\tilde{\varphi}_{13} = 0$, *i.e.* if $R_{13}$ is real or purely imaginary, as expected for the CP conserving constraints derived in Chapter 1.

The elements of the matrix $R$ must satisfy the orthogonality condition: $R_{11}^2 + R_{12}^2 + R_{13}^2 = 1$. Then, one can have $\epsilon_{1\tau,1o} \neq 0$ only if at least two of the three elements $R_{1j}$ of the first row of $R$ are different from zero. In the case of "small" lightest neutrino mass $m_1$ under consideration, the $R_{11}$ element does not appear in the expressions for $\epsilon_{1\tau}$, $\epsilon_{1o}$, $\widetilde{m}_{1\tau}$ and $\widetilde{m}_{1o}$, which are relevant for the calculation of the baryon asymmetry $Y_B$ (see Eq. (1.74)). In the following analysis, therefore, it is considered for simplicity only the possibility of relatively small $|R_{11}|$, so that the term $R_{11}^2$ in the orthogonality condition can be neglected. This is realized if $|R_{11}|^2 \ll \min(1, |R_{12}|^2|\sin 2\tilde{\varphi}_{12}|)$. Such condition is compatible with the hypothesis of decoupling of the heaviest RH Majorana neutrino $N_3$ [78, 79], leading effectively to the so-called "$3\times 2$" see-saw model [80]. For negligible $|R_{11}|^2$, the orthogonality condition for the elements of $R$ can be written in terms of two equations involving the absolute values and the phases of $R_{12}$ and $R_{13}$:

$$
|R_{12}|^2 \cos 2\tilde{\varphi}_{12} + |R_{13}|^2 \cos 2\tilde{\varphi}_{13} = 1, \tag{3.2}
$$

$$
|R_{12}|^2 \sin 2\tilde{\varphi}_{12} + |R_{13}|^2 \sin 2\tilde{\varphi}_{13} = 0, \tag{3.3}
$$

with the constraint: $\text{sign}(\sin 2\tilde{\varphi}_{12}) = -\text{sign}(\sin 2\tilde{\varphi}_{13})$. Using these equations one can express the

phases $\tilde{\varphi}_{12}$ and $\tilde{\varphi}_{13}$ in terms of $|R_{12}|^2$ and $|R_{13}|^2$ [74]

$$\cos 2\tilde{\varphi}_{12} = \frac{1 + |R_{12}|^4 - |R_{13}|^4}{2|R_{12}|^2}, \quad \sin 2\tilde{\varphi}_{12} = \pm\sqrt{1 - \cos^2 2\tilde{\varphi}_{12}}, \tag{3.4}$$

$$\cos 2\tilde{\varphi}_{13} = \frac{1 - |R_{12}|^4 + |R_{13}|^4}{2|R_{13}|^2}, \quad \sin 2\tilde{\varphi}_{13} = \mp\sqrt{1 - \cos^2 2\tilde{\varphi}_{13}}. \tag{3.5}$$

The fact that $-1 \leq \cos 2\tilde{\varphi}_{12(13)} \leq 1$ leads to the following conditions:

$$(1 + |R_{12}|^2)^2 \geq |R_{13}|^4, \quad (1 - |R_{12}|^2)^2 \leq |R_{13}|^4; \tag{3.6}$$

$$(1 + |R_{13}|^2)^2 \geq |R_{12}|^4, \quad (1 - |R_{13}|^2)^2 \leq |R_{12}|^4. \tag{3.7}$$

Alternatively, one can express $|R_{12}|^2$ and $|R_{13}|^2$ as functions of the $R-$phases:

$$|R_{12}|^2 = \frac{\sin 2\tilde{\varphi}_{13}}{\sin 2(\tilde{\varphi}_{13} - \tilde{\varphi}_{12})},$$

$$\tag{3.8}$$

$$|R_{13}|^2 = -\frac{\sin 2\tilde{\varphi}_{12}}{\sin 2(\tilde{\varphi}_{13} - \tilde{\varphi}_{12})}.$$

The $R-$phases $\tilde{\varphi}_{12}$ and $\tilde{\varphi}_{13}$ can take CP violating values in the interval $[0,2\pi]$. The the positivity of $|R_{12}|^2$ and $|R_{13}|^2$ allows to further constrain the ranges of $\tilde{\varphi}_{12}$ and $\tilde{\varphi}_{13}$:

$$k\pi \leq \tilde{\varphi}_{13} \leq (2k+1)\frac{\pi}{2}, \quad \tilde{\varphi}_{13} - \frac{\pi}{2} - k'\pi < \tilde{\varphi}_{12} \leq (k - k')\pi; \tag{3.9}$$

$$(2k+1)\frac{\pi}{2} \leq \tilde{\varphi}_{13} \leq (k+1)\pi, \quad (k - k')\pi \leq \tilde{\varphi}_{12} < \tilde{\varphi}_{13} - \frac{\pi}{2} - k'\pi, \tag{3.10}$$

where $k = 0, 1, 2, 3$ and $k' = 0, \pm1, \pm2, \pm3$.

The most interesting region of the parameter space, from a phenomenological point of view, is provided by those values of the relevant leptogenesis parameters for which the mixed term, proportional to $|R_{12}R_{13}|$ in the expression (3.1) for the CP asymmetry $\epsilon_{1\tau}$, is sufficiently large and gives either a dominant contribution to $\epsilon_{1\tau}$ or at least one comparable to that due to the high energy term. The latter is proportional to $|R_{13}|^2|U_{\tau3}|^2 \sin 2\tilde{\varphi}_{13}$, as already stated before. Accordingly, it is useful to know the values $|R_{12}|$ and $|R_{13}|$ which maximize the function:

$$F_1(|R_{12}|, |R_{13}|) = \frac{|R_{12}|\,|R_{13}|}{\left(\dfrac{\Delta m_\odot^2}{\Delta m_{\mathrm{A}}^2}\right)^{1/2}|R_{12}|^2 + |R_{13}|^2}. \tag{3.11}$$

The maximum of $F_1(|R_{12}|, |R_{13}|)$ is obtained for $|R_{12}|/|R_{13}| = (\Delta m_{\mathrm{A}}^2/\Delta m_\odot^2)^{1/4} \cong 2.4$ and at the maximum: $F_1^{\max} = 0.5\,(\Delta m_{\mathrm{A}}^2/\Delta m_\odot^2)^{1/4} \cong 1.2$. At $|R_{12}|/|R_{13}| = (\Delta m_{\mathrm{A}}^2/\Delta m_\odot^2)^{1/4}$, the corresponding function in the high energy term in $\epsilon_{1\tau}$,

$$F_3(|R_{12}|, |R_{13}|) = \frac{|R_{13}|^2}{\left(\dfrac{\Delta m_\odot^2}{\Delta m_{\mathrm{A}}^2}\right)^{1/2}|R_{12}|^2 + |R_{13}|^2}, \tag{3.12}$$

takes the value 0.5, which is smaller only by a factor of 2 than its largest possible value. The latter, however, takes place at $|R_{12}| = 0$, for which $\epsilon_{1\tau} = \epsilon_{1o} = 0$.

The wash-out mass parameters (see Eq. (1.75)) in the case of interest are given by:

$$
\begin{aligned}
\widetilde{m}_{1\tau} &= \sqrt{\Delta m_\odot^2}\,|R_{12}|^2\,|U_{\tau 2}|^2 \;+\; \sqrt{\Delta m_{\mathrm A}^2}\,|R_{13}|^2\,|U_{\tau 3}|^2 \\[2mm]
&\quad + \; 2(\Delta m_\odot^2 \Delta m_{\mathrm A}^2)^{1/4}|R_{12}||R_{13}|\mathrm{Re}\left(e^{i(\tilde\varphi_{12}-\tilde\varphi_{13})}U_{\tau 2}^* U_{\tau 3}\right)
\end{aligned}
\tag{3.13}
$$

$$
\widetilde{m}_{1o} = \sqrt{\Delta m_\odot^2}\,|R_{12}|^2 \;+\; \sqrt{\Delta m_{\mathrm A}^2}\,|R_{13}|^2 \;-\; \widetilde{m}_{1\tau}\,.
\tag{3.14}
$$

Below, the combined effects of the "high" energy and "low" energy CP violating phases on the generation of the baryon asymmetry are analyzed.

### 3.1.1 CP violation due to Majorana phases and $R-$phases

The first case considered is the possibility that the baryon asymmetry $|Y_B|$ is generated by the combined effect of CP violation due to the Majorana phases in the PMNS matrix $U$ and the phases $\tilde\varphi_{12}$ and $\tilde\varphi_{13}$ of the orthogonal matrix $R$. The Dirac phase $\delta$ is, therefore, assumed to take a CP conserving value: $\delta = k\pi$ $(k = 0, 1, 2, ...)$. The CP asymmetries $\epsilon_{1\tau}$ and $\epsilon_{1o}$ and the wash-out mass parameters $\widetilde{m}_{1\tau}$ and $\widetilde{m}_{1o}$, given above, depend explicitly on the Majorana phase difference $\alpha_{32} \equiv \alpha_{31} - \alpha_{21}$. Indeed, the CP asymmetry $\epsilon_{1\tau}$ can be written in the form [74]:

$$
\begin{aligned}
\epsilon_{1\tau} \;\cong\; &-\frac{3\,M_1\sqrt{\Delta m_{\mathrm A}^2}}{16\,\pi\,v^2}\left\{\, F_3\,|U_{\tau 3}|^2\,\sin 2\tilde\varphi_{13} \right. \\
&\left. -\left(\frac{\Delta m_\odot^2}{\Delta m_{\mathrm A}^2}\right)^{\frac14} F_1\,|U_{\tau 2}^* U_{\tau 3}|\left[\sin(\varphi_{23}+\frac{\alpha_{32}}{2}) + \left(\frac{\Delta m_\odot^2}{\Delta m_{\mathrm A}^2}\right)^{\frac12}\sin(\varphi_{23}-\frac{\alpha_{32}}{2})\right]\right\}\,,
\end{aligned}
\tag{3.15}
$$

where $\varphi_{23} = \tilde\varphi_{12} + \tilde\varphi_{13}$. The functions $F_1$ and $F_3$ are defined respectively by Eqs (3.11) and (3.12) and for $\delta = \pi k$ one has: $(\exp(-i\alpha_{32}/2)U_{\tau 2}^* U_{\tau 3}) = -(c_{12}s_{23} \pm s_{12}c_{23}s_{13})c_{23}c_{13} = -|U_{\tau 2}^* U_{\tau 3}|$. The CP asymmetry $\epsilon_{1o}$ can be obtained from Eq. (3.15) by replacing $|U_{\tau 3}|^2$ with $(1 - |U_{\tau 3}|^2)$ and by changing the minus sign in front of the term proportional to $F_1$ to plus sign (see Eq. (1.83)).

The expression for the baryon asymmetry $Y_B$ in the two-flavour regime, given in Eq. (1.74), can be written as

$$
Y_B \;\cong\; Y_B^0\,(A_{\mathrm{HE}} + A_{\mathrm{MIX}})\,,
\tag{3.16}
$$

where

$$
Y_B^0 \cong \frac{12}{37g_*}\,\frac{3\,M_1\sqrt{\Delta m_{\mathrm A}^2}}{16\,\pi\,v^2} \cong 3\times 10^{-10}\left(\frac{M_1}{10^9\ \mathrm{GeV}}\right)\left(\frac{\sqrt{\Delta m_{\mathrm A}^2}}{5\times 10^{-2}\ \mathrm{eV}}\right)\,.
\tag{3.17}
$$

The high energy term $A_{\mathrm{HE}}$ and the mixed term $A_{\mathrm{MIX}}$, introduced in Eq. (3.16), are defined below:

$$
A_{\mathrm{HE}} = F_3\,\sin 2\tilde\varphi_{13}\left[\,|U_{\tau 3}|^2\,\eta(0.66\widetilde{m}_{1\tau}) + (1 - |U_{\tau 3}|^2)\,\eta(0.71\widetilde{m}_{1o})\right]\,,
\tag{3.18}
$$

## 3.1 Neutrino Mass Spectrum with Normal Hierarchy

$$A_{\mathrm{MIX}} = -\left(\frac{\Delta m_\odot^2}{\Delta m_\mathrm{A}^2}\right)^{\frac{1}{4}} F_1 \, |U_{\tau 2}^* U_{\tau 3}| \, [\eta(0.66\widetilde{m}_{1\tau}) - \eta(0.71\widetilde{m}_{1o})]$$

$$\times \left[ \sin(\tilde{\varphi}_{12} + \tilde{\varphi}_{13} + \frac{\alpha_{32}}{2}) + \left(\frac{\Delta m_\odot^2}{\Delta m_\mathrm{A}^2}\right)^{\frac{1}{2}} \sin(\tilde{\varphi}_{12} + \tilde{\varphi}_{13} - \frac{\alpha_{32}}{2}) \right]. \qquad (3.19)$$

Note that for the best fit value of $s_{23}^2 = 0.5$, one has $|U_{\tau 3}|^2 = c_{23}^2 c_{13}^2 \cong 0.5 \cong (1 - |U_{\tau 3}|^2)^{1/2}$ and, therefore, one has effectively $A_{\mathrm{HE}} \propto (\eta(0.66\widetilde{m}_{1\tau}) + \eta(0.71\widetilde{m}_{1o}))$. For $\tilde{\varphi}_{12} = k\pi/2$ or $\tilde{\varphi}_{13} = k'\pi/2$, $(k, k' = 0, 1, 2, ...)$ the term $A_{\mathrm{HE}}$ is equal to zero and the expression for $Y_B$ corresponds to the case in which the only source of CP violation are the Majorana phases in the PMNS matrix $U$. [2] In this case successful leptogenesis is possible, provided $M_1 \gtrsim 4 \times 10^{10}$ GeV and $|\sin \alpha_{32}/2| \gtrsim 0.1$. The phase $\alpha_{32}$ is also present in the expression for the $(\beta\beta)_{0\nu}$-decay effective Majorana mass corresponding to the NH spectrum (see Section 1.2.4).

Few more comments are in order. It follows from Eq. (3.16) that the $\tau$ and $(e + \mu)$ CP asymmetries generated by the high energy term always add up, while the $\tau$ and $(e + \mu)$ CP asymmetries due to the mixed term tend to compensate each other. The contribution of the mixed term to $Y_B$ has the additional *suppression factor* $(\Delta m_\odot^2/\Delta m_\mathrm{A}^2)^{1/4} \cong 0.42$ in comparison to that due to the high energy term. For $\sin(\tilde{\varphi}_{12} + \tilde{\varphi}_{13} + \alpha_{32}/2) = 0$, the mixed term $|A_{\mathrm{MIX}}|$ is smaller at least by the factor $(\Delta m_\odot^2/\Delta m_\mathrm{A}^2)^{1/2} c_{12}/\sqrt{2} \cong 0.11$ than the high energy term $|A_{\mathrm{HE}}|$. Finally, the sign of $A_{\mathrm{HE}}$ is determined by the sign of $\sin 2\tilde{\varphi}_{13}$, while the sign of $A_{\mathrm{MIX}}$ depends on the signs of $\sin(\tilde{\varphi}_{12} + \tilde{\varphi}_{13} + \alpha_{32}/2)$ and $(\eta(0.66\widetilde{m}_{1\tau}) - \eta(0.71\widetilde{m}_{1o}))$.

The high energy term $A_{\mathrm{HE}} \propto F_3 \sin 2\tilde{\varphi}_{13}$ will be suppressed and will give a subdominant contribution in $|Y_B|$ if either the phase of $R_{13}^2$ is to a good approximation CP conserving so that $\sin 2\tilde{\varphi}_{13} \cong 0$ or $|R_{13}|/|R_{12}|$ is sufficiently small. For $\sin 2\tilde{\varphi}_{13} = 0$ and $|R_{13}|, |R_{12}| \neq 0$, however, one also has $\sin(2\tilde{\varphi}_{12}) = 0$, implying that $R_{12}^2$ and $R_{13}^2$ are real, while $R_{12} R_{13}$ is real or purely imaginary. If, on the other hand, $|R_{13}| = 0$, then $\epsilon_{1\tau} = \epsilon_{1o} = 0$, and, as a consequence, $Y_B = 0$. In order to have successful leptogenesis in the case of interest, the ratio $|R_{13}|/|R_{12}|$ should not be too small, *i.e.* should be larger than approximately 0.05.

The wash-out mass parameter $\widetilde{m}_{1\tau}$ in (3.13) takes the value [74]:

$$\widetilde{m}_{1\tau} = \sqrt{\Delta m_\odot^2} \, |R_{12}|^2 \, |U_{\tau 2}|^2 + \sqrt{\Delta m_\mathrm{A}^2} \, |R_{13}|^2 \, |U_{\tau 3}|^2$$

$$- 2 \, (\Delta m_\odot^2 \, \Delta m_\mathrm{A}^2)^{1/4} \, |R_{12}| \, |R_{13}| \, |U_{\tau 2}^* U_{\tau 3}| \cos\left(\tilde{\varphi}_{12} - \tilde{\varphi}_{13} + \frac{\alpha_{32}}{2}\right). \qquad (3.20)$$
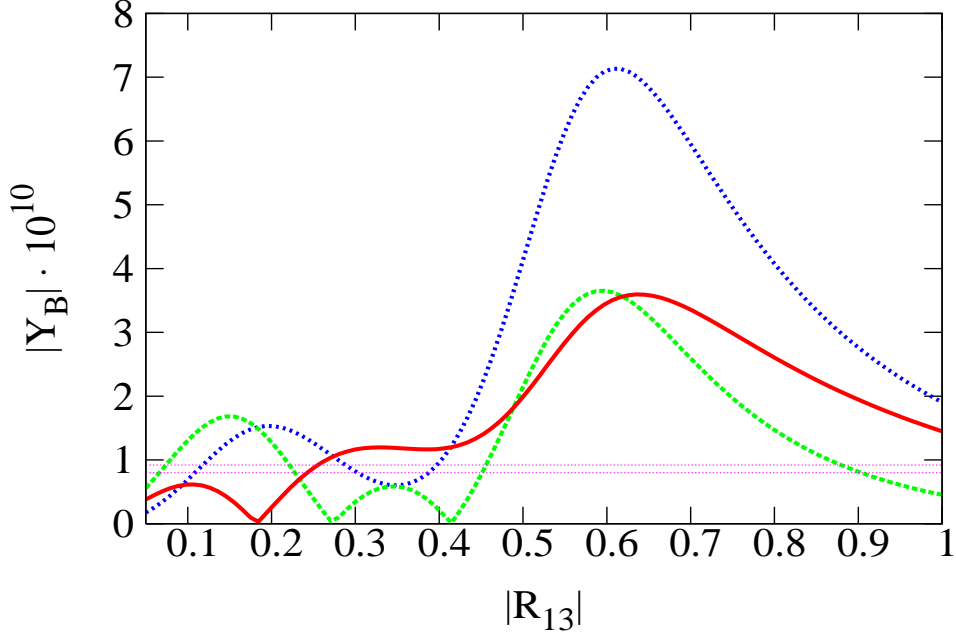
Thus, for given $|R_{12}|$ and $|R_{13}|$, $\widetilde{m}_{1\tau}$ satisfies the following inequalities:

$$\widetilde{m}_{1\tau} \geq \sqrt{\Delta m_\mathrm{A}^2} \, |R_{13}|^2 \, |U_{\tau 3}|^2 \left(1 - \left(\frac{\Delta m_\odot^2}{\Delta m_\mathrm{A}^2}\right)^{1/4} \frac{|R_{12}|}{|R_{13}|} \frac{|U_{\tau 2}|}{|U_{\tau 3}|}\right)^2, \qquad (3.21)$$

$$\widetilde{m}_{1\tau} \leq \sqrt{\Delta m_\mathrm{A}^2} \, |R_{13}|^2 \, |U_{\tau 3}|^2 \left(1 + \left(\frac{\Delta m_\odot^2}{\Delta m_\mathrm{A}^2}\right)^{1/4} \frac{|R_{12}|}{|R_{13}|} \frac{|U_{\tau 2}|}{|U_{\tau 3}|}\right)^2. \qquad (3.22)$$

It follows from Eq. (3.14) that the minimum (maximum) value of $\widetilde{m}_{1\tau}$ corresponds to the maximum (minimum) value of $\widetilde{m}_{1o}$.

---

[2] This particular scenario was studied in detail in [54].

**Figure 3.1:** The dependence of the *high energy term* $|Y_B^0 A_{\mathrm{HE}}|$ (blue dotted line), the *mixed term* $|Y_B^0 A_{\mathrm{MIX}}|$ (green dashed line) and of the *total baryon asymmetry* $|Y_B|$ (red continuous line) on $|R_{13}|$ in the case of NH spectrum, CP violation due to the Majorana phases in $U$ and $R$-phases, $\alpha_{32} = \pi/2$, $s_{23}^2 = 0.5$, $s_{13} = 0$, $|R_{12}| \cong 1$ and $M_1 = 10^{11}\,\mathrm{GeV}$. The horizontal dotted lines indicate the range of $|Y_B|$, compatible with observations: $|Y_B| \in [8.0, 9.2] \times 10^{-11}$.

**Analysis of the parameter space**

From the previous expressions, it is clear that for fixed $M_1$ and given values of the neutrino oscillations parameters, the asymmetry $Y_B$ and the relative contributions to $Y_B$ of the high energy and the mixed terms depend on $|R_{12}|$, $|R_{13}|$ and the Majorana phase $\alpha_{32}$, or equivalently, on the three phases $\tilde{\varphi}_{12}$, $\tilde{\varphi}_{13}$ and $\alpha_{32}$. One of the constraints that $\tilde{\varphi}_{12}$ and $\tilde{\varphi}_{13}$ should satisfy is: $\mathrm{sign}(\sin 2\tilde{\varphi}_{12}) = -\mathrm{sign}(\sin 2\tilde{\varphi}_{13})$ (see Eq. (3.3)). From Eqs (3.16)-(3.19) and (3.20) one can prove that

$$Y_B(\tilde{\varphi}_{12}, \tilde{\varphi}_{13}; \alpha_{32}) = -Y_B(-\tilde{\varphi}_{12}, -\tilde{\varphi}_{13}; 4\pi - \alpha_{32}). \tag{3.23}$$

Therefore, in what follows, it is enough to analyze the case: $\sin 2\tilde{\varphi}_{12} < 0$, $\sin 2\tilde{\varphi}_{13} > 0$. The results corresponding to $\sin 2\tilde{\varphi}_{12} > 0$, $\sin 2\tilde{\varphi}_{13} < 0$ can always be obtained from the indicated property of $Y_B$.

In what concerns the values of $|R_{12}|$ and $|R_{13}|$, there are several possibilities leading to quite different physical results: *i)* $|R_{13}| \leq |R_{12}|$ with $|R_{12}| \leq 1$; *ii)* $|R_{12}| \leq |R_{13}|$ with $|R_{13}| \leq 1$; *iii)* $|R_{12}| > 1$ or $|R_{13}| > 1$.

The overall parameter space compatible with successful leptogenesis is represented in Figs 3.1-3.6.
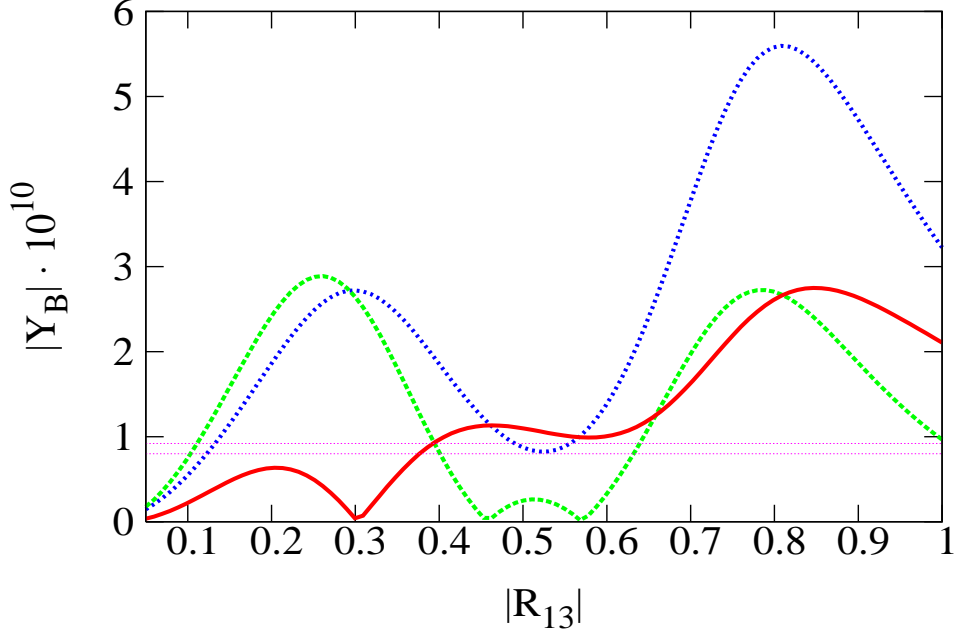
**Figure 3.2:** The same as in Fig. 3.1, but for $s_{23}^2 = 0.64$, $s_{13} = 0.2$ and $\delta = 0$.

**Case $|R_{13}| \leq |R_{12}| \leq 1$**

As it was already pointed out above, the baryon asymmetry $|Y_B|$ will be strongly suppressed if $|R_{13}|/|R_{12}| \ll 0.05$, so the discussion is referred to values of $|R_{13}|/|R_{12}| \gtrsim 0.05$. The results obtained depend on whether $|R_{13}| \lesssim 0.5$ or $|R_{13}| \gtrsim 0.5$.

For $|R_{13}| \leq 0.5$, one should have $|R_{12}| > \sqrt{0.75} \cong 0.87$ in order to have $\sin 2\tilde{\varphi}_{13} \neq 0$. In the case of $|R_{12}| = 1$ the relevant $R$-phases depend on $|R_{13}|$ in the following way: $\cos 2\tilde{\varphi}_{12} = 1 - 0.5|R_{13}|^4 \gtrsim 0.97$, $|\sin 2\tilde{\varphi}_{12}| = |R_{13}|^2 \leq 0.25$, $\cos 2\tilde{\varphi}_{13} = 0.5|R_{13}|^2 \leq 0.125$, $|\sin 2\tilde{\varphi}_{13}| \cong 1 - |R_{13}|^4/8 \gtrsim 1 - 7.8 \times 10^{-3}$. Thus, $0 < (-\tilde{\varphi}_{12}) \lesssim 0.12$ and $\tilde{\varphi}_{13} \cong \pi/4$. This implies that for $\alpha_{32}/2 \cong \pi/4$ one has $\sin(\tilde{\varphi}_{12} + \tilde{\varphi}_{13} + \alpha_{32}/2) \cong 1$, while if $\alpha_{32}/2 \cong 3\pi/4$ the mixed term will be strongly suppressed. It follows from these simple observations that the predictions for $|Y_B|$ will exhibit a strong dependence on $\alpha_{32}$. For $\alpha_{32}/2 \cong \pi/4$, $\cos(\tilde{\varphi}_{12} - \tilde{\varphi}_{13} + \alpha_{32}/2) \cong \cos \tilde{\varphi}_{12} \cong 1$, and for any given $|R_{13}| \leq 0.5$, $\widetilde{m}_\tau$ takes approximately its minimal value.

At $|R_{13}| = 0.5$ and $\alpha_{32}/2 = \pi/4$, one has (see Fig. 3.1): $\widetilde{m}_\tau \cong 5.7 \times 10^{-4}$ (weak wash-out), $\widetilde{m}_{1o} \cong 2.1 \times 10^{-2} \gg \widetilde{m}_\tau$ (strong wash-out), $\eta(0.66\widetilde{m}_{1\tau}) \cong 4.2 \times 10^{-2}$, and $\eta(0.71\widetilde{m}_{1o}) \cong 6.8 \times 10^{-3} < \eta(0.66\widetilde{m}_{1\tau})$. The mixed term and the high energy term have opposite signs and $A_{\text{MIX}} \cong -7.3 \times 10^{-3}$ and $A_{\text{HE}} \cong 1.40 \times 10^{-2}$. Therefore, the mixed term in $Y_B$ has the effect of partially compensating the contribution of the high energy term, so that the sum $(A_{\text{MIX}} + A_{\text{HE}})$ is approximately by a factor of 2 smaller than $A_{\text{HE}}$. As $|R_{13}|$ decreases starting from 0.5, the wash-out mass parameters $\widetilde{m}_\tau$, $\widetilde{m}_{1o}$ and the efficiency function $\eta(0.66\widetilde{m}_{1\tau})$ also decrease starting from the values given above. However,

$\eta(0.71\widetilde{m}_{1o})$ increases and at $|R_{13}| \cong 0.41$ [3] one has $\eta(0.66\widetilde{m}_{1\tau}) \cong \eta(0.71\widetilde{m}_{1o})$. As a consequence, at $|R_{13}| \cong 0.41$, $|A_{\mathrm{MIX}}|$ goes through a deep minimum and is strongly suppressed. The high energy term $|A_{\mathrm{HE}}|$ just decreases somewhat as $|R_{13}|$ changes from 0.50 to 0.41. At $|R_{13}| \cong 0.41$, the mixed term $A_{\mathrm{MIX}}$ changes sign: for $|R_{13}| \approx (0.3 \div 0.4)$ one has $\eta(0.66\widetilde{m}_{1\tau}) < \eta(0.71\widetilde{m}_{1o})$ and, consequently, $A_{\mathrm{MIX}} > 0$. Thus, $A_{\mathrm{HE}}$ and $A_{\mathrm{MIX}}$ have the same sign and add up constructively in $Y_B$. When $|R_{13}|$ decreases below 0.41, $\widetilde{m}_{1\tau}$, $\widetilde{m}_{1o}$ and $\eta(0.66\widetilde{m}_{1\tau})$ continue to decrease, while $\eta(0.71\widetilde{m}_{1o})$ continues to increase; $A_{\mathrm{MIX}}$ also increases rapidly, while $A_{\mathrm{HE}}$ decreases but rather slowly (see Fig. 3.1). At $|R_{13}| \cong (\Delta m_\odot^2/\Delta m_A^2)^{1/4} c_{12} \cong 0.35$, the wash-out mass parameter $\widetilde{m}_{1\tau}$ is approximately zero and $A_{\mathrm{MIX}}$ has a local maximum. At this point, $A_{\mathrm{MIX}} \cong A_{\mathrm{HE}} \cong 2 \times 10^{-3}$. As $|R_{13}|$ decreases further, $\widetilde{m}_\tau$ and $\eta(0.66\widetilde{m}_{1\tau})$ increase, $\widetilde{m}_{1o}$ decreases, but $\eta(0.71\widetilde{m}_{1o})$ increases. As a consequence, $A_{\mathrm{HE}}$ also increases, while $A_{\mathrm{MIX}}$ diminishes. At $|R_{13}| \cong 0.27$ one gets $\eta(0.66\widetilde{m}_{1\tau}) \cong \eta(0.71\widetilde{m}_{1o})$ and $A_{\mathrm{MIX}}$ exhibits a second deep minimum, $A_{\mathrm{MIX}} \cong 0$. At values of $|R_{13}| < 0.27$ the inequality $\eta(0.66\widetilde{m}_{1\tau}) > \eta(0.71\widetilde{m}_{1o})$ holds and $A_{\mathrm{MIX}}$ is negative, $A_{\mathrm{MIX}} < 0$. Therefore $A_{\mathrm{HE}}$ and $A_{\mathrm{MIX}}$ have opposite signs and their contributions to $Y_B$ tend to compensate each other. For decreasing $|R_{13}| < 0.27$, $\eta(0.66\widetilde{m}_{1\tau})$ and $F_1(\eta(0.66\widetilde{m}_{1\tau}) - \eta(0.71\widetilde{m}_{1o}))$ grow faster than $\eta(0.71\widetilde{m}_{1o})$ and $F_3(\eta(0.66\widetilde{m}_{1\tau}) + \eta(0.71\widetilde{m}_{1o}))$, respectively. At $|R_{13}| \cong 0.18$, $A_{\mathrm{HE}}$ has a local maximum. However, one also has $|A_{\mathrm{MIX}}| \cong A_{\mathrm{HE}}$. As a consequence, $A_{\mathrm{MIX}} + A_{\mathrm{HE}} \cong 0$, *i.e.* the high energy and the mixed terms cancel each other and $|Y_B|$ is strongly suppressed. This important feature of $|Y_B|$ persists for values of $\alpha_{32}/2$ up to $\pi/2$. The precise position of the considered deep minimum of $|Y_B|$ depends on the value of $\sin^2 \theta_{23}$ and, to less extent, on whether $\delta = 0$ or $\pi$ if $\sin \theta_{13}$ has a value close to the existing upper limit. As an illustration, Fig. 3.2 shows $|Y_B^0 A_{\mathrm{HE}}|$, $|Y_B^0 A_{\mathrm{MIX}}|$ and $|Y_B|$ as functions of $|R_{13}|$ for $s_{23}^2 = 0.64$, $s_{13} = 0.2$ and $\delta = 0$. From the figure one can see easily that, for $s_{23}^2 = 0.64$ and $|R_{13}| \cong 0.30$, the total contribution $A_{\mathrm{MIX}} + A_{\mathrm{HE}} \cong 0$ and correspondingly $Y_B \cong 0$. Note that both $|Y_B^0 A_{\mathrm{HE}}|$ and $|Y_B^0 A_{\mathrm{MIX}}|$ have relatively large values at $|R_{13}| \cong 0.30$ and thus each of the two terms separately could account for the observed value of $Y_B$ (see Fig. 3.2). Nevertheless, the generated baryon asymmetry is strongly suppressed, $|Y_B| = |Y_B^0(A_{\mathrm{HE}} + A_{\mathrm{MIX}})| \ll 8.6 \times 10^{-11}$ and it is impossible to reproduce the measured value of $Y_B$ for $M_1 \lesssim 10^{12}$ GeV. Finally, for $|R_{13}| < 0.17$, the mixed term is larger, in absolute value, than the high energy term, $|A_{\mathrm{MIX}}| > A_{\mathrm{HE}}$: at $|R_{13}| = 0.10$, for instance, $|A_{\mathrm{MIX}}| \cong 2A_{\mathrm{HE}}$. Since the two terms have opposite signs, $\mathrm{sign}(A_{\mathrm{MIX}}) = -\mathrm{sign}(A_{\mathrm{HE}})$, the contributions of the high energy term in $Y_B$ partially compensates the contribution of the mixed term.

Consider now the dependence of the baryon asymmetry $|Y_B|$ on the Majorana phase $\alpha_{32}$. This study corresponds to values of $|R_{13}| \leq |R_{12}| = 1$ in the interval $0.1 \lesssim |R_{13}| \lesssim 0.5$. Moreover, three values of $s_{23}$ ($s_{23}^2 = 0.36$; $0.50$; $0.64$) and two values of $s_{13}$ ($s_{13} = 0$; $0.2$) are considered. In the case of $s_{13} = 0.2$, the two CP conserving values of the Dirac phase, $\delta = 0$; $\pi$, are distinguished. These results are illustrated in Figs 3.3-3.5. As these figures indicate, the behavior of $|Y_B|$ as a function of $\alpha_{32}$ exhibits particularly interesting features when $\alpha_{32}$ changes in the interval $0 < \alpha_{32} \lesssim \pi$. Therefore, for $s_{13} = 0.2$ and given $s_{23}^2$, one can get very different dependence of $|Y_B|$ on $\alpha_{32}$ for the two values of $\delta = 0$; $\pi$ and that the dependence under discussion for, *e.g.* $s_{23}^2 = 0.50$ can differ drastically from those for $s_{23}^2 = 0.36$ and for $s_{23}^2 = 0.64$ (see Figs 3.4 and 3.5).

One can analyze in a similar manner the behavior of $A_{\mathrm{MIX}}$, $A_{\mathrm{HE}}$ and $|Y_B|$ as functions of $|R_{13}|$ in the interval $0.5 < |R_{13}| \leq 1.0$. As in the preceding discussion, the parameter space is fixed

---

[3] This value is obtained as a solution of the equation $0.66\widetilde{m}_\tau/(8.25 \times 10^{-3} \text{ eV}) = (0.71\widetilde{m}_{1o}/(2 \times 10^{-4} \text{ eV}))^{-1.16}$.
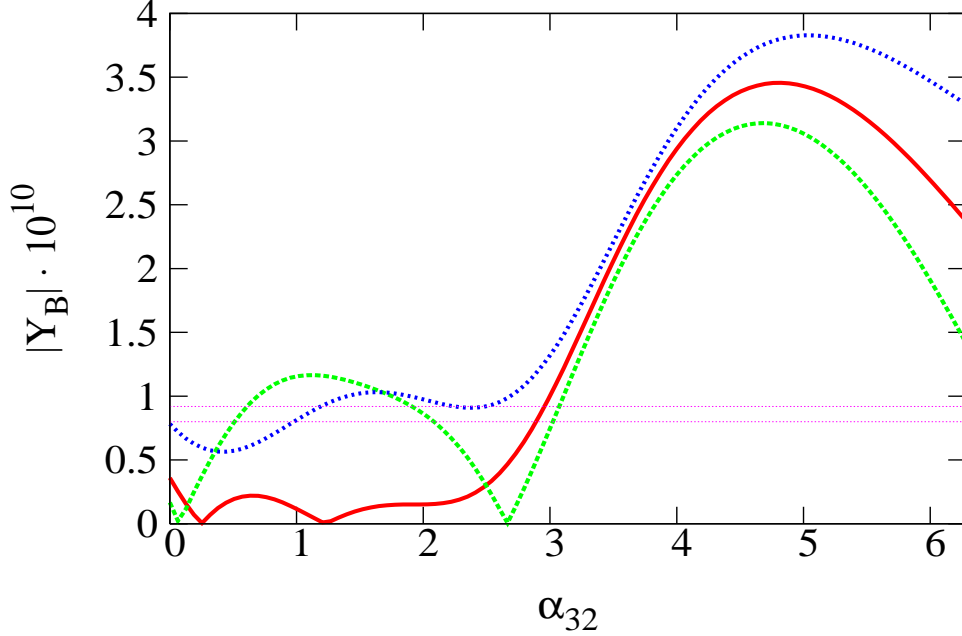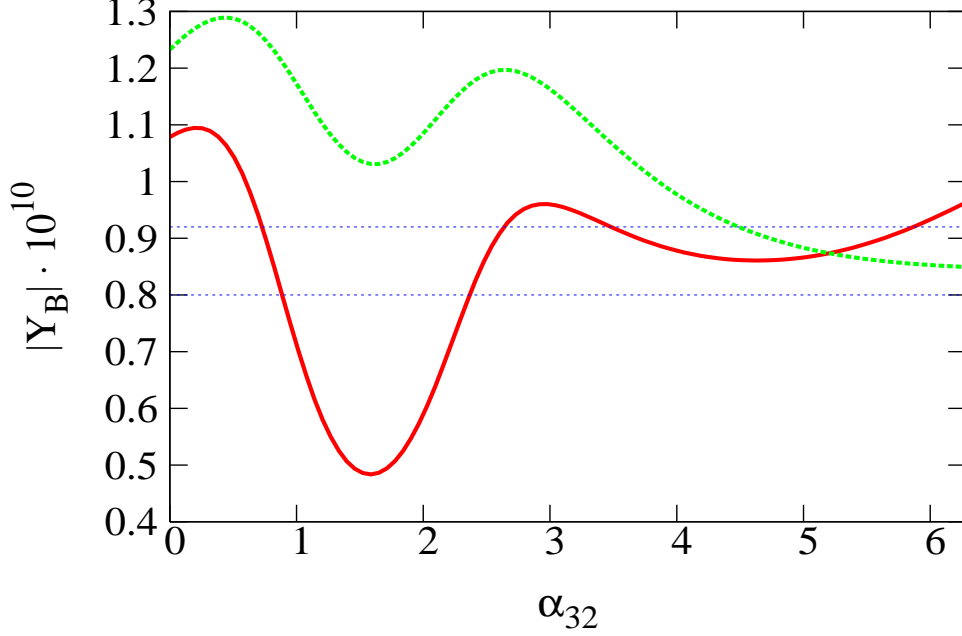
**Figure 3.3:** The dependence of $|Y_B|$ on the Majorana phase (difference) $\alpha_{32}$ in the case of NH spectrum, Majorana and $R$ matrix CP violation, $s_{23}^2 = 0.5$, $M_1 = 2 \times 10^{11}$ GeV, $R_{12} \cong 1$, $R_{13} = 0.19$, $i$) $s_{13} = 0$ (red continuous line), $ii$) $s_{13} = 0.2$, $\delta = 0$ (green dashed line), $iii$) $s_{13} = 0.2$, $\delta = \pi$ (blue dotted line).

with $|R_{13}| \leq |R_{12}| \leq 1.0$ and $\alpha_{32}/2 = \pi/4$. As can be easily verified, when $|R_{13}|$ increases from 0.5 to 1.0 under the indicated conditions, $i$) $F_1 \sin(\tilde{\varphi}_{12} + \tilde{\varphi}_{13} + \alpha_{32}/2)$ changes from 1.14 to 0.60, $ii$) $F_3 \sin 2\tilde{\varphi}_{13}$ increases from 0.59 to 0.74, $iii$) $\widetilde{m}_{1\tau}$ increases monotonically by a factor of about 20 from $5.7 \times 10^{-4}$ eV to $1.1 \times 10^{-2}$ eV and $iv$) $\widetilde{m}_{1o}$ increases only by a factor of approximately 2.3 from $2.1 \times 10^{-2}$ eV to $4.8 \times 10^{-2}$ eV. Correspondingly, the efficiency factor $\eta(0.66\widetilde{m}_{1\tau})$ first increases starting from the value $4.2 \times 10^{-2}$, reaches a maximum $\eta(0.66\widetilde{m}_{1\tau}) \cong 6.8 \times 10^{-2}$ at $|R_{13}| \cong 0.6$ when $0.66\widetilde{m}_{1\tau} \cong 1.1 \times 10^{-3}$ eV and then decreases monotonically to $1.52 \times 10^{-2}$. In contrast, when $|R_{13}|$ changes from 0.5 to 1.0, the efficiency factor $\eta(0.71\widetilde{m}_{1o})$ only decreases monotonically by a factor of about 2.6, from $6.7 \times 10^{-3}$ to $2.6 \times 10^{-3}$. Thus, the asymmetry in the $(e + \mu)$ lepton charge is generated in the regime of strong wash-out, while the wash-out effects in the production of the asymmetry in the $\tau$ lepton charge change from weak to strong, passing through a minimum. Clearly, the change of $A_{\mathrm{MIX}}$ and $A_{\mathrm{HE}}$ with $|R_{13}|$ is determined essentially by the behavior of $\eta(0.66\widetilde{m}_{1\tau})$. In particular, $\eta(0.66\widetilde{m}_{1\tau}) > \eta(0.71\widetilde{m}_{1o})$ in the case under discussion, implying that $\mathrm{sign}(A_{\mathrm{MIX}}) = -\mathrm{sign}(A_{\mathrm{HE}})$. For the considered range of $|R_{13}|$ one typically has $|A_{\mathrm{MIX}}| \cong (0.5 \div 0.6)A_{\mathrm{HE}}$, so that there is a partial cancellation between the two terms $A_{\mathrm{MIX}}$ and $A_{\mathrm{HE}}$ in $Y_B$ (see Fig. 3.1).

It should be clear that $A_{\mathrm{MIX}}$, $A_{\mathrm{HE}}$ and $|Y_B|$ will exhibit a different dependence on $|R_{13}|$ varying in the range $0.05 \lesssim |R_{13}| \leq |R_{12}| \leq 1$ if $\alpha_{32}/2$ differs significantly from $\pi/4$. If $\alpha_{32}/2 \cong 3\pi/4$, for

**Figure 3.4:** The dependence of $|Y_B|$ on $\alpha_{32}$ in the case of NH spectrum, Majorana and $R$ matrix CP violation, $|R_{12}| = 1$, $|R_{13}| = 0.51$, $M_1 = 3.5 \times 10^{10}$ GeV, $s_{23}^2 = 0.5$, $s_{13} = 0.2$ and $\delta = 0\,(\pi)$, red continuous (green dashed) line.

instance, one has $|A_{\text{MIX}}| \ll |A_{\text{HE}}|$. For $|R_{13}| \lesssim 0.5$ this is due to the fact that $\sin(\tilde{\varphi}_{12} + \tilde{\varphi}_{13} + \alpha_{32}/2) \ll 1$, while for $0.5 < |R_{13}| \leq 1$ and $|R_{12}| \cong 1$, it is a consequence of the fact that $\eta(0.66\widetilde{m}_{1\tau})$ and $\eta(0.71\widetilde{m}_{1o})$ have rather close values: when $|R_{13}|$ changes from 0.5 to 1.0, the efficiency function combination $\eta(0.66\widetilde{m}_{1\tau}) - \eta(0.71\widetilde{m}_{1o})$ decreases approximately from $7.6 \times 10^{-3}$ to $2.7 \times 10^{-3}$. At the same time the sum $\eta(0.66\widetilde{m}_{1\tau}) + \eta(0.71\widetilde{m}_{1o})$ changes from $3 \times 10^{-2}$ to $10^{-2}$, remaining by a factor four bigger than $\eta(0.66\widetilde{m}_{1\tau}) - \eta(0.71\widetilde{m}_{1o})$.

**Case $|R_{12}| > 1$**

One can perform a similar analysis in the case of $|R_{12}| > 1$ or $|R_{13}| > 1$. The results pertaining to $|R_{12}| > 1$ are illustrated in Fig. 3.6, which shows the dependence of $|Y_B^0 A_{\text{HE}}|$, $|Y_B^0 A_{\text{MIX}}|$ and of $|Y_B|$ on $|R_{13}|$ for $|R_{12}| = 1.2$, $\alpha_{32}/2 = \pi/4$ and $s_{23}^2 = 0.5$, $s_{13} = 0$. The figure exhibits some typical features, namely, the relevance of the mixed term in the region close to the minimal allowed value of $|R_{13}|$, *i.e.* for $|R_{13}| \lesssim 1$. If $|R_{12}| > 1$ (*e.g.* $|R_{12}| = 1.2$ as in Fig. 3.6), $|R_{13}|^2$ can take values in the interval $(|R_{12}|^2 - 1) \leq |R_{13}|^2 \leq (|R_{12}|^2 + 1)$. When $|R_{13}|^2$ changes from its minimal value to its maximum value, the phase $2\tilde{\varphi}_{13}$ decreases from $\pi$ to 0, whereas $2\tilde{\varphi}_{12}$ changes from 0 to $(-\pi)$, so that one always has $\sin 2\tilde{\varphi}_{12} \leq 0$. Obviously, at $|R_{13}|^2 = (|R_{12}|^2 - 1)$ one has $A_{\text{HE}} = 0$ since $\sin 2\tilde{\varphi}_{13} = 0$, while for $\alpha_{32}/2 \neq \pi k$ ($k = 0, 1, 2, ...$), one finds, in general, $A_{\text{MIX}} \neq 0$. For the value of $\alpha_{32}/2 = \pi/4$ (see Fig. 3.6), for instance: $A_{\text{MIX}} \cong -3.9 \times 10^{-3}$. The salient features of the
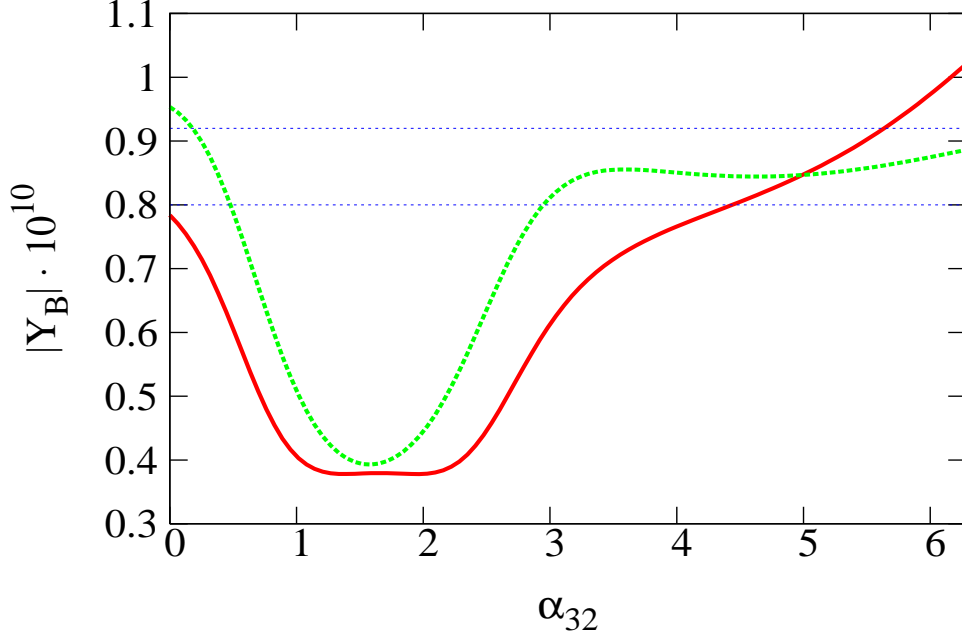
**Figure 3.5:** The same as in Fig. 3.4, but for $s_{23}^2 = 0.64$.

behavior of $A_{\mathrm{HE}}$ and $A_{\mathrm{MIX}}$ as functions of $|R_{13}|$, shown in Fig. 3.6, can be understood qualitatively from the behavior of $F_3 \sin(2\tilde{\varphi}_{13})\eta(0.66\widetilde{m}_{1\tau})$ and of $F_1 \sin(\tilde{\varphi}_{12} + \tilde{\varphi}_{13} + \alpha_{32}/2)\eta(0.66\widetilde{m}_{1\tau})$: both quantities grow monotonically as $|R_{13}|$ increases starting from its minimal value, but the former grows faster than the latter. There is always a value of $|R_{13}|$ relatively close to its minimal value at which $A_{\mathrm{HE}} = |A_{\mathrm{MIX}}|$. Obviously, at this point the baryon asymmetry is strongly suppressed: $Y_B = Y_B^0(A_{\mathrm{HE}} + A_{\mathrm{MIX}}) = 0$ (see Fig. 3.6). The behavior of $A_{\mathrm{HE}}$ and $|A_{\mathrm{MIX}}|$ when $|R_{13}|$ increases beyond the point at which $Y_B \cong 0$, is basically determined by $\eta(0.66\widetilde{m}_{1\tau})$, which goes through a maximum and after that decreases monotonically. Note also that at certain value of $|R_{13}| > 1$, $\sin(\tilde{\varphi}_{12} + \tilde{\varphi}_{13} + \alpha_{32}/2)$ can go through zero and changes sign. As a consequence, $A_{\mathrm{MIX}}$ also can change sign.

As the results described above show, in the case of NH light neutrino mass spectrum and CP violation due the "low" energy Majorana phases in $U$ and "high" energy $R$-phases, the predicted baryon asymmetry can exhibit strong dependence on the Majorana phase $\alpha_{32}$ if the latter has a value in the interval $0 < \alpha_{32} < \pi$ ($\sin 2\tilde{\varphi}_{12} < 0$, $\sin 2\tilde{\varphi}_{13} > 0$) or $3\pi < \alpha_{32} < 4\pi$ ($\sin 2\tilde{\varphi}_{12} > 0$, $\sin 2\tilde{\varphi}_{13} < 0$). In the most extreme cases both $Y_B \ll 8.77 \times 10^{-11}$ or $Y_B$ compatible with the observations are possible in a certain point of the relevant parameter space, depending on the value of $\alpha_{32}$.
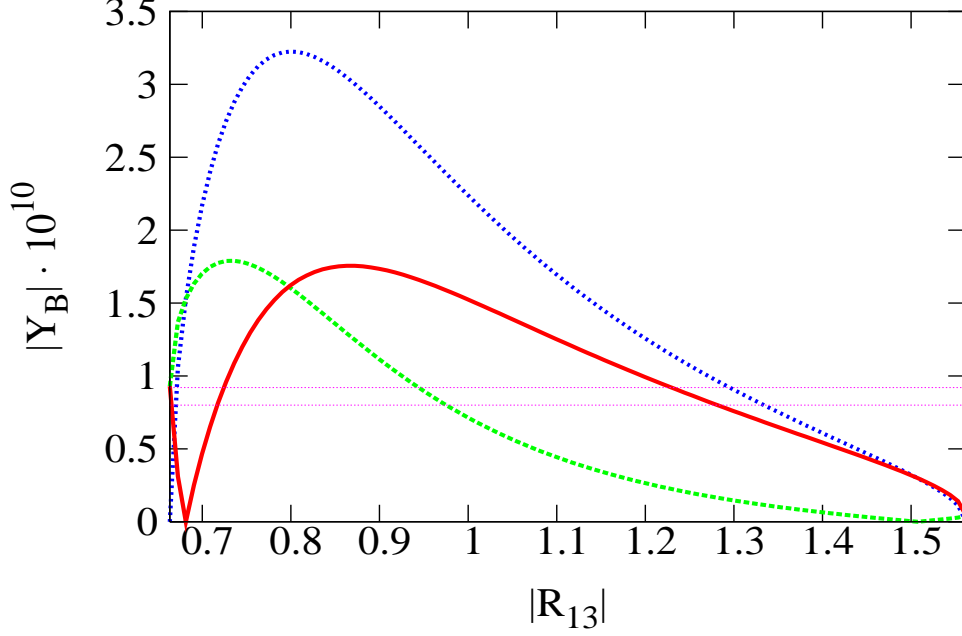
**Figure 3.6:** The dependence of $|Y_B^0 A_{\mathrm{HE}}|$ (blue line), $|Y_B^0 A_{\mathrm{MIX}}|$ (green line) and of $|Y_B|$ (red line) on $|R_{13}|$ in the case of NH spectrum, Majorana and $R$ matrix CP violation, $|R_{12}| = 1.2$, $\alpha_{32}/2 = \pi/4$, $s_{23}^2 = 0.5$, $s_{13} = 0$ and $M_1 = 10^{11}$ GeV.

### 3.1.2 CP violation due to Dirac phase and $R-$phases

Consider next the possibility that the CP violation in flavoured leptogenesis is due to the Dirac phase $\delta$ in the PMNS matrix $U$ and to the "high" energy phases $\tilde{\varphi}_{12}$ and $\tilde{\varphi}_{13}$ of the matrix $R$. It is assumed in this case that the Majorana phase $\alpha_{32}$ takes a CP conserving value: $\alpha_{32} = \pi k$ ($k = 0, 1, 2, ...$). The expression for the baryon asymmetry $Y_B$ also in this case can be cast in the form (3.16). The high energy term $A_{\mathrm{HE}}$ is the same as in the Majorana and R-matrix CP violation case and is given by Eq. (3.18). The mixed term has the following form for arbitrary $\alpha_{32}$:

$$
A_{\mathrm{MIX}}^{\mathrm{D}} = -\left(\frac{\Delta m_{\odot}^2}{\Delta m_{\mathrm{A}}^2}\right)^{1/4} F_1 \, c_{23} \, c_{13} \left[\eta(0.66\widetilde{m}_{1\tau}) - \eta(0.71\widetilde{m}_{1o})\right]
$$

$$
\times \ \left\{ c_{12}s_{23}\left(\sin\left(\tilde{\varphi}_{12} + \tilde{\varphi}_{13} + \frac{\alpha_{32}}{2}\right) + \sqrt{\frac{\Delta m_{\odot}^2}{\Delta m_{\mathrm{A}}^2}}\sin\left(\tilde{\varphi}_{12} + \tilde{\varphi}_{13} - \frac{\alpha_{32}}{2}\right)\right) + \Phi_{\mathrm{MIX}}^{\mathrm{D}} \right\},
$$

$$(3.24)$$

where

$$
\Phi_{\mathrm{MIX}}^{\mathrm{D}} = s_{12}c_{23}s_{13}\left[\sin\left(\tilde{\varphi}_{12} + \tilde{\varphi}_{13} + \frac{\alpha_{32}}{2} - \delta\right) + \sqrt{\frac{\Delta m_{\odot}^2}{\Delta m_{\mathrm{A}}^2}}\sin\left(\tilde{\varphi}_{12} + \tilde{\varphi}_{13} - \frac{\alpha_{32}}{2} + \delta\right)\right]. \quad (3.25)
$$
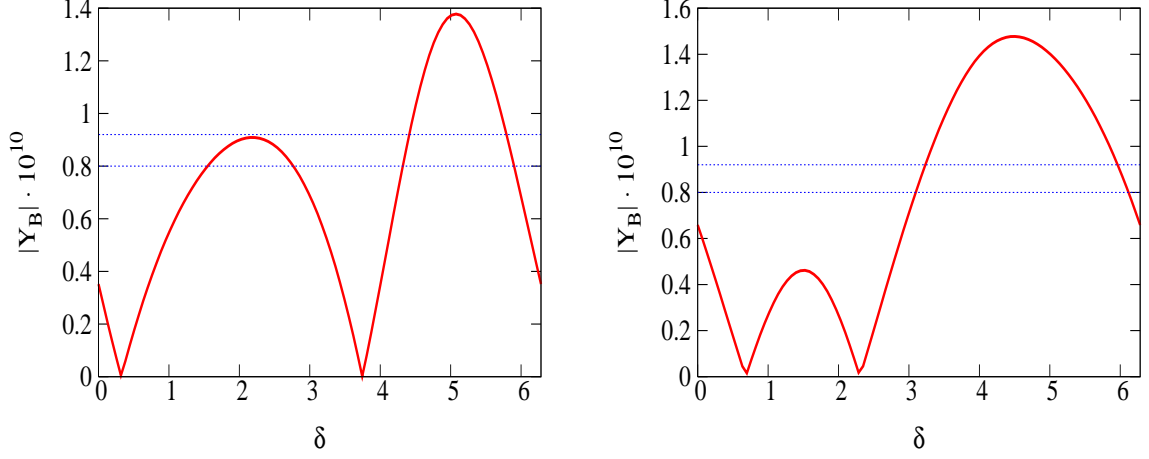
**Figure 3.7:** The dependence of $|Y_B|$ on the Dirac phase $\delta$ in the case of NH spectrum, Dirac and $R$ matrix CP violation, $s_{13} = 0.2$, $R_{12} \cong 1$, $M_1 = 5 \times 10^{11}$ GeV and for $i)$ $\alpha_{32} = 0$, $|R_{13}| \cong 0.16$ (left panel) and $ii)$ $\alpha_{32} = \pi$, $|R_{13}| \cong 0.12$ (right panel).

The wash-out mass parameter $\widetilde{m}_{1\tau}$ is given by

$$
\begin{aligned}
\widetilde{m}_{1\tau} &= \sqrt{\Delta m_\odot^2}\, |R_{12}|^2\, |U_{\tau 2}|^2 + \sqrt{\Delta m_A^2}\, |R_{13}|^2\, |U_{\tau 3}|^2 - 2\,(\Delta m_\odot^2\, \Delta m_A^2)^{1/4}\, |R_{12}|\, |R_{13}|\, c_{23} c_{13} \\
&\quad \times \left[ c_{12} s_{23} \cos\left( \tilde{\varphi}_{12} - \tilde{\varphi}_{13} + \frac{\alpha_{32}}{2} \right) + s_{12} c_{23} s_{13} \cos\left( \tilde{\varphi}_{12} - \tilde{\varphi}_{13} + \frac{\alpha_{32}}{2} - \delta \right) \right] . \quad (3.26)
\end{aligned}
$$

For *e.g.* $\alpha_{32} = 2\pi k$ $(k = 0, 1, 2, ...)$ and $\tilde{\varphi}_{12}, \tilde{\varphi}_{13} = 0, \pm\pi$, $R_{12}$ and $R_{13}$ are real, $A_{\mathrm{HE}} = 0$, while in the mixed term only the part proportional to $\Phi_{\mathrm{MIX}}^{\mathrm{D}}$ is non-zero, $A_{\mathrm{MIX}}^{\mathrm{D}} \propto \Phi_{\mathrm{MIX}}^{\mathrm{D}} \neq 0$. The CP violation in leptogenesis in this case is entirely due to the Dirac phase $\delta$ in the PMNS matrix. In particular, one can have successful leptogenesis for $M_1 \lesssim 5 \times 10^{11}$ GeV provided $|s_{13} \sin \delta| \gtrsim 0.1$. [4] For $\alpha_{32} = 0$ and $R_{12} R_{13} > 0$ $(R_{12} R_{13} < 0)$, the baryon asymmetry $|Y_B|$ has a maximum at $R_{12}^2 \cong 0.75$, $R_{13}^2 \cong 0.25$ $(R_{12}^2 \cong 0.85, R_{13}^2 \cong 0.15)$. Since the CP violation effects due to the Dirac phase are always suppressed by the relatively small experimentally allowed value of $s_{13}$, the regions of interest would correspond to $\tilde{\varphi}_{13} \sim 0, \pm\pi/2$, where $A_{\mathrm{HE}}$ is also suppressed. The case of $\tilde{\varphi}_{13} \sim 0, \pm\pi/2$, corresponds to $|R_{13}|$ taking values close to the boundaries: $|R_{13}|^2 \sim |\,|R_{12}|^2 \mp 1\,|$.

Note that the mixed term $A_{\mathrm{MIX}}^{\mathrm{D}}$ contains a piece which does not depend on the Dirac phase $\delta$. This $\delta$-independent piece is multiplied by $c_{12} s_{23}$ which is approximately at least by a factor seven larger than the corresponding mixing angle factor $s_{12} c_{23} s_{13}$ in the $\delta$-dependent term $\Phi_{\mathrm{MIX}}^{\mathrm{D}}$. In the region $|R_{13}|^2 \sim |\,|R_{12}|^2 \mp 1\,|$, one also has $\sin(\tilde{\varphi}_{12} + \tilde{\varphi}_{13} + \alpha_{32}/2) \cong 0$ for $\alpha_{32} = \pi k$ and the $\delta$-independent term in $A_{\mathrm{MIX}}^{\mathrm{D}}$ will also be suppressed. A detailed numerical analysis of this region of parameter space for CP violating values of the Dirac phase $\delta$ and a CP conserving Majorana

---

[4] Values of $s_{13} \gtrsim 0.1$ are within the range to be probed by future experiments with reactor $\bar{\nu}_e$ [38]. Future long baseline experiments will aim at measuring values of $\sin^2 \theta_{13}$ as small as $10^{-4} \div 10^{-3}$ and at constraining (or determining) $\delta$ (see *e.g.* [39]).

phase $\alpha_{32}$ shows that successful leptogenesis can still be realized for $|R_{13}|^2 \gtrsim ||R_{12}|^2 - 1|$ and $|R_{12}| \approx \mathcal{O}(1)$. Moreover, in the cases considered, the effects of the CP violating Dirac phase are relevant in order to reproduce the observed value of the baryon asymmetry. In Fig. 3.7 it is reported $|Y_B|$ as a function of $\delta$ for $|R_{12}| \cong 1$, $s_{13} = 0.2$, $\alpha_{32} = 0$ (left panel) and $\alpha_{32} = \pi$ (right panel). The value of $|R_{13}|$ is taken close to its lower bound. In both the shown cases, there is a significant interference between the high energy and the mixed terms that can suppress or enhance the baryon asymmetry. The latter is controlled by the Dirac phase $\delta$.

In conclusion, from the previous analysis one can say that if the Majorana phase $\alpha_{32}$ has a CP conserving value, there still will be regions in the parameter space where the effects of the CP violating Dirac phase in the PMNS matrix can be significant in flavoured leptogenesis, even if CP violation is due also to the "high" energy $R$ matrix phases.

## 3.2 Inverted Hierarchical Light Neutrino Mass Spectrum

Very different results are obtained for IH neutrino mass spectrum: $m_3 \ll m_{1,2} \cong \sqrt{|\Delta m_A^2|} \cong$ 0.05 eV. As follows, for such scenario there exist significant regions of the corresponding leptogenesis parameter space where the relevant "high" energy $R-$phases have large CP violating values, but the purely high energy contribution in $Y_B$ plays a subdominant role in the production of baryon asymmetry compatible with the observations. The requisite dominant term in $Y_B$ can arise due to the "low" energy CP violation in the neutrino mixing matrix $U$. In some of these regions the high energy contribution in $Y_B$ is so strongly suppressed that one can have successful leptogenesis only if the requisite CP violation is provided by the Majorana phase(s) in $U$.

The see-saw parameter space considered in this section is compatible with the two flavour regime of leptogenesis, $10^9$ GeV $\lesssim M_1 \lesssim 10^{12}$ GeV. For simplicity, the lightest neutrino mass is $m_3$ is set equal to zero and the heaviest RH neutrino $N_3$ is assumed to be decoupled from the theory. The latter condition is easily fulfilled if $R_{13} = 0$. As will be discussed below, all the results derived here are actually valid if the following more general conditions are fulfilled: $i)$ $|R_{13}|^2 \sin 2\tilde{\varphi}_{13} \ll \min(|R_{11}|^2 \sin 2\tilde{\varphi}_{11}, |R_{12}|^2 \sin 2\tilde{\varphi}_{12})$ and $ii)$ the terms proportional to $m_3|R_{13}|^2$ and $m_3^2|R_{13}|^2$ in the expressions of $\epsilon_{1\tau}$ and $\epsilon_{1o}$ are negligible. The first condition is satisfied not only in the $N_3-$decoupling limit but also for $R_{13} \neq 0$, but $\text{Im}(R_{13}^2) = 0$. The second condition is naturally verified in the case of inverted hierarchical light neutrino mass spectrum. Working in the framework defined by the constraints $i)$ and $ii)$, one can use the orthogonality of the $R$ matrix to express the two relevant "high" energy phases $\tilde{\varphi}_{11}$ and $\tilde{\varphi}_{12}$ in terms of the absolute values $|R_{11}|$, $|R_{12}|$ and of $R_{13}^2$ which is real:

$$\cos 2\tilde{\varphi}_{11} = \frac{\left(1 - R_{13}^2\right)^2 + |R_{11}|^4 - |R_{12}|^4}{2|R_{11}|^2 \left(1 - R_{13}^2\right)}, \qquad (3.27)$$

$$\cos 2\tilde{\varphi}_{12} = \frac{\left(1 - R_{13}^2\right)^2 - |R_{11}|^4 + |R_{12}|^4}{2|R_{12}|^2 \left(1 - R_{13}^2\right)}, \qquad (3.28)$$

with the further constraint: $\text{sign}(\sin 2\tilde{\varphi}_{11}) = -\text{sign}(\sin 2\tilde{\varphi}_{12})$. In the cases discussed below the sign is fixed as: $\sin 2\tilde{\varphi}_{11} < 0$.
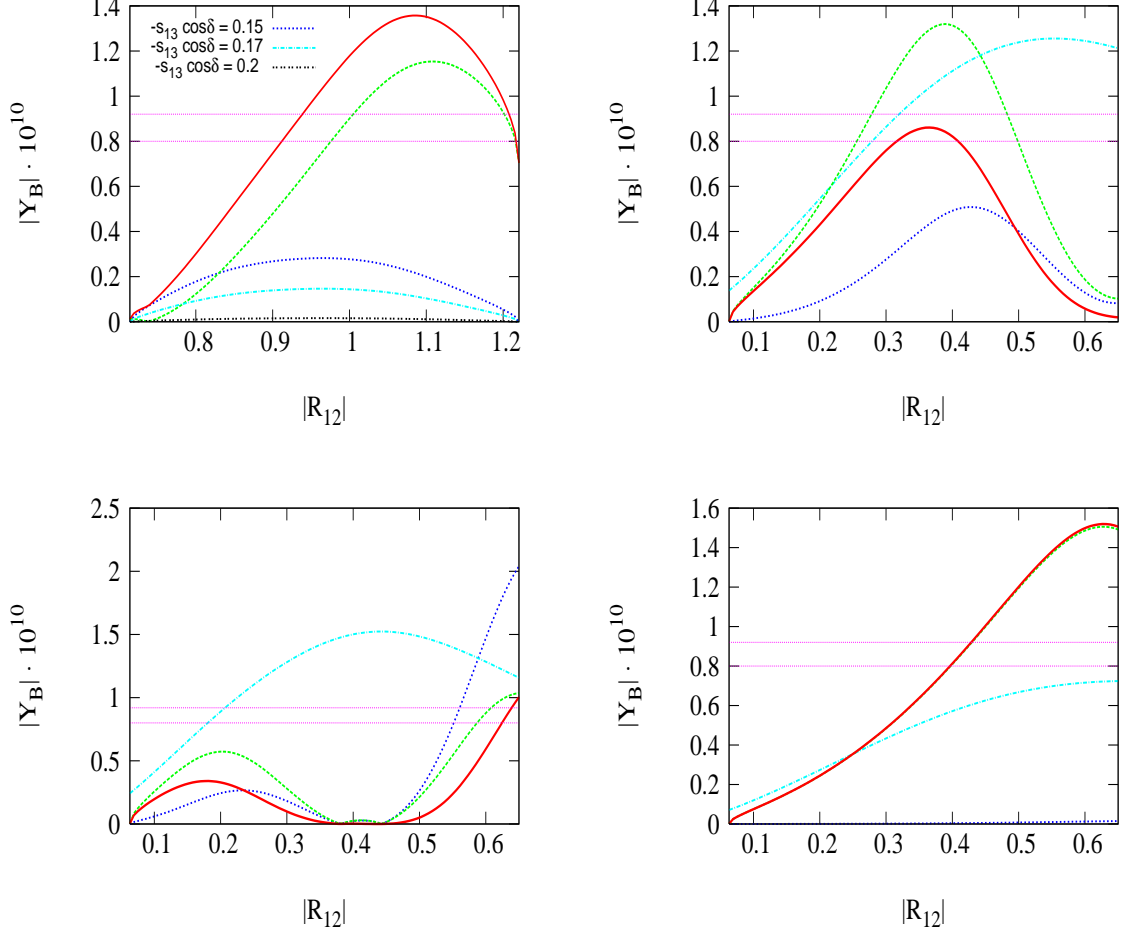
**Figure 3.8:** The dependence of the high energy term $|Y_B^0 A_{\mathrm{HE}}|$ (blue dotted line), the mixed term $|Y_B^0 A_{\mathrm{MIX}}|$ (green dashed line) and of the total baryon asymmetry $|Y_B|$ (red continuous line) on $|R_{12}|$ in the case of IH spectrum, CP violation due to the Majorana phase $\alpha_{21}$ and $R-$phases: $i$) $(-s_{13} \cos \delta) =$ 0.15; 0.17; 0.20, $\alpha_{21} = \pi/2$, $|R_{11}| = 0.7$ (upper left panel); $ii$) $\alpha_{21} = \pi/2$, $|R_{11}| \cong 1$, $s_{13} = 0$ (upper right panel), $s_{13} = 0.2$, $\delta = 0$ (lower left panel), $s_{13} = 0.2$, $\delta = \pi$ (lower right panel). The light-blue dot-dashed curve in the last three panels represents the dependence of $Y_B$ on $|R_{12}|$ for the given PMNS parameters and CP conserving matrix R, with $R_{11} R_{12} \equiv ik|R_{11} R_{12}|$, $k = -1$ and $|R_{11}|^2 - |R_{12}|^2 = 1$. In all the panels the lightest RH neutrino mass is $M_1 = 10^{11}$ GeV. The horizontal lines indicate the allowed range of $|Y_B|$, $|Y_B| \in [8.0, 9.2] \times 10^{-11}$.

The CP violating asymmetry $\epsilon_{1\tau}$, in the case considered, is given by [75]:

$$
\begin{aligned}
\epsilon_{1\tau} \;\cong\; & -\frac{3\,M_1}{16\,\pi\,v^2} \frac{\sqrt{|\Delta m_{\mathrm{A}}^2|}}{|R_{11}|^2 + |R_{12}|^2} \left\{ |R_{11}|^2 \sin(2\tilde{\varphi}_{11}) \left[ (|U_{\tau 1}|^2 - |U_{\tau 2}|^2) - \frac{\Delta m_{\odot}^2}{|\Delta m_{\mathrm{A}}^2|} |U_{\tau 1}|^2 \right] \right. \\
& + |R_{11}|\,|R_{12}| \left[ \frac{1}{2} \frac{\Delta m_{\odot}^2}{|\Delta m_{\mathrm{A}}^2|} \cos(\tilde{\varphi}_{11} + \tilde{\varphi}_{12}) \,\mathrm{Im}(U_{\tau 1}^* U_{\tau 2}) \right. \\
& \left. \left. + 2\left( 1 - \frac{1}{2} \frac{\Delta m_{\odot}^2}{|\Delta m_{\mathrm{A}}^2|} \right) \sin(\tilde{\varphi}_{11} + \tilde{\varphi}_{12}) \,\mathrm{Re}(U_{\tau 1}^* U_{\tau 2}) \right] \right\} .
\end{aligned}
\tag{3.29}
$$

For $\tilde{\varphi}_{11} = k\pi/2$, $\tilde{\varphi}_{12} = k'\pi/2$ ($k, k' = 0, 1, 2, ...$) $R_{11}$ and $R_{12}$ are either real or purely imaginary and the expression for $\epsilon_{1\tau}$ reduces to Eqs (1.78) or (1.79). Under these conditions successful leptogenesis is possible for $R_{13} = 0$ only if $R_{11}R_{12}$ is purely imaginary, *i.e.* if $|\sin(\tilde{\varphi}_{11} + \tilde{\varphi}_{12})| = 1$, the requisite CP violation being provided exclusively by the Majorana or Dirac phases in the PMNS matrix [54].

One can easily show that for the IH light neutrino mass spectrum of interest in the present analysis, the following relation holds [75]: [5]

$$\epsilon_{1o} = -\epsilon_{1\tau} \left( 1 + \mathcal{O}(\Delta m_\odot^2/|\Delta m_A^2|) \right) . \tag{3.30}$$

As in the NH case discussed in the previous section, the leptogenesis parameter space can be divided according to the different sources of CP violation that enter in the expression of the CP asymmetry $\epsilon_{1\tau}$. In particular, following the discussion reported at the end of Chapter 1, few considerations should be taken into account:

i) The $R$ matrix satisfies the CP invariance constraint if its elements $R_{ij}$ are real or purely imaginary (see Eq. (1.47)).

ii) In order to have CP violation, *e.g.* only due to the Majorana phase $\alpha_{21}$ in $U$, both $\text{Im}(U_{\tau 1}^* U_{\tau 2})$ and $\text{Re}(U_{\tau 1}^* U_{\tau 2})$ should be different from zero [41, 42], while the Dirac phase $\delta$ should have a CP conserving value, $\delta = k\pi$ ($k = 0, 1, 2, ...$) (*i.e.* the rephasing invariant $J_{CP}$, Eq. (1.18), associated to $\delta$ should satisfy $J_{CP} = 0$).

iii) Purely imaginary $R_{11}R_{12}$, *i.e.* $|\sin(\tilde{\varphi}_{11} + \tilde{\varphi}_{12})| = 1$, and $\text{Re}(U_{\tau 1}^* U_{\tau 2}) = 0$, $J_{CP} = 0$ corresponds to the case of CP invariance and therefore $\epsilon_{1\tau} = 0$.

iv) Purely imaginary $R_{11}R_{12}$ and $J_{CP} = 0$, $\text{Im}(U_{\tau 1}^* U_{\tau 2}) = 0$, but $\text{Re}(U_{\tau 1}^* U_{\tau 2}) \neq 0$, *i.e.* $\delta = k\pi$, $\alpha_{21} = 2\pi q$ ($k, q = 0, 1, 2, ...$), corresponds to CP violation due to the neutrino Yukawa couplings, *i.e.* due to the combined effect of the matrix $R$ and of the PMNS matrix $U$, and $\epsilon_{1\tau} \neq 0$. It is interesting that in this case both $U$ and $R$ satisfy the CP invariance constraints (see Eqs (1.46) and (1.47), respectively), while the neutrino Yukawa couplings do not satisfy these constraints, *i.e.* relation (1.50) is verified for the specific case considered. As a consequence, under the indicated conditions there will be no CP violation effects caused by the PMNS matrix $U$ in the low energy neutrino mixing phenomena (neutrino oscillations, $(\beta\beta)_{0\nu}$-decay, etc.) and there will be no CP violation effects in the "high" energy phenomena which depend only on the matrix $R$ (*i.e.* do not depend on the PMNS matrix $U$).

### 3.2.1 CP violation and baryon asymmetry

According to relation (3.30), the baryon asymmetry $Y_B$ can be expressed just in terms of $\epsilon_{1\tau}$, with good approximation, in analogy to the case of the a CP conserving matrix $R$, reported in the previous chapter. Therefore, one has:

$$
\begin{aligned}
Y_B &\cong -\frac{12}{37} \frac{\epsilon_{1\tau}}{g_*} \left( \eta\left(\frac{390}{589}\widetilde{m}_{1\tau}\right) - \eta\left(\frac{417}{589}\widetilde{m}_{1o}\right) \right) \\
&\equiv Y_B^0 (A_{\text{HE}} + A_{\text{MIX}}) ,
\end{aligned} \tag{3.31}
$$

---

[5] Note that this relation is valid not only for $R_{13} = 0$, but also for non-zero real $R_{13}^2$: $R_{13} \neq 0$, $\text{Im}(R_{13}^2) = 0$.

where $Y_B^0$ is the same as in Eq. (3.17) and $A_{\text{HE(MIX)}} \equiv C_{\text{HE(MIX)}}(\eta(0.66\widetilde{m}_{1\tau}) - \eta(0.71\widetilde{m}_{1o})$, with

$$C_{\text{HE}} = G_{11} \sin 2\tilde{\varphi}_{11} \left[ |U_{\tau 1}|^2 - |U_{\tau 2}|^2 \right] , \qquad (3.32)$$

$$C_{\text{MIX}} \cong 2 G_{12} \sin(\tilde{\varphi}_{11} + \tilde{\varphi}_{12}) \operatorname{Re}(U_{\tau 1}^* U_{\tau 2}) , \qquad (3.33)$$

and

$$G_{11} \equiv \frac{|R_{11}|^2}{|R_{11}|^2 + |R_{12}|^2} , \qquad (3.34)$$

$$G_{12} \equiv \frac{|R_{11} R_{12}|}{|R_{11}|^2 + |R_{12}|^2} . \qquad (3.35)$$

The wash-out mass parameters are in this case:

$$\widetilde{m}_{1\tau} \cong \sqrt{|\Delta m_A^2|} \left[ |R_{11}|^2 |U_{\tau 1}|^2 + |R_{12}|^2 |U_{\tau 2}|^2 \right.$$
$$\left. + 2 |R_{11}| |R_{12}| \operatorname{Re}\left( e^{i(\tilde{\varphi}_{11} - \tilde{\varphi}_{12})} U_{\tau 1}^* U_{\tau 2} \right) \right] , \qquad (3.36)$$

$$\widetilde{m}_{1o} = \sqrt{|\Delta m_A^2|} (|R_{11}|^2 + |R_{12}|^2) - \widetilde{m}_{1\tau} . \qquad (3.37)$$

Notice that the contributions proportional to the factor $0.5 \Delta m_\odot^2 / |\Delta m_A^2| \cong 0.016$ in the CP asymmetry $\epsilon_{1\tau}$, Eq. (3.29), are neglected. In Eq. (3.31), $Y_B^0 A_{\text{HE}}$ is the *high energy term* which vanishes in the case of a CP conserving matrix $R$, while $Y_B^0 A_{\text{MIX}}$ is the *mixed term* which, in contrast to $Y_B^0 A_{\text{HE}}$, does not vanish when $R$ conserves CP: it includes the "low" energy CP violation, *e.g.* due to the Majorana phase $\alpha_{21}$ in the neutrino mixing matrix. It is important to notice that the phase $\alpha_{21}$ enters also into the expression for the $(\beta\beta)_{0\nu}$-decay effective Majorana mass in the case of IH light neutrino mass spectrum (see Eq. (1.32)). As discussed above, in order to have CP violation due to the Majorana phase $\alpha_{21}$, both $\operatorname{Im}(U_{\tau 1}^* U_{\tau 2})$ and $\operatorname{Re}(U_{\tau 1}^* U_{\tau 2})$ should be different from zero [41, 42].

### 3.2.2   Baryon asymmetry and large $\theta_{13}$

Using the formalism described above, one can study the interplay between the CP violation arising from the "high" energy phases of the orthogonal matrix $R$ ($R$−phases) and the "low" energy CP violating Dirac and/or Majorana phases in the neutrino mixing matrix, as well as the relative contributions of the high energy and the mixed terms $Y_B^0 A_{\text{HE}}$ and $Y_B^0 A_{\text{MIX}}$ in $Y_B$, in analogy to the analysis performed in the previous section concerning the case of NH light neutrino mass spectrum. One can see now that there are large regions of the corresponding leptogenesis parameter space where the high energy contribution to $Y_B$ is subdominant, or even strongly suppressed. The results of this study are illustrated in Fig. 3.8.

Two representative examples of such a suppression of $Y_B^0 A_{\text{HE}}$, which can take place even when the "high" energy $R$−phases get large CP violating values, are analyzed below in the simple case

$R_{13} = 0$. In both scenarios the CP asymmetry $\epsilon_{1\tau}$ is produced in the regime of mild wash-out ($\widetilde{m}_{1\tau} \cong (1 \div 3) \times 10^{-3}$ eV), while $\epsilon_{1o}$ (3.30) is generated with strong wash-out effects. Under these conditions the two-flavour regime in leptogenesis is realized for $M_1 \lesssim 5 \times 10^{11}$ GeV [70, 71]. More precisely, there are small subregions of the parameter space where the two-flavour regime is realized for $M_1 \leq 7 \times 10^{11}$ GeV; in another subregion, the results are valid for $M_1 \leq 3 \times 10^{11}$ GeV. If, for instance, $|R_{11}| = 1$, the two-flavour regime of leptogenesis is realized for $M_1 \lesssim 5 \times 10^{11}$ GeV, provided that $|R_{12}| \leq 0.7$. For $|R_{11}| \leq 0.5$, the same conclusion is valid for $M_1 \lesssim 5 \times 10^{11}$ GeV in the whole interval of variability of $|R_{12}|$; for $|R_{11}| = 1.1$ and $|R_{12}| \leq 1$ this is realized for $M_1 \lesssim 3 \times 10^{11}$ GeV. In the latter case $|R_{12}|$ can vary in the interval $0.45 \lesssim |R_{12}| \lesssim 1.45$.

From Eqs (3.31) and (3.33) one can see that the term $Y_B^0 A_{\text{HE}}$ is strictly related to the Dirac phase $\delta$, for sufficiently large $\theta_{13}$. Indeed, the following combination of the elements of the neutrino mixing matrix is relevant in the computation of the CP asymmetry $\epsilon_{1\tau}$ [75]:

$$
\begin{aligned}
|U_{\tau 1}|^2 - |U_{\tau 2}|^2 &\cong (s_{12}^2 - c_{12}^2)s_{23}^2 - 4s_{12}c_{12}s_{23}c_{23}s_{13}\cos\delta \\
&\cong -0.20 - 0.92\, s_{13}\,\cos\delta\,,
\end{aligned}
\tag{3.38}
$$

where $s_{12}^2 = 0.30$ and $s_{23}^2 = 0.5$ are used. Therefore, for $s_{13} = 0.2$ and the Dirac phase assuming the CP conserving value $\delta = \pi$, one has: $|U_{\tau 1}|^2 - |U_{\tau 2}|^2 \cong (-0.016)$. At the same time, $|Y_B^0 A_{\text{MIX}}| \propto |U_{\tau 1}^* U_{\tau 2}| \cong 0.27$. As a consequence, if the Majorana phase $\alpha_{21}$ has a sufficiently large CP violating value, the contribution of $|Y_B^0 A_{\text{MIX}}|$ to $|Y_B|$ can be by an order of magnitude bigger than the other term, $|Y_B^0 A_{\text{HE}}|$. Actually, for $s_{12}^2 = 0.30$ and $s_{23}^2 = 0.5$, the high energy term in $Y_B$ is strongly suppressed by the factor $(|U_{\tau 1}|^2 - |U_{\tau 2}|^2)$, if $(-\sin\theta_{13}\cos\delta) \gtrsim 0.15$, independently of the values of the "high" energy phases $\tilde{\varphi}_{11}$ and $\tilde{\varphi}_{12}$. Even if the latter assume large CP violating values, the purely high energy contribution to $Y_B$ would play a subdominant role in the generation of the baryon asymmetry compatible with the observations if the above inequality holds. For $(-\sin\theta_{13}\cos\delta) > 0.17$ and $M_1 \lesssim 5 \times 10^{11}$ GeV, the observed value of the baryon asymmetry cannot be generated by the high energy term $Y_B^0 A_{\text{HE}}$ alone. One can have successful leptogenesis in this case only if there is an additional dominant contribution in $Y_B$ due to the CP violating Majorana phase $\alpha_{21}$ from the neutrino mixing matrix. This result is valid in the whole range of variability of the parameter $|R_{12}|$ ($R_{13} = 0$), $|(1 - |R_{11}|^2)| \leq |R_{12}|^2 \leq (1 + |R_{11}|^2)$, and for $|R_{11}|$ having values in the interval $0.3 \lesssim |R_{11}| \lesssim 1.2$. For values of $|R_{11}|$ outside the indicated interval successful leptogenesis is not realized in the two-flavour regime, for $M_1 \lesssim 5 \times 10^{11}$ GeV. For the $3\sigma$ allowed values of $s_{12}^2 = 0.38$ and $s_{23}^2 = 0.36$, the same conclusion is valid if $0.06 \lesssim (-\sin\theta_{13}\cos\delta) \lesssim 0.12$. The values of $\sin\theta_{13}$ and $\sin\theta_{13}\cos\delta$, for which the discussed strong suppression is possible of $Y_B^0 A_{\text{HE}}$, can be probed by the Double CHOOZ and Daya Bay reactor neutrino experiments [38] and by the planned accelerator experiments on CP violation in neutrino oscillations [39]. As already discussed in the first chapter, in the recent analysis of the global neutrino oscillation data [40], a nonzero value of $\sin^2\theta_{13}$ was reported at $1.6\sigma$. The best value and the $1\sigma$ allowed interval of values of $\sin\theta_{13}$ found in [40], $\sin\theta_{13} = 0.126$ and $\sin\theta_{13} = (0.077 \div 0.161)$, are in the range of interest for the present analysis. In addition, $\cos\delta = -1$ is reported to be preferred over $\cos\delta = +1$ by the atmospheric neutrino data.

The results discussed above are illustrated in Fig. 3.8, upper left panel, where the dependence of $|Y_B^0 A_{\text{HE}}|$, $|Y_B^0 A_{\text{MIX}}|$ and $|Y_B|$ on $|R_{12}|$ is reported, for a fixed value of $|R_{11}| = 0.7$ ($R_{13} = 0$) and $\alpha_{21} = \pi/2$, $s_{13} = 0.2$, $(-s_{13}\cos\delta) = 0.15$ and $M_1 = 10^{11}$ GeV. Note that varying $|R_{12}|$ in its allowed

range is equivalent to change the "high" energy CP violating phases, see Eqs (3.27) and (3.28). The behavior of the high energy term for two additional values of $(-s_{13} \cos \delta)$ is also shown. It is clear form the upper left panel of Fig. 3.8 that, for $(-s_{13} \cos \delta) \gtrsim 0.15$, $|A_{\mathrm{HE}}|$ is *strongly suppressed* and is much smaller than $|A_{\mathrm{MIX}}|$ in almost all the range of variability of $|R_{12}|$. [6] The same conclusion holds if $|R_{11}|$ varies in the range: $0.3 \lesssim |R_{11}| \lesssim 1.2$. Therefore, reproducing the observed value of the baryon asymmetry is problematic or can even be impossible, without a contribution due to the CP violating phases in the PMNS matrix. Similar results are valid in the more general case of $R_{13} \neq 0$, $\mathrm{Im}(R_{13}^2) = 0$, for $0 \lesssim |R_{13}| \lesssim 0.9$, $1.05 \lesssim |R_{13}| \lesssim 1.5$ and $0.3 \lesssim |R_{11}| \lesssim 1.2$.

### 3.2.3  Baryon asymmetry and the Majorana phase $\alpha_{21}$

Another case in which the contribution of the high energy term in $Y_B$ is subdominant is illustrated in Fig. 3.8, upper right and lower panels. The different contributions to the baryon asymmetry as function of $|R_{12}|$ are reported. The parameter space corresponds to $0.05 \leq |R_{12}| \leq 0.65$, $|R_{11}| \cong 1$, $R_{13} = 0$ and $i)$ $s_{13} = 0$ (upper right panel), $ii)$ $s_{13} = 0.2$, $\delta = 0$ (lower left panel), $iii)$ $s_{13} = 0.2$, $\delta = \pi$ (lower right panel). The behavior of the total baryon asymmetry generated when the CP violation is due exclusively to the Majorana phase $\alpha_{21}$ is also given. It is manifest from the figures that in most of the chosen range of $|R_{12}|$, the contribution of the mixed term $|Y_B^0 A_{\mathrm{MIX}}|$ in $|Y_B|$ is greater than that of the high energy term $|Y_B^0 A_{\mathrm{HE}}|$ and plays a dominant role in the generation of baryon asymmetry compatible with that observed. Indeed, it follows from Eqs (3.27) and (3.28) that in the case under discussion: $\sin 2\tilde{\varphi}_{11} \cong -|R_{12}|^2$ and $\sin 2\tilde{\varphi}_{12} \cong (1 - |R_{12}|^4/8)$. This implies $|A_{\mathrm{HE}}| \propto |G_{11} \sin 2\tilde{\varphi}_{11}| \propto |R_{11} R_{12}|^2$, while $|A_{\mathrm{MIX}}| \propto 2|G_{12} \sin(\tilde{\varphi}_{11} + \tilde{\varphi}_{12})| \propto \sqrt{2}|R_{11} R_{12}|$, being $|\sin(\tilde{\varphi}_{11} + \tilde{\varphi}_{12})| \cong 1/\sqrt{2}$. The latter approximation is rather accurate for $|R_{11}| = 1$ and $|R_{12}| \leq 0.5$. Thus, for $|R_{12}| = 0.4$, for instance, one has $\tilde{\varphi}_{11} \cong -0.08$, $\tilde{\varphi}_{12} \cong \pi/4$, and correspondingly for $s_{13} = 0$ and $\alpha_{21} = \pi/2$ the relative magnitude between the two contributions is: $|A_{\mathrm{MIX}}|/|A_{\mathrm{HE}}| \cong 2.6$ (see Fig. 3.8, upper right panel). Note also that, if $s_{13} = 0$, the generated $|Y_B|$ is largest when the "high" energy $R-$phases assume CP conserving values. The same feature is clearly observed also for $s_{13} = 0.2$ and $\delta = 0$ at $|R_{12}| \lesssim 0.55$. Moreover, for $0.25 \lesssim |R_{12}| \lesssim 0.50$, the baryon asymmetry generated in the case of CP conserving $R-$phases is significantly larger in absolute value than the asymmetry produced when the relevant $R-$phases get CP violating values (see Fig. 3.8, lower left panel). Finally, for $s_{13} = 0.2$ and $\delta = \pi$ (see Fig. 3.8, lower right panel), the high energy term $|Y_B^0 A_{\mathrm{HE}}|$ is strongly suppressed by the factor $(|U_{\tau 1}|^2 - |U_{\tau 2}|^2)$, as explained above. If, however, $|R_{12}| \gtrsim 0.8$ and $M_1 \gtrsim 7 \times 10^{10}$ GeV, the high energy term in $|Y_B|$ is the dominant one and can provide the requisite baryon asymmetry compatible with the observations.

In conclusion, the purely high energy contribution to the baryon asymmetry plays a subdominant/negligible role in the generation of the baryon asymmetry of the Universe for values of the Majorana phase $\alpha_{21}$ in the interval $0 < \alpha_{21} \lesssim 2\pi/3$ and roughly in half of the parameter space spanned by the relevant elements of the $R$ matrix. In all the cases considered the observed value of the baryon asymmetry can be reproduced for values of the lightest RH Majorana neutrino mass

---

[6]The mixed term $|Y_B^0 A_{\mathrm{MIX}}|$ is shown to give the dominant contribution to the baryon asymmetry in certain regions of the leptogenesis parameter when $s_{13} \sim 0.2$ and the "low" energy source of CP violation arises from the Dirac phase $\delta$ alone, provided $\alpha_{21} = (2k+1)\pi$ $(k = 1, 2, \ldots)$ [74]. However, in most of the parameter space relevant for successful leptogenesis, the observed baryon asymmetry is generated by the input of the high energy term $|Y_B^0 A_{\mathrm{HE}}|$ (see *e.g.* Figs 11 and 12 in [74]).

lying in the interval $5^{10}\,\mathrm{GeV} \lesssim M_1 \lesssim 7 \times 10^{11}\,\mathrm{GeV}$.

## 3.3 Summary

In the present chapter it was studied the region of see-saw parameter space where high energy contribution to the baryon asymmetry of the Universe in thermal flavoured leptogenesis is subdominant or even suppressed. More precisely, the interplay between the "low" energy CP violation, originating from the PMNS neutrino mixing matrix $U$ and the "high" energy CP violation present in the matrix of neutrino Yukawa couplings was investigated in detail.

Two types of light neutrino mass spectrum allowed by the existing data were taken into account, namely, the normal hierarchical (NH), $m_1 \ll m_2 < m_3$, and the inverted hierarchical (IH), $m_3 \ll m_1 < m_2$. The lightest neutrinos mass in both cases is assumed to be negligibly small. Analyzing the possibility of NH spectrum and CP violation due to the Majorana phase $\alpha_{32}$ and the $R-$phases $\tilde{\varphi}_{12}$ and $\tilde{\varphi}_{13}$, it results that there exists a relatively large region of the relevant parameter space in which the predicted value of the baryon asymmetry exhibits a strong dependence on the Majorana phase $\alpha_{32}$, provided the latter lies in the interval $0 < \alpha_{32} < \pi$ (if $\sin 2\tilde{\varphi}_{12} < 0$, $\sin 2\tilde{\varphi}_{13} > 0$) or $3\pi < \alpha_{32} < 4\pi$ (when $\sin 2\tilde{\varphi}_{12} > 0$, $\sin 2\tilde{\varphi}_{13} < 0$). These regions typically correspond to $0.05 \lesssim |R_{13}| \lesssim 0.5$, $|R_{13}| < |R_{12}| \leq 1$, and to $|R_{12}| > 1$, $|R_{13}|^2 \sim |R_{12}|^2 - 1$. Depending on the value of $\alpha_{32}$, one can have, for instance, either $|Y_B| \ll 8.6 \times 10^{-11}$ or $Y_B$ compatible with the observations in the indicated regions. The effects of the "low" energy CP violation due to $\alpha_{32}$ can be non-negligible in leptogenesis also for $0.5 \leq |R_{13}| \leq |R_{12}| \leq 1$.

Very different results are obtained for IH neutrino mass spectrum. In this case there are large regions of values of the corresponding parameters, for which the contribution to $Y_B$ due to the "low" energy CP violating Majorana phase $\alpha_{21}$ or Dirac phase $\delta$ (for $\alpha_{21} = (2k+1)\pi$), is comparable in magnitude or exceeds the purely high energy contribution in $Y_B$, originating from CP violation generated by the complex orthogonal matrix $R$. Moreover, in certain significant subregions of the indicated regions, the contribution to $Y_B$ due to the "high" energy CP violation is subdominant. In particular, for $(-\sin\theta_{13}\cos\delta) \gtrsim 0.1$, the high energy term in $Y_B$ is strongly suppressed by the difference $|U_{\tau 1}|^2 - |U_{\tau 2}|^2$. The "high" energy phases $\tilde{\varphi}_{11}$ and $\tilde{\varphi}_{12}$ in this case can have large CP violating values. Nevertheless, if the indicated inequality is fulfilled, the purely high energy contribution to $Y_B$, due to the CP violating $R-$phases, would play practically no role in the generation of baryon asymmetry compatible with the observations. One would have successful leptogenesis in this case only if the requisite CP violation is provided by the Majorana and/or Dirac phases in the neutrino mixing matrix.

The results obtained in this chapter, therefore, show that CP violation in the lepton sector, due to the "low" energy Majorana and Dirac phases in the PMNS matrix, can affect significantly the generation of baryon asymmetry compatible with the observation in the *flavoured leptogenesis* scenario, even in the presence of "high" energy CP violation, given by additional physical phases in the matrix of neutrino Yukawa couplings. In particular, in certain physical interesting cases, like IH light neutrino mass spectrum, relatively large value of $(-\sin\theta_{13}\cos\delta)$, etc., the contribution to $Y_B$ due to the low energy source of CP violation can be decisive in order to produce a sufficiently large baryon asymmetry.

# Chapter 4

# Leptogenesis in Models with $A_4$ Flavour Symmetry

In the present chapter the correlation between the Majorana CP violating phases in the PMNS matrix and leptogenesis is studied in detail in two rather generic supersymmetric see-saw models based on $A_4$ flavour symmetry, which naturally lead at leading order (LO) to tri-bimaximal (TB) mixing in the lepton sector. The TB mixing scheme was introduced in Section 1.2.2 and the corresponding form of the PMNS neutrino mixing is given in Eq. (1.17).

The analysis reported in the following is based mainly on the results obtained in [18].
The two models discussed in this chapter and in [18] employ the type I see-saw mechanism of neutrino mass generation and are variations of the supersymmetric $A_4$ models introduced in [81] and [82], which are summarized in Appendix B. They predict at leading order (LO) a diagonal mass matrix for charged leptons and lead to exact TB mixing in the neutrino sector. The main difference with respect to the original models is in the predicted right-handed (RH) neutrino mass scale. Indeed, the RH neutrino masses in the variations considered here and in [18] are set in the range $(10^{11} \div 10^{13})$ GeV, which is about two orders of magnitude smaller than the mass scale in reported in [81, 82]. This is realized, in practice, by adding a $Z_2$ symmetry which is able to suppress sufficiently the neutrino Yukawa couplings. As a consequence, the mass scale of the RH neutrinos is lowered as well. This choice was motivated in order to avoid possible potential problems with lepton flavour violating (LFV) processes within the two models considered. A detailed analysis of the LFV effects within the two original models of references [81, 82], in the framework of Minimal Supergravity, is reported in the next and last chapter of the thesis. The flavon superpotential in the modified models of interest is defined in Appendix C.

The results obtained at leading order and next-to-leading order (NLO) in the original models [81, 82] are still valid in the extensions considered in this chapter. In particular, the mass matrix of the RH neutrinos contains only two complex parameters $X$, $Z$ (see Section 4.2, further in this chapter). All low energy observables are expressed through only three independent quantities: the real parameter $\alpha = |3Z/X|$, the relative phase $\phi$ between $X$ and $Z$, and the absolute scale of the light neutrino masses. The latter is a combination of the neutrino Yukawa coupling and the parameter $|X|$ which determines the scale of RH neutrino masses. The analysis of the baryon asymmetry generation is performed in the one-flavour approximation. The latter is valid as long

as the masses of the RH neutrinos satisfy $M_i \gtrsim 5 \times 10^{11}(1 + \tan^2 \beta)$ GeV, where $\tan \beta$ is the ratio of the vacuum expectation values of the two Higgs doublets present in the SUSY extensions of the Standard Model. The one-flavour regime holds for, e.g. $\tan \beta \sim 3$ and $M_i \sim 10^{13}$ GeV. In the models we consider here relatively small values of $\tan \beta$ are indeed preferable (see Appendix B.3). Further, with masses of the RH neutrinos in the range of $(10^{11} \div 10^{13})$ GeV, one can safely neglect the effects of the $\Delta L = 2$ wash-out processes in leptogenesis [72]. This allows to use simple analytic approximations in the calculation of the relevant efficiency factors, already introduced in Chapter 1. The baryon asymmetry is computed for the two types of light neutrino mass spectrum allowed by data, *i.e.* pattern with normal ordering (NO) and inverted ordering (IO). Both types of spectrum are naturally predicted in the $A_4$ models.

In the class of models under consideration, the two Majorana phases of the PMNS matrix, $\alpha_{21}$ and $\alpha_{31}$, effectively play the role of leptogenesis CP violating parameters in the generation of the baryon asymmetry of the Universe. Notice that, this scenario is completely different from the one depicted in Chapters 2 and 3, where a model independent analysis of *flavoured* leptogenesis was done. In the models studied here, what matters in the computation of $Y_B$ are the total CP asymmetries, $\epsilon_k$. The dependance of $\epsilon_k$ on the "low" energy Majorana phases *is not due to flavour effects* (leptogenesis happens in the one-flavour regime), but rather to the *flavour symmetry* of the models, which constraints the see-saw parameter space and, in particular, the form of the Dirac and Majorana mass terms, $m_D$ and $M_N$, in the neutrino sector. In fact, the phases $\alpha_{21}$ and $\alpha_{31}$ and the ratio $r \equiv \Delta m_\odot^2 / |\Delta m_A^2|$, determined in such types of models, are functions of only one parameter, *e.g.* $\alpha$ or $\phi$. The resulting Majorana phases are the only source of CP violation in the CP asymmetries relevant for leptogenesis and are enough in order to generate the correct size and sign of the baryon asymmetry $Y_B$, within the two versions of $A_4$ models analyzed here. As was pointed out in [83], the CP asymmetries, originating in the decays of the RH neutrinos and sneutrinos fields and relevant for the generation of the baryon asymmetry of the Universe, always vanish at LO. Thus, successful leptogenesis is possible only if the NLO corrections are taken into account. The latter are different in the two specific models considered here, so that also the results for the CP asymmetries and the baryon asymmetry differ.

The chapter is organized as follows: in Section 4.1 the two models are introduced and the changes with respect the original ones, owing to the additional the $Z_2$ symmetry, are discussed. The possible light and heavy Majorana neutrino mass spectra are analyzed in Section 4.2. The Majorana phases are also introduced and their dependence on the parameter $\alpha$ is shown. Finally, in Section 4.3 results concerning the production of the baryon asymmetry of the Universe in the two specific model considered are presented.

## 4.1 Models with $A_4$ Flavour Symmetry

In this section two different models based on the flavour symmetry group $A_4$ are introduced and the main features discussed. The two flavour models are variations of the field and symmetry content studied in [81] and [82], whose basic features are summarized in Appendix B. In this class of models both the lepton doublets $\ell_1$, $\ell_2$ and $\ell_3$ and the neutrino singlets $\nu_1^c$, $\nu_2^c$ and $\nu_3^c$ are unified in triplet representations of $A_4$, respectively denoted as $\ell$ and $\nu^c$. Note that the states $\ell_j$ in $\ell$ are given in the basis in which the superpotential is defined, which does not coincides with the see-saw flavour

| Field | $\ell$ | $e^c$ | $\mu^c$ | $\tau^c$ | $\nu^c$ | $h_{u,d}$ | $\varphi_T$ | $\varphi_S$ | $\xi, \tilde{\xi}$ | $\zeta$ |
|-------|--------|-------|---------|----------|---------|-----------|-------------|-------------|--------------------|---------|
| $A_4$ | 3 | 1 | $1''$ | $1'$ | 3 | 1 | 3 | 3 | 1 | 1 |
| $Z_3$ | $\omega$ | $\omega^2$ | $\omega^2$ | $\omega^2$ | $\omega^2$ | 1 | 1 | $\omega^2$ | $\omega^2$ | 1 |
| $Z_2$ | $+$ | $+$ | $+$ | $+$ | $-$ | $+$ | $+$ | $+$ | $+$ | $-$ |

**Table 4.1:** Particle content of Model 1: transformation properties of lepton superfields, Minimal Supersymmetric (MSSM) Higgs and flavons under the flavor group $A_4 \times Z_3 \times Z_2$. The field $\ell$ denotes the three lepton doublets, $e^c$, $\mu^c$ and $\tau^c$ are the three $SU(2)_L$ singlets and $\nu^c$ are the three RH neutrinos forming an $A_4$-triplet. Apart from $\nu^c$ and the flavon $\zeta$ all fields are neutral under the additional $Z_2$ symmetry. Note that $\omega$ is the third root of unity, *i.e.* $\omega = \mathrm{e}^{\frac{2\pi i}{3}}$. Additionally, the model contains a $U(1)_R$ symmetry relevant for the alignment of the vacuum (see *e.g.* [81] for details).

basis, as discussed below.

### 4.1.1 Model 1

This model is based on the flavour symmetry group: $A_4 \times Z_3 \times Z_2 \times U(1)_{FN}$. It is a variation, through the addition of the $Z_2$ discrete group, of the model studied in [81]. The $U(1)_{FN}$ symmetry is used to accommodate the charged lepton mass hierarchy. As mentioned before, a further $Z_2$ symmetry is added to suppress the Dirac couplings of the neutrinos at leading order and, consequently, the RH neutrino mass scale. [1] Assuming that the RH neutrino superfields $\nu^c$ acquire a sign under $Z_2$, the renormalizable coupling with the left-handed lepton doublets $\ell$ and the Higgs doublet $h_u$ superfields becomes forbidden. [2] Alternatively, one could also let $h_u$ instead of $\nu^c$ transform under the $Z_2$ symmetry to forbid the Dirac Yukawa coupling at the renormalizable level. To allow a Yukawa coupling for neutrinos at all it is enough to introduce a new flavon $\zeta$ which only transforms under $Z_2$, with $\langle\zeta\rangle = z \approx \varepsilon\Lambda$, where $\Lambda$ is the cut-off of the theory and $\varepsilon \approx 0.04$. [3] The vacuum expectation value (VEV) of $z$ is the same as all other flavon VEVs. The symmetries and particle content of Model 1 are reported in Tab. 4.1.

At LO in the cut-off scale $\Lambda$, the neutrino masses are generated by superpotential: [4]

$$y_\nu(\nu^c\ell)h_u\zeta/\Lambda + a\,\xi(\nu^c\nu^c) + b\,(\nu^c\nu^c\varphi_S) \tag{4.1}$$

---

[1]See the see-saw mass relation in Eq. (1.9)

[2]Here and in the next chapter the particle fields are always denoted with the same symbol as the corresponding superfields. The supersymmetric partner is, instead, indicated with a tilde over the proper superfield notaion.

[3]The range of variability of the expansion parameter $\varepsilon$ in the class of models considered is reported in Appendix B.3.

[4]The field $\tilde{\xi}$ in Tab. 4.1 does not have a VEV at LO [81] and, therefore, is not relevant at this level.

with $(\cdots)$ denoting the contraction to an $A_4$-invariant (see Appendix A for details). The RH neutrino superfields $\nu^c$, which transform as a triplet of $A_4$ (see Tab. 4.1), are considered in the flavour basis. The mass matrices of the neutrinos are of the form:

$$m_D = y_\nu \begin{pmatrix} 1 & 0 & 0 \\ 0 & 0 & 1 \\ 0 & 1 & 0 \end{pmatrix} \frac{z}{\Lambda} v_u \quad \text{and} \quad M_N = \begin{pmatrix} -au - 2bv_S & bv_S & bv_S \\ bv_S & -2bv_S & bv_S - au \\ bv_S & bv_S - au & -2bv_S \end{pmatrix} , \qquad (4.2)$$

with $v_u = \langle h_u \rangle$, $\langle \xi \rangle = u$ and $\langle \varphi_{Si} \rangle = v_S$, according to the alignment given in [81] (see Appendix B). The light neutrino mass matrix is indeed obtained from $m_D$ and $M_N$ via the type I see-saw mechanism:

$$m_\nu = m_D^T M_N^{-1} m_D = U^* \operatorname{diag}(m_1, m_2, m_3) U^\dagger \qquad (4.3)$$

and has the generic size $\varepsilon v_u^2 / \Lambda$. At the same time, the effective dimension-5 operator $\ell h_u \ell h_u / \Lambda$, [5] which can also contribute to the light neutrino masses, is only invariant under the flavor group, if it involves two flavons of the type $\varphi_S$ and $\xi$ ($\tilde{\xi}$). Thus, its contribution to $m_1$, $m_2$ and $m_3$ scales as $\varepsilon^2 v_u^2 / \Lambda$, which is always subdominant, compared to the type I see-saw (leading order) term.

Considering the NLO corrections, note that they involve for the Dirac neutrino mass matrix either the two flavon combination $\varphi_T \zeta$ or the shift of the vacuum of $\zeta$. The first type gives rise to two different terms:

$$y_A \left( (\nu^c \ell)_{3_S} \varphi_T \right) h_u \zeta / \Lambda^2 + y_B \left( (\nu^c \ell)_{3_A} \varphi_T \right) h_u \zeta / \Lambda^2 \qquad (4.4)$$

with $(\cdots)_{3_{S(A)}}$ standing for the (anti-)symmetric triplet of the product $\nu^c \ell$ (see Eq. (A.9)). The correction due to the shift in $\langle \zeta \rangle$ can be simply absorbed into a redefinition of the coupling $y_\nu$. Thus, using the alignment of $\varphi_T$ as given in [81] (see Appendix B.2), $\langle \varphi_T \rangle = v_T (1, 0, 0)^T$, the structure of the NLO corrections to $m_D$ is the same as in the original model:

$$\delta m_D = \begin{pmatrix} 2y_A & 0 & 0 \\ 0 & 0 & -y_A - y_B \\ 0 & -y_A + y_B & 0 \end{pmatrix} \frac{v_T z}{\Lambda^2} v_u . \qquad (4.5)$$

The NLO corrections to the Majorana mass matrix of the RH neutrinos are lso unchanged:

$$a\, \delta\xi(\nu^c \nu^c) + \tilde{a}\, \delta\tilde{\xi}(\nu^c \nu^c) + b\, (\nu^c \nu^c \delta\varphi_S) \qquad (4.6)$$
$$+ x_A (\nu^c \nu^c)(\varphi_S \varphi_T)/\Lambda + x_B (\nu^c \nu^c)'(\varphi_S \varphi_T)''/\Lambda + x_C (\nu^c \nu^c)''(\varphi_S \varphi_T)'/\Lambda$$
$$+ x_D (\nu^c \nu^c)_{3_S}(\varphi_S \varphi_T)_{3_S}/\Lambda + x_E (\nu^c \nu^c)_{3_S}(\varphi_S \varphi_T)_{3_A}/\Lambda + x_F (\nu^c \nu^c)_{3_S}\varphi_T \xi/\Lambda + x_G (\nu^c \nu^c)_{3_S}\varphi_T \tilde{\xi}/\Lambda$$

where $\delta\varphi_S$, $\delta\xi$ and $\delta\tilde{\xi}$ indicate the shifted vacua of the flavons $\varphi_S$, $\xi$ and $\tilde{\xi}$. Taking into account the possibility of absorbing these corrections partly into the LO result, they give rise to four independent additional contributions to $M_N$ which can be effectively parametrized as

$$\delta M_N = \begin{pmatrix} -2\tilde{x}_D & -\tilde{x}_A & \tilde{x}_C - \tilde{x}_B \\ -\tilde{x}_A & -\tilde{x}_B - 2\tilde{x}_C & \tilde{x}_D \\ \tilde{x}_C - \tilde{x}_B & \tilde{x}_D & -\tilde{x}_A \end{pmatrix} \varepsilon^2 \Lambda . \qquad (4.7)$$

---

[5] All non-renormalizable operators are considered suppressed by the same cut-off scale $\Lambda$.

| Field | $\ell$ | $e^c$ | $\mu^c$ | $\tau^c$ | $\nu^c$ | $h_d$ | $h_u$ | $\varphi_T$ | $\xi'$ | $\varphi_S$ | $\xi$ | $\zeta$ |
|---|---|---|---|---|---|---|---|---|---|---|---|---|
| $A_4$ | 3 | 1 | 1 | 1 | 3 | 1 | $1''$ | 3 | $1'$ | 3 | 1 | $1'$ |
| $Z_4$ | $i$ | 1 | $i$ | $-1$ | $-1$ | 1 | 1 | $i$ | $i$ | 1 | 1 | $i$ |
| $Z_2$ | $+$ | $+$ | $+$ | $+$ | $+$ | $+$ | $-$ | $+$ | $+$ | $+$ | $+$ | $-$ |

**Table 4.2:** Particle content of the Model 2: transformation properties of lepton superfields, MSSM Higgs and flavons under the flavor group $A_4 \times Z_4 \times Z_2$ are shown. The nomenclature is as in Tab. 4.1. Apart from $h_u$ and the flavon $\zeta$ all fields are neutral under the additional $Z_2$ symmetry. Apart from $A_4 \times Z_4 \times Z_2$, the model also contains a $U(1)_R$ symmetry relevant for the alignment of the vacuum (see *e.g.* [82] for details).

Compared to these, NLO corrections involving the new flavon $\zeta$ are suppressed, since invariance under the $Z_2$ symmetry requires always an even number of $\zeta$ fields and invariance under the $Z_3$ at least one field of the type $\varphi_S$, $\xi$ or $\tilde{\xi}$. The NLO corrections to the charged lepton masses are also the same as in the original model and effects involving $\zeta$ can only arise at the level of three flavons. The VEV of the flavon $\zeta$ is naturally of the order $\varepsilon\Lambda$ as the VEVs of the other flavons and the shift of its VEV is of the size $\delta\text{VEV} \sim \varepsilon\text{VEV}$. Its effect on the vacuum alignment of the other flavons is computed in Appendix C.1 and it is shown that the results achieved in the original model [81], especially the alignment at LO, remain unchanged.

### 4.1.2 Model 2

The flavour symmetry in this case is: $A_4 \times Z_4 \times Z_2$. The model is a variation of the one studied in [82], which is based on the group $A_4 \times Z_4$ and predicts a tri-bimaximal neutrino mixing at leading order, as seen for Model 1. The additional $Z_2$ symmetry with respect to the original model is used to suppress the neutrino Yukawa couplings at renormalizable level. Moreover, only the Higgs field $h_u$ and the new flavon $\zeta$ transform under the $Z_2$ symmetry. Compared to the original model, the field $h_u$ transforms as a $1''$ under $A_4$ and trivially under $Z_4$. The flavon $\zeta$ is a $1'$ under $A_4$ and acquires a phase $i$ under $Z_4$. The transformation properties of leptonic superfields, MSSM Higgs and flavons can be found in Tab. 4.2.

The Dirac neutrino coupling at LO is indeed:

$$y_\nu(\nu^c l)h_u\zeta/\Lambda \,, \tag{4.8}$$

which leads to the same Dirac mass matrix $m_D$ as in the original model, suppressed by the factor $\varepsilon$ for $z/\Lambda \approx \varepsilon$. The Majorana mass termsfor the RH neutrinos remains unaffected by the changes of the model, at LO:

$$M(\nu^c\nu^c) + a\xi(\nu^c\nu^c) + b\,(\nu^c\nu^c\varphi_S)\,, \tag{4.9}$$

so that the contribution from the type I see-saw to the light neutrino masses arises from:

$$m_D = y_\nu \begin{pmatrix} 1 & 0 & 0 \\ 0 & 0 & 1 \\ 0 & 1 & 0 \end{pmatrix} \frac{z}{\Lambda} v_u \,, \tag{4.10}$$

$$M_N = \begin{pmatrix} -M - au - 2bv_S & bv_S & bv_S \\ bv_S & -2bv_S & -M - au + bv_S \\ bv_S & -M - au + bv_S & -2bv_S \end{pmatrix} \,. \tag{4.11}$$

The flavon alignment is the same as the one given in [82] and it is reported in Appendix B.2. Eq. (4.11) leads to exact TB mixing in the neutrino sector. For $M \approx \varepsilon \Lambda$, as argued in [82], one finds the generic size of the light neutrino masses to be $\varepsilon v_u^2 / \Lambda$. The effective dimension-5 operator $\ell h_u \ell h_u / \Lambda$ arises in this variant only at the two flavon level:

$$(\varphi_T \varphi_T)''(\ell\ell)h_u^2/\Lambda^3 + (\varphi_T \varphi_T)'(\ell\ell)'h_u^2/\Lambda^3 + (\varphi_T \varphi_T)(\ell\ell)''h_u^2/\Lambda^3 + ((\varphi_T \varphi_T)_{3_S}(\ell\ell)_{3_S})''h_u^2/\Lambda^3$$
$$+(\xi')^2(\ell\ell)h_u^2/\Lambda^3 + \xi'(\varphi_T \ell\ell)'h_u^2/\Lambda^3 + \zeta^2(\ell\ell)h_u^2/\Lambda^3 \,, \tag{4.12}$$

where order one couplings are omitted. Thus, its contributions to the light neutrino masses are of order $\varepsilon^2 v_u^2 / \Lambda$, *i.e.* of the same size as the expected NLO corrections to the type I see-saw contribution and, hence, subdominant.

The effect of the introduction of the $Z_2$ symmetry and the new field $\zeta$ on the charged lepton sector is the following: an insertion of three flavons, two of which are $\zeta$, gives a new LO contribution to the electron mass:

$$\zeta^2(e^c \ell \varphi_T)' h_d / \Lambda^3 \,. \tag{4.13}$$

Using the same vacuum alignment as in [82], its contribution resembles the one from the operator with $\xi'$ instead of $\zeta$ and thus gives also a non-vanishing term in the (11) entry of the charged lepton mass matrix. The latter is of the same size as those already encountered in the original version of the model [82]. Therefore in the variant considered here the charged lepton mass matrix is also diagonal at LO and the correct hierarchy among the charged lepton masses is predicted.

At NLO, the Dirac couplings of the neutrinos are:

$$y_\nu (\nu^c \ell)\delta \zeta h_u / \Lambda + y_A (\nu^c \ell)\xi \zeta h_u / \Lambda^2 + y_B ((\nu^c \ell)_{3_S}\varphi_S) \zeta h_u / \Lambda^2 + y_C ((\nu^c \ell)_{3_A}\varphi_S) \zeta h_u / \Lambda^2 \,. \tag{4.14}$$

The first two contributions can be absorbed into the LO coupling $y_\nu$. Compared to the original model, the other corrections are of the same type and generate the same structure

$$\delta m_D = \begin{pmatrix} 2y_B & -y_B - y_C & -y_B + y_C \\ -y_B + y_C & 2y_B & -y_B - y_C \\ -y_B - y_C & -y_B + y_C & 2y_B \end{pmatrix} \frac{v_S z}{\Lambda^2} v_u \,. \tag{4.15}$$

Note that, actually, the contribution associated to the coupling $y_B$ is still compatible with TB mixing so that only $y_C$ can lead to deviations from the TB mixing pattern. For this reason, also the CP asymmetries depend on the coupling $y_C$ alone (see Section 4.3).

All effects to the Majorana mass matrix of the RH neutrinos involving $\zeta$ are negligible, since one always needs at minimum two fields $\zeta$ and additionally the $Z_4$ charge of the operator must be balanced. Thus, the NLO corrections are only those already present in the original model:

$$x_A\,(\nu^c\nu^c)\xi^2/\Lambda + x_B\,(\nu^c\nu^c)(\varphi_S\varphi_S)/\Lambda + x_C(\nu^c\nu^c)_{3_S}(\varphi_S\varphi_S)_{3_S}/\Lambda + x_D(\nu^c\nu^c)_{3_S}\varphi_S\xi/\Lambda$$
$$+x_E\,(\nu^c\nu^c)'(\varphi_S\varphi_S)''/\Lambda + x_F\,(\nu^c\nu^c)''(\varphi_S\varphi_S)'/\Lambda\,. \tag{4.16}$$

The first four contributions can be absorbed into the LO result (or vanish). Effects from shifts in the vacua of $\varphi_S$ and $\xi$ can also be absorbed into the LO result. The new structures at NLO lead to a matrix $\delta M_N$ of the form:

$$\delta M_N = -3 \begin{pmatrix} 0 & x_E & x_F \\ x_E & x_F & 0 \\ x_F & 0 & x_E \end{pmatrix} \frac{v_S^2}{\Lambda}\,. \tag{4.17}$$

For the charged leptons, additional NLO corrections to the muon and the electron mass arise from three and four flavon insertions, respectively, involving the field $\zeta$. The operator

$$\zeta^2(\mu^c\ell\varphi_S)'h_d/\Lambda^3 \tag{4.18}$$

corrects the muon mass. This type of subleading contribution already exists in the original model in such a way that no new structures are introduced. The NLO corrections to the electron mass are induced through the operator $\zeta^2(e^c\ell\varphi_T)'h_d/\Lambda^3$, if the shifts in the vacua are taken into account, as well as through the four flavon operators

$$\zeta^2(e^c\ell(\varphi_T\varphi_S)_{3_S})'h_d/\Lambda^4 + \zeta^2(e^c\ell(\varphi_T\varphi_S)_{3_A})'h_d/\Lambda^4 + \zeta^2\xi(e^c\ell\varphi_T)'h_d/\Lambda^4 + \zeta^2\xi'(e^c\ell\varphi_S)h_d/\Lambda^4\,. \tag{4.19}$$

All structures arising from these terms are already generated by the NLO corrections present in the original model so that the analysis performed in [82] for the NLO corrections is still valid in the present variant.

In Appendix C.2 it is discussed how to give a VEV of the desired size to the field $\zeta$, the shift of this VEV from NLO corrections as well as the effects of $\zeta$ on the flavon superpotential of the original model, at LO and NLO.

## 4.2   Neutrino Masses and CP Violating Phases in the $A_4$ Models

The two models introduced in the previous section have in common that the Majorana mass matrix of RH neutrinos is of the form:

$$M_N = \begin{pmatrix} -X-2Z & Z & Z \\ Z & -2Z & Z-X \\ Z & Z-X & -2Z \end{pmatrix}, \tag{4.20}$$

while the neutrino Dirac mass matrix reads:

$$m_D = y_\nu \begin{pmatrix} 1 & 0 & 0 \\ 0 & 0 & 1 \\ 0 & 1 & 0 \end{pmatrix} \frac{z}{\Lambda} v_u\,. \tag{4.21}$$

The symmetry of this class of models implies that, at leading order, the see-saw Lagrangian depends only on few parameters: $X, Z$ and $y_\nu$. These parameters are, in general, complex numbers. One can set $y_\nu$ real by performing a global phase transformation of the lepton doublet fields. The CP violating phases, which enter in the CP asymmetries of the RH neutrino decays, are functions of the relative phase between $X$ and $Z$. The type I see-saw mechanism for the neutrino mass generation implies that the full parameter space of the neutrino sector can be constrained significantly by the low energy data.

The RH neutrino mass matrix (4.20) is diagonalized by the orthogonal matrix $U_{TB}$, given in Eq. (1.17):

$$\text{diag}(M_1 e^{i\varphi_1}, M_2 e^{i\varphi_2}, M_3 e^{i\varphi_3}) = U_{TB}^T M_N U_{TB}, \tag{4.22}$$

where

$$\begin{aligned}
M_1 &= |X + 3Z| \equiv |X||1 + \alpha e^{i\phi}|, \quad \varphi_1 = \arg(X + 3Z), & (4.23) \\
M_2 &= |X|, \quad \varphi_2 = \arg(X), & (4.24) \\
M_3 &= |X - 3Z| \equiv |X||1 - \alpha e^{i\phi}|, \quad \varphi_3 = \arg(3Z - X). & (4.25)
\end{aligned}$$

Here $\alpha \equiv |3Z/X|$ and $\phi \equiv \arg(Z) - \arg(X)$. Therefore the RH (s)neutrino mass eigenstates $N_i(\widetilde{N}_i)$ are related to the flavour fields $\nu_j^c$ ($\tilde{\nu}_j^c$) by the following transformation:

$$\nu_j^c = \left( U_{TB} \, \text{diag}(e^{i\phi_1/2}, e^{i\phi_2/2}, e^{i\phi_3/2}) \right)_{jk} N_k. \tag{4.26}$$

A light neutrino Majorana mass term is generated after electroweak symmetry breaking via the type I see-saw mechanism:

$$m_\nu = m_D^T M_N^{-1} m_D = U^* \text{diag}(m_1, m_2, m_3) U^\dagger, \tag{4.27}$$

where

$$U = U_{TB} \, \text{diag} \left( e^{i\varphi_1/2}, e^{i\varphi_2/2}, e^{i\varphi_3/2} \right) \tag{4.28}$$

and $m_{1,2,3}$ are the light neutrino masses,

$$m_i \equiv \frac{(y_\nu)^2 v_u^2}{M_i} \left( \frac{z}{\Lambda} \right)^2. \tag{4.29}$$

Note that one of the phases $\varphi_k$ in $U$, say $\varphi_1$, can be considered as a common phase of the neutrino mixing matrix and, therefore, has no physical relevance. For this reason, $\varphi_1$ is set equal to zero in the subsequent numerical computation. As discussed in the previous section, in the class of models considered here, the charged lepton mass matrix is always diagonal at LO. Therefore, the matrix $U$ which diagonalizes $m_\nu$ in (4.27) coincides with the PMNS neutrino mixing matrix (see Section 1.1). More precisely, assuming the standard parametrization of the neutrino mixing matrix (1.11) and the tri-bimaximal form (1.17), the PMNS matrix in the class models considered is at LO:

$$U = \text{diag}(1, 1, -1) U_{TB} \, \text{diag}(1, e^{i\varphi_2/2}, e^{i\varphi_3/2}) \tag{4.30}$$

From Eqs (1.11) and (4.30) one can identify the "low energy" Majorana phases as:

$$\alpha_{21} = \varphi_2 \quad \text{and} \quad \alpha_{31} = \varphi_3. \tag{4.31}$$
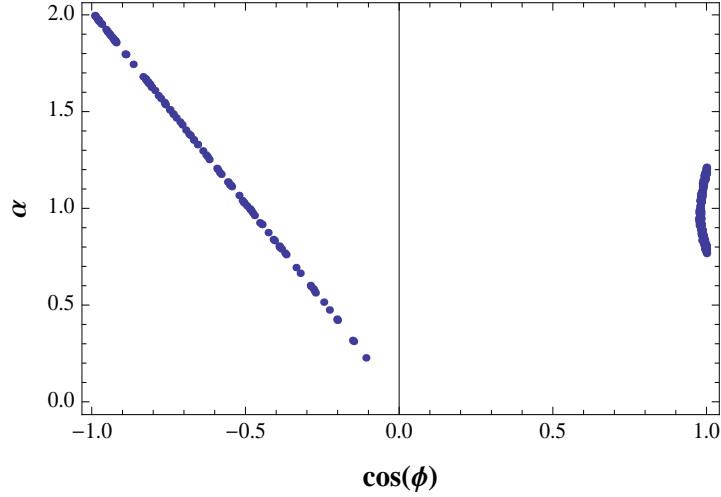
**Figure 4.1:** The correlation between the real parameter $\alpha$ and the phase $\phi$, which appear in the RH neutrino Majorana mass matrix. The figure is obtained by using the $3\sigma$ range of the parameter $r$ given in Eq. (4.32). See text for details.

At this order of perturbation theory, the CHOOZ mixing angle, $\theta_{13}$, is always zero as a consequence of the TB form of the neutrino mixing matrix, imposed by the broken $A_4$ discrete symmetry.

The parameters $|X|$, $\alpha$ and $\phi$ defined in (4.23)-(4.25), which determine the RH neutrino mass matrix, Eq. (4.20), can be constrained by the neutrino oscillation data. More specifically, one has for the ratio:

$$r \equiv \frac{\Delta m_\odot^2}{|\Delta m_A^2|} = \frac{(1 + \alpha^2 - 2\,\alpha\,\cos\phi)(\alpha + 2\cos\phi)}{4\,|\cos\phi|}\,, \tag{4.32}$$

where $\Delta m_\odot^2 = \Delta m_{21}^2 \equiv m_2^2 - m_1^2 > 0$ and $|\Delta m_A^2| = |\Delta m_{31}^2| \cong |\Delta m_{32}^2|$ are the neutrino mass squared differences responsible, respectively, for solar and atmospheric neutrino oscillations. Since $r$ is fixed by the data, Eq. (4.33), there is a strong correlation between the values of the parameters $\alpha$ and $\cos\phi$. Note that the sign of $\sin\phi$ cannot be constrained by the low energy data, but it is fixed by the sign of the baryon asymmetry of the Universe, computed in the leptogenesis scenario (see Section 4.3).

At $3\sigma$, the following experimental constraints must be satisfied (see Tab. 1.1):

$$\begin{aligned}
\Delta m_\odot^2 &> 0 \\
|\Delta m_A^2| &= (2.41 \pm 0.34) \times 10^{-3} \text{ eV}^2 \\
r &= 0.032 \pm 0.006\,.
\end{aligned} \tag{4.33}$$

The correlation between $\alpha$ and $\cos\phi$ is reported in Fig. 4.1. Depending on the sign of $\cos\phi$, the parameter space is divided into two physically distinct parts: $\cos\phi > 0$ corresponds to light neutrino mass spectrum with normal ordering, whereas for $\cos\phi < 0$ one obtains neutrino mass spectrum with inverted ordering.

In the models considered here the predicted RH neutrino masses are always rescaled by the additional factor $\varepsilon^2 \sim 10^{-3}$. Depending on the value of the neutrino Yukawa coupling $y_\nu$, the

lightest RH Majorana neutrino mass can be in the range from $(10^{11} \div 10^{12})$ GeV and up to $10^{13}$ GeV for a neutrino Yukawa coupling $y_\nu \sim \mathcal{O}(1)$.

A light neutrino mass spectrum with NO is generated through the see-saw mechanism if the RH neutrino masses show an approximately partial hierarchy: $M_1 \approx 2M_2 \approx 10M_3$. The lightest neutrino mass $m_1$, compatible with the experimental constraints given in (4.33), takes values in the interval:

$$3.8 \times 10^{-3}\text{eV} \lesssim m_1 \lesssim 6.9 \times 10^{-3}\text{eV} \,. \tag{4.34}$$

This implies that the light neutrino mass spectrum is with partial hierarchy as well. For the sum of the neutrino masses one has:

$$6.25 \times 10^{-2} \text{ eV} \lesssim m_1 + m_2 + m_3 \lesssim 6.76 \times 10^{-2} \text{ eV} \,. \tag{4.35}$$

In the case of IO spectrum, the overall range of variability of the lightest neutrino mass, $m_3$, is the following:

$$0.02 \,\text{eV} \lesssim m_3 \leq 0.50 \,\text{eV} \,, \tag{4.36}$$

where only the lower bound follows from the low energy constraints. The upper bound was chosen to be compatible with the "conservative" cosmological upper limit on the sum of the neutrino masses [30, 31]. Thus, the light neutrino mass spectrum can be with partial hierarchy or quasi-degenerate. If the spectrum is with partial hierarchy (*i.e.* $0.02 \,\text{eV} \lesssim m_3 < 0.10$ eV), for the RH Majorana neutrino masses, then to a good approximation: $M_1 \cong M_2 \cong M_3/3$. Quasi-degenerate light neutrino mass spectrum implies that, up to corrections $\sim \mathcal{O}(r)$, one has $M_1 \cong M_2 \cong M_3$. The sum of the light neutrino masses in the case of IO spectrum is predicted to satisfy:

$$m_1 + m_2 + m_3 \gtrsim 0.125 \text{ eV} \,. \tag{4.37}$$

The expressions for the lightest neutrino mass in the NO and IO spectrum as functions of $\alpha$ and $r$ are reported below. Recall that for fixed value of $r$, all the parameter space and the associated phenomenology is characterized by the parameter $\alpha$. In the numerical examples reported in the following, the value of the ratio $r$ is set equal to the best fit value: $r = 0.032$. The lightest neutrino mass in terms of $r$ is

$$m_1^2 \;=\; \Delta m_\text{A}^2 r \left( \frac{1}{1 + 2\alpha^2} + \frac{2(1 + \alpha^2)r}{(1 + 2\alpha^2)^3} \right) \,, \quad \text{for NO spectrum} \,, \tag{4.38}$$

$$m_3^2 \;=\; |\Delta m_\text{A}^2| \left( \frac{1}{2\alpha^2} + \frac{(1 + \alpha^2)r}{\alpha^2(1 + 2\alpha^2)} \right) \,, \quad \text{for IO spectrum} \,. \tag{4.39}$$

In the class of models considered here, the three light neutrino masses obey the general sum rule [84] (valid for both types of spectrum):

$$\frac{e^{i\varphi_3}}{m_3} \;=\; \frac{1}{m_1} - \frac{2e^{i\varphi_2}}{m_2} \tag{4.40}$$

This equation implies a strong correlation between the neutrino masses and the Majorana phases arising from the RH neutrino mass matrix. The Majorana phases are responsible for CP violation in leptogenesis and therefore they will be discussed in detail in the following subsection.
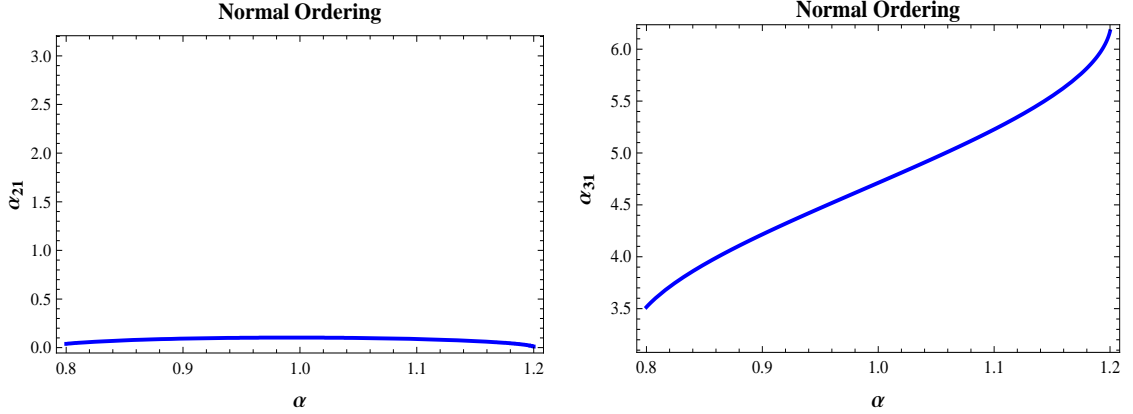
**Figure 4.2:** The Majorana phases $\alpha_{21}$ and $\alpha_{31}$ in the case of a light neutrino mass spectrum with normal ordering. The parameter $r$ is set to its best fit value, $r = 0.032$. The solutions of equations (4.41) and (4.42) shown in the figure correspond to $\sin\phi < 0$. See text for details.

### 4.2.1 The Majorana CPV phases and $(\beta\beta)_{0\nu}$-decay

In the models under discussion the Majorana phases $\alpha_{21}$ and $\alpha_{31}$ can also be constrained by using the neutrino oscillation data. After some algebraic manipulation, one obtains the following relations between the CP violating phases $\alpha_{21,31}$ and the see-saw parameters $\alpha$ and $\phi$ of the model:

$$\tan\alpha_{21} = -\frac{\alpha\sin\phi}{1 + \alpha\cos\phi} \tag{4.41}$$

$$\tan\alpha_{31} = 2\frac{\alpha\sin\phi}{\alpha^2 - 1}, \tag{4.42}$$

where $\alpha$ and $\cos\phi$ are correlated by Eqs (4.32) and (4.33).

In the case of NO spectrum one has $\phi = 0 \pm \rho, 2\pi \pm \rho$, with $\rho < 0.2$ and $0.8 \lesssim \alpha \lesssim 1.2$ (see Fig. 4.1). If $\rho \cong 0$, the two CP violating phases become unphysical. CP symmetry is preserved in this case. As regards the IO light neutrino mass spectrum, one has $2\cos\phi \approx -\alpha + \delta_\alpha(\alpha)$. The correction, $\delta_\alpha(\alpha)$ is given by:

$$\delta_\alpha(\alpha) = \frac{2\alpha r}{1 + 2\alpha^2}\left(1 - \frac{2(1 + \alpha^2)r}{(1 + 2\alpha^2)^2}\right). \tag{4.43}$$

For light neutrino mass spectrum with IO, the parameter $\alpha$ varies in the interval $0.07 \lesssim \alpha \lesssim 2$, where the lower limit of $\alpha$ comes from the indicative upper bound on the absolute neutrino mass scale cited before, $m_{1,2,3} \lesssim 0.5$ eV.

The behavior of the Majorana phases $\alpha_{21}$ and $\alpha_{31}$ as functions of $\alpha$ is shown in Figs 4.2 and 4.3, for the NO and IO mass spectrum, respectively. The solution corresponding to $\sin\phi < 0$ in (4.41) and (4.42) is chosen, in order to reproduce the correct sign of the baryon asymmetry (see Section 4.3). On the other hand, the relative sign of $\sin\alpha_{21}$ and $\sin\alpha_{31}$ is fixed by the requirement that the sum rule in Eq. (4.40) is satisfied. In the case of NO spectrum, the phase $\alpha_{21}$ is close
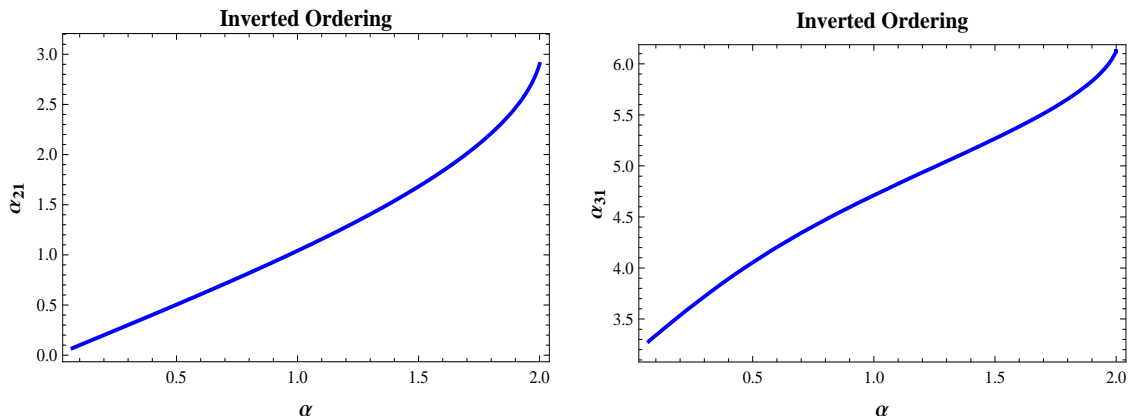
**Figure 4.3:** The same as in Fig. 4.2, but for a light neutrino mass spectrum with inverted ordering.

to zero. The maximum value of $\alpha_{21}$ is obtained for $\alpha \cong 1$. At $\alpha = 1$ one has approximately $\alpha_{21} = \sqrt{r/3} \cong 0.1$. The other Majorana phase $\alpha_{31}$ can assume large CP violating values. The largest $|\sin \alpha_{31}|$ is reached for $\alpha = 1$, where $\sin \alpha_{31} = -1$. If the light neutrino mass spectrum is with IO, both phases can have large CP violating values. Indeed, $\sin \alpha_{21} = 1$ and $\sin \alpha_{31} = -1$ for $\alpha \approx \sqrt{2}$ and $\alpha = 1$, respectively. The Majorana phase $\alpha_{21}$ can be probed, in principle, in the next generation of experiments searching for neutrinoless double beta decay (see Section 1.2.4). It is important to notice that in the class of models under discussion, $\sin^2 \theta_{12} = 1/3$, $\cos^2 \theta_{12} = 2/3$ and a non-zero value of $\theta_{13}$ arises only due to the NLO corrections to the superpotential of the lepton sector. As a consequence, the predicted value of $\theta_{13}$ is relatively small, $\theta_{13} \sim \mathcal{O}(\varepsilon) \sim 0.04$. Thus, the terms $\sim \sin^2 \theta_{13}$ in the effective Majorana mass $m_{ee}$, Eqs (1.31) and (1.32), give a negligible contribution. Further, since the Majorana phase $\alpha_{21} \cong 0$ (see Fig. 4.2), the two terms in the expression for $m_{ee}$ in the case of NO spectrum add up:

$$m_{ee} \;\cong\; \left| \frac{2}{3}\, m_1 + \frac{1}{3} \sqrt{m_1^2 + \Delta m_\odot^2} \right| , \quad \text{NO} , \tag{4.44}$$

where $m_1$ varies in the range (4.34). Therefore, $m_{ee}$ takes values in the interval: $6.5 \times 10^{-3}\,\text{eV} \lesssim m_{ee} \lesssim 7.5 \times 10^{-3}\,\text{eV}$. In what concerns the IO spectrum, the predicted full range of variability of the effective Majorana mass, compatible with neutrino oscillation data, is

$$\frac{1}{3} \sqrt{m_3^2 + |\Delta m_A^2|} \lesssim m_{ee} \lesssim \sqrt{m_3^2 + |\Delta m_A^2|} , \; \text{with} \; m_3 \gtrsim 0.02 \text{ eV} , \quad \text{IO} . \tag{4.45}$$

For $m_3 \gtrsim 0.02$ eV, this implies $m_{ee} \gtrsim 0.018$ eV. In Fig. 4.4, left panel (right panel) both the effective Majorana mass $m_{ee}$ and the lightest neutrino mass $m_1$ ($m_3$) are represented as function of the parameter $\alpha$, for a neutrino mass spectrum with normal (inverted) ordering.
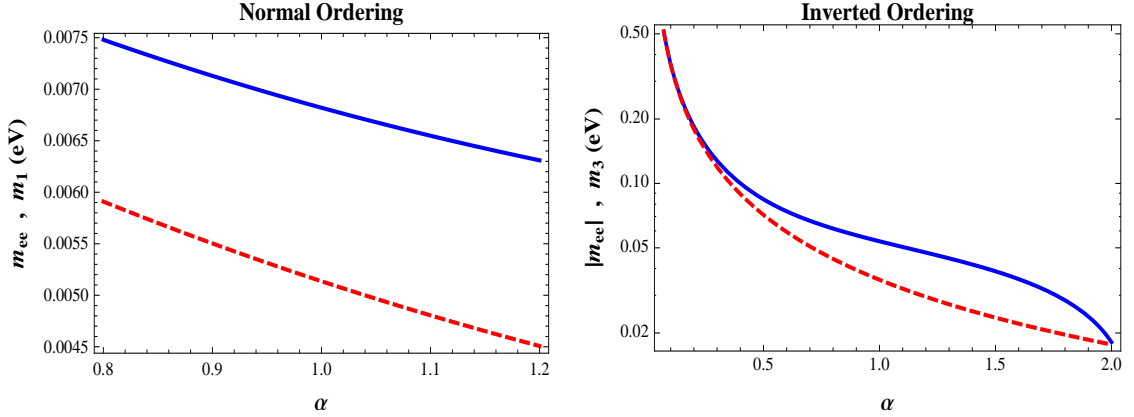
**Figure 4.4:** The effective Majorana mass $m_{ee}$ (blue continuous line) and the lightest neutrino mass (red dashed line) as function of the parameter $\alpha$ in the case of a light neutrino mass spectrum with normal ordering (left panel) and inverted ordering (right panel).

## 4.3  Leptogenesis Predictions

In this section the baryon asymmetry of the Universe is computed within the thermal leptogenesis scenario defined in Model 1 and Model 2, both introduced in Section 4.1. As mentioned earlier, leptogenesis cannot be realized if only the LO contribution to the neutrino superpotential are taken into account. In order to generate a sufficiently large CP asymmetry, higher order corrections to the Dirac mass matrix of neutrinos must be considered.

The RH neutrino mass spectrum in this class of models is not strongly hierarchical. Consequently, the standard thermal leptogenesis scenario, in which the relevant lepton CP violating asymmetry is mostly produced in the decays of the lightest RH (s)neutrino, is not applicable here and the contribution from the out-of-equilibrium decays of the heavier RH (s)neutrinos can play an important role in the generation of the observed baryon asymmetry. The lepton charge asymmetry produced in the decays of all the heavy RH (s)neutrinos $N_i$ ($\widetilde{N}_i$ ) (see Eq. (4.26)) is therefore considered in the computation of $Y_B$. According to the results obtained in Section 1.4.1, the neutrino and sneutrino CP asymmetries $\epsilon_i$, which are equal for lepton and slepton final states, are

$$\epsilon_i \;=\; \frac{1}{8\pi v_u^2} \sum_{j\neq i} \frac{\mathrm{Im}[(\hat{m}_D \hat{m}_D^\dagger)_{ji}^2]}{(\hat{m}_D \hat{m}_D^\dagger)_{ii}} \; f\left(\frac{m_i}{m_j}\right) \;, \tag{4.46}$$

where

$$\hat{m}_D = U_{TB}^T \, \mathrm{diag}\left(1, e^{-i\alpha_{21}/2}, e^{-i\alpha_{31}/2}\right) m_D \tag{4.47}$$

is the neutrino Dirac mass matrix in the mass eigenstate basis of RH neutrinos, and $m_i$ are, as usual, the light neutrino masses defined in Eq. (4.29). The MSSM loop function $f(x)$ in (4.46) was introduced in Eq. (1.63). This function is strongly affected by the hierarchy of light neutrino masses. Indeed, it can lead to a strong enhancement of the CP asymmetries if the light neutrino masses $m_i$ and $m_j$ are nearly degenerate. As discussed before, the neutrinos can be quasi-degenerate in

mass for the inverted ordered mass spectrum spectrum. In this case, to a good approximation: $f(m_i/m_j) \cong -f(m_j/m_i)$.

For the IO spectrum, the two lighter two heavy Majorana (s)neutrinos, $N_{1,2}$ ($\widetilde{N}_{1,2}$), have very close masses. However, the conditions for resonant leptogenesis [85] are not satisfied in the models under consideration. Indeed, in all the region of the relevant parameter space, $0.2 \lesssim \alpha \lesssim 2$, the relative mass difference of the two heavy Majorana (s)neutrinos in question is:

$$\left| \frac{M_2 - M_1}{M_1} \right| = 1 - \frac{m_1}{m_2} \cong (2 \div 14) \times 10^{-3} \gg \max \left| \frac{(\hat{m}_D \hat{m}_D^\dagger)_{12}}{16\pi^2 v_u^2} \right| \approx \frac{\varepsilon^3}{\pi^2} \approx 10^{-5} \qquad (4.48)$$

Under the above condition, the CP asymmetries for each (s)neutrino decay can be computed in perturbation theory as the interference between the tree level and one loop diagrams (see Section 1.4.1).

The general expression for the baryon asymmetry [86], where each RH (s)neutrino gives a non-negligible contribution, can be cast in the following form:

$$Y_B \equiv \frac{n_B - \bar{n}_B}{s} = -1.48 \times 10^{-3} \sum_{i,j=1}^{3} \epsilon_i \eta_{ij} . \qquad (4.49)$$

In the previous expression $\eta_{ij}$ represents the efficiency factor that accounts for the wash-out and decoherence effects of the lepton charge asymmetry $Y_{\ell_i}$, due to the $\Delta L = 1$ interactions involving $N_j$ and $\widetilde{N}_j$. The asymmetry $Y_{\ell_i}$ is generated in the decays $N_i \to \ell_i \, h_u, \, \tilde{\ell}_i \, \tilde{h}_u$ and $\widetilde{N}_i \to \tilde{\ell}_i \, h_u, \, \ell_i \, \tilde{h}_u$. In the following, only the number densities of lepton doublets will be considered. The same considerations apply for the interactions of the corrsponding slepton states.

The computation of the efficiency factors $\eta_{ij}$ in the models under discussion is considerably simplified [87, 88] (see also [89]). This is due to the fact that, to leading order, the heavy Majorana neutrinos eigenstates $N_1$, $N_2$ and $N_3$, as can be shown, couple to orthogonal leptonic states. As a consequence, the Boltzmann evolutions of the three lepton CP violating asymmetries, associated to the indicated three orthogonal leptonic states, are practically independent and one can compute the total baryon asymmetry as an incoherent sum of the contributions arising from decays of each of the three heavy RH neutrinos:

$$Y_B \approx \sum_{i=1}^{3} Y_{Bi} , \qquad (4.50)$$

where

$$Y_{Bi} \equiv -1.48 \times 10^{-3} \epsilon_i \, \eta_{ii} . \qquad (4.51)$$

In the class of models considered the RH neutrino mass scale is set below $10^{14}$ GeV, preventing possible wash-out effects from $\Delta L = 2$ scattering processes. In this case, the efficiency factors $\eta_{ii}$ can be expressed in terms of the wash-out mass parameters $\widetilde{m}_i$, through the analytic estimate given in Eq. (1.73), where $\widetilde{m}_i$ is now

$$\widetilde{m}_i \equiv \frac{(\hat{m}_D \hat{m}_D^\dagger)_{ii}}{M_i} . \qquad (4.52)$$

The computation of $Y_B$ within the two SUSY $A_4$ models defined before, is reported in the next subsections.

### 4.3.1   Leptogenesis in Model 1

Concerning Model 1, in the basis in which the RH Majorana neutrino mass term, Eq. (4.20), is diagonal, the relevant matrix that enters into the expression of the leptogenesis CP asymmetries (4.46) is given by

$$
\hat{m}_D\hat{m}_D^\dagger = \mathbf{1}\left(\frac{z}{\lambda}\right)^2 y_\nu^2 v_u^2
$$

$$
(4.53)
$$

$$
+ \begin{pmatrix} 2\,\mathrm{Re}(y_A) & 2\sqrt{2}e^{i\frac{\alpha_{21}}{2}}\,\mathrm{Re}(y_A) & \frac{2}{\sqrt{3}}e^{i\frac{\alpha_{31}}{2}}\,\mathrm{Re}(y_B) \\ 2\sqrt{2}e^{-i\frac{\alpha_{21}}{2}}\,\mathrm{Re}(y_A) & 0 & -2\sqrt{\frac{2}{3}}e^{i\frac{\alpha_{31}-\alpha_{21}}{2}}\,\mathrm{Re}(y_B) \\ \frac{2}{\sqrt{3}}e^{-i\frac{\alpha_{31}}{2}}\,\mathrm{Re}(y_B) & -2\sqrt{\frac{2}{3}}e^{i\frac{\alpha_{21}-\alpha_{31}}{2}}\,\mathrm{Re}(y_B) & -2\,\mathrm{Re}(y_A) \end{pmatrix} \left(\frac{v_T}{\Lambda}\right)\left(\frac{z}{\lambda}\right)^2 y_\nu v_u^2
$$

where $y_A$ and $y_B$ are the higher order (complex) Yukawa couplings defined in (4.4) and (4.5). All the flavon VEVs are taken real without loss of generality.

The CP asymmetries $\epsilon_k$ can be written in the following way:

$$
\epsilon_1 = -\frac{1}{6\pi}\left(\frac{z}{\lambda}\right)^2\left(\frac{v_T}{\Lambda}\right)^2\left(6f(m_1/m_2)\sin\alpha_{21}\,\mathrm{Re}(y_A)^2 + f(m_1/m_3)\sin\alpha_{31}\,\mathrm{Re}(y_B)^2\right) \tag{4.54}
$$

$$
\epsilon_2 = \frac{1}{3\pi}\left(\frac{z}{\lambda}\right)^2\left(\frac{v_T}{\Lambda}\right)^2\left(3f(m_2/m_1)\sin\alpha_{21}\,\mathrm{Re}(y_A)^2 + f(m_2/m_3)\sin(\alpha_{21}-\alpha_{31})\,\mathrm{Re}(y_B)^2\right) \tag{4.55}
$$

$$
\epsilon_3 = \frac{1}{6\pi}\left(\frac{z}{\lambda}\right)^2\left(\frac{v_T}{\Lambda}\right)^2\left(2f(m_3/m_2)\sin(\alpha_{31}-\alpha_{21}) + f(m_3/m_1)\sin\alpha_{31}\right)\mathrm{Re}(y_B)^2 \tag{4.56}
$$

where $m_k$ are the LO neutrino masses and $z/\Lambda \approx v_T/\Lambda \approx \varepsilon$. Thus, in the model under consideration we have

$$
|\epsilon_k| \propto \varepsilon^4 \approx 3\times 10^{-6}\,, \quad k = 1,2,3\,. \tag{4.57}
$$

This is the order of magnitude we expect for the CP asymmetry if we require successful leptogenesis. Depending on the loop factor $f(m_i/m_j)$ and the values of the Majorana phases, the CP asymmetry can be enhanced or suppressed.

The wash-out mass parameters (4.52), associated to each of the three lepton asymmetries, coincide to a good approximation with the light neutrino masses:

$$
\widetilde{m}_1 = m_1(1+\mathcal{O}(\varepsilon)) \tag{4.58}
$$

$$
\widetilde{m}_2 = m_2(1+\mathcal{O}(\varepsilon)) \tag{4.59}
$$

$$
\widetilde{m}_3 = m_3(1+\mathcal{O}(\varepsilon)) \tag{4.60}
$$

#### Results for NO Spectrum

The baryon asymmetry is computed in the region of the parameter space corresponding to a neutrino mass spectrum with normal ordering: $0.8 \lesssim \alpha \lesssim 1.2$. The lightest RH Majorana neutrino in this scenario is $N_3$. The Majorana phases, that provide the requisite CP violation for successful
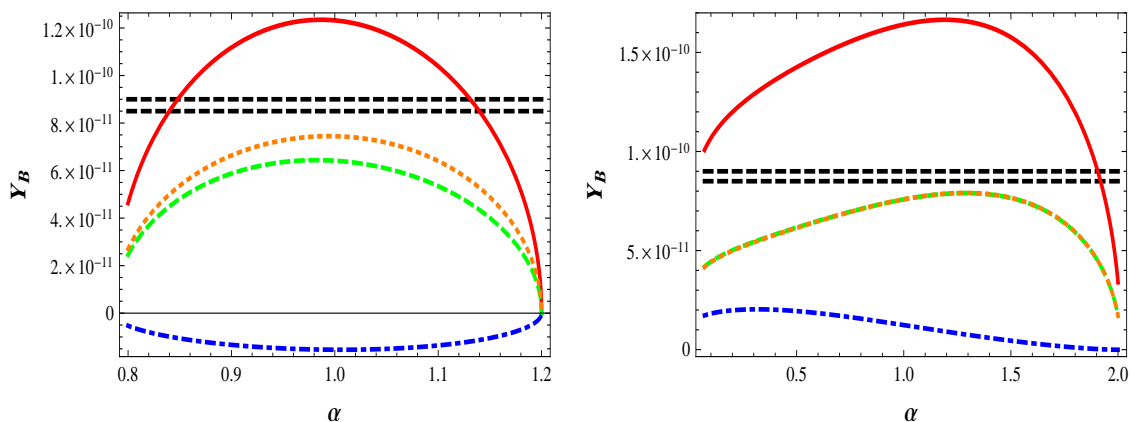
**Figure 4.5:** Model 1: baryon asymmetry $Y_B$ versus $\alpha$ in the cases of neutrino mass spectrum with normal (left panel) and inverted (right panel) ordering: $i$) total baryon asymmetry $Y_B$ (red continuous curve), $ii$) $Y_{B1}$ (green dashed curve), $iii$) $Y_{B2}$ (orange dotted curve) and $iv$) $Y_{B3}$ (blue dot-dashed curve). On the right panel, the lines corresponding to $Y_{B1}$ and $Y_{B2}$ overlap. In both cases $\sin\phi < 0$ and $\Delta m_A^2$ and $r$ are fixed at their best fit values. The results shown in the left (right) panel correspond to $y_A = 2.5$ and $y_B = 3$ ($y_A = 0.4$ and $y_B = 2$). The horizontal dashed lines represent the allowed range of the observed value of $Y_B$, $Y_B \in [8.5, 9] \times 10^{-11}$.

leptogenesis, are solutions of Eqs (4.41) and (4.42) corresponding to $\sin\phi < 0$. The dependence on $\alpha$ of each of the two CP violating phases is shown in Fig. 4.2. It is important to notice that only the solutions with $\sin\phi < 0$ give the correct sign of the total baryon asymmetry.

The dependence of the baryon asymmetry $Y_B$ on the parameter $\alpha$, in this case, is reported in Fig. 4.5, left panel. The individual contributions to $Y_B$ from the decays of each of the three RH Majorana neutrinos are also shown. The term $Y_{B3}$, originating from the lightest RH neutrino decays, is suppressed by largest wash-out effects, with respect to $Y_{B1}$ and $Y_{B2}$ (see Eq. (4.60)). The contribution to the total baryon asymmetry given by $Y_{B1}$ shows an interplay between two independent terms proportional to $y_A$ and $y_B$, respectively. Such terms have always the same signs and are of the same order of magnitude. The suppression caused by the Majorana phase $\alpha_{21} \lesssim 0.1$ of the term proportional to $y_A$ is compensated by the enhancement due to the loop factor: $6f(m_1/m_2)/f(m_1/m_3) \cong -(8 \div 20)$. The same considerations apply to $Y_{B2}$. Now $\sin\alpha_{21}$ and $\sin(\alpha_{21} - \alpha_{31})$ have the same sign and the ratio of the corresponding loop factors is approximately $3f(m_2/m_1)/f(m_2/m_3) \cong (20 \div 30)$.

In conclusion, in the case of NO light neutrino mass spectrum, each of the two Majorana phases $\alpha_{21}$ and $\alpha_{31}$, having values within the ranges allowed by neutrino oscillation data (see Fig. 4.2), can provide the CP violation required for successful leptogenesis. Even in the case in which the term proportional to $\sin\alpha_{31}$ in the CP asymmetries is strongly suppressed (which corresponds to a strong fine-tuning of $y_B \ll 1$), successful baryogenesis can be naturally realized for values of the Majorana phase $\alpha_{21} \approx (0.04 \div 0.10)$ and a moderately large neutrino Yukawa coupling $y_A \sim (2.5 \div 3.0)$.

**Results for IO Spectrum**

In the case of a light neutrino mass spectrum with inverted ordering, the baryon asymmetry is computed in all the allowed range of $\alpha$, *i.e.* for $0.2 < \alpha \lesssim 2$. The results shown for $0.07 < \alpha \lesssim 0.2$, which correspond to a quasi-degenerate spectrum, should be valid provided the renormalisation group effects [76] are sufficiently small in the indicated region [90].

In Fig. 4.5, right panel, the different contributions to the baryon asymmetry are reported, similarly to the case of NO mass spectrum. The Majorana CP violating phases which enter into the expressions of the CP asymmetries are reported in Fig. 4.3. The solutions of equations (4.41) and (4.42) corresponding to $\sin \phi < 0$ must be used also in this case in order to obtain the correct sign of the baryon asymmetry. Now $N_3$ is the heaviest RH Majorana neutrino and the wash-out effects for the CP asymmetry generated in the decays of this state are less strong since they are controlled to LO by the lightest neutrino mass $m_3$: $\widetilde{m}_3 \cong m_3$. Note, however, that even in this scenario the contribution of the term $Y_{B3}$ in $Y_B$ is always much smaller than the input given by the other terms, $Y_{B1}$ and $Y_{B2}$. This is a consequence of the strong enhancement in the self energy part of the loop function that enters into the expressions for $Y_{B1}$ and $Y_{B2}$. Indeed, if the spectrum is inverted hierarchical, then $f(m_1/m_2) \cong -f(m_2/m_1) \approx 50 f(m_3, m_{1,2})$. Finally, one should notice that the "low" energy CP violating phase $\alpha_{31}$ gives, in general, a subdominant contribution in the CP asymmetries $\epsilon_1$ and $\epsilon_2$, when the Yukawa couplings $y_A$ and $y_B$ are of the same order of magnitude. This conclusion is valid even in the region of the parameter space where $\alpha_{31} \approx 3\pi/2$.

The analysis of all the parameter space defined by $\alpha$, compatible with low energy neutrino oscillation data, in the Model 1, shows that in both the normal and inverted patterns of light neutrino masses, the Majorana phases can provide enough CP violation in order to have successful leptogenesis, even when only one of the phases $\alpha_{21}$ and $\alpha_{31}$, effectively, contributes in the generation of the CP asymmetry.

### 4.3.2 Leptogenesis in Model 2

In this subsection the generation of the baryon asymmetry of the Universe is realized via the leptogenesis mechanism within Model 2. The computation is performed in the one-flavour approximation, as in the analysis of the previous model. The quantity relevant for the calculation of the CP asymmetries is in this case:

$$
\hat{m}_D \hat{m}_D^\dagger = \mathbf{1} \left(\frac{z}{\Lambda}\right)^2 y_\nu^2 v_u^2
$$

$$
+ \begin{pmatrix} 6\,\mathrm{Re}(y_B) & 0 & 2\sqrt{3}e^{i\frac{\alpha_{31}}{2}}\,\mathrm{Re}(y_C) \\ 0 & 0 & 0 \\ 2\sqrt{3}e^{-i\frac{\alpha_{31}}{2}}\,\mathrm{Re}(y_C) & 0 & -6\,\mathrm{Re}(y_B) \end{pmatrix} \left(\frac{v_S}{\Lambda}\right)\left(\frac{z}{\Lambda}\right)^2 y_\nu v_u^2
$$

$$(4.61)$$
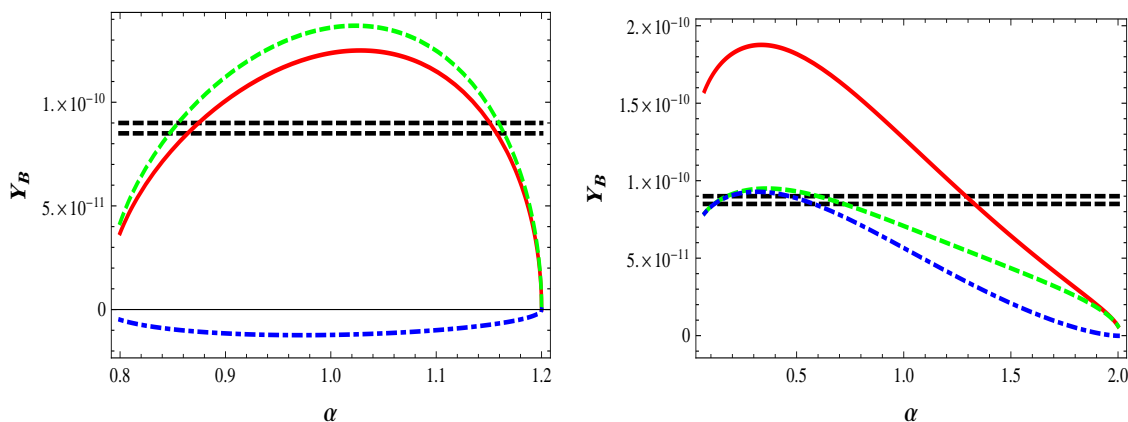
**Figure 4.6:** Model 2: the same as in Fig. 4.5. In both the figures, the relevant NLO Yukawa coupling is $y_C = 2$.

where the $y_B$ and $y_C$ are defined in Eqs (4.14) and (4.15). Again, all flavon VEVs are chosen to be real without loss of generality. The CP asymmetries in this model are given by

$$\epsilon_1 \quad = \quad -\frac{3}{2\pi}\left(\frac{z}{\Lambda}\right)^2\left(\frac{v_S}{\Lambda}\right)^2 f(m_1/m_3)\sin(\alpha_{31})\operatorname{Re}(y_C)^2 \qquad (4.62)$$

$$\epsilon_2 \quad = \quad 0 \qquad (4.63)$$

$$\epsilon_3 \quad = \quad \frac{3}{2\pi}\left(\frac{z}{\Lambda}\right)^2\left(\frac{v_S}{\Lambda}\right)^2 f(m_3/m_1)\sin(\alpha_{31})\operatorname{Re}(y_C)^2 \qquad (4.64)$$

where $m_{1,3}$ are again the LO neutrino masses (see Eq. (4.29)). The leptogenesis CP violating phase now coincides with the Majorana phase $\alpha_{31}$. Moreover, the CP asymmetries $\epsilon_{1,3} \neq 0$ are controlled by only one parameter, $y_C$, of the matrix of neutrino Yukawa couplings (4.14), the reason being that only this parameter breaks the TB form of the neutrino mixing pattern.

In this model, the heavy RH Majorana neutrino $N_2$ "decouples": the CP violating lepton asymmetry is produced in the out-of-equilibrium decays of the heavy Majorana neutrinos $N_1$ and $N_3$ alone. This constitutes a major difference with respect to Model 1. After the lepton asymmetries are converted into a baryon asymmetry by sphaleron processes, the final matter-antimatter asymmetry of the Universe can be estimated as:

$$Y_B \equiv Y_{B1} + Y_{B3} \qquad (4.65)$$

where $Y_{Bi}$, for $i = 1, 3$, are given in Eq. (4.51). The LO wash-out mass parameters $\widetilde{m}_{1,3}$ are the same as in the previous model:

$$\widetilde{m}_1 \quad = \quad m_1(1 + \mathcal{O}(\varepsilon)) \qquad (4.66)$$

$$\widetilde{m}_3 \quad = \quad m_3(1 + \mathcal{O}(\varepsilon)) \qquad (4.67)$$

In Fig. 4.6 the dependence of the baryon asymmetry on the parameter $\alpha$ is reported in the cases of neutrino mass spectrum with normal and inverted ordering. The ranges of possible values

of the Majorana phase $\alpha_{31}$ which provides the correct sign of the baryon asymmetry are shown for the NO and IO spectra in Figs 4.2 and 4.3, respectively.

As already seen for the previous model, the suppression of the term $Y_{B3}$ with respect to $Y_{B1}$ in the case of NO spectrum is due to the relatively larger wash-out effects in the generation of the CP asymmetry $\epsilon_3$. The maximum of the total baryon asymmetry $Y_B$ is reached for $\alpha \approx 1$ where the CP violating Majorana phase $\alpha_{31} \cong 3\pi/2$. (see Fig. 4.2, right panel).

In what concerns the IO spectrum, the two terms $Y_{B1}$ and $Y_{B3}$ enter with equal sign in the total baryon asymmetry and are of the same order of magnitude. The enhancement of the asymmetry for $\alpha < 0.7$ is explained by the increase of the loop function $f(m_1/m_3) \cong -f(m_3/m_1)$ in the region of quasi-degenerate light neutrino mass spectrum.

In this model, successful leptogenesis can be naturally realized for both types of neutrino mass spectrum and for an effective Yukawa coupling $y_C \gtrsim 1.5$.

## 4.4  Summary

In this chapter the thermal leptogenesis mechanism of generation of the baryon asymmetry of the Universe was investigated within two prominent see-saw supersymmetric models based on the $A_4$ flavour symmetry group in the lepton sector, which naturally predicts a tri-bimaximal neutrino mixing, at leading order in the flavour symmetry breaking parameter $\varepsilon$.

In these models, the only source of CP violation which enters in the expression of the CP asymmetries in the RH (s)neutrino decays, is provided by the two CP violating Majorana phases $\alpha_{21}$ and $\alpha_{31}$ in PMNS matrix. In the case of neutrino mass spectrum with normal ordering, $\alpha_{21}$ is shown to be small, $\alpha_{21} \lesssim 0.1$. In the types of models considered $\sin^2 \theta_{13}$ is also predicted to be small, $\sin^2 \theta_{13} \sim 10^{-3}$. As a consequence, the contributions of the terms proportional to $\sin^2 \theta_{13}$ in $m_{ee}$ are strongly suppressed. The lightest neutrino mass is predicted to lie in the interval: $3.8 \times 10^{-3}\,\text{eV} < m_1 < 6.9 \times 10^{-3}\,\text{eV}$. Thus the neutrino mass spectrum is with partial hierarchy. The effective Majorana mass $m_{ee}$ has a relatively large value, $m_{ee} \sim 7 \times 10^{-3}$ eV. Moreover, if $\alpha_{21}$ had a value close to $\pi$, one would have $m_{ee} \ll 10^{-3}$ eV. Conversely, depending on the parameter space, the phase $\alpha_{31}$ can take large CP violating values. For light neutrino mass spectrum with inverted ordering, the Majorana CP phases $\alpha_{21}$ and $\alpha_{31}$ vary (for $\sin \phi < 0$) between 0 and $\pi$ and $\pi$ and $2\pi$, respectively. The mass spectrum is also in this case with partial hierarchy and $0.02\,\text{eV} \lesssim m_3 < 0.10$ eV.

The correct size and sign of the baryon asymmetry $Y_B$ can be produced in both the models. The study of leptogenesis was performed in the framework of the one-flavor approximation. Since the mass spectrum of the RH neutrinos is generically not strongly hierarchical, the decays of all three RH (s)neutrinos contribute to the generation of the baryon asymmetry. The correct magnitude as well as the correct sign of the baryon asymmetry $Y_B$ can be easily obtained in the two models for most values of the allowed parameter space. The sign of $Y_B$ uniquely fixes the sign of $\sin \phi$. The latter cannot be determined by low energy observables since they exhibit only a $\cos \phi$-dependence.

In conclusion, the results of this chapter show that SUSY models with $A_4$ flavour symmetry and type I see-saw mechanism of neutrino mass generation, which naturally give rise to tri-bimaximal mixing and Majorana CP violation in the lepton sector, can also explain successfully the observed baryon asymmetry of the Universe, via the thermal leptogenesis mechanism.

# Chapter 5

# Lepton Flavour Violation in A$_4$ Models

In this chapter other phenomenological predictions concerning the class of SUSY $A_4$ models discussed so far are considered. In particular, the charged lepton flavour violating (LFV) radiative decays $e_\alpha \to e_\beta + \gamma$ are discussed in detail. [1] The results obtained are based on the study performed in [19].

These types of LFV processes as well as the electric dipole moments (EDMs) and magnetic dipole moments (MDMs) of the charged leptons, were thoroughly studied in the class of models under consideration using effective field theory methods in [91]. In this approach, a new physics scale $M$ is assumed to exist at $(1 \div 10)$ TeV. The charged LFV radiative decays are mediated by an effective dimension-6 operator, which is suppressed by the scale $M$. Thus, the rates of the LFV decays $e_\alpha \to e_\beta + \gamma$ and the EDM of the electron, can have values close to and even above the existing experimental upper limits. [2] Assuming that the flavour structure of the indicated dimension-6 operator is also determined by the $A_4$ symmetry, one finds that its form in flavour space is similar to the one of the charged lepton mass matrix. In [91] the dependence of the branching ratios $B(e_\alpha \to e_\beta + \gamma)$, the EDMs and MDMs on the symmetry breaking parameter $\varepsilon$ was analyzed in detail. It was found that the contributions of the new physics to the EDMs and MDMs arise at leading order (LO) in $\varepsilon$, whereas the LFV transitions are generated only at next-to-leading order (NLO). It was shown that $B(e_\alpha \to e_\beta + \gamma)$ scales as $\varepsilon^2$, independently of the type of the decaying lepton. Correspondingly, all charged LFV radiative decays are predicted to have similar branching ratios. The existing stringent experimental upper bound on $B(\mu \to e + \gamma)$ can be satisfied if the new physics scale $M > 10$ TeV. These results were shown to be independent of the generation mechanism of the light neutrino masses. An extensive review of articles in which the charged LFV radiative decays are studied can be found in [94].

In this chapter the branching ratios of charged LFV radiative decays are computed within the

---

[1] In this chapter $e_\alpha$, for $\alpha = 1, 2, 3$, denote the charged leptons: $e_1 \equiv e$, $e_2 \equiv \mu$ and $e_3 \equiv \tau$.

[2] As is well known, in the minimal extension of the Standard Model (SM) with massive neutrinos and neutrino mixing, the rates and cross sections of the LFV processes are suppressed by the factors [92] (see also [93]) $2.2 \times 10^{-4} |U_{ej} m_j^2 U_{\mu j}^*|^2 / M_W^4 \lesssim 5.2 \times 10^{-48}$, $M_W$, $m_j$ and $U_{\alpha j}$, $\alpha = e, \mu$, being the $W^\pm$ mass, light neutrino masses and elements of the PMNS matrix. This renders the LFV processes unobservable.

minimal supergravity (mSUGRA) framework, which provides flavour universal boundary conditions at the GUT scale $M_X \approx 2 \times 10^{16}$ GeV. [3] The SUSY breaking and the sparticle masses are completely specified by the flavour universal mass parameters $m_0$, $m_{1/2}$ and by the trilinear coupling $A_0$. Off-diagonal elements in the slepton mass matrices, which can lead to relatively large branching ratios of the LFV decays $e_\alpha \to e_\beta + \gamma$, are generated through renormalization group (RG) effects associated with the three heavy RH Majorana neutrinos [96].

The numerical analysis is referred to the two specific $A_4$ models, introduced in [81] and AM, whose main features are summarized in Appendix B. The branching ratios $B(e_\alpha \to e_\beta + \gamma)$ are calculated using the analytic approximations developed in [97, 98, 99]. In this approach $B(e_\alpha \to e_\beta + \gamma)$ depend only on the generated off-diagonal elements of the mass matrix of the left-handed sleptons, which are functions of the matrix of the neutrino Yukawa couplings $\lambda$, of the three RH Majorana neutrino masses $M_1$, $M_2$ and $M_3$ and of the SUSY breaking parameters $m_0$, $m_{1/2}$ and $A_0$.

The chapter is organized as follows: in Section 5.1 the formulae for the branching ratios of charge LFV radiative decay are introduced, identifying the LO and NLO contributions for the two specific models cited before. This is done within the framework of mSUGRA and for the two possible types of the light neutrino mass spectrum, with normal ordering (NO) and inverted ordering (IO). In Section 5.2 results of the numerical calculation as well as analytical estimates of the charged LFV radiative decay branching ratios are reported. Finally, a brief comment on predictions for $\mu - e$ conversion and the decays $e_\alpha \to 3e_\beta$ is given in Section 5.3.

## 5.1 Charged Lepton Flavour Violating Radiative Decays

The notation used here is defined in Appendix B, where the basic features of generic supersymmetric type I see-saw $A_4$ models are summarized.

### 5.1.1 Computation of the branching ratios $B(e_\alpha \to e_\beta + \gamma)$

The branching ratios of the LFV processes $e_\alpha \to e_\beta + \gamma$ ($m_{e_\alpha} > m_{e_\beta}$) are computed using the following expression [98, 99]:

$$B(e_\alpha \to e_\beta + \gamma) \approx B(e_\alpha \to e_\beta + \nu_\alpha + \overline{\nu}_\beta) \, B_0(m_0, m_{1/2}) \left| \sum_k (\lambda^\dagger)_{\alpha k} \log\left(\frac{M_X}{M_k}\right) (\lambda)_{k\beta} \right|^2 \tan^2\beta \,. \quad (5.1)$$

In Eq. (5.1) $\lambda$ is, as usual, the matrix of neutrino Yukawa couplings, evaluated taking into account all NLO effects in the basis in which the charged lepton and RH neutrino mass matrices are diagonal and have positive eigenvalues:

$$\lambda = V_R^T \, \Omega \, U_{TB}^T \, \widehat{\lambda} \, V_{eL} \,, \quad (5.2)$$

where $\Omega \equiv \text{diag}(e^{-i\varphi_1/2}, e^{-i\varphi_2/2}, e^{-i\varphi_3/2})$ and $\widehat{\lambda} \equiv m_D/v_u$ represents the matrix of neutrino Yukawa couplings in the basis in which the superpotential is defined (see Eq. (B.8)). The Dirac mass matrix

---

[3]Notice that, in the context of global supersymmetry (SUSY) [95], the presence of soft SUSY breaking terms in the flavon sector can lead to additional flavour non-universal contributions to the sfermion soft masses. These terms vanish in the limit of universal soft SUSY parameters in the flavon potential.

$m_D$ includes the generic NLO corrections given in Eq. (B.18). The unitary matrices $V_{eL}$ and $V_R$ are given in Eqs (B.22) and (B.24), respectively.

According to the mSUGRA scenario considered here, at the GUT scale $M_X \approx 2 \times 10^{16}$ GeV, the slepton mass matrices are diagonal and universal in flavour and the trilinear couplings are proportional to the Yukawa couplings:

$$(m_{\tilde{L}}^2)_{ij} = (m_{\tilde{e}}^2)_{ij} = (m_{\tilde{\nu}}^2)_{ij} = \delta_{ij} m_0^2 \,, \tag{5.3}$$

$$(A_\nu)_{ij} = A_0 (\lambda)_{ij} \,, \quad A_0 = a_0 m_0 \,, \tag{5.4}$$

where $m_{\tilde{L}}^2$ and $m_{\tilde{e}}^2$ are the left-handed and right-handed charged slepton mass matrices, respectively, while $m_{\tilde{\nu}}^2$ is the right-handed sneutrino soft mass term. The gaugino masses are assumed to have a common value at the high scale $M_X$:

$$M_{\tilde{B}} = M_{\tilde{W}} = M_{\tilde{g}} = m_{1/2} \,. \tag{5.5}$$

The scaling function $B_0(m_0, m_{1/2})$ contains all the dependence on the SUSY breaking parameters:

$$B_0(m_0, m_{1/2}) \approx \frac{\alpha_{em}^3}{G_F^2 m_S^8} \left| \frac{(3 + a_0^2) m_0^2}{8\pi^2} \right|^2 \,. \tag{5.6}$$

In Eq. (5.6), $G_F$ is the Fermi constant and $\alpha_{em} \approx 1/137$ is the fine structure constant. The SUSY mass parameter $m_S$ in Eq. (5.6) was obtained in [98] by performing a fit to the exact RG computation. The resulting analytic expression in terms of $m_0$ and $m_{1/2}$ has the form:

$$m_S^8 \approx 0.5 \, m_0^2 \, m_{1/2}^2 \, (m_0^2 + 0.6 \, m_{1/2}^2)^2 \,. \tag{5.7}$$

According to [98], deviations from the exact RG result can be present in the region of relatively large (small) $m_{1/2}$ and small (large) $m_0$.
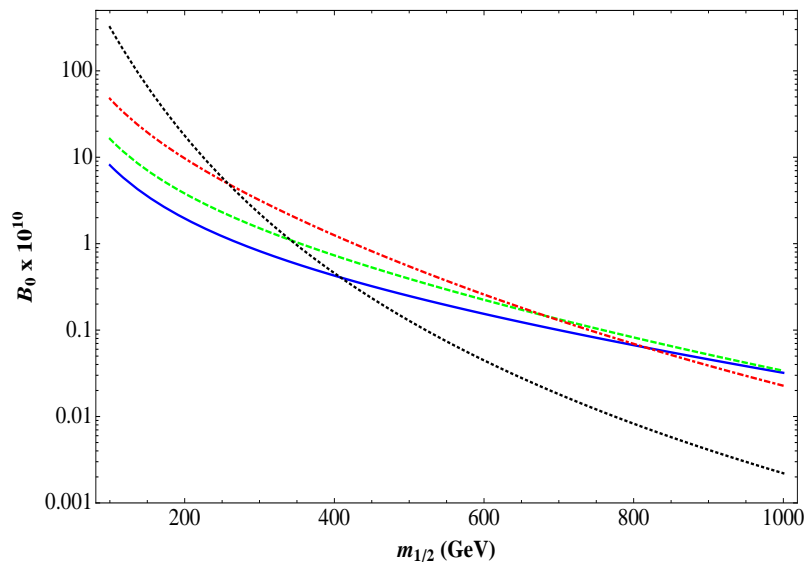
The dependence of $B_0(m_0, m_{1/2})$ on $m_{1/2}$ for fixed values of $m_0$ and $A_0 = 0$ is shown in Fig. 5.1. Note that the function $B_0$ and, consequently, the branching ratio in Eq. (5.1) can vary up to three or four orders of magnitude, depending on which point $(m_0, m_{1/2})$ of the parameter space is considered. The larger is the SUSY mass parameter $m_S$, the stronger is the suppression of the predicted branching ratio. Values of $A_0 \neq 0$ lead to larger values of $B_0(m_0, m_{1/2})$ (see Eq. (5.6)) and to an increase of the branching ratios.

### 5.1.2 Leading order contributions in $B(e_\alpha \rightarrow e_\beta + \gamma)$

In the following discussion, normalized charged LFV radiative decay branching ratios are defined, for convenience, as the ratios of Eq. (5.1) and the partial branching ratios of the $\mu$ or $\tau$ decays into one lighter charged lepton and two neutrinos:

$$B'(e_\alpha \rightarrow e_\beta + \gamma) = \frac{B(e_\alpha \rightarrow e_\beta + \gamma)}{B(e_\alpha \rightarrow e_\beta + \nu_\alpha + \overline{\nu}_\beta)} \,. \tag{5.8}$$

Consequently [22]: $B(\mu \rightarrow e + \gamma) \approx B'(\mu \rightarrow e + \gamma)$, $B(\tau \rightarrow e + \gamma) \approx 0.18 \, B'(\tau \rightarrow e + \gamma)$ and $B(\tau \rightarrow \mu + \gamma) \approx 0.17 \, B'(\tau \rightarrow \mu + \gamma)$.

**Figure 5.1:** The dependence of the scaling function $B_0(m_0, m_{1/2})$ (see Eq. (5.6)) on $m_{1/2}$ for $A_0 = 0$ and fixed $m_0$: *i*) $m_0 = 100$ GeV (black, dotted line), *ii*) $m_0 = 400$ GeV (red, dot-dashed line), *iii*) $m_0 = 700$ GeV (green, dashed line) and *iv*) $m_0 = 1000$ GeV (blue, continuous line).

It proves useful to analyze separately the contributions in the LFV branching ratios associated to each of the three heavy RH Majorana neutrinos. For this purpose, the terms in Eq. (5.1) are rearranged in the following way:

$$B'(e_\alpha \to e_\beta + \gamma) \propto \left| (\lambda^\dagger \lambda)_{ij} \log\left(\frac{m_1}{\overline{m}}\right) + (\lambda^\dagger)_{i2}(\lambda)_{2j} \log\left(\frac{m_2}{m_1}\right) + (\lambda^\dagger)_{i3}(\lambda)_{3j} \log\left(\frac{m_3}{m_1}\right) \right|^2, \quad (5.9)$$

with

$$\overline{m} = \frac{v_u^2 y_\nu^2}{M_X} \cong (1.5 \times 10^{-3}\,\text{eV})\, y_\nu^2 \sin^2\beta \approx 1.5 \times 10^{-3}\,\text{eV}. \quad (5.10)$$

The last expression is valid for $y_\nu = 1$ and $\sin^2\beta \approx 1$, which is a good approximation given the fact that $\tan\beta \gtrsim 2$ (see Appendix B.3). In Eq. (5.9). As usual, $m_k$ are the LO neutrino masses in the $A_4$ models, given by Eq. (B.10). The contributions to $m_k$ which arise from NLO corrections in the superpotential are neglected in (5.9) since the branching ratio depends only logarithmically on the light neutrino masses and, typically, all such relative corrections are of order $\varepsilon \approx (0.007 \div 0.05)$ (see Appendix B.3). The RG effects [76] in the calculation of the neutrino masses and mixings are neglected as well. The RG corrections can be relevant in the case of quasi-degenerate (QD) light neutrino mass spectrum, while they are relatively small or negligible if the spectrum is hierarchical or with partial hierarchy [76]. In the $A_4$ models under discussion, the lightest neutrino mass in the case of NO (IO) mass spectrum is constrained to lie in the interval $3.8 \times 10^{-3}\,\text{eV} \lesssim m_1 \lesssim 7 \times 10^{-3}\,\text{eV}$ $(0.02\,\text{eV} \lesssim m_3)$. [4] In the case of IO the results presented in the

---

[4]See Section 4.2 for a discussion of the (LO) light neutrino mass spectrum in the class of SUSY $A_4$ models reported here.

| $\mu \to e + \gamma$ | |
|:---:|:---:|
| $(\lambda^\dagger \lambda)_{21}$ | $y_\nu \left( w'' \overline{y}^\nu_{1'} + w' y^\nu_{1''} - x_2 (y^\nu_A + y^\nu_S) - x_3 (\overline{y}^\nu_A + \overline{y}^\nu_S) \right) \varepsilon + \mathcal{O}(\varepsilon^2)$ |
| $(\lambda^\dagger)_{22}(\lambda)_{21}$ | $\frac{1}{3} y^2_\nu + \mathcal{O}(\varepsilon)$ |
| $(\lambda^\dagger)_{23}(\lambda)_{31}$ | $\mathcal{O}(\varepsilon)$ |
| $\tau \to e + \gamma$ | |
| $(\lambda^\dagger \lambda)_{31}$ | $y_\nu \left( w'' y^\nu_{1'} + w' \overline{y}^\nu_{1''} + x_2 (\overline{y}^\nu_A - \overline{y}^\nu_S) + x_3 (y^\nu_A - y^\nu_S) \right) \varepsilon + \mathcal{O}(\varepsilon^2)$ |
| $(\lambda^\dagger)_{32}(\lambda)_{21}$ | $\frac{1}{3} y^2_\nu + \mathcal{O}(\varepsilon)$ |
| $(\lambda^\dagger)_{33}(\lambda)_{31}$ | $\mathcal{O}(\varepsilon)$ |
| $\tau \to \mu + \gamma$ | |
| $(\lambda^\dagger \lambda)_{32}$ | $y_\nu \left( w'' \overline{y}^\nu_{1'} + w' y^\nu_{1''} + 2 \, x_2 \, y^\nu_S + 2 \, x_3 \, \overline{y}^\nu_S \right) \varepsilon + \mathcal{O}(\varepsilon^2)$ |
| $(\lambda^\dagger)_{32}(\lambda)_{22}$ | $\frac{1}{3} y^2_\nu + \mathcal{O}(\varepsilon)$ |
| $(\lambda^\dagger)_{33}(\lambda)_{32}$ | $-\frac{1}{2} y^2_\nu + \mathcal{O}(\varepsilon)$ |

**Table 5.1:** Combination of elements of the matrix of neutrino Yukawa couplings, $\lambda$, which enter into the expression for the branching ratios of the LFV decay $e_\alpha \to e_\beta + \gamma$ (see Eq. (5.9)). The expression for the relevant $\mathcal{O}(\varepsilon)$ terms in $(\lambda^\dagger \lambda)_{\alpha\beta}$ ($\alpha \neq \beta$) is also given (see text for details).

following are valid for $0.02 \, \mathrm{eV} \lesssim m_3 \lesssim 0.10 \, \mathrm{eV}$. As pointed out in the following, the predictions for the branching ratios of the LFV decays $e_\alpha \to e_\beta + \gamma$ depend, in general, on the type of neutrino mass spectrum.

**Neutrino Mass Spectrum with Normal Ordering**

In the case of NO mass spectrum, the three logarithms in Eq. (5.9) are all positive and are of the same order (see Fig. 5.2, left panel). The dominant contribution to the decay amplitude depends strongly on the combination of the neutrino Yukawa matrix elements in Eq. (5.9). Note that the matrix elements of $\lambda$ take all $\mathcal{O}(1)$ values, except for the (31) entry which typically scales as the expansion parameter $\varepsilon$. This is due to the presence of the TB mixing matrix $U_{TB}$, Eq. (1.17), in the expression for the neutrino Yukawa couplings $\lambda$, Eq. (5.2).

The order of magnitude in $\varepsilon$ of the coefficients of the three logarithms, $(\lambda^\dagger \lambda)_{\alpha\beta}$, $(\lambda^\dagger)_{\alpha 2}(\lambda)_{2\beta}$ and $(\lambda^\dagger)_{\alpha 3}(\lambda)_{3\beta}$, which appear in the three branching ratios $B'(e_\alpha \to e_\beta + \gamma)$ of interest, is reported in Tab. 5.1. The VEVs of the flavon fields are assumed to be real for simplicity. As Tab. 5.1 shows, the coefficient of the $\log(m_2/m_1)$ term in each of the three LFV branching ratios under discussion is of order one. The same conclusion is valid for the coefficient of the $\log(m_3/m_1)$ term in $B'(\tau \to \mu + \gamma)$. In what concerns the coefficients of the term proportional to $\log(m_1/\overline{m})$, they always originate from NLO corrections in the superpotential. These coefficients correspond to the off-diagonal elements of the hermitian matrix $\lambda^\dagger \lambda$, in which the rotation matrices, $U_{TB}$, $\Omega$ and $V_R$, associated with the diagonalization of the RH neutrino Majorana mass term, do not appear. At order $\varepsilon$, they depend
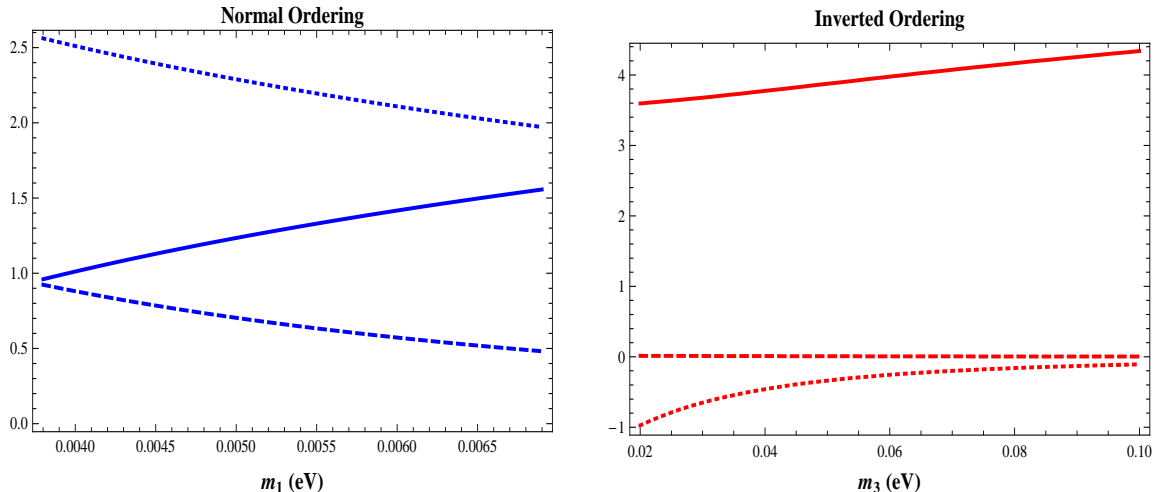
**Figure 5.2:** The three different contributions in $B'(e_\alpha \rightarrow e_\beta + \gamma)$, Eq. (5.9), in the case of light neutrino mass spectrum with normal (inverted) ordering (left (right) panel): $i)$ $\log(m_1/\overline{m})$ vs $m_1$ ($m_3$) (continuous line), $ii)$ $\log(m_2/m_1)$ vs $m_1$ ($m_3$) (dashed line) and $iii)$ $\log(m_3/m_1)$ vs $m_1$ ($m_3$) (dotted line). The results shown correspond to the best fit values reported in Tab. 1.1: $|\Delta m_A^2| = 2.40 \times 10^{-3}$ eV$^2$ and $r = \Delta m_\odot^2/|\Delta m_A^2| = 0.032$.

only on the parameters of the neutrino Dirac mass matrix (see Eqs (B.7) and (B.18)), as reported in Tab. 5.1.

Taking into account the magnitude of the different terms shown in Tab. 5.1, one has, in general, that in the case of NO neutrino mass spectrum:

$$B'(\mu \rightarrow e + \gamma) \approx B'(\tau \rightarrow e + \gamma) \approx B_0(m_0, m_{1/2}) \left| \frac{1}{3} y_\nu^2 \log\left(\frac{m_2}{m_1}\right) \right|^2 \tan^2\beta \propto 0.1 \, |y_\nu|^4 \ , \quad (5.11)$$

$$B'(\tau \rightarrow \mu + \gamma) \approx B_0(m_0, m_{1/2}) \left| \frac{1}{3} y_\nu^2 \log\left(\frac{m_2}{m_1}\right) - \frac{1}{2} y_\nu^2 \log\left(\frac{m_3}{m_1}\right) \right|^2 \tan^2\beta \propto |y_\nu|^4 \ . \quad (5.12)$$

From the analytical estimates, Eqs (5.11) and (5.12), one can conclude that in the case of NO mass spectrum, $B'(\tau \rightarrow \mu + \gamma)$ is approximately by one order of magnitude larger than $B'(\tau \rightarrow e + \gamma)$ and $B'(\mu \rightarrow e + \gamma)$.

### Neutrino Mass Spectrum with Inverted Ordering

As can be seen in Fig. 5.2 (right panel), in the case of IO mass spectrum the term proportional to $\log(m_2/m_1)$ is strongly suppressed with respect to the other terms. This is valid for all values of the lightest neutrino mass allowed in the models of interest, $m_3 \gtrsim 0.02$ eV. More specifically, one has: $\log(m_2/m_1) \approx 0.014$ (0.003) for $m_3 = 0.02$ eV (0.1 eV). In the case of non-QD neutrino mass spectrum ($m_3 \lesssim 0.1$ eV), $B'(e_\alpha \rightarrow e_\beta + \gamma)$ are determined practically by the sum of the terms proportional to $\log(m_1/\overline{m})$ and $\log(m_3/m_1)$. The second term increases as $m_3$ decreases towards

the minimal allowed value $m_3 \approx 0.02$ eV, so that $|\log(m_3/m_1)| \approx 1$ (0.1) for $m_3 = 0.02$ eV (0.1 eV). Thus, taking into account the results reported in Tab. 5.1, one has at LO in $\varepsilon$:

$$B'(\mu \to e + \gamma) \approx B'(\tau \to e + \gamma) \propto \mathcal{O}(\varepsilon^2) , \tag{5.13}$$

$$B'(\tau \to \mu + \gamma) \propto \left| \frac{1}{2} y_\nu^2 \log\left(\frac{m_3}{m_1}\right) \right|^2 \approx \left\{ \begin{array}{ll} 0.25 \, |y_\nu|^4 , & \text{for } m_3 = 0.02 \, \text{eV} , \\ 0.0025 \, |y_\nu|^4 , & \text{for } m_3 = 0.1 \, \text{eV} . \end{array} \right. \tag{5.14}$$

The shown order of magnitude estimates for $B'(\mu \to e + \gamma)$ and $B'(\tau \to e + \gamma)$ in Eq. (5.13) can be significantly modified by the rather large contribution of the term containing the factor $\log(m_1/\overline{m}) \approx (3.5 \div 4.5)$. It follows from Tab. 5.1 that for, e.g. $\varepsilon \approx 0.04$, the contribution in the LFV branching ratios due to the indicated term can be $\sim \varepsilon \log(m_1/\overline{m}) \approx 1/5 \sim \sqrt{\varepsilon}$ such that the branching ratios of the decays $\mu \to e + \gamma$ and $\tau \to e + \gamma$ scale as $\mathcal{O}(\varepsilon)$. For $m_3 \approx 0.1$ eV, $B'(\mu \to e+\gamma)$ and $B'(\tau \to e+\gamma)$ can be comparable to the normalized branching ratio of $\tau \to \mu+\gamma$ decay, Eq. (5.14). Indeed, for $m_3 \approx 0.1$ eV and $\varepsilon \approx 0.04$, owing to the interplay between the leading term in the expansion parameter $\varepsilon$, $\log(m_3/m_1)$, whose absolute value decreases with increasing of $m_3$, and the contribution from $\log(m_1/\overline{m})$, $B'(\tau \to \mu + \gamma)$ scales as few times $\varepsilon$.

Comparing the results for the NO and the IO neutrino mass spectrum one can see that in a model with generic NLO corrections to the matrix of neutrino Yukawa couplings, the magnitude of the branching ratio $B'(\tau \to \mu + \gamma)$ practically does not depend on the type of neutrino mass spectrum. For $\varepsilon \approx 0.007$, $B'(\mu \to e+\gamma)$ and $B'(\tau \to e+\gamma)$ in the case of IO spectrum can be by one order of magnitude smaller than in the case of NO spectrum, while if $\varepsilon \approx 0.04$, these two branching ratios are predicted to be essentially the same for the two types of spectrum. Independently of the type of the spectrum and of the value of $\varepsilon$, one always has: $B'(\mu \to e + \gamma) \approx B'(\tau \to e + \gamma)$.

In the next section a numerical study of the LFV processes discussed before will be performed within the the two $A_4$ models defined in [81] and [82]. One important difference between the two models is in the predicted off-diagonal elements of the hermitian matrix $\lambda^\dagger \lambda$. In the model introduced in [82] they are all of $\mathcal{O}(\varepsilon)$ and originate from the NLO corrections to the Dirac mass matrix, Eq. (B.20). The exact expressions for the matrix elements can be derived using Tab. 5.1 and setting $w' = w'' = 0$ and $(x_1, x_2, x_3) = (1, 1, 1) v_S$. In what concerns the model in [81], the VEV structure of the flavon fields, $w' = w'' = 0$ and $(x_1, x_2, x_3) \propto (1, 0, 0)$, implies that the leading term in the off-diagonal elements of the matrix $\lambda^\dagger \lambda$ is of $\mathcal{O}(\varepsilon^2)$. This receives contributions from the Dirac mass term, see Eq. (B.19), as well as from the charged lepton sector (through $V_{eL}$, see Eq. (B.22)). This difference in the $\varepsilon$ dependence of the elements of $\lambda^\dagger \lambda$ in the two models leads to different predictions for the LFV branching ratios for the IO neutrino mass spectrum. As a consequence, in the models reported in [82] the branching ratios of the decays $\mu \to e + \gamma$ and $\tau \to e + \gamma$ are up to two orders of magnitude larger than those in the other model. In contrast, for $m_3 < 0.1$ eV, one expects similar results in both models for the decay $\tau \to \mu + \gamma$ since the coefficient of the term proportional to $\log(m_3/m_1)$ is of order $\varepsilon^0$. Note that in the case of a QD light (heavy) neutrino mass spectrum, $m_3 \gtrsim 0.1$ eV, the term proportional to $\log(m_1/\overline{m})$ in Eq. (5.9) gives the dominant contribution, in both the models under discussion, and thus the magnitude of the non-diagonal elements of $\lambda^\dagger \lambda$ determines the magnitude of the branching ratios of the LFV decays.

The preceding study shows that in the $A_4$ models, the LO structure of the matrix of neutrino Yukawa couplings $\lambda$, which is determined by $U_{TB}$, together with the possibility of having a heavy

RH neutrino mass spectrum with partial hierarchy, leads to LFV decay rates scaling as $\mathcal{O}(\varepsilon^0)$. This prediction differs significantly from the one obtained in the effective field theory approach. In [91] the branching ratios of the charged LFV radiative decays were shown to scale as $\varepsilon^2$ in a generic effective field theory framework, and could even be stronger suppressed (scaling as $\varepsilon^4$) in a specific supersymmetric scenario. However, the absolute magnitude of the branching ratios are expected to be of similar size in both approaches, because the suppression due to (positive) powers of the expansion parameter $\varepsilon$, present in the effective field theory approach, corresponds in the current analysis to the suppression factor associated to the fact that flavour violating soft slepton masses are generated only through RG running.

The scales $m_S$ and $M$, which are the relevant scales for charged LFV radiative decays, in the approach used in this chapter and in the effective field theory one [91], respectively, can be related to each other. Indeed, assuming that the mass scale $M$ arises from one-loop effects of new particles, such as SUSY particles, one can see that the mass $m_S$ of these new particles is identified with $M$ weighted with the coupling $g$ of these particles to the charged leptons and divided by the loop factor $4\pi$:

$$m_S \approx \frac{gM}{4\pi}\,. \tag{5.15}$$

## 5.2 Numerical Results

In the following, the numerical computation of the branching ratios of the LFV decays $\mu \to e + \gamma$, $\tau \to e + \gamma$ and $\tau \to \mu + \gamma$ is reported in the form of scatter plots showing the correlations between two of the indicated branching ratios. The calculations are performed in the framework defined by the models [81, 82]. The expansion parameter $\varepsilon$ is set equal to 0.04.

The sparticle mass spectrum considered here is moderately heavy and is defined by the following set of mSUGRA parameters:

$$m_0 = 150 \text{ GeV}, \quad m_{1/2} = 700 \text{ GeV}, \quad A_0 = 0 \text{ GeV}, \quad \tan\beta = 10. \tag{5.16}$$

The parameters in Eq. (5.16) lead to squark masses between 1.1 TeV and 1.5 TeV, gluino masses around 1.6 TeV and masses of right-handed sleptons of about 300 GeV. Thus, these sparticles are accessible at LHC. This point in the mSUGRA parameter space belongs to the stau co-annihilation region [100, 101, 102], in which the amount of DM in the Universe can be explained through the lightest sparticle (LSP). The latter is a bino-like neutralino and has a mass of approximately 280 GeV. [5] As was shown in [104], the stau co-annihilation and the bulk regions are hardly affected, if RH neutrinos are included into the mSUGRA context. For the set of parameters in Eq. (5.16), all decay rates scale with the factor $B_0(m_0, m_{1/2})\tan^2\beta \approx 3.8 \times 10^{-10}$.

The scatter plots are obtained by varying all the $\mathcal{O}(1)$ parameters that enter in the matrix of neutrino Yukawa couplings $\lambda$, defined in Eq. (5.2). Some of these parameters are equal to zero or have a common value (see Appendix B). The NLO corrections to the Dirac mass matrices for the two models under discussion are given in Eqs (B.19) and (B.20), respectively. In the calculations of the normalized branching ratios $B'(e_\alpha \to e_\beta + \gamma)$, the LO neutrino Yukawa parameter $y_\nu$ was set

---

[5]The sparticle masses quoted above were calculated with ISAJET 7.69 [103].

equal to one. The absolute values of all the other (complex) parameters in the neutrino Yukawa matrix $\lambda$ were varied in the interval $[0.5, 2]$. The corresponding phases are varied between $0$ and $2\pi$.

The results obtained for the two models are presented graphically in Figs 5.3 and 5.4, respectively, for both the NO and IO light neutrino mass spectrum. The scatter plots correspond to three values of the lightest neutrino mass: $i$) $m_1 = 3.8 \times 10^{-3}$ eV, $5 \times 10^{-3}$ eV and $7 \times 10^{-3}$ eV (NO spectrum); $ii$) $m_3 = 0.02$ eV, $0.06$ eV and $0.1$ eV (IO spectrum). In all numerical calculations the RG effects on neutrino masses and mixings were neglected. This is a sufficiently good approximation provided the light neutrino mass spectrum is not QD.

### 5.2.1 Model predictions

The results for the $A_4$ model given in [81] are shown in Fig. 5.3. In the case of NO spectrum (left panels in Fig. 5.3), the normalized branching ratios $B'(\mu \to e + \gamma)$ and $B'(\tau \to e + \gamma)$, defined in Eq. (5.8), are approximately the same, as the analysis performed in Section 5.1 suggested. The branching ratios are larger for smaller values of the lightest neutrino mass $m_1$, the dominant contribution being due to the term $\propto \log(m_2/m_1)$ which is a decreasing function of $m_1$ (Fig. 5.2, left panel). The same feature is exhibited by the term $\propto \log(m_3/m_1)$. The latter is multiplied by a coefficient of $\mathcal{O}(\varepsilon)$. As was indicated before, the term $\propto \log(m_1/\overline{m})$ in such model is suppressed, being of $\mathcal{O}(\varepsilon^2)$, and has a negligible effect on the results. Due to the fact that the coefficient of the term $\propto \log(m_3/m_1)$ in $B'(\tau \to \mu + \gamma)$ is of order one, the normalized branching ratio of $\tau \to \mu + \gamma$ decay is approximately by a factor of ten larger than those of $\mu \to e + \gamma$ and $\tau \to e + \gamma$ decays, which is consistent with the analytic estimates given in Eqs (5.11) and (5.12).

Note that, for the set of mSUGRA boundary conditions chosen, Eq. (5.16), the MEGA upper limit [105] on $B(\mu \to e + \gamma)$ is not satisfied for $m_1 = 3.8 \times 10^{-3}$ eV. This important experimental constraint can be fulfilled for larger values of the lightest neutrino mass and, in particular, for the two other chosen values of $m_1$, $m_1 = 5 \times 10^{-3}$ eV and $m_1 = 7 \times 10^{-3}$ eV. However, $B(\mu \to e + \gamma)$ is always larger than $10^{-12}$ and thus is within the range of sensitivity of the MEG experiment [106], $B(\mu \to e + \gamma) \gtrsim 10^{-13}$, which is currently taking data. The predicted rates of the $\tau$ LFV radiative decays are always below the current experimental upper bounds [107] as well as below the sensitivity planned to be reached at a SuperB factory [108].

In the case of IO mass spectrum, the predicted $B(\mu \to e + \gamma)$ is always compatible with the existing experimental upper limit [105]. In this scenario the MEG experiment will probe a relatively large region of the parameter space of the model. The branching ratios of $\mu \to e + \gamma$ and $\tau \to e + \gamma$ decays are, in general, smaller by up to two orders of magnitude than in the case of a neutrino spectrum with NO. As explained earlier, this is partly due to the fact that the term $\propto \log(m_2/m_1)$, which in the case of NO mass spectrum gives the dominant contribution, is strongly suppressed since $m_2$ and $m_1$ are nearly equal, $m_2 \cong m_1$, and partly due to the fact that the coefficient of the term proportional to $\log(m_1/\overline{m})$ is of order $\varepsilon^2$. This conclusion is valid for all allowed values of the lightest neutrino mass, $m_3 \gtrsim 0.02$ eV (Fig. 5.2, right panel). In contrast to the case of a NO neutrino mass spectrum, the branching ratios of $\mu \to e + \gamma$ and $\tau \to e + \gamma$ decays do not show any significant dependence on the lightest neutrino mass, $m_3$. At the same time, the $\tau \to \mu + \gamma$ decay branching ratio exhibits a strong dependence on the value of $m_3$. Indeed, it varies by up to two orders of magnitude when $m_3$ is varied from $0.02$ eV to $0.1$ eV (Fig. 5.3, right bottom panel). The magnitude and the behavior of $B'(\tau \to \mu + \gamma)$ as a function of $m_3$ is determined by the term pro-
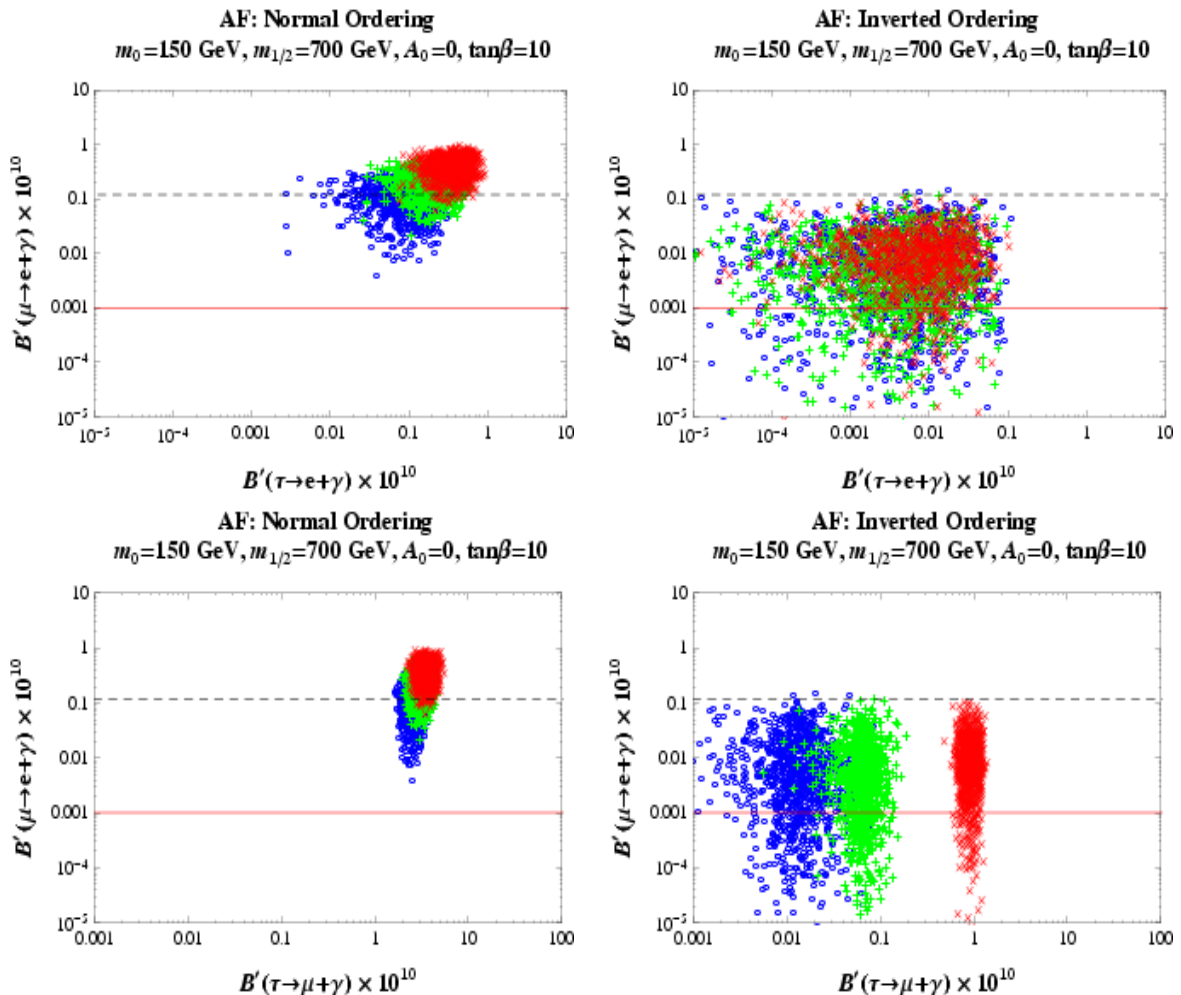
**Figure 5.3:** Correlation between $B'(\mu \to e + \gamma)$, $B'(\tau \to e + \gamma)$ and $B'(\tau \to \mu + \gamma)$, calculated within the model defined in [81]. The results shown are obtained for three different values of the lightest neutrino mass for both types of neutrino mass spectrum: $i$) with normal ordering (left panels), $m_1 = 3.8 \times 10^{-3}$ eV (red $\times$), $m_1 = 5 \times 10^{-3}$ eV (green $+$) and $m_1 = 7 \times 10^{-3}$ eV (blue $\circ$); $ii$) with inverted ordering (right panels), $m_3 = 0.02$ eV (red $\times$), $m_3 = 0.06$ eV (green $+$) and $m_3 = 0.1$ eV (blue $\circ$). The horizontal dashed line corresponds to the MEGA bound, $B'(\mu \to e + \gamma) \leq 1.2 \times 10^{-11}$. The horizontal continuous line corresponds to $B'(\mu \to e + \gamma) = 10^{-13}$, which is the prospective sensitivity of the MEG experiment.

portional to $\log(m_3/m_1)$ in the right-hand side of Eq. (5.9). It has a maximal value for $m_3 = 0.02$ eV and decreases as $m_3$ increases, following the decreasing of $\log(m_3/m_1)$. As a consequence of the suppression of the coefficient of the $\log(m_1/\overline{m})$ term, the analytic estimates reported in Eqs (5.13) and (5.14) are valid. Thus, the $\tau \to \mu + \gamma$ decay has a branching ratio which, at least for $m_3 \approx 0.02$ eV, is by approximately two orders of magnitude larger than those of the two other charged LFV
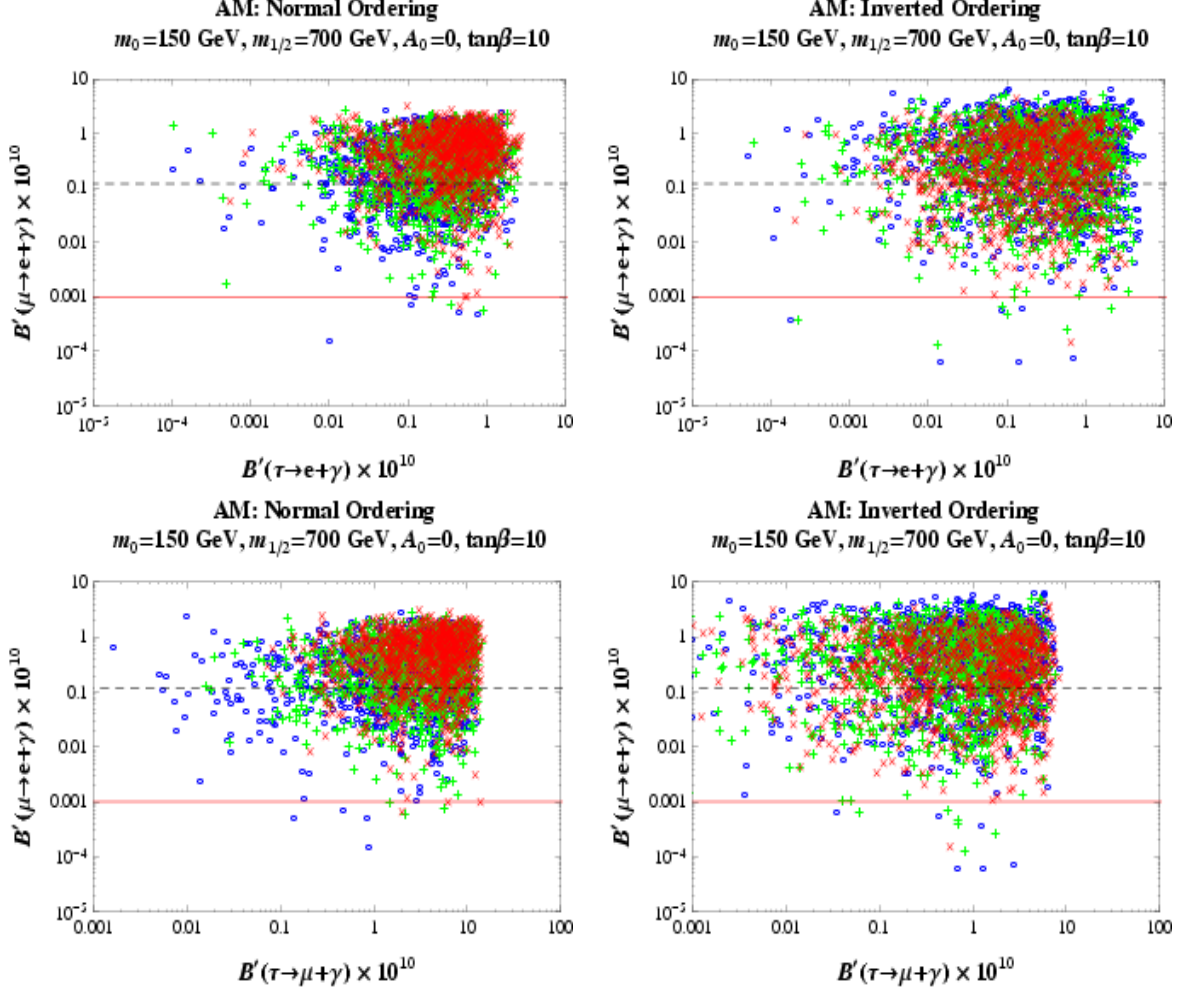
**Figure 5.4:** The same as in Fig. 5.3, but for the model defined in [82].

radiative decays. For $m_3 = 0.02$ eV we have $B'(\tau \to \mu + \gamma) \approx 10^{-10}$. Therefore as in the case of NO spectrum, the predicted $B'(\tau \to \mu + \gamma)$ for the values of mSUGRA parameters considered is below the sensitivity range of the currently planned experiments.

Concerning the model defined in [82], the associated numerical results for the charged LFV radiative decays are illustrated in Fig. 5.4, for both types of neutrino mass spectrum. As was discussed above, the main difference with respect to the previous case is in the prediction for the coefficient of the $\log(m_1/\overline{m})$ term in the expression of the branching ratio (5.9). In fact, now this coefficient is of $\mathcal{O}(\varepsilon)$ for the three radiative decays and, therefore, the term $\propto \log(m_1/\overline{m})$ is not negligible. Obviously, $\log(m_1/\overline{m})$ is a monotonically increasing function of the lightest neutrino mass (see Fig. 5.2). Since the coefficient of this logarithm is a number with absolute value of order one, for both types of neutrino mass spectrum the $\mu \to e + \gamma$, $\tau \to e + \gamma$ and $\tau \to \mu + \gamma$
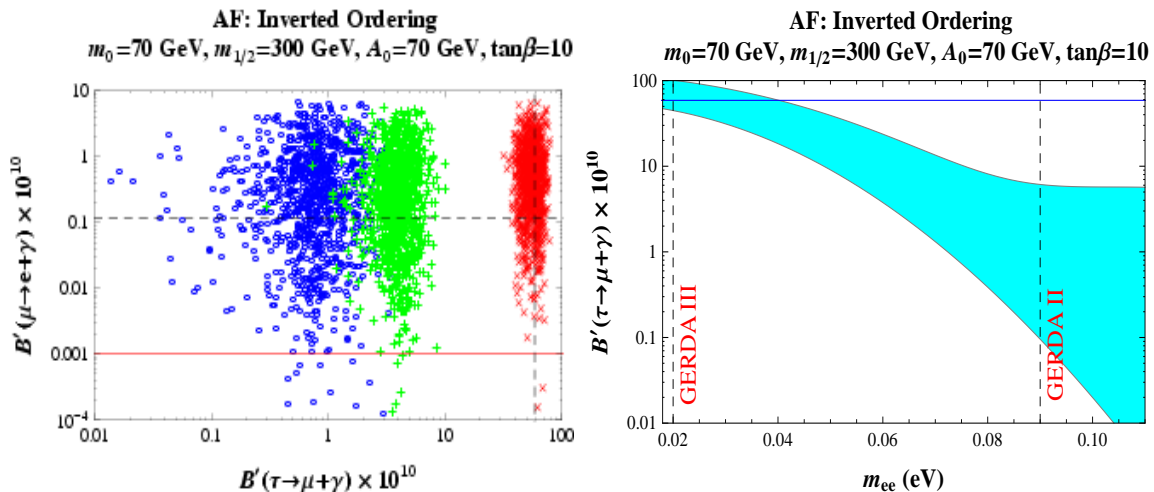
**Figure 5.5:** Left panel: correlation between $B'(\mu \to e + \gamma)$ and $B'(\tau \to \mu + \gamma)$ in the model defined in [81] for three different values of the lightest neutrino mass: $m_3 = 0.02$ eV (red $\times$), $m_3 = 0.06$ eV (green $+$) and $m_3 = 0.1$ eV (blue $\circ$). The horizontal dashed line shows the current upper bound from the MEGA experiment, while the continuous line corresponds to the foreseen sensitivity of the MEG experiment. The vertical dashed line indicates the possible future bound on $\tau \to \mu + \gamma$ from a SuperB factory. Right panel: correlation between $B'(\tau \to \mu + \gamma)$ and the effective Majorana mass $m_{ee}$. The horizontal continuous line shows the prospective reach of a SuperB factory. The two dashed vertical lines indicate the expected sensitivity of the GERDA II and GERDA III phase.

decay branching ratios exhibit much weaker dependence on the lightest neutrino mass compared to the dependence they show in the previous model. Most importantly, as a consequence of the contribution due to the term $\propto \log(m_1/\overline{m})$, $B'(\mu \to e + \gamma)$ and $B'(\tau \to e + \gamma)$ in the case of IO spectrum are predicted to be of the same order of magnitude as in the case of NO spectrum. This is in sharp contrast to the predictions of the first model (see Fig. 5.3).

Concerning $B'(\tau \to \mu + \gamma)$, the predictions in the cases of NO and IO spectrum essentially do not differ and are similar to those obtained in the previous model. As Fig. 5.4 shows, for both the NO and IO mass spectrum one has $B(\mu \to e + \gamma) < 1.2 \times 10^{-11}$ in roughly half of the parameter space explored. At the same time, in practically all the parameter space considered, $B(\mu \to e + \gamma) \gtrsim 10^{-13}$. The tau LFV radiative decays are predicted to proceed with rates which are below the sensitivity range of the planned experiments.

## 5.2.2 Case of $B(\mu \to e + \gamma) > 10^{-13}$ and $B(\tau \to \mu + \gamma) \approx 10^{-9}$

The numerical analysis reported before and summarized in Figs 5.3 and 5.4 shows clearly that for the point in the mSUGRA parameter space considered, Eq. (5.16), the $\tau \to e + \gamma$ and $\tau \to \mu + \gamma$ decay branching ratios are predicted to be compatible with the existing experimental upper bounds and below the sensitivity of the future planned experiments. However, the decay $\tau \to \mu + \gamma$ might have a rate within the sensitivity range of the future experiments if the SUSY particle masses are smaller (*i.e.* the effective SUSY mass scale $m_S$, Eq. (5.7), is lower) than those resulting from

Eq. (5.16). This possibility can be realized for smaller values of the mass parameters $m_0$ and $m_{1/2}$, compared to those reported in (5.16). Indeed, consider the following set:

$$m_0 = 70 \text{ GeV}, \quad m_{1/2} = 300 \text{ GeV}, \quad A_0 = 70 \text{ GeV}, \quad \tan\beta = 10. \tag{5.17}$$

For the values given in Eq. (5.17) squarks can be as light as 500 GeV, gluinos have masses of approximately 700 GeV and all sleptons have masses smaller than 250 GeV. The LSP providing the correct amount of DM in the Universe is bino-like and has a mass of 115 GeV. The parameters given in Eq. (5.17) correspond also to a point in the stau co-annihilation region, very close to the region excluded by the LEP2 data [100, 101, 102]: the mass of the lightest Higgs boson is near 114.4 GeV. For the indicated values of the SUSY breaking parameters the predicted LFV branching ratios are larger than those corresponding to the mSUGRA point in Eq. (5.16) since $B_0(m_0, m_{1/2}) \tan^2\beta \approx 2.3 \times 10^{-8}$. As a result, the model given in [82] is strongly disfavored by the experimental limit on $B(\mu \to e + \gamma)$. Concerning the other model, the latter constraint cannot be satisfied, if the neutrino mass spectrum is with NO. However, in the case of IO mass spectrum, the predicted $B(\mu \to e + \gamma)$ is compatible with the MEGA bound in nearly half of the region of the relevant parameter space and (with the exception of singular specific points) is within the sensitivity reach of the MEG experiment. This case is analyzed in Fig. 5.5, left panel, where the correlation between the normalized branching ratios of the decays $\mu \to e + \gamma$ and $\tau \to \mu + \gamma$ is represented, assuming the boundary conditions reported in (5.17). The prospective sensitivity of the searches for the $\tau \to \mu + \gamma$ decay, which can be reached at a SuperB factory, $B(\tau \to \mu + \gamma) \approx 10^{-9}$ [108], is also indicated. Assuming a scenario in which in the MEG experiment it is found that $B(\mu \to e + \gamma) > 10^{-13}$ and the SUSY particles with masses, as predicted above, are observed at LHC, one can see from Fig. 5.5, left panel, that $B(\tau \to \mu + \gamma)$ might be detectable at a SuperB factory if the lightest neutrino mass $m_3 \approx 0.02$ eV. For $m_3 = 0.02$ eV, the $(\beta\beta)_{0\nu}$-decay effective Majorana mass is predicted to lie in the interval $m_{ee} \approx (0.018 \div 0.054)$ eV (see Section 4.2.1). Values of $m_{ee}$ in the indicated interval might be probed in some of the next generation of $(\beta\beta)_{0\nu}$-decay experiments (see, e.g. [46, 47]). In Fig. 5.5, right panel, the correlation between the normalized branching ratio of $\tau \to \mu + \gamma$ decay and the effective Majorana mass $m_{ee}$ is shown. As was explained in Chapter 1, the relation between $m_{ee}$ and the lightest light neutrino mass is in this case: $m_{ee} \cong \sqrt{m_3^2 + |\Delta m_{\rm A}^2|}\, \left| 2 + e^{i\alpha_{21}} \right| /3$, where $m_3$ and $\alpha_{21}$ are both functions of one parameter and thus their values are correlated. The prospective sensitivity of the GERDA II and GERDA III phase are, $m_{ee} = 0.09$ eV and $m_{ee} = 0.02$ eV, respectively [46]. As one can see form the figure, with a positive signal of $B(\tau \to \mu + \gamma) \approx 10^{-9}$ at a SuperB factory values of $m_{ee}$ up to $m_{ee} \approx 0.04$ eV can be probed.

Finally, the sum of neutrino masses in this class of models, for IO light neutrino mass spectrum, is $\sum m_i \approx 0.125$ eV for $m_3 \approx 0.02$ eV (see Section 4.2.1). This value is smaller than the current cosmological bounds [31], but is within the sensitivity expected to be reached by combining data on weak lensing of galaxies by large scale structure with data from WMAP and PLANCK experiments (see, e.g. [30]).

### 5.2.3 Specific features of the predictions for $B(\mu \to e + \gamma)$

Apart from the detailed numerical analysis performed before for two specific models, it is interesting to perform an analysis of the parameter space of *generic $A_4$ models*, focusing on particular points
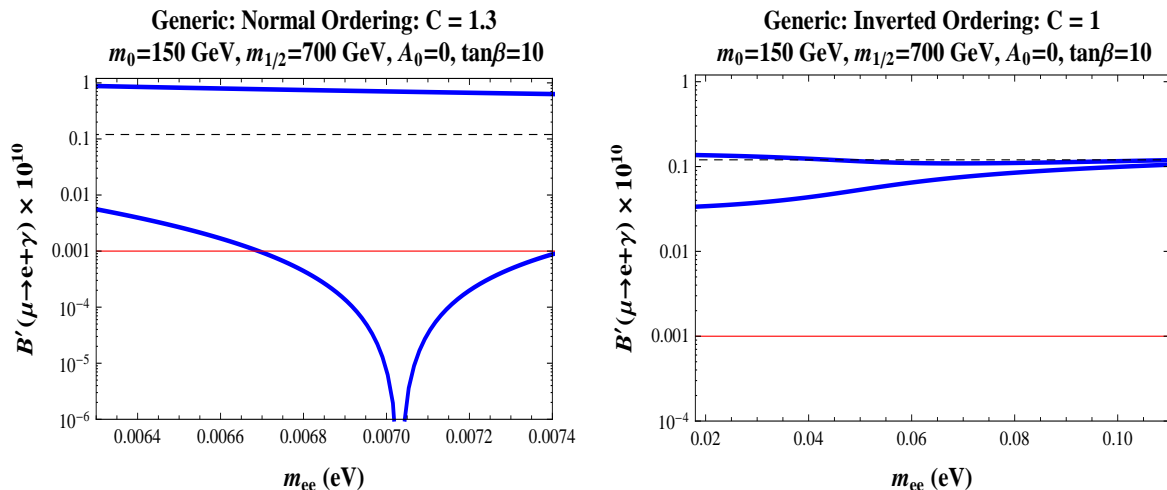
**Figure 5.6:** $B'(\mu \to e + \gamma)$ vs $m_{ee}$ for NO (left panel) and IO (right panel) light neutrino mass spectrum calculated for an $A_4$ model with generic NLO corrections, see Eq. (B.18). Lower and upper limits on $B'(\mu \to e + \gamma)$ are shown, which can be found by using Eq. (5.18) for all possible combinations of $\sigma_{1,2,3}$. The horizontal dashed line corresponds to the MEGA bound [105], $B'(\mu \to e + \gamma) \leq 1.2 \times 10^{-11}$. The horizontal continuous line corresponds to $B'(\mu \to e + \gamma) = 10^{-13}$, which is the prospective sensitivity of the MEG experiment [106]. The results shown correspond to the best fit values reported in Tab. 1.1: $|\Delta m_A^2| = 2.40 \times 10^{-3}$ eV$^2$ and $r = \Delta m_\odot^2 / |\Delta m_A^2| = 0.032$.

which result phenomenologically relevant. In order to do so one can use the analytic formula given in Section 5.1, Eq. (5.9), for the branching ratio of the decay $\mu \to e + \gamma$ together with the results given in Tab. 5.1 and assume that the coefficients of the $\mathcal{O}(\varepsilon)$ terms are real and have the same absolute value $C > 0$:

$$B'(\mu \to e + \gamma) \propto \left| \frac{1}{3} y_\nu^2 \log\left(\frac{m_2}{m_1}\right) + C\,\varepsilon \left( \sigma_1 \log\left(\frac{m_1}{\overline{m}}\right) + \sigma_2 \log\left(\frac{m_2}{m_1}\right) + \sigma_3 \log\left(\frac{m_3}{m_1}\right) \right) \right|^2 .$$
(5.18)

The relative sign of these terms is not fix and all the eight combinations $\sigma_{1,2,3} = \pm 1$ are allowed. The set of mSUGRA parameters is taken equal to Eq. (5.16). Moreover, $\varepsilon = 0.04$, $y_\nu = 1$ and the best fit values of $r$ and $|\Delta m_A^2|$ are assumed. In Fig. 5.6, left panel, the branching ratio of $\mu \to e + \gamma$ versus the effective Majorana mass $m_{ee}$ is reported in the case of light neutrino mass spectrum with normal ordering. The constant $C$ is fixed to the value: $C = 1.3$. The effective Majorana mass is now: $m_{ee} \cong |2\,m_1 + \sqrt{m_1^2 + \Delta m_\odot^2}|/3$. Only the two curves which correspond to the upper and lower bound of the branching ratio are shown. They correspond to two out of the eight different combinations of $\sigma_{1,2,3}$. As one can see, there exists the possibility of cancellations between the terms contributing to the branching ratio of the $\mu \to e + \gamma$ decay, so that the value of the latter can be strongly suppressed. [6] The value of $m_{ee}$ at which the suppression takes place depends on the value

---

[6]Note that the value of $B(\mu \to e + \gamma)$ will still be non-zero in general, because of the $\mathcal{O}(\varepsilon)$ corrections to the coefficients of the different logarithms in the expression of the branching ratio (5.9).

of the constant $C$. In Fig. 5.6, right panel, the corresponding plot for IO neutrino mass spectrum is shown. In this case: $C = 1$. In contrast to the case of NO spectrum, no strong suppression of $B(\mu \to e + \gamma)$ is possible, because the term $\propto \log(m_1/\overline{m})$ always dominates (see Fig. 5.2, right panel). This result holds for all values of the constant $C$ from the interval $0.1 \lesssim C \lesssim 6$. Allowing for arbitrary relative phases between the different contributions in the right-hand side of Eq. (5.18), one can find that for a NO light neutrino mass spectrum the curve for $\sigma_{1,2,3} = +1$ corresponds to an upper bound on $B(\mu \to e + \gamma)$, whereas the curve for $\sigma_{1,2,3} = -1$ is an absolute lower bound with the exception of few points in the parameter space. For the IO spectrum, the bounds obtained for real coefficients are also upper and lower bounds in the case of arbitrary relative phases between the different terms in Eq. (5.18).

As mentioned earlier, the preceding analysis holds for an $A_4$ model with generic NLO corrections, as is the model defined in [82]. A similar analysis can be done for the model given in [81], where the coefficient of the logarithm $\log(m_1/\overline{m})$ is of order $\varepsilon^2$, by replacing $\sigma_1 \log(m_1/\overline{m})$ in with $\varepsilon\,\sigma_1 \log(m_1/\overline{m})$ in Eq. (5.18). One can see that deep cancellations between the different contributions in $B(\mu \to e + \gamma)$ can occur now in both the cases of NO and IO neutrino mass spectrum. For the IO spectrum, the cancellations leading to a strong suppression of branching ratio $B(\mu \to e + \gamma)$ take place for $m_{ee}$ around 0.09 eV for almost all values of $C$ in the range considered, $0.1 \lesssim C \lesssim 6$.

## 5.3 The $\mu - e$ Conversion and $e_\alpha \to 3\,e_\beta$ Decay Rates

In this section further constraints on the $A_4$ models are analyzed. These come from other LFV rare processes, *i.e.* the $\mu - e$ conversion and the decays $e_\alpha \to 3e_\beta$. In the mSUGRA scenario, these LFV processes are dominated by the contribution coming from the $\gamma-$penguin diagrams. As a consequence, for $\mu - e$ conversion, the following relation holds with a good approximation [97]:

$$CR(\mu\,\mathrm{N} \to e\,\mathrm{N}) \equiv \frac{\Gamma(\mu\mathrm{N} \to e\mathrm{N})}{\Gamma_{\mathrm{capt}}} = \frac{\alpha_{em}^4 G_F^2 m_\mu^5 Z}{12\pi^3 \Gamma_{\mathrm{capt}}} Z_{eff}^4 |F(q^2)|^2 B(\mu \to e + \gamma)\,. \tag{5.19}$$

In Eq. (5.19) $Z$ is the proton number in the nucleus N, $F(q^2)$ is the nuclear form factor at momentum transfer $q$, $Z_{eff}$ is an effective atomic charge and $\Gamma_{\mathrm{capt}}$ is the experimentally known total muon capture rate. For $^{48}_{22}\mathrm{Ti}$ one has $Z_{eff} = 17.6$, $F(q^2 = -m_\mu^2) \approx 0.54$ and $\Gamma_{\mathrm{capt}} = 2.590 \times 10^6\ \mathrm{sec}^{-1}$ [109]. In the case of $^{27}_{13}\mathrm{Al}$ one finds $Z_{eff} = 11.48$, $F(q^2 = -m_\mu^2) \approx 0.64$ and $\Gamma_{\mathrm{capt}} = 7.054 \times 10^5\ \mathrm{sec}^{-1}$ [110]. According to Eq. (5.19), the $\mu - e$ conversion ratios in $^{48}_{22}\mathrm{Ti}$ and $^{27}_{13}\mathrm{Al}$ are given by:

$$CR(\mu\,^{48}_{22}\mathrm{Ti} \to e\,^{48}_{22}\mathrm{Ti}) \approx 0.005 B(\mu \to e + \gamma)\,, \tag{5.20}$$

$$CR(\mu\,^{27}_{13}\mathrm{Al} \to e\,^{27}_{13}\mathrm{Al}) \approx 0.0027 B(\mu \to e + \gamma)\,. \tag{5.21}$$

Future experimental searches for $\mu - e$ conversion can reach the sensitivity: $CR(\mu\,^{48}_{22}\mathrm{Ti} \to e\,^{48}_{22}\mathrm{Ti}) \approx 10^{-18}$ [109], and $CR(\mu\,^{27}_{13}\mathrm{Al} \to e\,^{27}_{13}\mathrm{Al}) \approx 10^{-16}$ [110]. The upper bound $B(\mu \to e + \gamma) < 10^{-13}$ which can be obtained in the MEG experiment would correspond to the following upper bounds on the $\mu - e$ conversion ratios under discussion: $CR(\mu\,^{48}_{22}\mathrm{Ti} \to e\,^{48}_{22}\mathrm{Ti}) < 5 \times 10^{-16}$ and $CR(\mu\,^{27}_{13}\mathrm{Al} \to e\,^{27}_{13}\mathrm{Al}) < 2.7 \times 10^{-16}$. The latter could be probed by future experiments on $\mu - e$ conversion, which have higher prospective sensitivity. Therefore, it is easy to realize that for

the mSUGRA points considered in Section 5.2, both the specific models analyzed can be further constrained by the experiments on $\mu - e$ conversion if the $\mu \to e + \gamma$ decay will not be observed in the MEG experiment.

In what concerns the decay of a charged lepton into three lighter charged leptons, the branching ratio is approximately given by [97]:

$$B(e_\alpha \to 3e_\beta) \approx \frac{\alpha}{3\pi} \left( \log\left( \frac{m_{e_\alpha}^2}{m_{e_\beta}^2} \right) - \frac{11}{4} \right) B(e_\alpha \to e_\beta + \gamma) \,. \tag{5.22}$$

The searches for $\tau \to \mu + \gamma$, $\tau \to 3\mu$ and $\tau \to 3e$ decays at SuperB factories [108] will be sensitive to $B(\tau \to \mu + \gamma), B(\tau \to 3\mu), B(\tau \to 3e) \geq 10^{-9}$. Therefore, if in the experiments at SuperB factories it is found that $B(\tau \to \mu + \gamma) < 10^{-9}$, obtaining the upper limits $B(\tau \to 3\mu), B(\tau \to 3e) < 10^{-9}$ would not constrain further the $A_4$ models considered here. However, the observation of the $\tau \to 3\mu$ decay with a branching ratio $B(\tau \to 3\mu) \geq 10^{-9}$, combined with the upper limit $B(\tau \to \mu + \gamma) < 10^{-9}$, or the observation of the $\tau \to \mu + \gamma$ decay with a branching ratio $B(\tau \to \mu + \gamma) \geq 10^{-9}$, would rule out the $A_4$ models under discussion.

The current limit on the $\mu \to 3e$ decay branching ratio is $B(\mu \to 3e) < 10^{-12}$ [111]. There are no plans at present to perform a new experimental search for the $\mu \to 3e$ decay with higher precision.

## 5.4   Summary

The main topic of this chapter is the numerical and analytical study of lepton flavour violation in a class of supersymmetric $A_4$ models with three heavy RH Majorana neutrinos, in which the lepton (neutrino) mixing is predicted to leading order to be tri-bimaximal. The flavour violating radiative decays, $\mu \to e + \gamma$, $\tau \to \mu + \gamma$ and $\tau \to e + \gamma$ are analyzed in detail, within the framework of the minimal supergravity scenario, which provides flavour universal boundary conditions at the scale of grand unification. The analytic estimates of the branching ratios $B(e_\alpha \to e_\beta + \gamma)$ were made for the case of generic NLO corrections to the neutrino Yukawa matrix. The numerical results presented, however, are obtained for two explicit realizations of the $A_4$ models, those reported in [81] and [82], respectively and discussed thoroughly in Appendix B.

The predictions of the $e_\alpha \to e_\beta + \gamma$ decay branching ratios, $B(e_\alpha \to e_\beta + \gamma)$, for both the models, are derived for a specific point in the mSUGRA parameter space lying in the stau co-annihilation region, which is compatible with direct bounds on sparticle masses and the requirement of explaining the amount of dark matter in the Universe. From the numerical analysis performed, it follows that in the case of NO light neutrino mass spectrum, both the models considered predict $B(\mu \to e + \gamma) > 10^{-13}$ in practically all the parameter space considered (see Figs 5.3 and 5.4). The same conclusion is valid for the IO mass spectrum in the case of the model defined in [82], whereas in the other one this result holds roughly in half of the parameter space of the model. Values of $B(\mu \to e + \gamma) \gtrsim 10^{-13}$ can be probed in the MEG experiment which is taking data at present.

In the case of NO spectrum for light neutrinos, the model given in [81] predicts for all the three branching ratios $B(e_\alpha \to e_\beta + \gamma)$ a noticeable dependence on the value of the lightest neutrino mass, as the numerical analysis shows. Furthermore, the dependence of $B(\tau \to \mu + \gamma)$ on $\min(m_j)$

is particularly strong in the case of IO spectrum. In contrast, $B(\mu \to e + \gamma)$ and $B(\tau \to e + \gamma)$ in this case vary relatively little with $\min(m_j)$. Concerning the branching ratios $B(e_\alpha \to e_\beta + \gamma)$ computed in the model given in [82], they do not exhibit significant dependence on $\min(m_j)$.

The branching ratios $B(\tau \to e + \gamma)$ and $B(\tau \to \mu + \gamma)$, in both the models examined, are always predicted to be below the sensitivity of the present and future planned experiments. It was shown, however, that if the SUSY particles are lighter, one can have, within the model defined in [81], $B(\mu \to e + \gamma) \gtrsim 10^{-13}$ and $B(\tau \to \mu + \gamma) \approx 10^{-9}$, if the light neutrino mass spectrum is with inverted ordering. A value of $B(\tau \to \mu + \gamma) \approx 10^{-9}$ requires the lightest neutrino mass to be $m_3 \approx 0.02$ eV. Sensitivity to such a value of $B(\tau \to \mu + \gamma)$ can be achieved, in principle, at a SuperB factory [108].

Estimates of the predicted rate of $\mu - e$ conversion in the $A_4$ models considered are also reported and it is shown that future experiments can further constrain these models if the $\mu \to e + \gamma$ decay will not be observed in the MEG experiment. The observation at the SuperB factories of the $\tau \to 3\mu$ decay with a branching ratio $B(\tau \to 3\mu) \geq 10^{-9}$, combined with the upper limit $B(\tau \to \mu + \gamma) < 10^{-9}$ or the observation of the $\tau \to \mu + \gamma$ decay with branching ratio $B(\tau \to \mu + \gamma) \geq 10^{-9}$, would rule out the $A_4$ models under discussion. If $B(\tau \to \mu + \gamma)$ is found to satisfy $B(\tau \to \mu + \gamma) < 10^{-9}$, the prospective sensitivity of SuperB factories to the decay modes $\tau \to 3\mu$ and $\tau \to 3e$ would not allow to obtain additional constraints on the parameter space of the $A_4$ models from non-observation of the $\tau \to 3\mu$ and $\tau \to 3e$ decays.

The results of the MEG experiment and of the upcoming experiments at LHC can provide significant tests of and can severely constrain the class of $A_4$ models predicting tri-bimaximal neutrino mixing.

# Conclusions

An important link between neutrino physics and cosmology is certainly provided by the leptogenesis mechanism for the generation of the matter-antimatter asymmetry of the Universe (*baryogenesis* via *leptogenesis*), which is the main topic studied in this Ph.D. thesis. As discussed in Chapter 1, the basic scheme in which this mechanism can be implemented is the type I see-saw model of neutrino mass generation. In its minimal version it includes the Standard Model particle content plus two or three right-handed (RH) heavy Majorana neutrinos. In the standard thermal leptogenesis scenario, under the assumption of a hierarchical spectrum for the RH heavy fields, the lightest RH Majorana neutrino is produced by thermal scatterings, via its Yukawa interactions with left-handed lepton and Higgs doublets. If CP is not preserved by the neutrino Yukawa couplings, a lepton number asymmetry can be dynamically generated through the out-of-equilibrium decays of the lightest RH Majorana field, thus satisfying all the three Sakharov's criteria. The lepton asymmetry is subsequently converted into a baryon number density due to the effect of non perturbative $B + L$ violating sphaleron interactions, which exist within the Standard Model.

An explicit connection between leptogenesis and low energy observables related to neutrino physics is realized in the scenario when *lepton flavour effects* play a dynamical role in the generation of the lepton asymmetry (*flavoured leptogenesis*). In this case, the high energy CP violation responsible for leptogenesis can be easily related to low energy CP violation in the lepton sector. Low energy CP violation in the lepton sector is provided by one Dirac and two Majorana CP violating phases in the Pontecorvo-Maki-Nakagawa-Sakata (PMNS) neutrino mixing matrix and can manifest itself in a non zero CP asymmetry in neutrino oscillations (Dirac CP violation) and, in an indirect way, in the effective Majorana mass in neutrinoless double beta decay. In Chapter 2 the effects of the lightest neutrino mass in flavoured leptogenesis were thoroughly analyzed when the amount of CP violation necessary for the generation of the baryon asymmetry of the Universe is provided exclusively by the Dirac and/or Majorana phases in the PMNS matrix. Results for the normal and inverted ordering (hierarchy) were derived. It was shown in particular that, for a non vanishing lightest neutrino mass, in some specific regions of the leptogenesis parameter space, the predicted baryon asymmetry can be larger, up to two orders of magnitude, than the corresponding asymmetry generated in the scenario with one massless neutrino.

In Chapter 3 the flavoured leptogenesis is further investigated in a model independent way. The main results obtained are related to the interplay between the low energy CP violation, originating from the PMNS matrix, and the high energy CP violation which can be present in the matrix of neutrino Yukawa couplings and can manifest itself only in "high" energy scale processes, like *e.g.* leptogenesis. Both normal and inverted hierarchical light neutrino mass spectra are considered in

the limit of decoupling of the heaviest RH Majorana field. It is shown that taking into account the contribution to the baryon asymmetry due to the CP violating phases in the neutrino mixing matrix can change drastically the predictions for baryogenesis, obtained assuming that only the high energy CP violation, which arises from the other phases in the neutrino Yukawa matrix, is operative in leptogenesis. In particular, in the case of inverted hierarchical light neutrino mass spectrum, there exist large regions in the corresponding leptogenesis parameter space where the relevant high energy phases have large CP violating values, but one can have successful leptogenesis only if the requisite CP violation is provided by the Majorana phases in the neutrino mixing matrix.

The related issues of Majorana CP violation in the lepton sector and leptogenesis are further analyzed in Chapter 4, where supersymmetric models based on type I see-saw mechanism of neutrino mass generation and $A_4$ flavour symmetry are considered. In this class of models, the three generations of left-handed leptons and right-handed neutrinos are unified into triplet representations of the $A_4$ group, whereas the right-handed charged leptons are $A_4-$singlets. The $A_4$ symmetry is spontaneously broken at high energies by the vacuum expectation values of a set of scalar fields, called flavons, which transform trivially under the gauge symmetry group. Such models predict at leading order a diagonal mass matrix for charged leptons and naturally lead to tri-bimaximal mixing in the neutrino sector, which is compatible with the present experimental data on the neutrino mixing angles. At leading order, the neutrino sector is described by two real parameters and one phase. The Majorana phases in the PMNS matrix depend on just one parameter and can be easily constrained by neutrino physics experiments. They play the role of leptogenesis CP violating parameters in the generation of the baryon asymmetry of the Universe. Moreover, the sign of one of the fundamental parameters of the model can be uniquely fixed by the requirement that the sign of the baryon asymmetry is correct.

Large values of the RH neutrino masses can lead in SUSY theories with see-saw mechanism to tension with the existing experimental upper limits on the rates of lepton flavour violating (LFV) decays and reactions. In Chapter 5, a detailed numerical analysis of the branching ratios of radiative LFV decays $\mu \to e + \gamma$, $\tau \to e + \gamma$ and $\tau \to \mu + \gamma$ was performed in supersymmetric $A_4$ models with three RH Majorana neutrinos. All sfermion mass matrices are assumed to be universal at the grand unification scale, as in the mSUGRA context, and off-diagonal elements in slepton mass matrices, which induce LFV decays, are only generated through RG running. Two different models based on $A_4$ discrete symmetry are analyzed in detail. Estimates of the predicted rate of $\mu - e$ conversion in the $A_4$ models considered show that future experiments can further constrain these models if the $\mu \to e + \gamma$ decay will not be observed by the MEG experiment, which is currently taking data. Further constraints and exclusion bounds on the models can be derived by other rare lepton flavour violating processes like three lepton tau decays. In particular, if SuperB factories will discover $\tau \to 3\mu$ decay with a branching ratio $B(\tau \to 3\mu) \geq 10^{-9}$ and at the same time $B(\tau \to \mu + \gamma) < 10^{-9}$, the $A_4$ models considered would be ruled out. The same conclusion is reached if $\tau \to \mu + \gamma$ decays with $B(\tau \to \mu + \gamma) \geq 10^{-9}$ will be detected.

The oncoming data from the MEG experiment as well as upcoming measurements of LHC can provide significant tests of supersymmetric $A_4$ models predicting tri-bimaximal neutrino mixing.

# Appendix A

# The discrete group $A_4$

A brief review of the basic features of the discrete group $A_4$ is reported in the following (see *e.g.* [112] and references therein for a further discussion about the properties of $A_4$ symmetry).

$A_4$ corresponds to the group of permutation of four objets (alternating group of order 4) and consists of 12 elements. From a geometrical point of view, it is the subgroup of the three dimensional rotation group which leaves invariant a regular tetrahedron. It has only two generators, $S$ and $T$. Each element of the group can be expressed in terms of $S$ and $T$:

$$1,\ S,\ T,\ ST,\ TS,\ T^2,\ ST^2,\ STS,\ TST,\ T^2S,\ TST^2,\ T^2ST. \tag{A.1}$$

The two generators of the group obey the following relation:

$$S^2 = T^3 = (ST)^3 = 1 \tag{A.2}$$

There are four inequivalent irreducible representations: one three-dimensional representation (3) and three of dimension one (1, 1′ and 1″). It is easy to check that two-dimensional representations do not exist in the group, because only $\det(T^3) = -1$ is in this case compatible with the conditions $S^2 = (ST)^3 = 1$ and, therefore, the relation given in (A.2) cannot be satisfied. The form of each irreducible representation, in the basis in which $T$ is diagonal, is given by:

$$1\ :\ S = 1, \qquad T = 1 \tag{A.3}$$
$$1'\ :\ S = 1, \qquad T = \omega^2 \tag{A.4}$$
$$1''\ :\ S = 1, \qquad T = \omega \tag{A.5}$$

$$3 : S = \frac{1}{3}\begin{pmatrix} -1 & 2 & 2 \\ 2 & -1 & 2 \\ 2 & 2 & -1 \end{pmatrix}, \qquad T = \begin{pmatrix} 1 & 0 & 0 \\ 0 & \omega^2 & 0 \\ 0 & 0 & \omega \end{pmatrix} \tag{A.6}$$

The product of two triplets decomposes as follows:

$$3 \times 3 = 1 + 1' + 1'' + 3_S + 3_A. \tag{A.7}$$

More explicitly, given two triplets $a = (a_1, a_2, a_3)$ and $b = (b_1, b_2, b_3)$, the product reads:

$$(ab)_k = \sum_{i,j} a_i A_{ij}^k b_j, \tag{A.8}$$

for $k = 1$, $1'$, $1''$ and

$$(ab)_k = \sum_{i,j} \left( a_i (B_1^k)_{ij} b_j,\, a_i (B_2^k)_{ij} b_j,\, a_i (B_3^k)_{ij} b_j \right) , \tag{A.9}$$

for the symmetric and anti-symmetric triplet combinations, $k = 3_S$, $3_A$. The matrices $A^k$ ($k = 1$, $1'$, $1''$) and $B_j^k$ ($k = 3_S$, $3_A$ and $j = 1$, 2, 3) are reported below:

$$A^1 = \begin{pmatrix} 1 & 0 & 0 \\ 0 & 0 & 1 \\ 0 & 1 & 0 \end{pmatrix}, \qquad A^{1'} = \begin{pmatrix} 0 & 1 & 0 \\ 1 & 0 & 0 \\ 0 & 0 & 1 \end{pmatrix}, \qquad A^{1''} = \begin{pmatrix} 0 & 0 & 1 \\ 0 & 1 & 0 \\ 1 & 0 & 0 \end{pmatrix}, \tag{A.10}$$

$$B_1^{3_S} = \frac{1}{3} \begin{pmatrix} 2 & 0 & 0 \\ 0 & 0 & -1 \\ 0 & -1 & 0 \end{pmatrix}, \; B_2^{3_S} = \frac{1}{3} \begin{pmatrix} 0 & -1 & 0 \\ -1 & 0 & 0 \\ 0 & 0 & 2 \end{pmatrix}, \; B_3^{3_S} = \frac{1}{3} \begin{pmatrix} 0 & 0 & -1 \\ 0 & 2 & 0 \\ -1 & 0 & 0 \end{pmatrix}, \tag{A.11}$$

$$B_1^{3_A} = \frac{1}{2} \begin{pmatrix} 0 & 0 & 0 \\ 0 & 0 & 1 \\ 0 & -1 & 0 \end{pmatrix}, \; B_2^{3_A} = \frac{1}{2} \begin{pmatrix} 0 & 1 & 0 \\ -1 & 0 & 0 \\ 0 & 0 & 0 \end{pmatrix}, \; B_3^{3_A} = \frac{1}{2} \begin{pmatrix} 0 & 0 & -1 \\ 0 & 0 & 0 \\ 1 & 0 & 0 \end{pmatrix}. \tag{A.12}$$

The group $A_4$ has two subgroups: $G_S \simeq Z_2$, the reflection subgroup generated by $S$, and $G_T \simeq Z_3$, which is generated by $T$. It is immediate to see that the VEVs

$$\langle \varphi_T \rangle \;\; \propto \;\; (1, 0, 0), \tag{A.13}$$
$$\langle \varphi_S \rangle \;\; \propto \;\; (1, 1, 1), \tag{A.14}$$

break $A_4$ respectively to $G_T$ and $G_S$.

# Appendix B

# Basic Features of $A_4$ Models

A general discussion about the basic features of $A_4$ models is reported in this appendix. A particular emphasis is given to the properties and relative differences between two prominent and rather generic supersymmetric $A_4$ models introduced in [81, 82], whose phenomenology is in part studied in Chapter 5.

## B.1  Leading Order Terms

The $A_4$ models discussed in this thesis have in common that the three left-handed lepton doublets $\ell$ and the three RH neutrinos $\nu^c$ transform as triplets under $A_4$. In contrast, the right-handed charged lepton fields $e^c$, $\mu^c$ and $\tau^c$ are singlets under $A_4$. [1] The Majorana mass matrix $M_N$ of the RH neutrinos is generated through the couplings:

$$a\,\xi(\nu^c\nu^c) + b\,(\nu^c\nu^c\varphi_S) \tag{B.1}$$

where $(\cdots)$ denotes the contraction to an $A_4$ invariant (see Appendix A) [2] and $\varphi_S \sim 3$ and $\xi \sim 1$ under $A_4$. The vacuum alignment of $\xi$ and $\varphi_S$ achieved, e.g. in [81, 82], is given by:

$$\langle\varphi_S\rangle = v_S\,\varepsilon\,\Lambda(1,1,1)^T \quad\text{and}\quad \langle\xi\rangle = u\,\varepsilon\,\Lambda \tag{B.2}$$

where $v_S$ and $u$ are assumed to be complex numbers having an absolute value of order one. The (real and positive) parameter $\varepsilon$ is associated with the ratio of a typical VEV of a flavon and the cut-off scale $\Lambda$ of the theory. The generic size of $\varepsilon$ is around 0.01. The exact range of variability of $\varepsilon$ is specified in the following. The matrix $M_N$ can be parametrized as

$$M_N = \begin{pmatrix} -X - 2Z & Z & Z \\ Z & -2Z & Z - X \\ Z & Z - X & -2Z \end{pmatrix}. \tag{B.3}$$

---

[1] In the model discussed in [81] they transform as the three inequivalent one-dimensional representations 1, 1′ and 1″ (see Appendix A), whereas in [82] all three right-handed charged lepton fields transform trivially under $A_4$.

[2] There might exist an additional direct mass term, as in the model defined in [82], $M(\nu^c\nu^c)$. However, this term leads to the same contribution as the term $\xi(\nu^c\nu^c)$.

It contains two complex parameters $X$ and $Z$ which are conveniently expressed through their ratio $\alpha = |3Z/X|$, their relative phase $\phi = \arg(Z) - \arg(X)$ and $|X|$. The parameter $|X|$ determines the absolute mass scale of the RH neutrinos. The matrix $M_N$ is diagonalized by $U_{TB}$ (see Eq. 1.17) so that:

$$\hat{U}_{TB} = U_{TB}\,\Omega \quad \text{with} \quad \Omega = \text{diag}(e^{-i\varphi_1/2}, e^{-i\varphi_2/2}, e^{-i\varphi_3/2}) \tag{B.4}$$

leads to

$$\hat{U}_{TB}^T M_N \hat{U}_{TB} = \text{diag}(M_1, M_2, M_3)\,, \tag{B.5}$$

$M_i$ being the physical RH neutrino masses.

The neutrino Yukawa couplings in the generic class of $A_4$ models considered here, read:

$$y_\nu(\nu^c l)h_u \tag{B.6}$$

so that the neutrino Dirac mass matrix has the simple form:

$$m_D = y_\nu \begin{pmatrix} 1 & 0 & 0 \\ 0 & 0 & 1 \\ 0 & 1 & 0 \end{pmatrix} v_u \tag{B.7}$$

where $v_u$ denotes the VEV of the MSSM Higgs doublet $h_u$. Therefore, the matrix of neutrino Yukawa couplings (in the basis defined by the flavour symmetry) is:

$$\widehat{\lambda} = \frac{m_D}{v_u}\,. \tag{B.8}$$

The light neutrino mass matrix arises from the type I see-saw mechanism:

$$m_\nu = m_D^T M_N^{-1} m_D\,. \tag{B.9}$$

It is diagonalized by $U_{TB}$. The light neutrino masses $m_i$ $(i = 1, 2, 3)$ are given by:

$$m_i = \frac{y_\nu^2 v_u^2}{M_i}\,. \tag{B.10}$$

At LO, the charged lepton mass matrix $m_\ell$ is diagonal in this class of models. In the model given in [81] the charged lepton masses are generated by the coupling to the flavon $\varphi_T$ with its alignment $\langle\varphi_T\rangle \propto (1, 0, 0)^T$ (and the coupling to a Froggatt-Nielsen field), whereas in the model defined in [82] they appear due to the couplings with the flavons $\varphi_T$ and $\xi'$, having the alignments $\langle\varphi_T\rangle \propto (0, 1, 0)^T$ and $\langle\xi'\rangle \neq 0$. Note, in particular, that the mass of the $\tau$ lepton stems from a non-renormalizable coupling:

$$y_\tau(\tau^c l\varphi_T)h_d/\Lambda\,. \tag{B.11}$$

Since $m_\ell$ is diagonal at this level, the lepton mixing originates only from the neutrino sector.

## B.2    Next-to-Leading Order Corrections

The LO results given above get corrected by multi-flavon insertions, as well as by shifts in the VEVs of the flavon fields. As a consequence, the matrices $M_N$, $m_D$ and $m_\ell$ receive corrections. Correspondingly, the lepton masses and mixings receive relative corrections of order $\varepsilon$. The form of the corrections of the neutrino Yukawa couplings is of special interest for the study of leptogenesis and lepton flavour violation in such class of models (see analysis reported in Chapters 4 and 5). The general parametrization of the form of these corrections depends on all the possible covariants that can be realized with the two fields $\nu^c \sim 3$ and $\ell \sim 3$ under $A_4$:

$$(\nu^c \ell) = \nu_1^c \ell_1 + \nu_3^c \ell_2 + \nu_2^c \ell_3 \quad \sim \quad 1 \,, \tag{B.12}$$

$$(\nu^c \ell)' = \nu_3^c \ell_3 + \nu_2^c \ell_1 + \nu_1^c \ell_2 \quad \sim \quad 1' \,, \tag{B.13}$$

$$(\nu^c \ell)'' = \nu_2^c \ell_2 + \nu_3^c \ell_1 + \nu_1^c \ell_3 \quad \sim \quad 1'' \,, \tag{B.14}$$

$$(\nu^c \ell)_S = \begin{pmatrix} 2\nu_1^c \ell_1 - \nu_3^c \ell_2 - \nu_2^c \ell_3 \\ 2\nu_3^c \ell_3 - \nu_2^c \ell_1 - \nu_1^c \ell_2 \\ 2\nu_2^c \ell_2 - \nu_3^c \ell_1 - \nu_1^c \ell_3 \end{pmatrix} \quad \sim \quad 3_S \,, \tag{B.15}$$

$$(\nu^c \ell)_A = \begin{pmatrix} \nu_3^c \ell_2 - \nu_2^c \ell_3 \\ \nu_2^c \ell_1 - \nu_1^c \ell_2 \\ -\nu_3^c \ell_1 + \nu_1^c \ell_3 \end{pmatrix} \quad \sim \quad 3_A \,, \tag{B.16}$$

where $3_{S(A)}$ is the (anti-)symmetric triplet in the product $3 \times 3$ (see Eq. (A.9) for details). As one can see, the structure of $m_D$ at LO coincides with the structure coming from the $A_4$ invariant in Eq. (B.12). The higher order contributions to $m_D$, given by the expressions reported above, arise at the next-to-leading order (NLO) level through multi-flavon insertions. Such contributions are assumed to arise at the level of one flavon insertions and are thus suppressed by $\varepsilon$ relative to the LO result. This is true in the two realizations given in [81] and [82]. All the NLO contributions, which are of the same form as the LO result, can be simply absorbed into the latter. Contributions which cannot be absorbed give rise to NLO terms of the form:

$$y_{1'}^\nu (\nu^c \ell)' \psi'' h_u / \Lambda + y_{1''}^\nu (\nu^c \ell)'' \psi' h_u / \Lambda + y_S^\nu \left( (\nu^c \ell)_S \phi \right) h_u / \Lambda + y_A^\nu \left( (\nu^c \ell)_A \phi \right) h_u / \Lambda \,, \tag{B.17}$$

where $\psi'$ and $\psi''$ stand for flavons which transform as $1'$ and $1''$ under $A_4$, respectively. Here $\phi$ denotes a triplet under $A_4$ and, for simplicity, only such contribution is taken into account. For $\langle \psi' \rangle = w' \, \varepsilon \, \Lambda$, $\langle \psi'' \rangle = w'' \, \varepsilon \, \Lambda$ and $\langle \phi \rangle = (x_1, x_2, x_3)^T \, \varepsilon \, \Lambda$ (with $w'$, $w''$ and $x_i$ being complex numbers whose absolute value is of order one) it results that these induce matrix structures of the type:

$$\begin{aligned} \delta m_D &= y_{1'}^\nu w'' \varepsilon \begin{pmatrix} 0 & 1 & 0 \\ 1 & 0 & 0 \\ 0 & 0 & 1 \end{pmatrix} v_u + y_{1''}^\nu w' \varepsilon \begin{pmatrix} 0 & 0 & 1 \\ 0 & 1 & 0 \\ 1 & 0 & 0 \end{pmatrix} v_u \\ &+ y_S^\nu \varepsilon \begin{pmatrix} 2x_1 & -x_3 & -x_2 \\ -x_3 & 2x_2 & -x_1 \\ -x_2 & -x_1 & 2x_3 \end{pmatrix} v_u + y_A^\nu \varepsilon \begin{pmatrix} 0 & -x_3 & x_2 \\ x_3 & 0 & -x_1 \\ -x_2 & x_1 & 0 \end{pmatrix} v_u \,. \end{aligned} \tag{B.18}$$

Apart from this type of contribution one could, in principle, find contributions arising at the relative order $\varepsilon$ due to the perturbation of the VEVs of the flavons at this relative order, when

NLO corrections are included into the flavon (super-)potential. However, the coupling from which the LO term in Eq. (B.6) originates is generated at the renormalizable level, *i.e.* without involving a flavon. Thus, the most general NLO corrections to the neutrino Dirac mass matrix, $\delta m_D$, are of the form given in Eq. (B.18). In explicit models the term $\delta m_D$ has usually a special form. On the one hand, the flavons in triplet representations have a certain alignment, such as $(1,1,1)^T$, $(1,0,0)^T$, $(0,1,0)^T$ or $(0,0,1)^T$. On the other hand, in such models usually there exist two different flavour symmetry breaking sectors which are separated by an additional cyclic symmetry. In most cases each of these sectors contains one triplet of flavons. Considering NLO corrections arising at the level of one flavon insertions, at most fields from one of the two flavour symmetry breaking sectors can couple at the NLO level to give rise to corrections to the neutrino Dirac mass matrix. Thus, there is only one flavon triplet contributing to $\delta m_D$ at this level. In the specific framework of the model in [81], the NLO terms are given by the triplet flavon $\varphi_T$ with $\langle \varphi_T \rangle = v_T \, \varepsilon \, \Lambda (1,0,0)^T$ ($v_T$ is complex with $|v_T| \sim \mathcal{O}(1)$), so one has:

$$\delta m_D = y_S^\nu \, v_T \, \varepsilon \begin{pmatrix} 2 & 0 & 0 \\ 0 & 0 & -1 \\ 0 & -1 & 0 \end{pmatrix} v_u \; + \; y_A^\nu \, v_T \, \varepsilon \begin{pmatrix} 0 & 0 & 0 \\ 0 & 0 & -1 \\ 0 & 1 & 0 \end{pmatrix} v_u \,. \tag{B.19}$$

In contrast, in the model reported in [82] the triplet $\varphi_S$ has $\langle \varphi_S \rangle = v_S \, \varepsilon \, \Lambda (1,1,1)^T$, which gives rise to the NLO terms such that: [3]

$$\delta m_D = y_S^\nu \, v_S \, \varepsilon \begin{pmatrix} 2 & -1 & -1 \\ -1 & 2 & -1 \\ -1 & -1 & 2 \end{pmatrix} v_u \; + \; y_A^\nu \, v_S \, \varepsilon \begin{pmatrix} 0 & -1 & 1 \\ 1 & 0 & -1 \\ -1 & 1 & 0 \end{pmatrix} v_u \,. \tag{B.20}$$

Similar to the neutrino Dirac mass matrix, the matrices $M_N$ and $m_\ell$ also receive corrections at the NLO level through multi-flavon insertions and shifts in the flavon VEVs. These corrections generate small off-diagonal elements in the charged lepton mass matrix $m_\ell$. If the corrections are of general type, the matrix $V_{eL}$ which satisfies

$$V_{eL}^\dagger m_\ell^\dagger m_\ell \, V_{eL} = \mathrm{diag}(m_e^2, m_\mu^2, m_\tau^2) \,, \tag{B.21}$$

has the form:

$$V_{eL} \approx \begin{pmatrix} 1 & z_A \varepsilon & z_B \varepsilon \\ -\overline{z_A} \varepsilon & 1 & z_C \varepsilon \\ -\overline{z_B} \varepsilon & -\overline{z_C} \varepsilon & 1 \end{pmatrix} \tag{B.22}$$

where $\overline{z}$ denotes the complex conjugate of $z$. The parameters $z_i$ are, in general, complex numbers and $|z_i| \sim \mathcal{O}(1)$. The Majorana mass matrix $M_N$ of the RH neutrinos also gets contributions from NLO corrections $\delta M_N$, so that it is no longer exactly diagonalized by $U_{TB}$:

$$V_R^T \hat{U}_{TB}^T \left( M_N + \delta M_N \right) \hat{U}_{TB} V_R = \mathrm{diag}(\widetilde{M_1}, \widetilde{M_2}, \widetilde{M_3}) \,, \tag{B.23}$$

where $V_R$ is defined by:

$$V_R \approx \begin{pmatrix} 1 & w_A \varepsilon & w_B \varepsilon \\ -\overline{w_A} \varepsilon & 1 & w_C \varepsilon \\ -\overline{w_B} \varepsilon & -\overline{w_C} \varepsilon & 1 \end{pmatrix} \,. \tag{B.24}$$

---

[3] A contribution from the flavon $\xi$ transforming as a trivial singlet under $A_4$ can be absorbed into the LO result.

The mass eigenvalues $\widetilde{M}_i$ are expected to differ from those calculated at LO, $M_i$, by relative corrections of order $\varepsilon$. Also here the complex parameters $w_i$ have absolute values $|w_i| \sim \mathcal{O}(1)$. For each matrix element in $V_{eL}$ and $V_R$, the leading term in the expansion in $\varepsilon$ is shown. In the two models discussed in [81, 82], one finds that, due to the structure of the NLO terms, not all parameters $z_i$ and $w_i$ in $V_{eL}$ and $V_R$, respectively, are arbitrary: in [81] one has $z_A = z_B = z_C$ with no constraints on $w_i$, while in [82] it results that $z_i$ are not related, but $w_A = 0$ and $w_C = 0$.

## B.3   Constraints on the Expansion Parameter $\varepsilon$

The size of the expansion parameter $\varepsilon$ is strictly related to the possible value of $\tan\beta = \langle h_u \rangle / \langle h_d \rangle = v_u/v_d$. Indeed, the upper bound on $\varepsilon$ comes from the requirement that the discussed NLO corrections to the lepton mixing angles do not lead to too large deviations from the experimental best fit values. The strongest constraint results from the data on the solar neutrino mixing angle and implies $\varepsilon \lesssim 0.05$. A lower bound on $\varepsilon$ can be obtained by taking into account the fact that the Yukawa coupling of the $\tau$ lepton should not be too large. As mentioned, a rather generic feature of the models of interest is that the $\tau$ lepton mass is generated through a non-renormalizable operator involving one flavon. As a consequence, the following relation holds:

$$m_\tau \approx |y_\tau| \varepsilon \langle h_d \rangle = |y_\tau| \varepsilon v \cos\beta \approx |y_\tau| \varepsilon v \frac{1}{\tan\beta} \qquad (\text{B.25})$$

where $v \approx 174$ GeV. Taking $m_\tau$ at the $Z$ mass scale, $m_\tau(M_Z) \approx 1.74$ GeV [113], one has:

$$0.01 \approx |y_\tau| \frac{\varepsilon}{\tan\beta} \; . \qquad (\text{B.26})$$

Reasonable values for $|y_\tau|$ are between $1/3$ and $3$. Using $|y_\tau| = 3$ and $\tan\beta = 2$ gives: [4]

$$\varepsilon \approx 0.007 \; . \qquad (\text{B.27})$$

This is the minimal value of $\varepsilon$ in this type of models. For $\varepsilon \approx 0.05$ one finds that $|y_\tau| = 3$ corresponds to the largest allowed value of $\tan\beta = 15$. All smaller values of $\tan\beta \gtrsim 2$ are possible as well.

---

[4]As is well known, $\tan\beta$ cannot be too small [114]. The smallest value of $\tan\beta$ considered here is: $\tan\beta = 2$.

# Appendix C

# Flavon Superpotential in Models of Chapter 4

## C.1 Flavon Superpotential in Model 1

In the construction of the flavon superpotential for Model 1 defined in Section 4.1.1 an additional $U(1)_R$ symmetry introduced under which driving fields have charge $+2$, superfields containing SM fermions $+1$ and flavons, $h_{u,d}$ and FN field(s) are uncharged. To give a VEV of order $\varepsilon\Lambda$ to $\zeta$ a new driving field $\zeta_0$ is considered, which is a singlet under all symmetries of the model, apart from carrying a $U(1)_R$ charge $+2$. The terms contributing to the flavon superpotential containing $\zeta_0$ at LO read [1]

$$w_d^\zeta = M_\zeta^2 \zeta_0 + g_a \zeta_0 \zeta^2 + g_b \zeta_0 (\varphi_T \varphi_T) \,. \tag{C.1}$$

Analogously to the original model given in [81], one requires a vanishing $F-$term of $\zeta_0$:

$$M_\zeta^2 + g_a \zeta^2 + g_b (\varphi_{T1}^2 + 2\varphi_{T2}\varphi_{T3}) = 0 \,. \tag{C.2}$$

At the same time, the field $\zeta$ does not couple to the other driving fields, $\varphi_0^T \sim (3,1)$, $\varphi_0^S \sim (3,\omega^2)$ and $\xi_0 \sim (1,\omega^2)$ under $(A_4, Z_3)$, in the model at LO. Thus, their $F-$terms read as in the model defined in [81]. The solution of the previous equation is

$$z^2 = -\frac{1}{g_a} \left( M_\zeta^2 + g_b v_T^2 \right) \tag{C.3}$$

and the same results for the VEVs of $\varphi_T$, $\varphi_S$, $\xi$ and $\tilde\xi$ as in [81] are obtained. For the mass parameter $M_\zeta$ being of order $\varepsilon\Lambda$ the VEV $z$ is also of order $\varepsilon\Lambda$.

Concerning the NLO contributions stemming from $\zeta$ to the alignment of the flavons $\varphi_T$, $\varphi_S$, $\xi$ and $\tilde\xi$, there is just one term:

$$\frac{t_z}{\lambda} \zeta^2 \left( \varphi_0^T \varphi_T \right) \,, \tag{C.4}$$

---

[1]Terms such as $\zeta_0 h_u h_d$ are not relevant, since the flavor symmetry is broken much above the electroweak scale.

which gives an additional contribution

$$\frac{3t_z}{2gg_a}\left(g_b+\frac{M_\zeta^2}{v_T^2}\right)\frac{v_T^2}{\lambda} \tag{C.5}$$

to the shift $\delta v_{T1}$ of $\varphi_T$. Its size is $\varepsilon^4\Lambda$, as expected. Furthermore, the shifts $\delta v_{T2,3}$ remain unchanged and thus still equal. The shifts in the vacuum of $\varphi_S$ and $\tilde{\xi}$ are also unchanged and the VEV of $\xi$ is still a free parameter. The NLO terms affecting $w_d^\zeta$ read

$$\Delta w_d^\zeta = \frac{1}{\lambda}\sum_{i=1}^{8}z_i I_i^Z \tag{C.6}$$

with

$$\begin{array}{llll}
I_1^Z = \zeta_0(\varphi_T\varphi_T\varphi_T)\,, & I_2^Z = \zeta_0(\varphi_S\varphi_S\varphi_S)\,, & I_3^Z = \zeta_0\xi(\varphi_S\varphi_S)\,, & I_4^Z = \zeta_0\tilde{\xi}(\varphi_S\varphi_S)\,, \\
I_5^Z = \zeta_0\xi^3\,, & I_6^Z = \zeta_0\xi^2\tilde{\xi}\,, & I_7^Z = \zeta_0\xi\tilde{\xi}^2\,, & I_8^Z = \zeta_0\tilde{\xi}^3\,.
\end{array} \tag{C.7}$$

The result for the shift in the VEV of $\zeta$, $z+\delta z$, in the usual linear approximation, is

$$\begin{aligned}
\delta z &= \frac{g_b\tilde{g}_4}{2g\tilde{g}_3g_a}\left(t_{11}+\frac{\tilde{g}_4^2}{3\tilde{g}_3^2}(t_6+t_7+t_8)\right)\frac{u^3}{z\lambda}-\frac{3g_bt_z}{2gg_a^2}\left(g_b-\frac{g_at_3}{t_z}+\frac{M_\zeta^2}{v_T^2}\right)\frac{v_T^3}{z\lambda} \\
&\quad -\frac{1}{2g_a}\left(z_1\left(\frac{v_T^3}{u^3}\right)+\frac{\tilde{g}_4^2}{3\tilde{g}_3^2}z_3+z_5\right)\frac{u^3}{z\lambda}
\end{aligned} \tag{C.8}$$

with $g_4=-\tilde{g}_4^2$ and $g_3=3\tilde{g}_3^2$ as introduced in [81]. This shift $\delta z$ in $\langle\zeta\rangle$ is of order $\lambda_c^4\lambda$. Additionally, it is easy to prove that, unless some non-trivial relation among the couplings in the flavon superpotential is fulfilled, the VEVs of all driving fields vanish at the minimum.

## C.2 Flavon Superpotential in Model 2

Concerning Model 2 defined in Section 4.1.2, in order to induce a VEV for the flavon $\zeta$, it is necessary to introduce a driving field $\zeta_0$ which transforms as $1'$ under $A_4$, with $-1$ under $Z_4$ and which is invariant under the $Z_2$ symmetry. Since it is responsible for the vacuum alignment, its charge under the $U(1)_R$ symmetry is $+2$. The LO potential for $\zeta_0$ is of the form:

$$w_d^\zeta = g_a\zeta_0\zeta^2 + g_b\zeta_0(\varphi_T\varphi_T)'' + g_c\zeta_0(\xi')^2\,. \tag{C.9}$$

From the $F$-term of $\zeta_0$ one can derive

$$g_a\zeta^2 + g_b(\varphi_{T2}^2+2\varphi_{T1}\varphi_{T3}) + g_c(\xi')^2 = 0\,. \tag{C.10}$$

Thus, $z$ takes the value

$$z^2 = -\frac{1}{g_a}\left(g_bv_T^2+g_c(u')^2\right) = -\frac{1}{g_a}\left(\frac{g_bh_1^2}{4h_2^2}+g_c\right)(u')^2\,, \tag{C.11}$$

sin such a way that $z \propto u'$ holds in case of no accidental cancellations. The parameter $u'$ is not fixed a priori and in [82] it take a value of the order $\varepsilon \Lambda$.

As one can check, the field $\zeta$ does not have renormalizable interactions with the driving fields, $\varphi_0^T \sim (3, -1)$, $\varphi_0^S \sim (3, 1)$ and $\xi_0 \sim (1, 1)$ under $(A_4, Z_4)$, of the original model given in [82]. Thus, the results for the vacuum alignment found in [82] still hold.

At NLO the field $\zeta$ contributes to the flavon superpotential of the original model through

$$\frac{1}{\Lambda} \zeta^2 (\varphi_0^T \varphi_S)', \tag{C.12}$$

while it does not introduce any contribution at this level involving $\varphi_0^S$ or $\xi_0$.

The NLO effects on the vacuum alignment of the field $\zeta$ stem from (order one coefficients are omitted)

$$\frac{1}{\Lambda} \zeta_0 \zeta^2 \xi + \frac{1}{\Lambda} \zeta_0 (\varphi_T \varphi_T \varphi_S)'' + \frac{1}{\Lambda} \zeta_0 \xi (\varphi_T \varphi_T)'' + \frac{1}{\Lambda} \zeta_0 \xi' (\varphi_T \varphi_S)' + \frac{1}{\Lambda} \zeta_0 \xi' \xi' \xi. \tag{C.13}$$

Computing the effect of all NLO terms on the vacuum alignment one finds that all shifts $\delta v_{Si}$ are still equal, *i.e.* the shifts do not change the structure of the vacuum. Therefore the generic size of all shifts, for mass parameters and VEVs of order $\varepsilon \Lambda$, is $\varepsilon^2 \Lambda$. The free parameter $u'$ is still undetermined.

Eventually, it is easy to prove that all driving fields can have a vanishing VEV at the minimum.

# Bibliography

[1] A. S. Beach *et al.*, *Measurement of the cosmic-ray antiproton to proton abundance ratio between 4-GeV and 50-GeV*, Phys. Rev. Lett. **87** (2001) 271101. Citation page:

[2] G. Steigman, *Observational tests of antimatter cosmologies*, Ann. Rev. Astron. Astrophys. **14** (1976) 339. Citation page:

[3] A. G. Cohen, A. De Rujula and S. L. Glashow, *A matter-antimatter Universe ?*, Astrophys. J. **495** (1998) 539. Citation page:

[4] B. Fields and S. Sarkar, *Big-bang nucleosynthesis (PDG mini-review)*, arXiv:astro-ph/0601514. Citation page:

[5] J. Dunkley *et al.* [**WMAP Collaboration**], *Five-Year Wilkinson Microwave Anisotropy Probe (WMAP) observations: likelihoods and parameters from the WMAP data*, Astrophys. J. Suppl. **180** (2009) 306. Citation page:

[6] A. D. Sakharov, *Violation of CP invariance, C asymmetry, and baryon asymmetry of the Universe*, Pisma Zh. Eksp. Teor. Fiz. **5** (1967) 32. Citation page:

[7] F. R. Klinkhamer and N. S. Manton, *A saddle point solution in the Weinberg-Salam theory*, Phys. Rev. D **30** (1984) 2212. Citation page:

[8] V. A. Kuzmin, V. A. Rubakov and M. E. Shaposhnikov, *On the anomalous electroweak baryon number non-conservation in the early Universe*, Phys. Lett. B **155** (1985) 36.

[9] N. Cabibbo, *Unitary symmetry and leptonic decays*, Phys. Rev. Lett. **10** (1963) 531. Citation page:

[10] M. Kobayashi and T. Maskawa, *CP violation in the renormalizable theory of weak interaction*, Prog. Theor. Phys. **49** (1973) 652. Citation page:

[11] M. Trodden, *Electroweak baryogenesis*, Rev. Mod. Phys. **71** (1999) 1463.

[12] C. Jarlskog, *Commutator of the quark mass matrices in the standard electroweak model and a measure of maximal CP violation*, Phys. Rev. Lett. **55** (1985) 1039. Citation page:

[13] K. Jansen, *Status of the finite temperature electroweak phase transition on the lattice*, Nucl. Phys. Proc. Suppl. **47** (1996) 196. Citation page:

[14] S. Davidson, E. Nardi and Y. Nir, *Leptogenesis*, Phys. Rept. **466** (2008) 105. Citation page:

[15] M. Fukugita and T. Yanagida, *Baryogenesis without Grand Unification*, Phys. Lett. B **174** (1986) 45. Citation page:

[16] Y. Fukuda *et al.* [**Kamiokande Collaboration**], *Solar neutrino data covering solar cycle 22*, Phys. Rev. Lett. **77** (1996) 1683; J. Hosaka *et al.* [**Super-Kamiokande Collaboration**], *Solar neutrino measurements in Super-Kamiokande-I*, Phys. Rev. D **73** (2006) 112001; J. N. Abdurashitov *et al.* [**SAGE Collaboration**], *Measurement of the solar neutrino capture rate by the Russian-American gallium solar neutrino experiment during one half of the 22-year cycle of solar activity*, J. Exp. Theor. Phys. **95** (2002) 181; W. Hampel *et al.* [**GALLEX Collaboration**], *GALLEX solar neutrino observations: results for GALLEX IV*, Phys. Lett. B **447** (1999) 127; M. Altmann *et al.* [**GNO Collaboration**], *Complete results for five years of GNO solar neutrino observations*, Phys. Lett. B **616** (2005) 174; Q. R. Ahmad *et al.* [**SNO Collaboration**], *Measurement of the charged current interactions produced by $^8B$ solar neutrinos at the Sudbury Neutrino Observatory*, Phys. Rev. Lett. **87** (2001) 071301; Q. R. Ahmad *et al.* [**SNO Collaboration**], *Measurement of day and night neutrino energy spectra at SNO and constraints on neutrino mixing parameters*, Phys. Rev. Lett. **89** (2002) 011302; C. Arpesella *et al.* [**Borexino Collaboration**], *First real time detection of $^7Be$ solar neutrinos by Borexino*, Phys. Lett. B **658** (2008) 101; C. Arpesella *et al.* [**The Borexino Collaboration**], *Direct measurement of the $^7Be$ solar neutrino flux with 192 days of Borexino data*, Phys. Rev. Lett. **101** (2008) 091302; K. Eguchi *et al.* [**KamLAND Collaboration**], *First results from KamLAND: evidence for reactor anti-neutrino disappearance*, Phys. Rev. Lett. **90** (2003) 021802; T. Araki *et al.* [**KamLAND Collaboration**], *Measurement of neutrino oscillation with KamLAND: evidence of spectral distortion*, Phys. Rev. Lett. **94** (2005) 081801; S. Abe *et al.* [**KamLAND Collaboration**], *Precision measurement of neutrino oscillation parameters with KamLAND*, Phys. Rev. Lett. **100** (2008) 221803; M. Apollonio *et al.* [**CHOOZ Collaboration**], *Search for neutrino oscillations on a long base-line at the CHOOZ nuclear power station*, Eur. Phys. J. C **27** (2003) 331; P. Adamson *et al.* [**MINOS Collaboration**], *Search for active neutrino disappearance using neutral-current interactions in the MINOS long-baseline experiment*, Phys. Rev. Lett. **101** (2008) 221804; P. Adamson *et al.* [**MINOS Collaboration**], *Measurement of neutrino oscillations with the MINOS detectors in the NuMI beam,"* Phys. Rev. Lett. **101** (2008) 131802. Citation page:

[17] P. Minkowski, $\mu \to e + \gamma$ *a rate of one out of 1-billion muon decays?*, Phys. Lett. B **67** (1977) 421. M. Gell-Mann, P. Ramond and R. Slansky, *Proceedings of the Supergravity Stony Brook Workshop*, New York 1979, eds. P. Van Nieuwenhuizen and D. Freedman; T. Yanagida, *Proceedinds of the Workshop on Unified Theories and Baryon Number in the Universe*, Tsukuba, Japan 1979, eds. A. Sawada and A. Sugamoto; R. N. Mohapatra and G. Senjanovic, *Neutrino mass and spontaneous parity non-conservation*, Phys. Rev. Lett. **44** (1980) 912. Citation page:

[18] C. Hagedorn, E. Molinaro and S. T. Petcov, *Majorana phases and leptogenesis in see-saw models with $A_4$ symmetry*, JHEP **0909** (2009) 115. Citation page:

[19] C. Hagedorn, E. Molinaro and S. T. Petcov, *Charged lepton flavour violating radiative decays $\ell_i \to \ell_j + \gamma$ in see-saw models with $A_4$ symmetry*, JHEP **1002** (2010) 047.

[20] S. M. Bilenky and S. T. Petcov, *Massive neutrinos and neutrino oscillations*, Rev. Mod. Phys. **59** (1987) 671. Citation page:

[21] B. Pontecorvo, *Mesonium and antimesonium*, Sov. Phys. JETP **6** (1957) 429; Z. Maki, M. Nakagawa and S. Sakata, *Remarks on the unified model of elementary particles*, Prog. Theor. Phys. **28** (1962) 870. Citation page:

[22] C. Amsler *et al.* [**Particle Data Group**], *Review of particle physics*, Phys. Lett. B **667** (2008) 1. Citation page:

[23] S. M. Bilenky, J. Hosek and S. T. Petcov, *On oscillations of neutrinos with Dirac and Majorana masses*, Phys. Lett. B **94** (1980) 495. Citation page:

[24] J. Schechter and J. W. F. Valle, *Neutrino masses in $SU(2) \times U(1)$ theories*, Phys. Rev. D **22** (1980) 2227. Citation page:

[25] M. Doi, T. Kotani, H. Nishiura, K. Okuda and E. Takasugi, *CP violation in Majorana neutrinos*, Phys. Lett. B **102** (1981) 323. Citation page:

[26] T. Schwetz, M. A. Tortola and J. W. F. Valle, *Three-flavour neutrino oscillation update*, New J. Phys. **10** (2008) 113011. Citation page:

[27] C. Kraus *et al.*, *Final results from phase II of the Mainz neutrino mass search in tritium $\beta$ decay*, Eur. Phys. J. C **40** (2005) 447. Citation page:

[28] V. M. Lobashev *et al.*, *Direct search for mass of neutrino and anomaly in the tritium beta-spectrum*, Phys. Lett. B **460** (1999) 227. Citation page:

[29] M. Beck [**KATRIN Collaboration**], *The Katrin experiment*, J. Phys. Conf. Ser. **203** (2010) 012097. Citation page:

[30] M. Fukugita, K. Ichikawa, M. Kawasaki and O. Lahav, *Limit on the neutrino mass from the WMAP three year data*, Phys. Rev. D **74** (2006) 027302; G. L. Fogli *et al.*, *Observables sensitive to absolute neutrino masses (addendum)*, Phys. Rev. D **78** (2008) 033010; M. Tegmark, *Cosmological neutrino bounds for non-cosmologists*, Phys. Scripta **T121** (2005) 153; S. Hannestad, H. Tu and Y. Y. Y. Wong, *Measuring neutrino masses and dark energy with weak lensing tomography*, JCAP **0606** (2006) 025; J. Lesgourgues, L. Perotto, S. Pastor and M. Piat, *Probing neutrino masses with CMB lensing extraction*, Phys. Rev. D **73** (2006) 045021. Citation page:

[31] E. Komatsu *et al.* [WMAP Collaboration], *Five-Year Wilkinson Microwave Anisotropy Probe (WMAP) Observations:Cosmological Interpretation*, Astrophys. J. Suppl. **180** (2009) 330. Citation page:

[32] P. F. Harrison, D. H. Perkins and W. G. Scott, *Tri-bimaximal mixing and the neutrino oscillation data*, Phys. Lett. B **530**, 167 (2002); P. F. Harrison, D. H. Perkins and W. G. Scott, *Symmetries and generalisations of tri-bimaximal neutrino mixing*, Phys. Lett. B **535** (2002) 163; Z. Z. Xing, *Nearly Tri-bimaximal neutrino mixing and CP violation*, Phys. Lett. B **533**, 85 (2002); X. G. He and A. Zee, *Some simple mixing and mass matrices for neutrinos*, Phys. Lett. B **560**, 87 (2003); L. Wolfenstein, *Oscillations among three neutrino types and CP violation*, Phys. Rev. D **18** (1978) 958; Y. Yamanaka, H. Sugawara and S. Pakvasa, *Permutation symmetries and the fermion mass matrix*, Phys. Rev. D **25**, 1895 (1982). Citation page:

[33] P. I. Krastev and S. T. Petcov, *Resonance amplification and T violation effects in three neutrino oscillations in the Earth*, Phys. Lett. B **205** (1988) 84. Citation page:

[34] C. Jarlskog, *A basis independent formulation of the connection between quark mass matrices, CP violation and experiment*, Z. Phys. C **29** (1985) 491. Citation page:

[35] C. Jarlskog, *Matrix representation of symmetries in flavor space, invariant functions of mass matrices and applications*, Phys. Rev. D **35** (1987) 1685. Citation page:

[36] N. Cabibbo, *Time reversal violation in neutrino oscillation*, Phys. Lett. B **72** (1978) 333. Citation page:

[37] V. D. Barger, K. Whisnant and R. J. N. Phillips, *CP violation in three neutrino oscillations*, Phys. Rev. Lett. **45** (1980) 2084. Citation page:

[38] F. Ardellier *et al.* [**Double CHOOZ Collaboration**], *Double CHOOZ: a search for the neutrino mixing angle* $\theta_{13}$, arXiv:hep-ex/0606025; H. Steiner [**Daya Bay Collaboration**], *The Daya Bay experiment to measure* $\theta_{13}$, Prog. Part. Nucl. Phys. **64** (2010) 342. Citation page:

[39] C. H. Albright *et al.* [**Neutrino Factory/Muon Collider Collaboration**], *The neutrino factory and beta beam experiments and development*, arXiv:physics/0411123; G. De Lellis *et al.*, *Neutrino factories and superbeams, Proceedings*, 7th International Workshop, NuFact05, Frascati, Italy, June 21-26, 2005; Y. Itow *et al.* [**T2K Collaboration**], *The JHF-Kamioka neutrino project*, arXiv:hep-ex/0106019; D. S. Ayres *et al.* [**NOvA Collaboration**], *NOvA proposal to build a 30-kiloton off-axis detector to study neutrino oscillations in the Fermilab NuMI beamline*, arXiv:hep-ex/0503053; A. Bandyopadhyay *et al.* [**ISS Physics Working Group**], *Physics at a future neutrino factory and super-beam facility*, Rept. Prog. Phys. **72** (2009) 106201. Citation page:

[40] G. L. Fogli, E. Lisi, A. Marrone, A. Palazzo and A. M. Rotunno, *Hints of* $\theta_{13} > 0$ *from global neutrino data analysis*, Phys. Rev. Lett. **101** (2008) 141801. Citation page: J. Escamilla, D. C. Latimer and D. J. Ernst, *Atmospheric, long baseline, and reactor neutrino data constraints on* $\theta_{13}$, Phys. Rev. Lett. **103** (2009) 061804. Citation page:

[41] J. F. Nieves and P. B. Pal, *Minimal re-phasing invariant CP violating parameters with Dirac and Majorana fermions*, Phys. Rev. D **36** (1987) 315; J. F. Nieves and P. B. Pal, *Rephasing-invariant CP violating parameters with Majorana neutrinos*, Phys. Rev. D **64** (2001) 076005. Citation page:

[42] J. A. Aguilar-Saavedra and G. C. Branco, *Unitarity triangles and geometrical description of CP violation with Majorana neutrinos*, Phys. Rev. D **62** (2000) 096009. Citation page:

[43] P. Langacker, S. T. Petcov, G. Steigman and S. Toshev, *On the Mikheev-Smirnov-Wolfenstein (MSW) mechanism of amplification of neutrino oscillations in matter*, Nucl. Phys. B **282** (1987) 589. Citation page:

[44] F. T. Avignone, *Strategies for next generation neutrinoless double-beta decay experiments*, Nucl. Phys. Proc. Suppl. **143** (2005) 233; C. Aalseth *et al.*, *Neutrinoless double beta decay and direct searches for neutrino mass*, arXiv:hep-ph/0412300. Citation page:

[45] F. Bellini [**CUORE Collaboration**], *Neutrinoless double beta decay search with Cuoricino and Cuore experiments*, Nucl. Phys. Proc. Suppl. **188** (2009) 65. Citation page:

[46] A. A. Smolnikov *et al.* [**GERDA Collaboration**], *Status of the GERDA experiment aimed to search for neutrinoless double beta decay of $^{76}Ge$*, arXiv:0812.4194 [nucl-ex]. Citation page:

[47] A. Giuliani [**CUORE Collaboration**], *From CUORICINO to CUORE: Investigating the inverted hierarchy region of neutrino mass*, J. Phys. Conf. Ser. **120** (2008) 052051. Citation page:

[48] C. E. Aalseth *et al.* [**MAJORANA Collaboration**], *The Majorana neutrinoless double-beta decay experiment*, Phys. Atom. Nucl. **67** (2004) 2002. Citation page:

[49] S. M. Bilenky, S. Pascoli and S. T. Petcov, *Majorana neutrinos, neutrino mass spectrum, CP-violation and neutrinoless double beta-decay. I: the three-neutrino mixing case*, Phys. Rev. D **64** (2001) 053010. Citation page:

[50] S. Pascoli, S. T. Petcov and W. Rodejohann, *On the CP violation associated with Majorana neutrinos and neutrinoless double-beta decay*, Phys. Lett. B **549** (2002) 177; S. Pascoli, S. T. Petcov and T. Schwetz, *The absolute neutrino mass scale, neutrino mass spectrum, Majorana CP violation and neutrinoless double-beta decay*, Nucl. Phys. B **734** (2006) 24; S. Pascoli and S. T. Petcov, *Majorana neutrinos, neutrino mass spectrum and the $|m_{ee}| \sim 10^{-3}$ eV frontier in neutrinoless double-beta decay*, Phys. Rev. D **77** (2008) 113003. Citation page:

[51] A. Faessler, G. L. Fogli, E. Lisi, V. Rodin, A. M. Rotunno and F. Simkovic, *QRPA uncertainties and their correlations in the analysis of neutrinoless double beta decay*, Phys. Rev. D **79** (2009) 053001. Citation page:

[52] J. A. Casas and A. Ibarra, *Oscillating neutrinos and $\mu \to e + \gamma$*, Nucl. Phys. B **618** (2001) 171. Citation page:

[53] S. F. King, *Invariant see-saw models and sequential dominance*, Nucl. Phys. B **786** (2007) 52. Citation page:

[54] S. Pascoli, S. T. Petcov and A. Riotto, *Leptogenesis and low energy CP violation in neutrino physics*, Nucl. Phys. B **774** (2007) 1. Citation page:

[55] S. Pascoli, S. T. Petcov and A. Riotto, *Connecting low energy leptonic CP violation to leptogenesis*, Phys. Rev. D **75** (2007) 083511. Citation page:

[56] E. W. Kolb and S. Wolfram, *Baryon number generation in the early Universe*, Nucl. Phys. B **172** (1980) 224. Citation page:

[57] L. Covi, E. Roulet and F. Vissani, *CP violating decays in leptogenesis scenarios*, Phys. Lett. B **384** (1996) 169; M. Flanz, E. A. Paschos and U. Sarkar, *Baryogenesis from a lepton asymmetric Universe*, Phys. Lett. B **345** (1995) 248; M. Flanz,, E. A. Paschos, U. Sarkar and J. Weiss, *Baryogenesis through mixing of heavy Majorana neutrinos*, Phys. Lett. B **389** (1996) 693. Citation page:

[58] J. A. Casas, A. Ibarra and F. Jimenez-Alburquerque, *Hints on the high-energy seesaw mechanism from the low-energy neutrino spectrum*, JHEP **0704** (2007) 064. Citation page:

[59] G. C. Branco, R. Gonzalez Felipe and F. R. Joaquim, *A new bridge between leptonic CP violation and leptogenesis*, Phys. Lett. B **645** (2007) 432. Citation page:

[60] S. Blanchet and P. Di Bari, *Flavor effects on leptogenesis predictions*, JCAP **0703** (2007) 018. Citation page:

[61] A. Anisimov, S. Blanchet and P. Di Bari, *Viability of Dirac phase leptogenesis*, JCAP **0804** (2008) 033. Citation page:

[62] R. Barbieri, P. Creminelli, A. Strumia and N. Tetradis, *Baryogenesis through leptogenesis*, Nucl. Phys. B **575** (2000) 61. Citation page:

[63] H. B. Nielsen and Y. Takanishi, *Baryogenesis via lepton number violation and family replicated gauge group*, Nucl. Phys. B **636** (2002) 305. Citation page:

[64] T. Endoh, T. Morozumi and Z. h. Xiong, *Primordial lepton family asymmetries in seesaw model*, Prog. Theor. Phys. **111** (2004) 123. Citation page:

[65] A. Abada, S. Davidson, F. X. Josse-Michaux, M. Losada and A. Riotto, *Flavour issues in leptogenesis*, JCAP **0604** (2006) 004. Citation page:

[66] E. Nardi, Y. Nir, E. Roulet and J. Racker, *The importance of flavor in leptogenesis*, JHEP **0601** (2006) 164. Citation page:

[67] A. Abada, S. Davidson, A. Ibarra, F. X. Josse-Michaux, M. Losada and A. Riotto, *Flavour matters in leptogenesis*, JHEP **0609** (2006) 010. Citation page:

[68] S. Antusch, S. F. King and A. Riotto, *Flavour-dependent leptogenesis with sequential dominance*, JCAP **0611** (2006) 011. Citation page:

[69] J. M. Cline, K. Kainulainen and K. A. Olive, *Protecting the primordial baryon asymmetry from erasure by sphalerons*, Phys. Rev. D **49** (1994) 6394. Citation page:

[70] S. Blanchet, P. Di Bari and G. G. Raffelt, *Quantum Zeno effect and the impact of flavor in leptogenesis*, JCAP **0703** (2007) 012. Citation page:

[71] A. De Simone and A. Riotto, *On the impact of flavour oscillations in leptogenesis*, JCAP **0702** (2007) 005. Citation page:

[72] G. F. Giudice, A. Notari, M. Raidal, A. Riotto and A. Strumia, *Towards a complete theory of thermal leptogenesis in the SM and MSSM*, Nucl. Phys. B **685** (2004) 89. Citation page:

[73] E. Molinaro, S. T. Petcov, T. Shindou and Y. Takanishi, *Effects of lightest neutrino mass in leptogenesis*, Nucl. Phys. B **797** (2008) 93. Citation page:

[74] E. Molinaro and S. T. Petcov, *The interplay between the 'low' and 'high' energy CP violation in leptogenesis*, Eur. Phys. J. C **61** (2009) 93. Citation page:

[75] E. Molinaro and S. T. Petcov, *A case of subdominant/suppressed 'high energy' contribution to the baryon asymmetry of the universe in flavoured leptogenesis*, Phys. Lett. B **671** (2009) 60. Citation page:

[76] P. H. Chankowski and Z. Pluciennik, *Renormalization group equations for seesaw neutrino masses*, Phys. Lett. B **316** (1993) 312; K. S. Babu, C. N. Leung and J. T. Pantaleone, *Renormalization of the neutrino mass operator*, Phys. Lett. B **319** (1993) 191; S. Antusch, M. Drees, J. Kersten, M. Lindner and M. Ratz, *Neutrino mass operator renormalization revisited*, Phys. Lett. B **519** (2001) 238; S. Antusch, J. Kersten, M. Lindner and M. Ratz, *Running neutrino masses, mixings and CP phases: Analytical results and phenomenological consequences*, Nucl. Phys. B **674** (2003) 401; S. Antusch, J. Kersten, M. Lindner, M. Ratz and M. A. Schmidt, *Running neutrino mass parameters in see-saw scenarios*, JHEP **0503** (2005) 024; S. T. Petcov, T. Shindou and Y. Takanishi, *Majorana CP-violating phases, RG running of neutrino mixing parameters and charged lepton flavour violating decays*, Nucl. Phys. B **738** (2006) 219. Citation page:

[77] S. M. Bilenky, S. Pascoli and S. T. Petcov, *Majorana neutrinos, neutrino mass spectrum, CP violation and neutrinoless double beta-decay: II. mixing of four neutrinos*, Phys. Rev. D **64** (2001) 113003; S. Pascoli and S.T. Petcov, *The SNO solar neutrino data, neutrinoless double-beta decay and neutrino mass spectrum*, Phys. Lett. B **544** (2002) 239; S. Pascoli and S. T. Petcov, *Addendum: the SNO solar neutrino data, neutrinoless double beta-decay and neutrino mass spectrum*, Phys. Lett. B **580** (2004) 280. Citation page:

[78] S. T. Petcov, W. Rodejohann, T. Shindou and Y. Takanishi, *The see-saw mechanism, neutrino Yukawa couplings, LFV decays $\ell_i \to \ell_j + \gamma$ and leptogenesis*, Nucl. Phys. B **739** (2006) 208. Citation page:

[79] A. Ibarra and G. G. Ross, *Neutrino phenomenology: the case of two right handed neutrinos*, Phys. Lett. B **591** (2004) 285; P. H. Chankowski, J. R. Ellis, S. Pokorski, M. Raidal and K. Turzynski, *Patterns of lepton flavor violation motivated by decoupling and sneutrino inflation*, Nucl. Phys. B **690** (2004) 279. Citation page:

[80] P. H. Frampton, S. L. Glashow and T. Yanagida, *Cosmological sign of neutrino CP violation*, Phys. Lett. B **548** (2002) 119; M. Raidal and A. Strumia, *Predictions of the most minimal see-saw model*, Phys. Lett. B **553** (2003) 72. Citation page:

[81] G. Altarelli and F. Feruglio, *Tri-bimaximal neutrino mixing, $A_4$ and the modular symmetry*, Nucl. Phys. B **741** (2006) 215. Citation page:

[82] G. Altarelli and D. Meloni, *A simplest $A_4$ model for tri-bimaximal neutrino mixing*, J. Phys. G **36** (2009) 085005. Citation page:

[83] E. E. Jenkins and A. V. Manohar, *Tri-bimaximal mixing, leptogenesis and $\theta_{13}$*, Phys. Lett. B **668** (2008) 210. Citation page:

[84] G. Altarelli, F. Feruglio and C. Hagedorn, *A SUSY $SU(5)$ Grand Unified Model of tri-bimaximal mixing from $A_4$*, JHEP **0803** (2008) 052. Citation page:

[85] A. Pilaftsis, *CP violation and baryogenesis due to heavy Majorana neutrinos*, Phys. Rev. D **56** (1997) 5431. Citation page:

[86] J. A. Harvey and M. S. Turner, *Cosmological baryon and lepton number in the presence of electroweak fermion number violation*, Phys. Rev. D **42** (1990) 3344. Citation page:

[87] G. Engelhard , Y. Grossman, E. Nardi and Y. Nir, *The importance of $N_2$ leptogenesis*, Phys. Rev. Lett. **99** (2007) 081802. Citation page:

[88] G. Engelhard, Y. Grossman and Y. Nir, *Relating leptogenesis parameters to light neutrino masses*, JHEP **0707** (2007) 029. Citation page:

[89] H. B. Nielsen and Y. Takanishi, *Baryogenesis via lepton number violation and family replicated gauge group*, Nucl. Phys. B **636** (2002) 305. Citation page:

[90] Y. Lin, L. Merlo and A. Paris, *Running effects on lepton mixing angles in flavour models with type I see-saw*, Nucl. Phys. B **835** (2010) 238. Citation page:

[91] F. Feruglio, C. Hagedorn, Y. Lin and L. Merlo, *Lepton flavour violation in models with $A_4$ flavour symmetry*, Nucl. Phys. B **809** (2009) 218. Citation page:

[92] S. T. Petcov, *The processes $\mu \to e + \gamma$, $\mu \to e + e + \overline{e}$, $\nu \to \nu + \gamma$ in the Weinberg-Salam model with neutrino mixing*, Sov. J. Nucl. Phys. **25** (1977) 340. Citation page:

[93] S. M. Bilenky, S. T. Petcov and B. Pontecorvo, *Lepton mixing, $\mu \to e + \gamma$ decay and neutrino oscillations*, Phys. Lett. B **67** (1977) 309. Citation page:

[94] M. Raidal *et al.*, *Flavour physics of leptons and dipole moments*, Eur. Phys. J. C **57** (2008) 13. Citation page:

[95] F. Feruglio, C. Hagedorn and L. Merlo, *Vacuum alignment in SUSY $A_4$ models*, JHEP **1003** (2010) 084. Citation page:

[96] F. Borzumati and A. Masiero, *Large muon and electron number violations In supergravity theories*, Phys. Rev. Lett. **57** (1986) 961. Citation page:

[97] J. Hisano, T. Moroi, K. Tobe, M. Yamaguchi and T. Yanagida, *Lepton flavor violation in the supersymmetric standard model with seesaw induced neutrino masses*, Phys. Lett. B **357** (1995) 579. Citation page: J. Hisano and D. Nomura, *Solar and atmospheric neutrino oscillations and lepton flavor violation in supersymmetric models with the right-handed neutrinos*, Phys. Rev. D **59** (1999) 116005. Citation page:

[98] S. T. Petcov, S. Profumo, Y. Takanishi and C. E. Yaguna, *Charged lepton flavor violating decays: leading logarithmic approximation versus full RG results*, Nucl. Phys. B **676** (2004) 453. Citation page:

[99] S. T. Petcov, W. Rodejohann, T. Shindou and Y. Takanishi, *The see-saw mechanism, neutrino Yukawa couplings, LFV decays $\ell_i \to \ell_j + \gamma$ and leptogenesis*, Nucl. Phys. B **739** (2006) 208. Citation page:

[100] H. Baer, C. Balazs, A. Belyaev, T. Krupovnickas and X. Tata, *Updated reach of the CERN LHC and constraints from relic density, $b \to s + \gamma$ and $a(\mu)$ in the mSUGRA model*, JHEP **0306** (2003) 054. Citation page:

[101] J. R. Ellis, K. A. Olive, Y. Santoso and V. C. Spanos, *Supersymmetric dark matter in light of WMAP*, Phys. Lett. B **565** (2003) 176. Citation page:

[102] H. Baer and A. D. Box, *Fine-tuning favors mixed axion/axino cold dark matter over neutralinos in the minimal supergravity model*, Eur. Phys. J. C **68** (2010) 523. Citation page:

[103] F. E. Paige, S. D. Protopopescu, H. Baer and X. Tata, *ISAJET 7.69: a Monte Carlo event generator for p p, anti-p p, and $e^+$ $e^-$ reactions,*" arXiv:hep-ph/0312045. Citation page:

[104] V. Barger, D. Marfatia and A. Mustafayev, *Neutrino sector impacts SUSY dark matter*, Phys. Lett. B **665** (2008) 242. Citation page:

[105] M. L. Brooks *et al.* [**MEGA Collaboration**], *New limit for the family-number non-conserving decay $\mu^+ \to e^+ \gamma$*, Phys. Rev. Lett. **83** (1999) 1521. Citation page:

[106] A. Maki, *Status of the MEG experiment*, AIP Conf. Proc. **981** (2008) 363. Citation page:

[107] B. Aubert [**The BABAR Collaboration**], *Searches for lepton flavor violation in the decays $\tau \to e\,\gamma$ and $\tau \to \mu\,\gamma$*, arXiv:0908.2381 [hep-ex]. Citation page:

[108] M. Bona *et al.*, *SuperB: a high-luminosity asymmetric $e^+e^-$ super flavor factory. conceptual design report*, arXiv:0709.0451 [hep-ex]; A. G. Akeroyd *et al.* [**SuperKEKB Physics Working Group**], *Physics at super B factory*, arXiv:hep-ex/0406071. Citation page:

[109] Y. Mori *et al.* [**The PRIME Working Group**], *An experimental search for $\mu^- \to e^-$ conversion process at an ultimate sensitivity of the order of $10^{-18}$ with PRISM*, LOI-25. Citation page:

[110] E. C. Dukes *et al.* [**Mu2e Collaboration**]**,** *Proposal to search for* $\mu^- N \to e^- N$ *with a single event sensitivity below* $10^{-16}$, FERMILAB-PROPOSAL-0973.

[111] U. Bellgardt *et al.* [**SINDRUM Collaboration**], *Search for the decay* $\mu^+ \to e^+ e^+ e^-$, Nucl. Phys. B **299** (1988) 1. Citation page:

[112] G. Altarelli and F. Feruglio, *Discrete flavor symmetries and models of neutrino mixing*, arXiv:1002.0211 [hep-ph]. Citation page:

[113] Z. z. Xing, H. Zhang and S. Zhou, *Updated values of running quark and lepton masses*, Phys. Rev. D **77** (2008) 113016. Citation page:

[114] S. Schael *et al.* [**ALEPH, DELPHI, L3 and OPAL Collaborations and LEP Working Group for Higgs Boson Searches**], Search for neutral MSSM Higgs bosons at LEP, Eur. Phys. J. C **47** (2006) 547. Citation page: